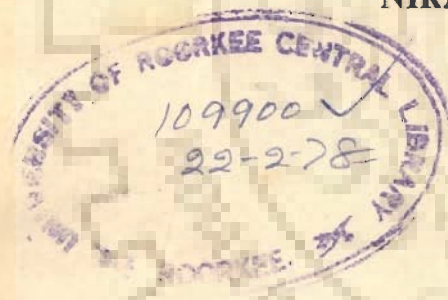# MASS TRANSFER IN COCURRENT GAS-LIQUID FLOW IN A HORIZONTAL TUBE WITH AND WITHOUT TWISTED TAPE INSERTS

A THESIS
submitted in fulfilment
of the requirements for the Degree
of
DOCTOR OF PHILOSOPHY
in
CHEMICAL ENGINEERING
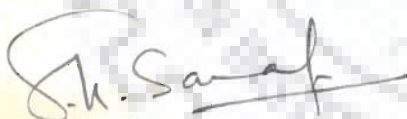
By

NIRANJAN PRASAD SHUKLA

DEPARTMENT OF CHEMICAL ENGINEERING
UNIVERSITY OF ROORKEE
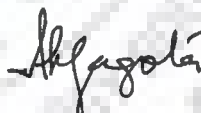ROORKEE, 247667 INDIA
November, 1976

CERTIFICATE

It is certified that the thesis entitled "Mass Transfer in Cocurrent Gas-Liquid Flow in a Horizontal Tube with and without Twisted Tape Inserts" which is being submitted by Niranjan Prasad Shukla in fulfillment of the requirement for the award of the degree of DOCTOR OF PHILOSOPHY in Chemical Engineering at the University of Roorkee, Roorkee, is a record of the candidate's own work carried out by him under the supervision and guidance of the undersigned. The matter embodied in this thesis has not been submitted for the award of any other degree.

This is further certified that the candidate has worked for a period of three and a half years since October 1972 for preparing this thesis.

S.K. Saraf
Department of Chemical Engineering
University of Roorkee
Roorkee, U.P. 247667

A. K. Jagota
International Research and
    Technology Corporation
1501 Wilson Boulevard
Arlington, Virginia 22209
U.S.A.

ACKNOWLEDGEMENTS

(iv)

CONTENTS

LIST OF FIGURES

Figure

LIST OF TABLES

LIST OF PHOTOGRAPHS

NOMENCLATURE

a   -   interfacial area, m^2/m^3 test section

A   -   cross sectional area of test section, m^2

A   -   gas phase component, concentration of gas phase component in liquid phase, g mole / lit.

B   -   reactive component in liquid phase, concentration of reactive component in liquid, g mole / lit.

C   -   concentration, g mole / lit

$C*$ -   equilibrium concentration Equation 3.20, 3.23, g mole / lit.

C_P -   heat capacity Equation 3.15

D   -   pipe diameter, m

D_A -   diffusion coefficient of dissolved gas in liquid phase, as specified or m^2/sec

D_i -   internal diameter, m

D_P -   pipe diameter, as specified units or m

E   -   effectiveness factor, (parameter with twisted tape inserts)/(parameter in empty tube)

E_C -   Chawla f_3 volume fraction, Equation 2.8

E_G -   volume fraction of gas

E_L -   volume fractionof liquid

Eu   -   Euler number, dimensionless, Equation 5.4

f   -   friction factor, dimensionless

f, f'   -   quantities defined by Equation 3.29

Fr   -   Froude number, dimensionless, Equation

G   -   gas flow rate, as specified or m^3/sec

g, g'   -   quantities defined by Equation 3.29

g_c -   Newton's gravitation constant, as specified or $g\text{-}m/g\,f\,sec^2$

h' -   quantity defined by Equation 3.29

H -   pitch length for 360 degrees, m

H_W -   Henry's law constant for water, (atm.lit)/g mole

H_S -   Henry's law constant for solution, (atm.lit)/g mole

I -   Enhancement factor $\equiv (k_L a)/(k_L^o a)$

j_D -   mass transfer factor, Equation 2.19

j_H -   heat transfer factor, Equation 2.18

k_2 -   second order reaction rate constant, lit/g.mole/sec

k_L^o -   individual liquid phase physical mass transfer coefficient, specified units or m/sec

$k_L^o a$ -   volumetric liquid phase physical mass transfer coefficient, sec^{-1}

$k_L a$ -   volumetric liquid phase chemical mass transfer coefficient, sec^{-1}

K_B -   dimensionless parameter in Bankoff void fraction correlation, Equation 2.4

K_H -   dimensionless parameter in Hughmark void fraction correlation, Equation 2.5

L -   test section length, m

L -   liquid mass or volume flow rate

m_1, m_2, m_3 -   quantities defined by Equation 3.42

M -   parameter modulus, (parameter)/$(\Delta P/\Delta L)$

M -   quantity define and used in Equation 3.57

n -   exponent constant, Equation 2.14 and Equation 3.14

N -   velocity numbers, Equation 2.3

N -   normality of a component in solution

p -   partial pressure as specified or kN/m^2

P	-	total pressure as specified or kN/m^2
$\Delta P/\Delta L$	-	pressure gradient, kN/m^3
Pe	-	Pedet number, dimensionless, Equation 5.4
q	-	quantity defined by Equation 3.31
Q	-	volumetric flow rate, specified or m^3/sec
Re	-	Reynold's number, dimensionless, $D_P v \rho / \mu$
Sc	-	Schmidt number, dimensionless, Equation 5.4
T	-	temperature, as specified or $^\circ K$
u	-	velocity, m/sec
v	-	velocity, m/sec
V	-	test section volume, m^3
V_{GO}	-	average superficial gas velocity, m/sec
V_{LO}	-	average superficial liquid velocity, m/sec
V_{SG}	-	superficial gas velocity, m/sec
V_{SL}	-	superficial liquid velocity, m/sec
x	-	mass fraction of gas
X	-	Lockhart-Martinelli parameter, Equation 2.11
y	-	pitch ratio (H/D for 360 degrees)
Y	-	mole fraction of gas A
z	-	number of moles B reacting with one mole of A
Z	-	distance from inlet or length of the test section, m

Subscripts

0, 1, 2, 3	-	inlet, point 1, point 2 and point 3 of the test section
av	-	average
cal or CAL		calculated
ex or EX		experimental
g or G	-	gas phase
H	-	Hughmark
i	-	inlet
i	-	instantaneous
l or L	-	liquid phase
l l	-	laminar gas - laminar liquid
LM	-	Lockhart - Martinelli
M	-	mixture
pred	-	predicted
S	-	liquid solution
t t	-	turbulent gas - turbulent liquid
TP	-	two-phase (gas-liquid)
TP-1 or 2		Twisted tape insert 1 or 2
W	-	water

Greek Symbols

δ -   partial differential

ϵ_B -   Banerjee's energy dissipation parameter, Equation 6.30, N/sec

ϵ_J -   Jepsen's energy dissipation parameter, Equation 2.24, $kN/(m^2 sec)$

θ -   contact time, sec

λ -   empirical coefficient, Equation 1.1

μ -   viscosity, as specified or g/m.sec

π -   constant, (circumference/diameter)

ρ -   density, as specified or g/m^3

σ -   interfacial tension, N/m^2

τ -   quantity defined by Equation 3.47

ϕ -   Lockhart - Martinelli parameter, Equations 2.9 and 2.10

ψ -   empirical coefficient, Equation 1.1

SYNOPSIS

A thesis entitled " Mass Transfer in Cocurrent Gas - Liquid Flow in a Horizontal Tube with and without Twisted Tape Inserts " submitted in fulfilment of the requirements for the degree of Doctor of Philosophy in Chemical Engineering by Niranjan Prasad Shukla at the University of Roorkee, Roorkee in November, 1976.

The two-phase gas-liquid flow in pipes has become increasingly important to engineers in recent years because this type of flow is encountered in large number of situations and a clear understanding of transport rates is necessary for logical and complete design and operations of a very wide variety of engineering equipments and processes. Hydrodynamic and heat transfer studies in two-phase system have been carried out to some extent earlier but the available information about the two-phase mass transfer rates under different flow regimes is extremely limited and only during the last two decades some efforts have been made to systematically study the two-phase mass transfer rates in different types of contacting equipments.

Literature survey revealed that only very few mass transfer studies have been made in horizontal cocurrent gas-liquid flow in the slug flow regime and there has been no reported information about the effect of the presence of twisted tape inserts on mass transfer rates. Therefore, the present investigations were undertaken to understand and analyze the hydrodynamic and

mass transfer phenomena in horizontal two-phase gas-liquid flow
in slug flow regime with and without twisted tape inserts.
Pressure drop and mass transfer studies with and without
chemical reaction are carried out for horizontal gas-liquid flow
in the slug flow regime. The systems studied are carbondioxide -
humidified air mixture as the gas phase and water as the liquid
phase for physical absorption and aqueous sodiumhydroxide
solutions for chemical absorption studies. The velocity ranges
investigated are : 0.13 to 0.73 m/sec for liquid and 0.60 to 10.0
m/sec for the gas. Test section consisted of a smooth 13.5 mm
internal diameter and about 4.0 metre long perspex tube. Twisted
tapes were made from smooth 0.75 mm thick, 12.50 mm wide and
2.50 metre long stainless steel strips. Experiments were carried
out using empty tube and tube with twisted tapes throughout the
test section length. The pitch (360 degrees) to diameter ratios of
5.00 and 9.32 were used.

     The generation of swirl flow in pipe-lines by the use of
internal twisted tapes results in the formation of complex flow
patterns when used with two-phase gas-liquid flow. The main
effect of this "swirling motion" is its ability to increase the
dispersion of gas into liquid but at high swirl intensity there is a
tendency for the liquid to be thrown to the wall of the horizontal
tube and the flow of gas is largely restricted in the central core.
Thus, the swirling flow has a significant effect on the interfacial
area and liquid phase mass transfer coefficient.

Samples were withdrawn at three points for analysis but
some experimental runs could not be used for calculation of
required parameters because the concentration of carbondioxide
in the liquid phase tended to approach the saturation value at a
short distance from the inlet in the case of physical absorption
in tube with lower pitch ratio twisted tape insert when high gas
flow rates and low liquid flow rates were used. In the case of
chemical absorption under similar conditions, almost 100 percent
absorption of carbondioxide gas from the gas mixture was observed.

The pressure drop per unit length of the test section
increased to a high magnitude when twisted tape insert of lower
pitch ratio was used. Increase in gas and liquid flow rates also
resulted in higher pressure drop. This increase in pressure
losses due to the presence of twisted tapes reduces the effective-
ness of using the twisted tape inserts to certain extent. The
pressure drop values were always calculated by using the
following modified friction factor equation developed from
Smithberg-Landis correlation for Reynolds number range of
2100 to 10^6 :

$$f = 0.0014 + \left[0.125 + 2.51 (H/D - 0.5)^{-1.07} \right] Re^{-n}$$

where
$$n = 0.32 \left[1 + 0.65 (H/D)^{-0.5} \right]$$

H/D = pitch to diameter ratio for 360 degrees twist

Re = Reynolds number = $D_H . V . \rho / \mu$

D_H = hydraulic diameter

XXV

The pressure drop in two-phase gas-liquid flow was calculated using Hughmark method of two-phase Reynolds number and Lockhart-Martinelli method. The values of pressure drop predicted by Hughmark method were always lower than the pressure drop measured experimentally with an average under-prediction of 37.7 percent. The Lockhart-Martinelli method of calculating the two-phase pressure drop was found better since this method under-predicted the pressure drop values for only 80 percent data points while the predicted values for the remaining 20 percent data points were more than the experimental pressure drop. The average under-prediction from Lockhart-Martinelli method is only 11.3 percent. The pressure drop values calculated by Lockhart-Martinelli method can be further improved using the following relationship :

$$(\Delta P / \Delta L) = 1.134 (\Delta P / \Delta L)_{LM}^{1.018} \quad ; \text{ standard error} = 17.9\%$$

where

$(\Delta P / \Delta L)$ = predicted two-phase pressure drop, kN/m^3.

$(\Delta P / \Delta L)_{LM}$ = two-phase pressure drop values estimated by Lockhart-Martinelli method, kN/m^3.

The volumetric liquid mass transfer coefficient, $k_L^o a$, was observed to increase with an increase in superficial fluid velocities or decrease in the pitch ratio. It was correlated in terms of pressure drop, two-phase Reynolds number and Jepsen's energy dissipation parameter. Jepsen's energy dissipation parameter, ϵ_J, was found to be the most suitable

for the correlation. The volumetric mass transfer coefficients correlated most satisfactorily by :

Empty tube :

$$k_L{}^{o}a = 0.0331 \ \epsilon_J^{0.515} \ ; \quad \epsilon_J \leqslant 4.0 \ , \ \text{standard error} = 15.8\%$$

$$k_L{}^{o}a = 0.0234 \ \epsilon_J^{0.765} \ ; \quad \epsilon_J \geqslant 4.0 \ , \ \text{standard error} = 38.4\%$$

Tube with twisted tape inserts :

$$k_L{}^{o}a = 0.0853 \ \epsilon_J^{0.277} \ ; \quad \epsilon_J \leqslant 8.0, \ \text{standard error} = 23.6\%$$

$$k_L{}^{o}a = 0.0384 \ \epsilon_J^{0.660} \ ; \quad \epsilon_J \geqslant 8.0, \ \text{standard error} = 22.7\%$$

where $k_L{}^{o}a$ is in sec^{-1} and ϵ_J is in kN/m^2 sec.

From practical point of view it is more desirable to know the effect of twisted tape on volumetric mass transfer modulus, $M_{k_L{}^{o}a}$, that is, $k_L{}^{o}a / (\Delta P/\Delta L)$. At lower gas velocities the twisted tape with larger pitch ratio ($H/D = 9.32$) gave the maximum value of $M_{k_L{}^{o}a}$ at superficial liquid velocity upto 0.8 m/sec. But at higher gas velocity the maximum value of $M_{k_L{}^{o}a}$ was found to be limited to a much lower value of liquid velocity.

The effective interfacial area, a , was observed to increase with an increase in superficial gas velocity or decrease in the pitch ratio. Interfacial area increased initially with an increase in superficial liquid velocity upto a value of 0.4 m/sec. but further increase in superficial liquid velocity, in general, decreases the interfacial area. The effect of difference in pitch ratio ($H/D = 5.0$ and 9.32) was found to be marginal but the observed values

of interfacial area were 1.5 to 4.0 times the values obtained in empty tube.

The effective interfacial area is correlated by Banerjee energy dissipation parameter, two-phase Reynolds number and Jepsen's energy disspation parameter. Area creation rate, first defined by Kasturi and Stepanek, was also correlated by pressure drop. The correlations based on Jepsen's energy dissipation parameter, ϵ_J, and area creation rate, $(a Q_L) / E_L$, were found to be most suitable. The effective interfacial area correlations with Jepsen's energy dissipation parameter are :

Empty tube :

$a = 163.9 \ \epsilon_J^{0.313}$; standard error = 31.0 %

Tube with twisted tape inserts

$a = 253.9 \ \epsilon_J^{0.231}$; standard error = 31.2 %

where a is in m^2 / m^3.

Kasturi and Stepanek's area creation rate correlations with pressure drop are given as :

Empty tube :

$(a Q_L) / E_L = 0.0224 \ (\Delta P / \Delta L)^{1.034}$; standard error = 32.3%

Tube with twisted tape inserts

$(a Q_L) / E_L = 0.00778 \ (\Delta P / \Delta L)^{1.064}$;

standard error = 32.8 %

where $a Q_L / E_L$ is rate of area creation in m^2 / sec.

From practical consideration it may be more desirable to estimate the area modulus, $a / (\Delta P / \Delta L)$, or area creation rate modulus, $(a Q_L / E_L) / (\Delta P / \Delta L)$. Area modulus was found dependent on superficial gas and liquid velocities, but the value of area creation rate modulus can be found quite easily by :

Empty tube :

$$\frac{(a Q_L / E_L)}{(\Delta P / \Delta L)} = 0.0224 (\Delta P / \Delta L)^{0.034} \simeq 0.0224$$

Tube with twisted tape inserts

$$\frac{(a Q_L / E_L)}{(\Delta P / \Delta L)} = 0.00778 (\Delta P / \Delta L)^{0.064} \simeq 0.00778$$

The liquid phase mass transfer coefficient, k_L^{o}, was calculated from the volumetric liquid phase mass transfer coefficient, $k_L^{o} a$, and the value of interfacial area, a, at the similar hydrodynamic condition, that is, at the same value of two-phase Reynolds number. k_L^{o} was found to increase with an increase in superficial gas velocity and decrease in the pitch ratio.

k_L^{o} was correlated using the correlating parameters proposed by Jepsen, Banerjee, Lamont and Scott and Kasturi and Stepanek. The Jepsen energy dissipation parameter and the method of Kasturi and Stepanek were found most satisfactory. These correlations are given as below :

Empty tube and tube with twisted tape inserts

$$k_L^{\,O} = 1.500 \times 10^{-4} \; \epsilon_J^{\,0.375} \; ; \; \text{standard error} = 28.8\%$$

where $k_L^{\,O}$ is in m/sec.

Empty tube :

$$Sh_L = 0.1243 \; Pe_L \; Eu_L \; Sc_L^{-\frac{1}{2}} \; ; \; \text{standard error} = 30.5\%$$

Tube with twisted tape inserts

$$Sh_L = 0.07863 \; Pe_L \; Eu_L \; Sc_L^{-\frac{1}{2}} \; ; \; \text{standard error} = 31.2\%$$

where Sh_L, Pe_L, Eu_L and Sc_L are liquid phase Sherwood, Pedet, Euler and Schmidt numbers respectively.

It may be noted that in most of the cases the numerical values of the constants in all correlations for tube with twisted tape inserts were found to be independent of the pitch-to-diameter ratio of the twisted tapes investigated. However, these values differed considerably when compared with those for empty tube.

Following values selected from the range of parameters studied in the present investigation, show the effectiveness of the use of twisted tape inserts on mass transfer coefficients and interfacial area :

Effectiveness Factor	ϵ_J, kN/m^2 sec.						
	0.1	0.4	1	4	10	40	100
$\dfrac{(k_L^o a)_{twisted\ tape}}{(k_L^o a)_{empty\ tube}}$	4.45	3.29	2.42	1.68	1.33	1.19	1.02
$\dfrac{(a)_{twisted\ tape}}{(a)_{empty\ tube}}$	1.88	1.67	1.53	1.40	1.28	1.12	1.07
$\dfrac{(k_L^o)_{twisted\ tape}}{(k_L^o)_{empty\ tube}}$	1.72	1.43	1.27	1.09	0.88	0.89	0.90

The value of effectiveness factor greater than unity proves the utility of twisted tape inserts, and the above values clearly show that the use of twisted tape inserts is attractive to increase the mass transfer rates and interfacial area only upto a limited increase in liquid and gas velocities.

The results of the present investigation clearly show that the mass transfer rates can be increased by using the twisted tape inserts and this increase is maximum at low gas and liquid velocities. The effectiveness of twisted tape inserts is maximum at low values of Jepsen's energy dissipation parameter, ϵ_J, and as ϵ_J increases to a sufficiently high value the use of twisted tape inserts may even retard the mass transfer rates when compared with those for empty

tube. Thus, absorber volume can be reduced considerably by using twisted tape inserts but at a considerably high pressure drop. When pressure loss considerations are important it is recommended to use twisted tapes with very large pitch to diameter ratio especially at lower liquid and gas velocities. It is hoped that the correlations developed in the present investigations will be useful in the design of tubular absorbers and reactors.
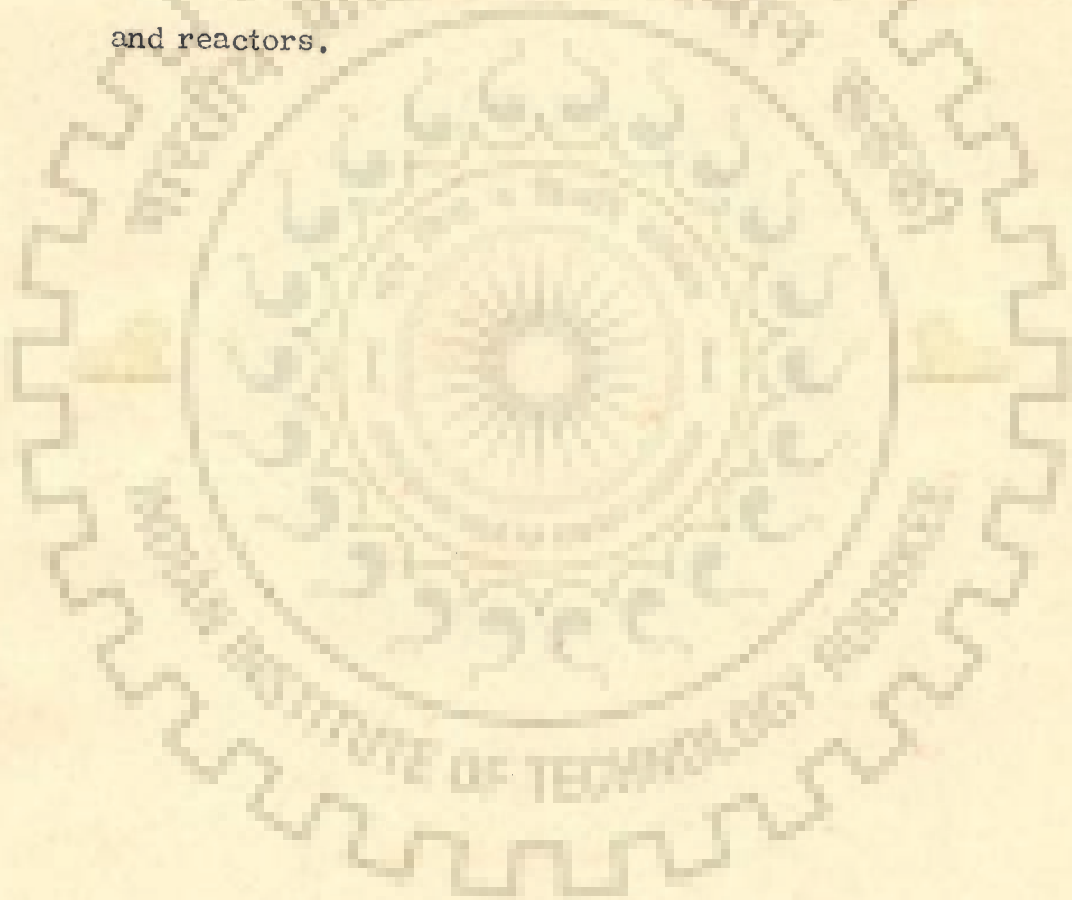
CHAPTER I

INTRODUCTION

The two-phase gas-liquid flow in pipes has become increasingly important to engineers in recent years. This type of flow is encountered in large number of important situations, and a clear understanding of the rates of transfer of momentum, heat and material will be necessary for logical and complete design and operation of a very wide variety of engineering equipments and processes.

1.1   SCOPE AND APPLICATIONS OF TWO-PHASE FLOW

Two-phase gas-liquid flow is encountered in a large number of important situations (1), such as :-

(i)   The production and transport of the crude and the products of petroleum where the prediction of pressure drop is important.

(ii)   Operation of heat transfer equipment, such as steam generators, refrigeration equipment, evaporators, reboilers and partial condensers where the prediction of pressure drop and heat transfer rates is important.

(iii)   Nuclear reactors, water cooled or other change of phase types, where heat transfer rates and maximum temperatures are important.

(iv)   Jet propulsion systems-where liquid films are used to protect nozzle surface from the hot, fast moving

combustion gases and where the prediction of
temperature gradient and stability of the film is
important.

(v)   Cryogenic processes for which prediction of heat loss
and vaporization is important for the proper design of
these low temperature systems.

(vi)   Space programmes, a typical example is the estimation
of the amount of liquid likely to be removed by shearing
during the re-entry of missiles in the atmosphere
where frictional heat is absorbed by the melting and
evaporation at the surface.

(vii) Design of chemical reactors - involving gas-liquid or
immiscible liquid-liquid reactions with reactions
occuring in one or both phases. Such reactors find
extensive use in inorganic, organic and metallurgical
processing industries.

(viii) Waste-water treatment - in recent years cocurrent
aerators have been developed to enhance the rates of
aeration in biological treatment (activated sludge
method) of waste-water.

In some of these operations the prime concern is the
prediction of pressure losses, but in heat-exchange-equipment
the prediction of heat transfer rates become more important.
The accurate estimation of rates of mass transfer, alongwith the
rates of heat transfer and the pressure drop data are essential for

satisfactory design of chemical process equipment for two-phase gas-liquid or liquid-liquid systems.

Information about the two-phase mass transfer rates is very limited and only during the last two decades some efforts have been made to systematically study the two-phase mass transfer rates in different types of contacting equipments.

1.2 CLASSIFICATION OF TWO-PHASE FLOW SYSTEMS

Initial classification of the two-phase flow systems may be based on the following factors :-

(i) Composition : two-phase system containing a single component (a pure liquid and its vapor) or more than one components with one or more components present in both phases or they may be present essentially in one or the other phase.

(ii) Thermal conditions : isothermal or adiabatic or heat regulated processes.

(iii) Phase Transfer : involving mass transfer between phases such as absorption, desorption, evaporation etc.

Classification may also be done by combination of the above factors.

1.3 CHARACTERISTICS OF TWO-PHASE GAS-LIQUID COCURRENT FLOW

Two-phase cocurrent flow has variety of possible flow patterns, ranging from a small quantity of gas dispersed as bubbles in a continuous liquid medium, to the opposite extreme of

a small amount of liquid dispersed as droplets in a continuous gas stream. Some well known facts regarding two-phase flow are as follows (1) :-

(i)   The gas and liquid velocities are rarely equal although this may be assumed as approximation in certain cases.

(ii)   At identical values of the flow variables it is sometimes possible to have two distinctly different flow patterns depending upon factors such as the inlet arrangement.

(iii)   Flow patterns vary not only with flow rates and fluid properties but depend also upon the flow geometry such as pipe diameter and inclination of the pipe.

(iv)   The frictional pressure drop is always higher for two-phase flow as compared to the single-phase flow. This higher pressure drop is caused by the increased velocity of the phase due to the reduction in cross-sectional area available for flow and also the interactions occuring at the extended gas-liquid interface which exists in essentially all the possible flow patterns.

(v)   Heat flux is higher for the two-phase flow for the same situation as compared to single-phase flow at the same liquid flow rate.

(vi)   Mass transfer is higher and depends upon both the extent of the gas liquid interface and the relative velocity between the two flowing phases.

(vii)   The variation in the rate of transport with the change in
the flow rate of one phase, while keeping the flow rate of
the second phase as constant, may show a minima or
maxima in different flow ranges demonstrating the effect
of the possible change in the flow pattern.

(viii)   The apparent visual changes in flow pattern may not always
coincide with observed change in transport behavior.

(ix)   Unstable regions of transition exist between one flow
pattern and the next, making precise definition of these
patterns based on visual appearance alone extremely
difficult.

(x)   As the gas and liquid velocities are not equal, and it has
been observed that they can differ widely, the volume
fraction of a component flowing in the pipe will not be
the same as the volume fraction of that component in the
feed at the inlet, thus the volume fractions of the two
phases are unknown and must depend on the same variables
that govern the flow pattern.

1.4   FLOW PATTERNS IN HORIZONTAL TUBES

It is necessary to distinguish between a physical or visual
description of the state of flow in two-phase mixtures and a
phenomenological one. Large varieties of flow patterns differing
in visual appearance have been given by many investigators ( )
and different correlations have been proposed. The classification

Flow →

A Bubble

B Plug

C Stratified

Increasing gas flow ↓

D Wavy

E Slug

F Annular

G Spray
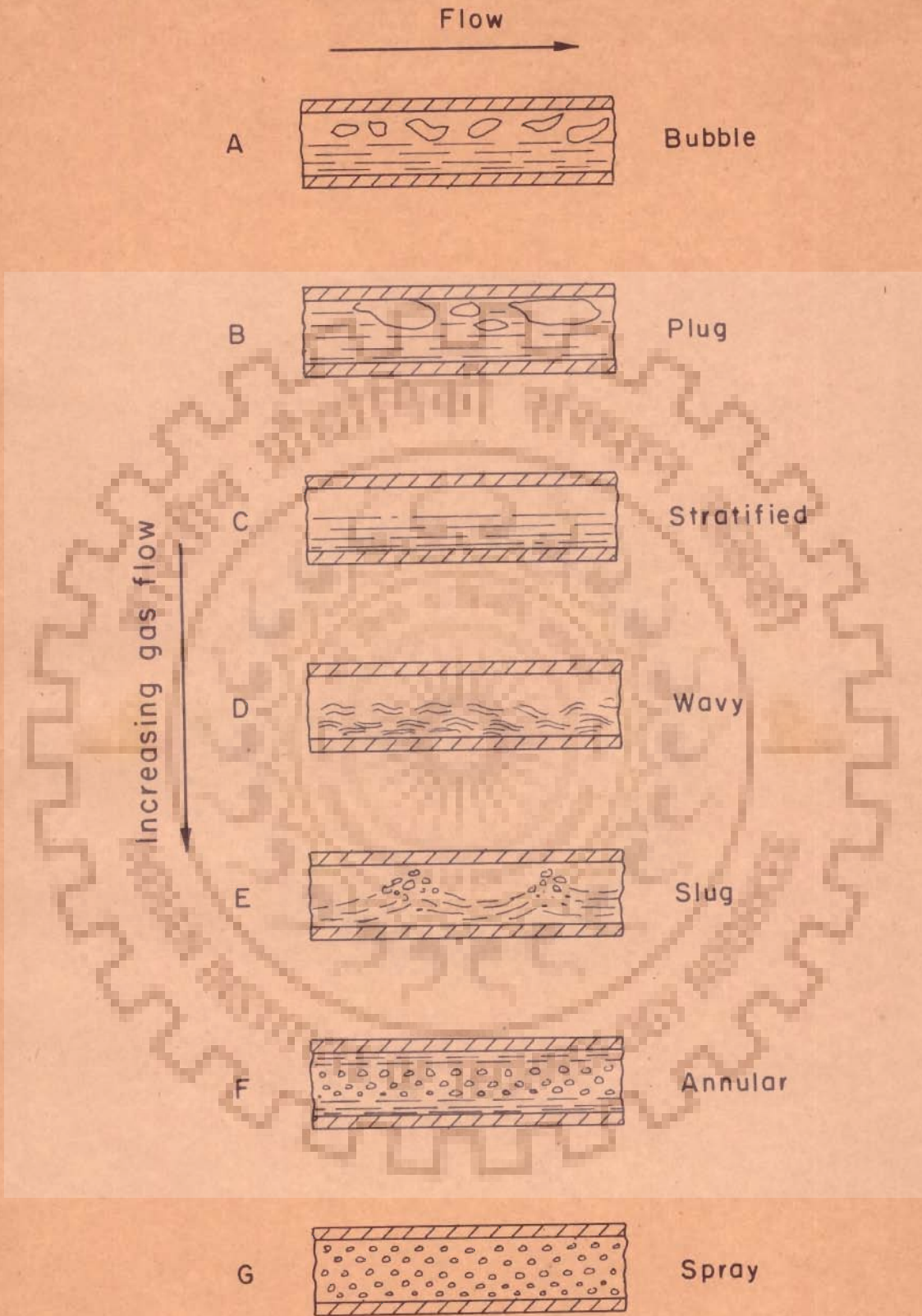
Fig. 1·1 Flow patterns in horizontal two phase flow

of two-phase cocurrent flow can be done as follows:-

Visual appearance

Flow pattern behaviour

1.4.1   Visual Appearance

The following patterns are clearly observable as classified by Alves (2) and shown in Fig. 1.1:-

A.   Bubble Flow :   Discrete gas bubbles move along the upper surface of the pipe at approximately the same velocity as the liquid. At high liquid rates, bubbles get dispersed throughout the liquid, a pattern frequently referred as froth flow.

B.   Plug Flow :   As the gas flow increases the gas bubbles tend to walse forming gas plugs filling a large part of the cross-sectional area of smaller tubes.

C.   Stratified Flow : Complete stratification of gas and liquid occurring at lower liquid flow rates and in larger tubes.

D.   Wavy Flow : At higher gas rates waves of increasing amplitude at the stratified gas-liquid interface are produced.

E.   Slug Flow : A frothy slug passing through the pipe at a much greater velocity than the average liquid velocity. Slug flow is also formed from plug flow as the gas flow rate is increased at constant liquid rate.

F.   <u>Annular or Film Flow</u> : The gas moves at a high velocity in the core of the tube and carries with it some of the liquid as a spray while the liquid is mainly carried as a thin film along the tube wall.

G.   <u>Spray or Mist Flow</u> : All the liquid is entrained in the gaseous core in the form of small drops flowing in the gas. This pattern has also been called dispersed flow or fog flow.

The order of these flow patterns may change depending upon the initial low or high liquid flow rates.

1.4.2   Flow Pattern Behaviour

Attempts have been made to classify flow based on the knowledge of flow variables (3). The graphical representation of such classification usually takes a form of a set of curves outlining the regions in which different flow patterns might be expected to occur. Flow pattern maps developed by different workers have a number of different coordinates and there is little agreement amongst them. A comparison of various maps is given by Govier and Aziz (4).

A flow pattern map based upon coordinates of G/λ and $L\psi\lambda/G$ proposed by Baker and modified by Scott (5) is shown in Fig. 1.2. G/λ is proportional to the mass velocity of the gas and $L\psi\lambda/G$ depends on the ratio of mass velocity of the liquid to that of the gas. The quantities λ and ψ are defined as :-
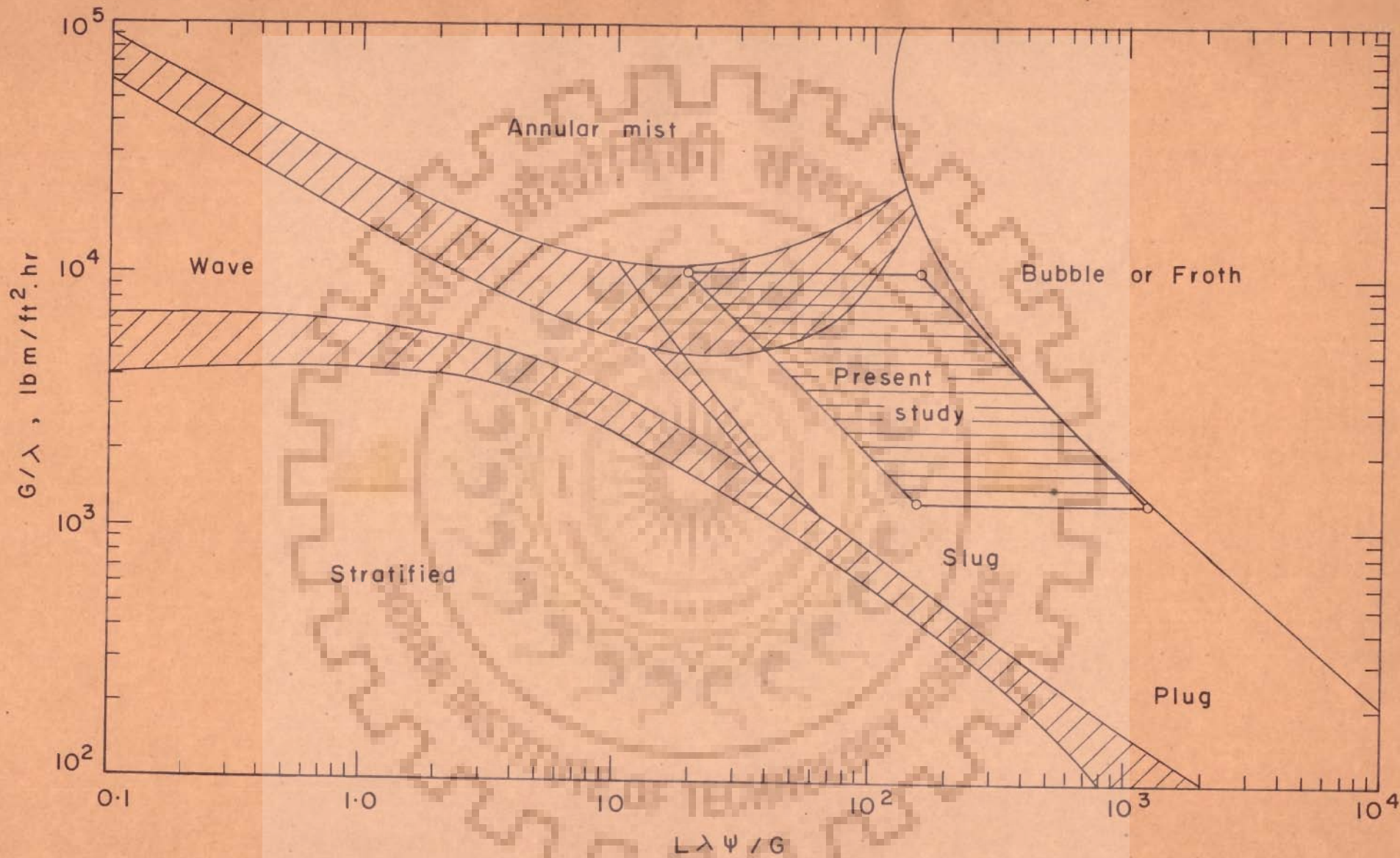
Fig. 1·2 Modified Baker's flow pattern map [1]

$$\lambda = (\rho_G/0.075)(\rho_L/62.3)^{\frac{1}{2}} \quad \cdots \quad (1.1)$$

$$\psi = \frac{73}{\sigma}\left(\frac{\mu L}{1}\right)\left(\frac{62.3}{\rho_L}\right)^{2^{1/3}} \quad \cdots \quad (1.2)$$

and are wholly empirical coefficients designed to bring the transition lines for systems other than air (ρ = 0.075 lb m / ft^3) and water (ρ = 62.3 lb m / ft^3 , σ = 73 dynes/cm and μ = 1 cp) into coincidence with the air-water system. Baker's coordinates reduce to G and L/G for the air-water system. Figure 1.2 is a Baker's plot as modified by Scott using more recent data. Baker's classification is widely used in the petroleum industry.

1.5   AIMS AND OBJECTIVES OF THE PRESENT STUDY

A review of the earlier investigations on cocurrent gas-liquid flow with and without the presence of twisted-tape inserts, reported in Chapter 2, shows that a good deal of experimental work is done to determine the pressure drop, gas holdup and heat transfer coefficients. However, the mass-transfer studies are very limited and there has been no reference in the literature about the effect of the presence of twisted-tape inserts on the mass transfer rates in two-phase cocurrent gas-liquid flow in the slug-flow regime. Therefore, the present investigation was undertaken to increase our knowledge of mass transfer in horizontal two-phase gas-liquid cocurrent flow.

In the present work, the investigations were undertaken to study the following at different gas and liquid flow rates :-

(i)   Pressure drop

(ii)   Volumetric liquid mass transfer coefficients $k_L^o a$

(iii)   Interfacial area 'a'

(iv)   Liquid phase mass transfer coefficient k_L^o

(v)   Effect of twisted tape inserts and its pitch ratio on the above parameters.

The results reported in the present investigation are useful for the design of cocurrent flow gas-liquid contacting equipment. Attempt has been made to correlate mass transfer characteristics with energy consumption rates for the two-phase cocurrent flow.

"Slug' flow was chosen for the investigation because it is obtained with about 50 % of the normal range of flow variables (2) and has been suggested as a flow regime which provides high mass transfer rates for relatively low energy consumption (6).

CHAPTER 2

LITERATURE REVIEW

A brief survey of the published work in the horizontal

flow of gas-liquid is being presented here. At first the hydrodynamic

studies illustrating the general nature of the flow patterns, hold up,

pressure gradient and the use of augmentative techniques are

considered. Then the mass transfer studies dealing with funda-

mental concepts and their application to the two-phase flow as well

as the presence of augmentative devices is taken.

2.1.1 Flow Patterns

It is useful to consider the flow pattern developed for two

immiscible fluids in half-pipe because the symmetry about the pipe

axis exists for horizontal flow in pipes. Flow pattern maps are

useful in predicting the type of flow if the flow characteristics, that

is, physical properties and fluid velocities are known.

Charles et. al. (8) obtained the data in a 1-inch pipe for

the flow of water with hydrocarbon oils of three different viscosities

in the range of 6.29 to 65.0 centipoise whose densities were

increased to that of water through addition of carbon tetrachloride.

They observed essentially the same flow patterns under similar

conditions of superficial oil and water velocities for all oil

viscosities. It was also observed that the sizing and spacing of the

bubbles were not fully fixed by the fluid properties, flow rates, and

pipe geometry but depend upon the mode of introduction of the two fluids.

Russel et. al. (9) observed that the flow patterns in a 1-inch pipe with water and oil of specific gravity 0.834 and 18.0 centipoise viscosity were generally similar to those for the equidensity system but with the distortion and eccentricity expected with the density contrast. Flow pattern map was made by plotting superficial velocities of the two phases with the help of actual photographs and hold-up measurements.

Govier and Omer (10) studied air-water system by visual and photographic observations of the flow pattern. They proposed relationships between the flow patterns for a pair of fluids of very different densities and those for the equidensity and explained the differences in the observed patterns.

Several empirical flow patterns have also been developed. Most of the correlations are expressed as flow pattern maps and a number of different parameters have been proposed for use in the maps. Bergelin and Gazley (11) introduced the flow pattern maps for horizontal flow based upon the data for air-water system using liquid and gas mass flow rates as coordinates.

Alves (12) studied the horizontal flow of air-water and air-oil (SAE 10) mixture in a 1-inch pipe for the full range of flow patterns. He found that a single flow pattern map using superficial liquid and gas velocities as coordinates could represent both systems.
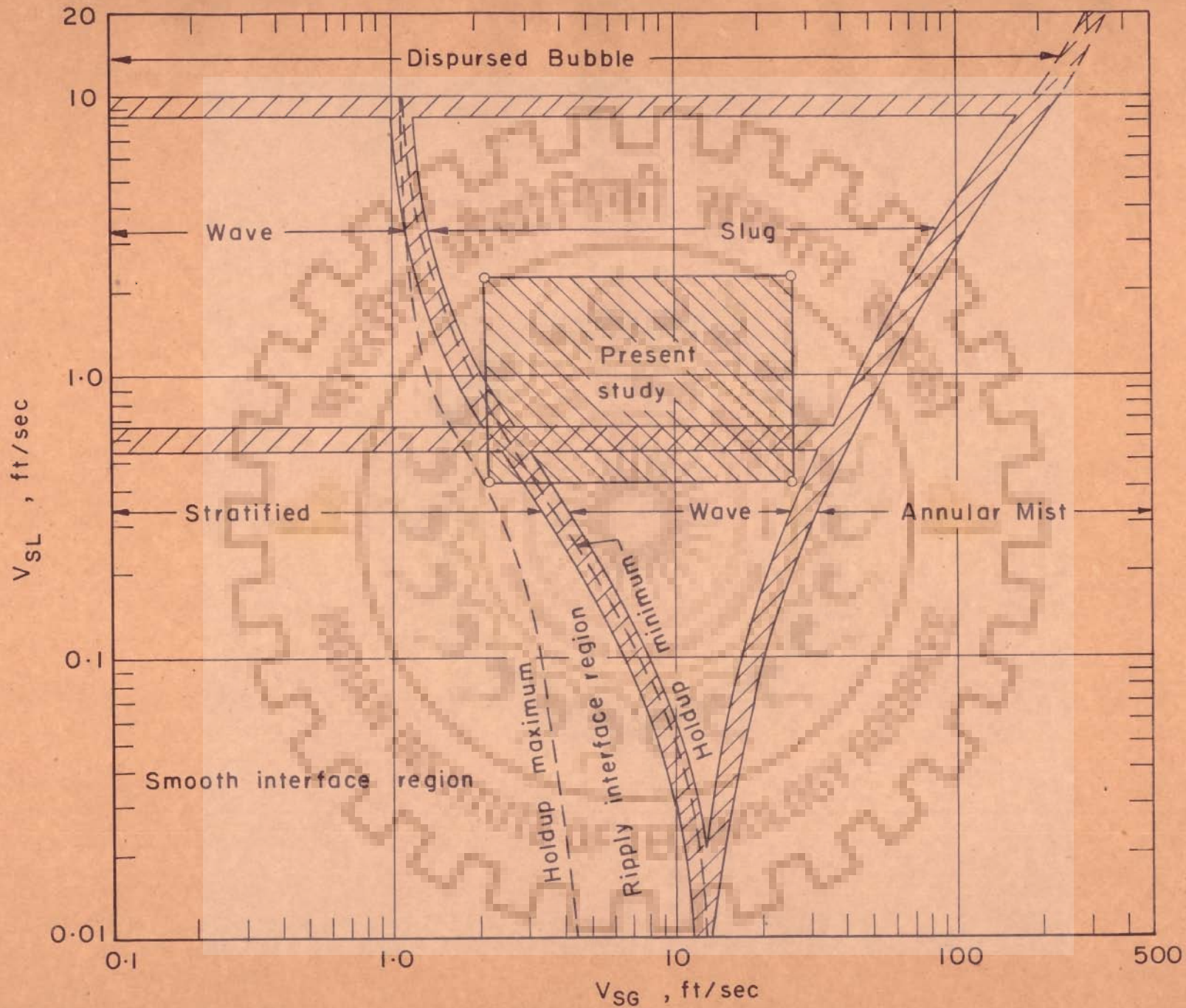
Fig. 2·1 Revised Govier–Omer flow pattern map [18]

White and Huntington (13) presented a flow pattern map for low liquid velcoties based on their data in 1-, 1½-, and 2-inch pipes with oil and natural gas, oil and air, and water and air systems.

Baker (14) proposed a flow pattern map based on the coordinates G/λ and $L\psi\lambda/G$. G/λ is proportional to mass velocity of the gas and $L\psi\lambda/G$ is the ratio of the mass velocity of the liquid to that of the gas (see fig. 1.2). The quantities λ and ψ are empirical parameters designed to bring the flow transition lines for systems other than air-water, into coincidence with those for air-water system. Scott (15) has modified the Baker's correlation using the data of Hoogendoorn (16) and Govier and Omer (10).

Hoogendoorn (16) and also Hoogendoorn and Buitelaar (17) found from their data that the influence of pipe diameter and of liquid and gas properties on the position of the flow transition lines was modest for air-oil systems except for high liquid viscosities.

Govier and Aziz (18) have revised the flow pattern map developed by Govier and Omer (10) and found it to closely agree (Fig. 2.1) with the flow pattern maps of Baker (14) and Hoogendoorn (16).

Eaton et. al. (19) studied the flow of natural gas-water, natural gas-crude oil, and natural gas-distillate systems in 2-, 4- and 17- inch pipe lines. They found all the existing flow pattern

correlations to be inadequate and developed a totally different correlation incorporating the fluid properties and the in-situ volume fraction of the phases. They also defined two-phase Reynolds number and Weber number to correlate their data.

Al-Sheikh et. al. (20) developed their correlation from the data covering a considerably greater range. Instead of defining lines of separation between flow patterns, they consider entire areas enclosing all data corresponding to particular flow patterns. The correlation takes the form of a set of twelve figures on ten different coordinate systems.

Mandhane et. al. (21) proposed a map based on coordinates of superficial gas and liquid velocity constructed from a larger data base. They showed that over 1000 data points for the air-water system in horizontal pipes ranging in size from 1.3 to 15 centimeter diameter gave a good fit. No theoretical basis is given for this method of mapping and the goodness of fit is observed to vary with pipe size and fluid properties. They have also indicated the transition boundaries in their map.

Taitel and Dukler (22) recently proposed criteria for predicting flow regime transitions in horizontal and near horizontal gas-liquid flow. Considering five basic flow regimes theoretical solutions resulted in five dimensionless groups which could be determined from the operating conditions since velocities and pressure gradients are calculated from superficial conditions.

Particular transitions are shown to be controlled by three or less combinations of the dimensionless groups. Satisfactory agreement is found both with respect to the trends of the curves and their absolute locations upto a pipe diameter of 5 centimeter. However, for the larger size pipes, such as 30 centimeter diameter, the displacement of the boundaries is significant when compared with the flow maps based on the superficial gas and liquid velocities only. Although the generalized map presented by Taitel and Dukler is for the turbulent flow of both phases but they found that the laminar flow of liquid had little effect on flow patterns.

2.1.2 Holdup

The holdup ratio, the ratio of the average in situ velocity of light phase to that of heavy phase in horizontal flow is observed to pass through a maximum and then to decrease to values below unity as the flow rate of light phase is increased since continuous phase changes from heavier to lighter phase. In case of air-water system (10) much higher hold-up ratios are observed both for horizontal and vertical flow. Various empirical methods for estimating the hold-up for horizontal flow are proposed and some of the widely used correlations are given below.

Lockhart and Martinelli (23) presented a correlation for the average insitu volume fraction of the liquid phase as a function of parameter X, which is defined as

$$X = \sqrt{\left[\left(\frac{\Delta P}{\Delta L} \right)_{SL} \Big/ \left(\frac{\Delta P}{\Delta L} \right)_{SG} \right]} \qquad (2.1)$$

where $\left(\frac{\Delta P}{\Delta L} \right)_{SL}$ is the

pressure gradient if the liquid is flowing alone at a velocity equal to its superficial velocity, $(\triangle P/\triangle L)_{SG}$ is the pressure gradient if the gas is flowing alone at its superficial velocity. Lockhart and Martinelli based their correlations on the data obtained for air-liquid flow in tubes upto one inch in diameter. Baker (14) compared his data for larger diameter pipes, 8 and 10 inches, and found his hold-up values to be higher than those predicted by Lockhart Martinelli correlations.

Hoogendoorn and Buitelaar (17) developed an empirical correlation for the use insitu volume fraction of gas phase, E_G, based on air-oil systems. It incorporates superficial gas velocity, V_{SG}, and the ratio of superficial velocity of liquid to that of gas V_{SL}/V_{SG}, and is expressed as

$$\frac{E_G}{1 - E_G} = 0.60 \left[V_{SG} \left\{ 1 - \frac{E_G}{1 - E_G} \left(\frac{V_{SL}}{V_{SG}} \right) \right\} \right]^{0.85} \quad ..\ (2.2)$$

It may be noted that the correlation suggests that the value of E_G is independent of pipe diameter and fluid properties.

Eaton et. al. (19) proposed a correlation based upon their data on flow of natural gas-water mixtures in 2- and 4- inch horizontal pipes. Their correlation incorporates three dimensionless ratios and a dimensionless pressure term to account for the variation in the density of the natural gas with pressure. For the range of variables studied they observed sigmoid shape curve when in-situ volume fraction of liquid, E_L, is plotted as a function

of correlating parameter given as :

$$\left(\frac{N_{VL}^{0.575}}{N_{VG} \cdot N_D^{0.0277}} \right) \left(\frac{P}{14.65} \right)^{0.05} \left(\frac{N_L}{0.00266} \right)^{0.10} \qquad \ldots (2.3)$$

where N_{VL}, N_{VG}, N_D, N_L and P are liquid velocity number, gas velocity number, diameter number, viscosity number (all dimensionless) and P is pressure in psia. 0.00266 is the value of N_L for water at 14.65 psia. and $60^{\circ}F$.

Hughmark (24) developed a correlation based on his own data for the vertical flow in a 1-inch pipe for the flow of air with water, saturated aqeous solution of Na_2CO_3, kerosene, trichloroethylene and oils of 5.8 and 28.6 centipoise and selected data of other investigators. The volume average insitu volume fraction of the gas phase, $\overline{E}_G$, expressed as Bankoff's (25) K_B factor

$$K_B = \overline{E}_G \left(\frac{V_{SL} + V_{SG}}{V_{SG}} \right) \qquad \ldots (2.4)$$

is correlated with Z factor defined by,

$$Z = Re_H^{1/6} \overline{Fr}_M^{1/8} C_L^{-1/4}$$

where Re_H is Hughmark Reynold number and $\overline{Fr}_M$ is Froude number of gas liquid mixture and C_L is lift coefficient. Hughmark (24) showed that the correlation for hold up in vertical flow applies also to horizontal flow which is also confirmed by Dukler et. al. (26).

Hughmark (27) gave an empirical correlation for determining the overall volume fraction gas and pressure gradient in the slug flow region. He used the data of Alves (12), Baker (14), Hoogendoorn (17) and Oliver and Wright (28) covering pipe diameter from 0.25 to 7.75 inches for slug flow conditions to obtain a relationship between mixture Reynolds number coefficient K_H. Average volume fraction gas phase, E_G, and pressure gradient, $\triangle P/ \triangle L$ are defined as ;

$$\overline{E}_G = \frac{1}{1 + K_H} \frac{V_{SG}}{V_{SG} + V_{SL}} \qquad \dots (2.5)$$

and

$$\triangle P/\triangle L = 2 f \rho_L V_L^2 / g_c D \qquad \dots (2.6)$$

where f is single phase friction factor based on actual liquid phase Reynolds number, $DV_L \rho_L / \mu_L$ and actual liquid velocity V_L which is $V_{LS} / (1 - E_G)$. Hughmark has correlated his coefficient K_H as a function of mixture Reynolds number and presented graphically where

$$Re_M = D \rho_L (V_{SL} + V_{SG}) / \mu_L \qquad \dots (2.7)$$

He observed that the value of K_H approaches 0.22 at Re_M greater than 4×10^5.

Chawla (29) presented a correlation for insitu volume fraction liquid in terms of the liquid content factor E_C,

$$E_C = 9.1 \left(\frac{1 - x}{x}\right) (Re_L Fr_L)^{-1/6} (\rho_G/ \rho_L)^{0.9} (\mu_G/ \mu_L)^{0.5} \qquad 2.8$$

$$\text{for } E_C < 2 \times 10^{-3}$$

where x is the mass fraction of gas, Re_L is liquid Reynold number, $\overline{Fr}_L$ is liquid Froude number and ρ and μ are density and viscosity. A graphical correlation is also presented to find in situ liquid fraction E_L as a function of Chawla factor E_C with μ_L / μ_G as a parameter.

Mamaev (30) proposed a simple correlation between input volume fraction and the mixture Froude number modified subsequently by Guzhov et. al. (31) and Greskovich et. al. (32). For Froude number greater than 4 and at high values of the input gas fraction, they observed that slug flow pattern predominates. For this region the correlation gives a good check with the Hughmark correlation;

$$\overline{E}_G = 0.82 \ V_{SG} / (V_{SG} + V_{SL}) \qquad (2.5)$$

for slug flow at Reynolds number of mixture, Re_M, 4×10^5. Below this value of Re_M, Hughmark's (27) correlation indicates a dependence of $\overline{E}_G$ on Reynolds number. It is interesting to note that Bankoff's factor K_B is related to Hughmark factor K_H as $K_B = 1 / (1 + K_H)$ and constant value of 0.82 for K_B is equivalent to the constant value of 0.22 of K_H value of Re_M greater than 4×10^5.

2.1.3 Pressure Gradient

The pressure gradient for two phase flow has been observed (18) to be higher than that for single phase flow. Lockhart and Martinelli (23) developed a general pressure drop correlation for two phase flow in horizontal pipes. The correlation is based

upon the concept that the pressure drop for the liquid phase must equal the pressure drop for the gas phase regardless of the flow pattern. Two phase pressure drop relating parameters ϕ_L or ϕ_G with X defined as below:-

$$\phi_L = \sqrt{\left[(\Delta P/\Delta L)_{TP} / (\Delta P/\Delta L)_{SL} \right]} \qquad (2.9)$$

$$\phi_G = \sqrt{\left[(\Delta P/\Delta L)_{TP} / (\Delta P/\Delta L)_{SG} \right]} \qquad (2.10)$$

$$X = \sqrt{\left[(\Delta P/\Delta L)_{SL} / (\Delta P/\Delta L)_{SG} \right]} \qquad (2.11)$$

are presented graphically.

The relationships were determined by Lockhart and Martinelli using their extensive experimental data for widely varying flow conditions of two phases. They provided separate correlations for four flow regimes, namely, laminar liquid-laminar gas, laminar liquid-turbulent gas, turbulent liquid-laminar gas, turbulent liquid-turbulent gas. Individual phase Reynolds number based on superficial velocity is used to characterize the flow and flow is considered turbulent if Re value is greater than 1000. The use of Re value of 1000 to characterize the flow for individual phases is justified because of the presence of the two phases.

Bertuzzi et. al. (33) proposed a pressure drop correlation based upon the mechanical energy balance where the kinetic energy term is negligible and no work is done on or by the system. In order to find the value of appropriate friction factor they defined their Reynolds number as an empirical function of

superficial liquid and gas Reynolds number and mass ratio of gas
to liquid and calculated the pressure drop using mixture velocity.
Gallyamov and Goldzberg (34) have used the above method and
found that the deviation of the experimental data is less than 30
percent of the predicted values.

Hoogendoorn and Buitelaar (17) correlated two phase
friction factor to the ratio of the liquid phase friction factor,
each based on total mass flow rate, as a function of the ratio of
density and the ratio of mass flow rate of two phases.

Dukler et. al. (26) developed a general pressure drop
correlation through a similarity analysis. This correlation is
based upon an assumption of constant holdup. The pressure
gradient due to the friction is expressed as a function of the total
mass flow rate and a specially defined two phase friction factor
which is calculated from single phase friction factor, physical
properties and in-situ volume fraction of two phases.

The correlation proposed by Hughmark (27) has already
been discussed earlier in the section on hold up. It is relatively
simpler to use because the average volume fraction gas phase
needed to evaluate actual liquid velocity can easily be obtained
from the value of Hughmark factor K_H which depends only on
mixture Reynolds number. Gregory and Scott (35) found that
Hughmark pressure drop correlations predicted reasonable values
but the predicted values were 15 to 20 percent lower.

Govier and Aziz (18) have given an excellent review of hydrodynamic studies on the two-phase flow of complex mixtures in horizontal, vertical and inclined pipes.

2.1.4 Studies with Augmentative techniques

An augmentative technique is an extension of a system characteristic. These are employed to enhance the boundary layer, and/or interfacial turbulence which results in an increase in the heat or mass transfer rates. It is also possible to increase the interfacial area or to change the flow pattern in a contactor by augmentative techniques. The commonly used techniques are (36) :-

(i)   Rough heated surface - corrugated or rifled pipes.

(ii)   Heated surface vibrator,

(iii)   Fluid vibrator or pulsed flow,

(iv)   Electrostatic field generator,

(v)   Displaced promoters,

(vi)   Vortex generators   a)   Swirling flow,

                             b)   Twisted tape generated flow.

Ultimate selection of the augmentative technique depends upon large number of factors. Most of the considerations revolve around economics such as development cost, initial cost, operating cost, maintenance cost etc; but there are other factors, notably amongst them are reliability and safety. Most of the studies have been done in the single phase and complex data, such as pumping power and transducer power are generally not reported.

Thus comparison between different augmentative techniques is rather difficult.

Vortex generating techniques are widely used. Some of the important methods of inducing vortex or swirl flow include :

A)   Tangential entry of fluids

B)   Short twisted ribbons

C)   Helical finning on the inside tube surface

D)   Helical ribs.

Twisted tape inserts have been used in industrial applications for over forty years (37). Kirov (38) reported a series of tests which indicated that overall boiler efficiency was improved by about 6 percent by utilising inserts in the flue gas tubes of the air pre-heater.

Gambill et. al. (39) obtained improvements in swirl flow heat transfer to subcooled water in short small diameter tubes. Swirl flow was obtained by inserting a twisted ribbon, of width equal to the tube's internal diameter, along the full length of the heater tube. It was observed that even though swirl flow increases the pumping power requirements, the gain in critical heat flux more than offsets the pumping loss. Gambill and Bundy (40) showed that at constant pumping power, the ratio of the swirl flow to axial flow critical heat fluxes can be as much as 2.5 at centrifugal intensities of 6×10^4 gees. The greatest benefit achieved with swirl flow results from a considerable increase of an improved flow pattern. The centrifugal forces tend to throw

liquid against the tube wall and prevent dry wall conditions.

A summary of some of the reported investigations using twisted - tape inserts is given in the table 2.1.

Table 2.1

Studies on Twisted Tape swirl flow

Investigator and reference	Fluid	Di	y (360°)	Tape fit	Heating	Cooling	Pressure drop
Royds (41)	Air	2.625	less than 20	loose		x	x
Colburn (42)	"	"	5.34-6.10	"		x	x
Siegel (41)	Water	0.527	5-5.68	snug	x		
Evans (43)	gases	3.00	5.8-11.8	loose		x	x
Koch (41)	air	1.97	4.9-22.0	un-known	x		x
Judd (41)	Santowax	0.48	5.2-14.6	snug	x		
Kreith (44)	air water	0.53	5.16-14.6	"	x	x	x
Greene (41)	water	0.89	0.56-2.24	un-known	x		x
Gambill (45)	"	0.136-0.25	4.6-24.06	tight	x		x
Ibragimov (41)	(water & (liquid (metals	0.473	4.24-9.14	"	x	x	x
Smithberg (46)	air-water	1.382	3.62-22	snug	x		x
Gambill (47)	et.glycol	.136-.25	4.6-24.06	tight	x	x	x
Seymous (48)	air	0.87	3.6-28.0	"	x		x
Lopina (49)	water	0.194	4.96-18.4	"	x	x	x
Thorsen (50)	air	0.587	3.16-8.0	snug	x	x	x
Kidd (51)	N₂ gas	0.4	4.68-29.34	tight	x		x
Narasimhamurty (52)	air + water	0.854	3.46-6.92	loose			x
Klepper (53)	N₂ gas	0.429	4.76-16.1	loose (short tapes)	x		x
Cumo (54)	Freon 12	0.298	8.8	tight	x		

The geometry of the twisted tapes can be generally specified in terms of the pitch ratio ' y ', number of tube diameters per 360° twist. A ' tight ' tape fit is considered when no measurable gap between the tape and tube wall exists and ' snug ' fit represents a gap of less than 0.01 inch and a loose fit involves a gap greater than 0.01 inch between the tape and tube wall.

One of the earliest experiments involving heat transfer and pressure drop with twisted tape turbulence promoters was reported in 1921 by Royds (41). Using pre-heated air flowing through an externally cooled tube, Royds noticed that the presence of a twisted tape increased the heat transfer and pressure drop significantly. More detailed results were reported in 1931 by Colburn and King (42). These investigators employed hot air and water cooled tube that contained a twisted tape with a y value of about three. At constant velocity the addition of the tape increased the heat transfer coefficient by 50 percent while the pressure drop was observed to increase to nearly four times.

Interest in twisted tape inserts was revived in late fifties. Koch (41) used air to cool tubes containing tapes with ' y ' ranging from 5.0 to 22. He also reported that with y equal to 5.0 the heat transfer coefficient was doubled but pressure drop increased to four times.

Kreith and Margolis (44) reported experiments with tapes of y from 5.16 to 14.60 using both air and water as fluid. At a Reynolds number of 50, 000 and y of 5.16 they observed Nusselt

modulus to increase by 30 percent for air with corresponding increase in pressure drop by 40 percent. More favourable results were obtained with water.

Gambill et. al. (45) collected available data and showed a great diversity in experimental results. Those investigators themselves conducted boiling and single phase experiments with water and ethylene glycol with an emphasis on burnout heat transfer conditions. Their results suggest that the microscopic surface roughness had a significant effect on the performance of twisted tapes and this may explain some of the scatter in the reported data especially with regard to the frictional pressure drop. The importance of fluid buoyancy in swirl flow heat transfer was also recognised by these workers.

Smithberg and Landis (46) reported heat transfer and pressure drop with twisted tapes of y from 3.62 - to 22.0 for Reynolds number upto 150,000. Nusselt number and friction factors were correlated reasonably well when ratio of wall to bulk fluid temperature was taken into account. Smithberg and Landis developed a modified equation to find the friction factor to account for losses due to axial, tangential and vortex mixing in single phase swirling flow. The rigorous equation proposed by them is

$$f = 0.464\sqrt{f} \ (1/y)^2 + \frac{0.0498}{Re} \ (\frac{Af}{Ac} \ \frac{1}{y}) \left[1125 \ \ln \ (Re\sqrt{f}) - 3170 \right]$$
$$+ \ 0.046 \ Re^{-0.20} \qquad \ldots \ (2.12)$$

which predicts pressure drop within 5% in the Reynolds number range of 5×10^3 to 10^5. Since the use of the above equation is not straight forward they also proposed a simplified equation

$$f = \left[0.046 + 2.1 (y - 0.5)^{-1.2} \right] Re^{-n} \quad \ldots (2.13)$$

where $\quad n = 0.2 (1 + 1.7 y^{-0.5})$ $\quad\quad\quad \ldots (2.14)$

which predicts friction factor to within 11% of the rigorous equation. It is to be noted that both these equations reduces to equation for empty pipe when pitch ratio y becomes infinity.

Lopina and Bergles (49) carried out pressure drop and heat transfer studies with twisted tapes using water as the coolant. They reported a friction factor relationship which takes into account the ratio of the bulk fluid viscosities to the fluid viscosity at the wall also. The use of this equation permitted them to correlate their own data and data obtained with air by other investigators to within 30%. Thorsen and Landis (50) conducted experiments on pressure drop and heat transfer studies by heating and cooling the air with twisted tape inserts.

Kidd (51) reported his studies on pressure drop and heat transfer for the flow of nitrogen using pitch ratio from 5.0 to 28. The effect of tube surface roughness on the heat transfer performance and pressure drop was investigated by Bergles et. al. (55). Electrically heated copper tubes containing Inconel twisted tapes with pitch ratio y ranging from 5.10 to 12.32 using water as coolant. The tube surface ranged from smooth to roughness of 300 micro-inch. The roughened surface tubes showed increase in

both pressure drop and heat transfer coefficient. Seymour (56) investigated the effect of the tape length by using short pieces of tapes and arranging with and without gaps for a twist ratio of 5.26 and concluded that for 75 percent decrease in tape length keeping the total flow length constant the overall friction factor was decreased by 40 percent.

Klepper (53) showed that heat transfer coefficient evaluated at constant pumping power, the tubes containing twisted taps performed upto 22% better than empty tubes. Meagerlin et. al. (57) studied the augmentation of heat transfer in tubes by use of mesh and brush inserts. Considerable improvements in heat transfer coefficient was observed over empty tube, both of these inserts produced very large pressure drops.

Hicks and Mandersloot (58) gave a systematic approach to the study of the effect of viscous forces on heat and mass transfer in systems with turbulence promoters and in packed beds. According to them the transfer rates depend only on the viscous forces at the transfer surfaces and may therefore be predicted from the measurements of the total surface area per unit volume, void fraction and viscous energy factor. They report the studies using expanded aluminium, corrugated perforated PVC and porous spheres as turbulence promoters. Their data gives good correlation between j_D , j_H factors and the modified Reynolds number.

The presence of a twisted tape increases the pressure drop because of friction against the inserts and also because of the increase in fluid velocity. The increase in friction factor is (59) a function of the tape thickness, roughness and method of installation. Simple correlations for the effect of tape pitch on friction factor have been suggested. Gambill et. al. (45) suggested that f varies as $y^{-0.6}$ for y between 4 and 6.

In two phase flow with twisted tapes the method of Lockhart - Martinelli (23) to estimate the pressure drop is found to be valid as long as the Lockhart-Martinelli parameters ϕ_1 and ϕ_g are calculated using the pressure drop for liquid or gas flowing alone in the same geometry and by taking into account the effect of tape geometry. Narasimhamurty and Vara Prasad (52) correlated their data for air-water system in two-phase flow with twisted tapes by means of Lockhart - Martinelli parameters using modified friction factor equation developed by Smithberg and Landis (39). Pressure drop measurements were obtained for three pitch ratios 3.46, 4.32 and 6.92 and the data was within 30 percent of the predicted value.

Gambill and Bundy (40) gave an evaluation of status of swirl-flow heat transfer and pressure drop. Sharma (60) studied the momentum transfer and stability of swirling flow in long horizontal tubes and gave detailed status of swirl flow induced by tangential entry or by putting in the flow inhibitors like twisted tapes. Collier and Wallis (59) have discussed the general

considerations in two phase flow and heat transfer. Date (61)
analyzed theoretically the problem of fully developed flow in tube
containing a twisted tape. He defined a new term called turbulent-
viscosity which accounted for about 10 percent correction but still
predicted friction factor was noticed to be about 30 percent lower
than the experimental data.

2.2. MASS TRANSFER STUDIES

Important problems of practical interest in mass transfer
involve the transfer of material from one fluid phase to another.
The basic principles for such industrial problems are discussed
by Sherwood and Pigford (62). Scott (15) has given an early review
of mass transfer in two phase flow.

2.2.1 Interfacial Mass Transfer - Theories

In the absorption of a gas by a liquid or in the extraction
of a solute from a liquid by a second liquid immiscible with the
first, the solute diffuses from one fluid into the second fluid phase.
In such cases when two fluids are in motion relative to the interface
between them then the two films can be visualized through which
the solute must diffuse. This "two film concept" first suggested
by Whitman (63) in 1923, has proved extremely useful to understand
transfer of mass between two phases. However, since the
individual mass transfer coefficients k_L^o and k_G^o along with
the interfacial concentrations in the two phases are difficult to
measure experimentally. The concept of overall mass transfer
coefficient is found to be more practical in usage (62).

Modified two film theory proposed by Lewis and Whitman (64) gave satisfactory results in some cases and in some other cases discrepancies were found possibly due to faults either in the basic concept or in its interpretations.

According to the film theory it is asumed (65) that close to any fluid interface there is a stagnant film of thickness through which the transport process takes place by simple molecular diffusion. The conditions in the bulk of the phase are assumed to be constant, with the sole exception of the stagnant film itself, so that the overall driving force is entirely used up by the molecular transport in the film. The film thickness depends upon the hydrodynamic conditions of the liquid phase and under equal hydrodyanmic conditions the mass transfer coefficient k_L^o is expected to be proportional to the molecular diffusivity D_A. However, most of the experimental data show $\sqrt{D_A}$ dependence of k_L^o.

Higbie (66) proposed a model of the hydrodynamic - conditions known as "penetration - theory" based on the hypothesis that the gas liquid interface was made up of a variety of small liquid elements, which are continuously brought upto the surface from the bulk of the liquid and vice versa by the convective motion of the liquid. Each element of liquid is considered to be stagnant, as long as it stays at the surface, and the concentration of the dissolved gas in the element is uniform and is equal to the bulk liquid concentration at a time when the element was brought to the surface. Accordingly,

absorption takes place by unsteady molecular diffusion in the various elements of the liquid surface. Higbic further assumed that all the surface elements stayed at the surface for the same amount of time and hence he was able to explain $\sqrt{D_A}$ dependence of $k_L^{\,o}$.

Danckwerts (67) modified the penetration theory by rejecting the concept of equal life for all surface elements of liquid. He used the concept of the age distribution function and the probability to estimate the rate of surface renewal. Danckwerts observed that his theory predicted $\sqrt{D_A}$ dependence of $k_L^{\,o}$ regardless of the nature of the surface renewal rate.

Dobbins (69) pointed out that the proportionality of $k_L^{\,o}$ with D_A predicted by film theory is analogous to an assumption that a time exposure of the surface elements is sufficiently long for the concentration profile within the film to be characteristic of the steady state value whereas the Higbic's penetration theory and Danckwert's surface renewal theories giving $\sqrt{D_A}$ dependence of $k_L^{\,o}$ assume that the surface elements are of essentially infinite depth and the diffusing solute never reach the region of constant concentration. The observed dependency of $k_L^{\,o}$ to $D_A^{\,n}$ could be explained by assuming a finite depth of the surface elements or eddies for a limited time. The value of 'n' depends upon the flow conditions and varies from 0.65 to 0.985. Smaller value of n is observed for greater turbulence corresponding to higher rates of surface renewal. Toor and Marchelto (70) also

confirmed the above observation.

2.2.2   Analogies in Mass Transfer

Analogies help to extend the extensive theoretical and experimental information on momentum and heat transfer to yield corresponding information about the mass transfer. Reynolds analogy (71) relating heat transfer to momentum transfer is the earliest record of this approach and establishes a relationship between heat transfer coefficient h and friction factor f :-

$$\frac{h}{C_P \rho \, U_{av}} = \frac{f}{2} \qquad \ldots \quad (2.15)$$

Von Karman (72) obtained a similar relationship between mass and momentum transfer.

$$(\frac{k_L{}^o}{U_{av}}) \quad (\frac{\mu}{\rho \, D_v}) = \frac{f}{2} \qquad \ldots \quad (2.16)$$

The first important modification of the Reynolds analogy was made by Prandtt and also Taylor (73) by visualising that heat transfer takes place through resistances in series; a laminar layer at the tube wall and a turbulent layer for which the Reynold's analogy is applicable. Corresponding analogy for mass transfer was derived by Colburn (74) who obtained the equation for gases

$$K_C = \frac{\frac{1}{2} f \, U_{av} \, (P/p_{BM})}{1 - a_1 + a_1 \, (\mu/\rho \, D_v)} \qquad \ldots \quad (2.17)$$

where a_1 is a constant, P is total pressure and p_{BM} is the average partial pressure of nontransferable component B. This equation compared well with the experimental data for the

evaporation of water but gave poor results for organic liquids.

Chilton and Colburn (75) altered the denominator of Prandtt-Taylor form and defined two new functions, heat transfer factor j_H and mass transfer factor j_D

$$j_H \quad = \quad \frac{h}{C_p \rho \ U_{av}} \quad \left(\frac{C_p \ \mu}{K}\right)^{2/3} \quad = \quad \tfrac{1}{2} \ f \qquad \dots \quad (2.18)$$

$$j_D \quad = \quad \frac{k_C}{U_{av}} \ \frac{p_{BM}}{P} \quad \left(\frac{\mu}{\rho \ D_v}\right)^{2/3}$$

$$= \quad \frac{k_G}{G_M} \ \frac{p_{BM}}{} \quad \left(\frac{\mu}{\rho \ D_v}\right)^{2/3} = \tfrac{1}{2} f \quad .. \ (2.19)$$

j_H and j_D have been found experimentally to approximate $f/2$ for certain simple streamline shapes but for flow past bluff objects, including spheres and cylinders, they are much smaller than $f/2$.

The mass transfer data of Sherwood and Gilliland (76) covering values of Reynolds number from 2000 to 35000, Schmidt number from 0.6 to 2.5 and gas pressures from 0.1 to 3 atm. and that of Lintan and Sherwood (77) by extending the range of Schmidt number to 3000 by using water over series of pipes made by casting soluble solids correlated satisfactorily by

$$S \ h_{av} \quad = \quad 0.023 \ \left(Re^{0.83} \right) \ Sc^{1/3}$$

Over the range of Re from 5000 to 200,000 the friction factor for flow in smooth pipes can be satisfactorily correlated by

$$f/2 \quad = \quad 0.023 \ / \ Re^{0.20} \qquad \dots \qquad (2.20)$$

and, therefore,

$$S \ h_{av} \ / \ (Re^{1.03} . \ Sc^{1/3}) \quad = \quad f/2 \quad = \quad 0.023 \ / \ Re^{0.20} \quad .. \ (2.21)$$

2.2.3   Mass Transfer Studies in Two Phase Flow

Varlamov et. al. (78) used the gas-lift pump to study overall gas absorption coefficients and observed their coefficients are nearly 100 times than those obtained in packed-tower operation. Baird and Davidson (79), Beek and Van Heuven (80) investigated absorption of carbon dioxide from rising gas bubbles in water and obtained 50 percent and 30 percent higher absorption rates respectively as compared to the predicted values for absorption from the upper surface of a spherical cap bubble.

Heuss et. al. (81) reported on liquid side controlled absorption (of oxygen and gas side controlled absorption) of ammonia into water in a horizontal flow under froth conditions. They applied the model of transfer from a stagnant sphere to the gas side controlled mass transfer data and presented an emperical correlation for the liquid side mass transfer coefficients.

Collins (82) measured volumetric liquid side mass transfer coefficients for the absorption of carbon dioxide into water in 50.8 millimeter internal diameter tube under cocurrent and counter-current annular flow conditions and observed similar values for the mass transfer coefficients at the same value of Reynolds number. However with cocurrent flow, the operation at higher Reynods number is possible and, therefore, six to seven times higher mass transfer coefficient can be achieved than the highest possible value obtainable in countercurrent flow.

Jepsen (83) reported measurements on liquid phase controlled mass transfer in two-phase gas-liquid flow in 1 and 4 inch diameter horizontal pipes 4 inch short radius bend and tubes wound in spirals. He studied the effect of mean gas and liquid flow rates, pipe diameter, and pipe orientation on the mean liquid-phase film mass transfer coefficients. General correlations were developed for $k_L^o a$, the volumetric mass transfer coefficient as a function of the two-phase frictional energy dissipation ϵ_J liquid phase physical properties like viscosity, diffusivity, inter-facial tension and pipe diameter D_P

$$\frac{k_L^o a D_P^{0.68}}{(D_A \cdot \sigma \cdot \mu)^{0.05}} = 18.75 \, \epsilon_J^{0.40} ; \epsilon_J < 0.05 \frac{atm.}{Sec.} \quad \dots (2.22)$$

and

$$\frac{k_L^o a}{(D_A \cdot \sigma \cdot \mu)^{0.05}} = 18.75 \, \epsilon_J^{0.79} ; \epsilon_J < 0.05 \frac{atm.}{Sec.} \quad \dots (2.23)$$

where energy dissipation parameter ϵ_J is defined as

$$\epsilon_J = (\frac{\Delta P}{\Delta L})_{TP} (V_{SG} + V_{SL}) \quad \dots (2.24)$$

Banerjee et. al. (84) obtained liquid side mass transfer coefficients for absorption of carbon dioxide into water and aqueous sodium hydroxide in helical coils with annular flow. They suggested a model for mass transfer in a liquid film under shear based on the assumption that the process is governed by small scale turbulent eddies. The mass transfer coefficient is expressed in terms of the time scale of smallest eddies which, in turn, is related to the

condition of local isotropy. Their correlation

$$k_L^o = \left[2.25 \lambda \ D_P \ V_L \ D_A \ \left(\frac{\Delta P}{\Delta L} \ \frac{D_P}{4 \rho_\ell} \right)^{0.5} \right]^{0.5} \quad \dots \quad (2.25)$$

is reported to give reasonable agreement between experimental
and predicted values of the mass transfer coefficients.

Kulic (85) made the measurements in helical coils using
slug flow conditions. The liquid phase mass transfer coefficient
k_L^o and the interfacial area were obtained using the method
proposed by Danckwerts (86). He observed that Banerjee
correlation are valid to explain his results also.

Jagota et. al. (87) reported mass transfer in upward
co-current gas-liquid annular flow using carbon dioxide water
system and observed that the Jepsen's energy dissipation parameter
does not correlate the k_L^o a values. They also observed that the
data correlated better by using energy dissipation parameter based
only on the liquid flow rate with a standard deviation of 15.6 percent.
A modified model of the energy dissipation parameter was proposed
to account for interchange of drops between the liquid film and the
gas core.

Golding and Mah (88) reported studies in gas absorption
using vertical slug flow. The gas phase consisted of nitrogen,
helium and freon-14 while the liquid phase was light and heavy
paraffin oil and hexane. The data was correlated by the penetration
theory, but predicted values were always high by at least a factor
of two.

Wicks and Duckler (89) studied cocurrent gas-liquid flow in horizontal pipes and correlated their data assuming absorption equilibrium between droplets and gas. Anderson et. al. (90) investigated gas side controlled mass transfer in horizontal annular flow by absorbing ammonia from air into water in a tube of 1 inch diameter and 40 feet long. Interchange of liquid between the film and the entrained droplets was found to increase the rate of mass transfer. They noticed their values to agree with the values of entrainment reported by Wicks and Duckler (89).

Cibrowski and Rychlicki (91) presented empirical correlations for gas and liquid mass transfer coefficients obtained respectively by absorbing carbondioxide and ammonia into water under wavy flow condition in horizontal tube. They correlated their data using the analogy suggested by Kropholler and Carr (92).

Gas absorption in horizontal cocurrent bubble and plug flow is reported by Scott and Hayduk (93). Carbondioxide and helium were used as gas phase and water, ethanol and ethylene glycol as liquid phase over a wide range of operating conditions. They correlated their data to within $\pm$ 15 percent using the transfer unit concept coupled with Levenspiel and Weinstein (94) equation as follows

$$k_L^o \, a = \frac{V_{SL} \, (NTU)}{L} = 6.88 \times 10^{-3} \, V_{SL} \, \left(\frac{V_{SG}}{V_{SG} + V_{SL}} \right)^{0.774}$$

$$\frac{\delta^{0.511} \, \mu^{0.038} \, D_A^{0.39}}{D_p^{1.88}} \qquad .. \ (2.26)$$

Physical as well as chemical absorption of carbon dioxide
into water and sodium hydroxide solution was studied by Wales (95)
in annular and dispersed horizontal flow and reported unusually
high values of interfacial area and low values of volumetric mass
transfer coefficient k_L^o a. Certain doubts have been raised
regarding these results by Cichy et. al. (96) and Jepsen (83).

Lamont and Scott (97) and Zamont (98) reported a study of
physical absorption of carbon dioxide into water in cocurrent
horizontal and vertical bubble flow using 5/16 and 5/8 inch
internal diameter pipe. They correlated their data by using the
dimensionless correlation :-

$$Sh_{(bubble)} = 9.3 \, Re_{(bubble)}^{1/2} \, Sc^{1/3} \qquad \ldots \quad (2.27)$$

Gregory and Scott (99) absorbed carbon dioxide in water
and sodium hydroxide solutions in the slug flow regime in a
horizontal tube of 3/4 inch diameter. Pressure drop data is
correlated both by Hughmark (100) and Lockhart Martinelli (23)
methods and observed that both methods in general underpredict
the pressure drop values but Lockhart Martinelli correlation
appears to correlate the data better. The mass transfer
coefficients are correlated using Jepsen (83) energy dissipation
parameter ϵ_J but a stronger dependence on ϵ_J is observed
than that given by Jepsen. Comparison of the data with the model
developed for annular flow by Banerjee et. al. (84) showed a
deviation by a factor of about three. Gregori and Scott (99) later
modified the Banerjee (84) model tofit the data obtained under slug

flow condition using the correlation

$$k_L^o = \left[\frac{D_A \ D_P \ (E_G)}{4 \ /\mu \ n} \right]^{1/2} \frac{\Delta P}{\Delta L} \qquad \ldots \quad (2.28)$$

where $n = 10^9 / (Re \ TP)^{1.7}$ (approximately) is introduced to

account for the thickness of interfacial viscous layer required for

energy dissipation.

Hughmark (100) proposed a correlation for mass transfer

in horizontal annular gas-liquid flow using mass and momentum

transfer analogies. Davison and Kessler (101) reported mass

transfer studies in horizontal two phase cocurrent annular flow

using carbon dioxide - aqueous monoethanolamine system and used

Higbies theory to find the interfacial areas.

Kasturi and Stepanek (102) measured the interfacial area

in cocurrent gas liquid flow using 6 milimeter internal diameter

and 1524 millimetre long vertical tube mostly in the annular flow

regime. They absorbed carbon dioxide from air mixture in

aqueous sodium hydroxide to obtain interfacial area and reported

that interfacial area increases with the liquid flow rate but a

maximum is observed for each liquid rate when plotted against gas

flow rates. The position of the maxima is virtually independent

of the liquid flow rate. They correlated their data in terms of

the rate of creation of the interfacial area against the pressure drop,

$$Q \ a \ / \ E_L = 0.226 \ (\Delta P/ \Delta L)_{TP}^{1.07} \qquad \ldots \quad (2.29)$$

Kasturi and Stepanek (103) also reported the gas side mass

transfer coefficients by absorbing sulfur dioxide into sodium

hydroxide solution and liquid side mass transfer coefficients by absorbing carbondioxide into sodium carbonate - sodium bicarbonate solution. The liquid side mass transfer coefficient k_L^O is found to increase with gas velocity but a maximum is observed when plotted against the liquid velocity. A model based on the analogy between momentum and mass transfer is proposed for the mass transfer in the liquid phase and they proposed a dimensionless relationship.

$$Sh_L = 0.25 \ Sc_L^{-1/2} \cdot Pe_L \cdot Eu_L \qquad \ldots \qquad (2.30)$$

to correlate liquid phase Sherwood number with Schmidt, Peclet and Euler numbers.

Horvath et. al. (104) reported measurements of radial transport in slug flow using enzyme tubes. They observed that in straight tubes radial mass transfer increases rapidly with decreasing slug length and increasing Reynolds number and quickly reaches a limiting value. In coiled tubes the radial mixing was higher than in straight tubes, particularly with relatively long slugs.

Shah and Sharma (105) studied mass transfer of gas-liquid flow in horizontal pipelines with stratified and slow slug flow regimes. Carbon dioxide - sodium carbonate - sodium bicarbonate and oxygen - sodium dithionite systems were employed for estimating k_L^O a and interfacial area respectively. Correlation proposed by Scott and Hayduk (93) is found to correlate the data well. They reported the reproducibility of their data to within $\pm$ 10 percent.

The study of mass transfer in swirling flow has not attracted much attention so far Thomas (106) studied the sublimation

rate of naphthalene using wires near the edge of laminar boundary layer and reported that the local values of the mass transfer coefficient increased 240 percent in the turbulent region. Bergles (36) has also reported that it is possible to increase the mass transfer rates by vortex devices. He further comments that thorough investigation is necessary before these devices can be put to extensive usage.

Zarnett (107) reported mass transfer studies using carbon dioxide and carbon dioxide nitrogen mixture for absorption into water and aqueous diethanolamine solutions in horizontal two-phase flow in rifled tubes. Smooth 3/4 inch internal diameter lucite tubes were fitted with 1/8 inch x 1/8 inch spiral ribs with pitch to diameter ratio of 1.57 and 2.79. They correlated their interfacial areas with Jepsen energy dissipation parameter and the liquid phase mass transfer coefficient by

$$k_L^o \; / \; (D_A)^{1/2} \;\; = \;\; K \; Re_L^b \qquad \ldots \qquad (2.31)$$

They found that the exponent 'b' is negative for flow in smooth tube and positive for flow in rifled tubes.

Morris and Misson (108) reported their observations of mass transfer and flow resistance in a circular tube fitted with alternate rotation helical inserts, called 'kenics static mixer'. The presence of these helics is shown to produce significant improvement in the mass transfer from the inside surface of the tube and the level of enhancement is dependent on the number of helics

fitted. They also reported that the increase in flow resistance is greater than the corresponding enhancement of mass transfer in relation to a circular tube.

CHAPTER 3

THEORETICAL DEVELOPMENT FOR THE
ANALYSIS OF THE DATA

3.1 PRESSURE DROP CORRELATIONS

Two approaches may be noted to the problem of predicting
pressure drop and holdup in two-phase gas-liquid flow. One method
is by considering the mechanistic approach which involves the detailed
study of hydroxynamics of individual flow patterns or groups of related
patterns and, in general, is more difficult to apply quantitatively.
The second method is by finding semi-theoretical or empirical
correlations using single-phase flow in the hope that equally widely
applicable relationships in terms of dimensionless groups or other
parameters might result. Lockhart - Martinelli (23) employed the
second approach and their approach may be termed as "friction factor"
methods or "homogeneous flow" method. The details of the Lockhart -
Martinelli method and other correlations available in the literature
are already discussed in Chapter 2. In the following sections the basic
correlations and their modifications used to test the experimental data
are discussed briefly.

3.1.1 Single Phase Pressure Drop in Tubes fitted with Twisted Tape Inserts

In order to predict friction losses in the twisted tape
assembly a model of boundary layer must be formulated in addition to

the core flow pattern. The actual boundary layer will reflect the influence of both the axial and the tangential velocity components and in all likelihood it will be highly skewed. In addition, the sublayer should be expected to be thinner than in pure axial flow (no tapes or turbulance promoters) due to the superposed vortex motion.

Assuming incompressible flow and an assumption that mechanical energy losses, due to axial, tangential and vortex mixing flow, can be added in form of equivalent pressure drop terms to define the overall friction factor. Based on rigorous theoretical analysis, Smithberg and Landis (46) proposed that the total pressure drop in twisted tape generated swirling flow can be calculated using the correlation for friction factor as given below:

$$f = 0.464 \ \sqrt{f} \ (D/H)^2 + (0.0498/Re)(D\,Af/HAc) \ (1125 \ \ln \ (Re \ \sqrt{f})$$

$$- 3170) + 0.046/Re^{0.2} \qquad (3.1)$$

where H/D is the pitch ratio for 360°.

Af and Ac are frontal area with and without twisted tape. For very thin tapes Af/Ac is close to unity. The first term in the above equation represents loss due to tangential flow, second term represents loss due to vortex mixing and the last term represents loss due to axial flow. The use of the above equation involves trial and error and Smithberg and Landis (46) also proposed an approximate simplification which can be used directly;

$$f = (0.046 + 2.1 \ (H/D - 0.5)^{-1.2}) \ Re^{-n} \qquad (3.2)$$

where

$$n = 0.2 \ (1 + 1.7 \ \sqrt{(D/H)}$$

Equation 3.2 is found to predict f'' within 11 percent to that calculated

from Equation 3.1 over the Reynolds number range from 5×10^3 to 10^5.

It is to be noted that both the above equations approach simplified equation

used extensively in heat and momentum analogy for smooth pipe

conditions as H/D approaches infinity, that is, axial flow without swirls,

$$f = 0.046 \, (Re)^{-0.2} \tag{3.3}$$

Unfortunately, the approximate Equation 3.3 is not very suitable for

Reynolds number much less than 3×10^4 where Blasius approximation

given by,

$$f = 0.0791 \, (Re)^{-0.25} \tag{3.4}$$

predicts f'' values more accurately. However, in the present study

superficial flow of single phase was in the Reynolds number range of

from approximately 1800 to 30,000; therefore, a more accurate equation

that is valid over a wider range of Reynolds number is to be used.

Accordingly, Drew's empirical equation,

$$f = 0.00140 + 0.125 \, Re^{-0.32} \tag{3.5}$$

was chosen which has been found to be valid in the Reynolds number range

of 2.1×10^3 to 3×10^6 (112) within ± 5 percent error.

In order to improve the applicability of Smitherbg-Landis equation

over wider Reynolds number, the Equation 3.1 is modified by replacing

the last term with Equation (3.5) to represent loss due to axial flow:

$$f = 0.464 \sqrt{f} \left(\frac{D}{H}\right)^2 + \frac{0.0498}{Re}\left[\left(\frac{DAf}{HAc}\right)\left\{1125 \ln (Re \sqrt{f}) - 3170\right\}\right]$$

$$+ 0.0014 + 0.125 \, Re^{-0.32} \tag{3.6}$$

The above equation is difficult to use and involves trial and error solution and is simplified to the following form as suggested by Smithberg and Landis for their simplified equation :

$$f = 0.0014 + \left[0.125 + x \, (H/D - 0.5)^y \right] \, Re^{-n} \qquad (3.7)$$

where $n = 0.32 \left[1 + x' \, (H/D)^{-y'} \right]$ \hfill (3.8)

However, the values of constant x, y, x' and y' used in equations 3.7 and 3.8 were evaluated in the following manner:

For thin twisted taps A_F/A_c can be assumed equal to 1.0 and equation 3.6 may be written as :

$$f = \left[0.464 \sqrt{f} \, (\frac{D}{H})^2 + \frac{0.0498}{Re} \, (\frac{D}{H}) \left\{ 1125 \ln (Re \sqrt{f}) - 3170 \right\} \right.$$
$$\left. + 0.0014 + 0.125 \, Re^{-0.32} \right] \qquad (3.9)$$

For analysis three values of D/H, 0.2, 0.1 and 0 (empty tube or flat tape without twists) and five values of Reynolds numbers, that is, 3×10^3, 1×10^4, 3×10^4, 1×10^5 and 3×10^5 were chosen. For any given values of 'D/H' and 'Re' the value of 'f' can only be calculated by trial and error procedure. IBM 1620 computer was used to calculate 'f' values and initial guess of f was made by using only last two terms of Equation (3.9). For chosen D/H, new value of f was calculated from Equation 3.9 and this new value was compared with initial value. If the difference was more than 0.2 % of the new value, the calculations were repeated using the last computed value of f as the initial guess. The convergence was achieved rapidly and only 3 to 4 iterations were

required. For each value of D/H, a set of five f values corresponding to five different Re values was available. Equation (3.7) was rewritten in the following form

$$\ln (f - 0.0014) = \ln P - n \ln Re \qquad (3.10)$$

where $\quad P = 0.125 + x \left(\dfrac{H}{D} - 0.5 \right)^y \qquad (3.11)$

For each value of D/H, the set of five f - Re values were used and the value of constants P and n were calculated using linear regression analysis. Thus, for three values of D/H we obtained three values of P and three values of n and these values were then used to find the constants x, y, x' and y'.

The values x and y were calculated by linear regression analysis after rewritting Equation (3.10) in the following form:

$$\ln (P - 0.125) = \ln x + y \ln \left(\dfrac{H}{D} - 0.5 \right) \qquad (3.11)$$

Similary, the values of x' and y' were calculated by linear regression analysis using the Equation (3.8) rewritten as:

$$\ln \left(\dfrac{n}{0.32} - 1.0 \right) = \ln x' + y' \ln (D/H) \qquad (3.12)$$

The final form of the equations obtained using above procedure is:

$$f = 0.0014 + \left[0.125 + 2.51 \left(\dfrac{H}{D} - 0.5 \right)^{-1.07} \right] Re^{-n} \qquad (3.13)$$

where $\quad n = 0.32 \left[1 + 0.65 \left(\dfrac{D}{H} \right)^{0.50} \right] \qquad (3.14)$

The above equations reduce to Drew's empirical correlation, equation (3.5), when D/H is equal to zero. For the twist ratio D/H range of 0 to 0.2 and Reynolds number Re range of 3×10^3 to 2×10^5, the values of f calculated from Equations (3.13) and (3.14) are found to be within $\pm$ 8 % to those obtained from Equation (3.9) by using iterative solution procedure.

3.1.2 Two phase pressure drop in tubes fitted with twisted tapes (Hughmark's Method) :

This method gives two phase pressure drops when gas and liquid superficial velocities are known. Reynolds number based on mixture velocity, Re_M is used to obtain Hughmark's K_H factor from K_H versus Re_M graph (27) discussed earlier in section 2.1.3. This K_H factor is used to obtain the fractional gas holdup, E_G

$$ E_G = \frac{V_{SG}}{(1 + K_H) (V_{SL} + V_{SG})} $$

and true average liquid velocity is then obtained using

$$ V_L = \frac{V_{SL}}{(1 - E_G)} \qquad (3.15) $$

where $(1 - E_G)$ is E_L, volume fraction occupied by liquid. Two phase Reynolds number Re_{TP} based on this true liquid velocity and liquid properties:

$$ Re_{TP} = \frac{D_P V_L L}{\mu_L} \qquad (3.16) $$

is in turn used to calculate a friction factor for the calculation of the

pressure drop in two phase flow in the usual manner as applied for single phase flow. This Re_{TP} when used in Equation (3.13) gives a value of friction factor for two phase flow with twisted tape inserts.

The value of two phase pressure drop is then calculated, using this friction factor and true liquid velocity V_L by the usual Darcy formula, that is,

$$\left(\frac{\Delta P}{\Delta L}\right)_{TP} = \frac{2 f V_L^2 \rho_L}{gc \, D_P} \tag{3.17}$$

It may, however, be noted that the pressure drop values predicted by the above method assumes that the two phase pressure drop is equal to the pressure drop for liquid phase alone provided the liquid phase velocity is corrected by estimating the volume fraction occupied by liquid during two-phase flow. These predicted values of pressure drop are expected to be lower than the experimental values for two phase flow because of the additional loss due to gas flow and exchange of momentum between gas and liquid phases. Gregory and Scott (99) have used the above method for predicting two-phase slug flow pressure drop in empty tube and observed an under prediction of 22 percent in physical absorption and 15 percent in the case of chemical disorption.

3.1.3 Two Phase Pressure Drop in tubes fitted with twisted tapes (Lockhart - Martinelli Method) :

This method can be used to estimate the pressure drop in two phase gas liquid flow, if the pressure drop in gas and liquid phase are known separately at their superficial velocities. The square root of the ratio of pressure drop in single phases ,

$$X = \sqrt{\left[(\Delta P/\Delta L)_L / (\Delta P/\Delta L)_G \right]}$$

is related to the square root of the ratio of two phase to single

phase pressure drop,

$$\phi_G = \left[(\Delta P/\Delta L)_{TP} / (\Delta P/\Delta L)_G \right]^{1/2}$$

or

$$\phi_L = \left[(\Delta P/\Delta L)_{TP} / (\Delta P/\Delta L)_L \right]^{1/2}$$

as discussed earlier in section 2.1.3.

Experimental values of the superficial liquid and gas velocities, V_{SL} and V_{SG}, in two-phase flow with and without twisted tapes, are used to calculate single phase presence drop using Darcy formula and Equations (3.13) and (3.14) for the calculation of the modified friction factor. These pressure drop values are used to determine the parameter X and corresponding to this X value ϕ can be obtained either by the graphs given by Lockhart - Martinelli (23) as discussed earlier or by a polynomial approximation of the curve (111).

A six degree polynomial in X is used to calculate the value of ϕ. The values of constants for four regimes of flow, liquid laminar - gas laminar, liquid turbulent - gas laminar, etc. are given by Hewit-et.al. (111) and are reproduced below :

Coefficients of fitted Polynomial Relations for Lockhart-Martinelli Pressure Drop Correlations

	Turbulent liquid turbulent gas	Laminar liquid turbulent gas	Turbulent liquid laminar gas	Laminar liquid-laminar gas
a_0	1.4450574	1.2386656	1.2502036	9.7950655×10^{-1}
a_1	$4.9572 14 \times 10^{-1}$	5.3137894×10^{-1}	5.5586231×10^{-1}	5.6919828×10^{-1}
a_2	5.7617506×10^{-2}	7.1746540×10^{-2}	6.6838261×10^{-2}	9.5809158×10^{-2}
a_3	$-1.1699323 \times 10^{-3}$	$-4.3863795 \times 10^{-3}$	$-5.1185552 \times 10^{-3}$	$-5.2155316 \times 10^{-3}$
a_4	$-4.2882670 \times 10^{-4}$	$-6.9122899 \times 10^{-4}$	$-5.7824134 \times 10^{-4}$	$-1.4334631 \times 10^{-3}$
a_5	3.1502187×10^{-5}	1.1996845×10^{-5}	1.1641920×10^{-5}	1.0692395×10^{-4}

These constants are used in polynomial expressed as,

$$\ln (\phi) = \sum_{n=0}^{5} \left[a_n \, (\ln \, X)^n \right] \tag{3.18}$$

The flow regimes are discriminated by calculating the Reynolds number using superficial single phase velocities. If Reynolds number is less than 1000, flow is considered as laminar and if it is 1000 or greater than it, flow is considered turbulent. The flow regimes used in the present investigations are liquid laminar-gas turbulent and liquid turbulent-gas turbulent.

3.2 PHYSICAL ABSORPTION

3.2.1 General

Material balance for carbon dioxide transfer can be written as,

moles of carbon dioxide gas absorbed by the liquid =

moles of carbon dioxide gas lost by gaseous mixture

or $\quad Q_L \ (C - C_i) = G_a. \ (Y_i - Y)$ $\qquad$ (3.19)

where $\quad Q_L$ = liquid flow rate, lit/sec.

$\qquad G_a$ = air flow rate, lit/sec.

$\qquad C$ = carbon dioxide concentration in liquid, g mole/lit.

$\qquad Y$ = moles of carbon dioxide per mole of air

and subscript i refers to inlet condition.

For absorption of carbon dioxide in water at very low (carbon dioxide) concentration in liquid, Henry's law is applicable, that is,

$$p = H C^*$$ $\qquad$ (3.20)

where p = partial pressure of carbon dioxide gas in bulk of gas,

$\qquad$ in atm, and is equal to total pressure 'P' multiplied by

$\qquad$ mole fraction of carbon dioxide gas 'y'

H = Henry's law constant, atm. lit/gmole

C^* = concentration of carbon dioxide gas at interface, in

$\qquad$ equilibrium with gas at interface, g. mole/lit.

noting that,

$$Y = \frac{y}{1 - y} \quad \text{and} \quad y = \frac{HC^*}{P}$$ $\qquad$ (3.21)

we can obtain from Equation 3.19 and 3.21

$$\left[Y_i - \frac{Q_L C}{G_a} \right] = \left[\frac{\frac{H}{P} C^*}{1 - \frac{H}{P} C^*} \right]$$
(3.22)

if water free of carbon dioxide is used at the inlet for absorption,

that is $C_i = 0$. The value of C^* can now be obtained in terms of measurable

quantities by rearranging Equation 3.22 in the following form,

$$C^* = \left[\frac{\frac{P}{H} \left(Y_i - \frac{Q_L C}{G_a} \right)}{1 + Y_i - \frac{Q_L C}{G_a}} \right]$$
(3.23)

However, it may be noted that pressure used in above equation

is the point value and varies with distance z, due to the pressure

drop in the test section.

The liquid phase volumetric mass transfer coefficient $'k_L^o a'$

can be calculated by writing the material balance equation for carbon dio-

xide over differential volume of the test section, dV.

$$Q_L \, d \, C = k_L^o \, a \, (C^* - C) \, dV$$
(3.24)

since volumetric liquid flow rate Q_L is essentially constant,

$$\frac{k_L^o a}{Q_L} \, dV = \frac{dC}{(C^* - C)}$$
(3.25)

substituting C^* from Equation 3.23 in Equation 3.25, we get an

rearrangement,

$$\frac{k_L^{\,o}\,a\quad dV}{Q_L} = \frac{dC}{\left[\dfrac{(Y_i - \dfrac{Q_L C}{Ga})}{(1 + Y_i - \dfrac{Q_L C}{Ga})}\quad \dfrac{P}{H} - C\right]} \tag{3.26}$$

equation 3.26 on rearrangement gives

$$(k_L^{\,o}a)_{1-2}\,V_{1-2} = \int_1^2 \frac{(1 + Y_i - \dfrac{Q_L}{Ga}C)\,dC}{(Y_i\dfrac{P}{H} - (1 + Y_i + \dfrac{Q_L P}{GaH})C + \dfrac{Q_L}{P}C^2)} \tag{3.27}$$

where V_{1-2} is volume of test section between point 1 and 2.

Integrand in Equation 3.27 can not be integrated, because no known relationships to express pressure 'P' as a function of carbon dioxide concentration in liquid phase 'C' is available and the Equation 3.27 cannot therefore, be reduced to variable separable form for integration if the variation of pressure P within the test section is significant. Since maximum pressure drop in the test section was much below 10 percent of the pressure in the test section for most of the runs, except for those taken at the high liquid and high gas flow rates with tapes, integration is carried out by taking the average test section pressure P_{av}, for the terms containing P in the denominator of the integrand.

With the assumption of the constancy of pressure P, the integrand of Equation 3.27 reduces to a standard form

$$(k_L{}^o a)_{1-2} \cdot V_{1-2} = \int_1^2 \frac{f + .g\, C}{f' + g' + h'\, C^2} \, dC \qquad (3.28)$$

where

$$f = 1 + Y_i \quad , \qquad g = - \frac{Q_L}{G_a}$$

$$f' = Y_i \, \frac{P_{av}}{H} \quad , \qquad g' = - \left(1 + Y_i + \frac{Q_L \, P_{av}}{G_a \, H} \right)$$

$$h' = \frac{Q_L}{G_a} \qquad\qquad\qquad\qquad\qquad (3.29)$$

on integration we obtain,

$$(k_L{}^o a)_{1-2} V_{1-2} = \left[\left(- \frac{gg'}{2h'} + f \right) \left(\frac{1}{\sqrt{-q}} \right) \ln \left(\frac{2h'C + g' - \sqrt{-q}}{2h'C + g' + \sqrt{-q}} \right) \right.$$

$$\left. + \left(\frac{g}{2 \, h'} \right) \ln (h' + g'C + h' C^2) \right]_{C_1}^{C_2} \qquad (3.30)$$

where $\quad q = (4 f'h' - g'^2) \qquad\qquad\qquad (3.31)$

3.2.2 Simplified Procedure

The general procedure described above may be simplified for cases where the following conditions (113) hold;

(i)   the mean partial pressure of the inert carrier gas remains essentially constant or equal to the total pressure throughout the apparatus,

(ii)   coefficient $k_L{}^o$ a remains constant throughout the apparatus,

(iii)   equilibrium curve is linear, that is, Henry's law is applicable over the range, in which they are to be used.

(iv)   operating line is linear over the range

In view of the above assumptions, Equation 3.26 can now be integrated directly to give,

$$(k_L^o a)_{1-2} = \frac{Q_L}{V_{1-2}} \frac{C_2 - C_1}{(C* - C) \text{ log mean}}$$ (3.32)

where

$$(C* - C) \text{ log mean} = \frac{(C* - C)_2 - (C* - C)_1}{\ln \frac{(C* - C)_2}{(C* - C)_1}}$$ (3.33)

The value of C* for using in the above equation can be calculated from Equation 3.23. Few sample calculations were made covering different operating conditions to calculate the values of volumetric mass transfer coefficients using the Equation 3.30 and simplified Equation 3.32 and it was found that the two values did not differ by $\pm$ 2.0 percent. This difference is very small as compared to other uncertainties in the data and the measurements and, therefore, all values of volumetric liquid phase mass transfer coefficient '$k_L^o a$' are calculated using simplified Equation 3.32 along with equations 3.23 and 3.33.

3.3   CHEMICAL ABSORPTION

3.3.1   Mass Transfer Coefficient

The system consisted of carbondioxide and air as the gas phase and sodiumhydroxide solution as the liquid phase. Overall reaction taking place can be written as (86)

$$CO_2^- + 2\ OH^+ \longrightarrow CO_3^{--} + H_2O \qquad (3.34\ A)$$

$$\text{or} \quad CO_2 + 2\ NaOH \xrightarrow{\ k_2\ } Na_2CO_3 + H_2O$$

$$A + b_2\ B \longrightarrow X + Y \qquad (3.34\ B)$$
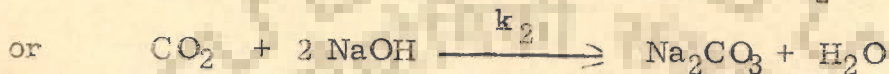
Material balance for carbondioxide over differential volume of test section of cross sectional area A and length dz can be written as

$$-\ \tfrac{1}{2}\ Q_L \cdot dB = k_L a\ (C_s^* - C)\ A\ dz \qquad (3.35)$$

where

$k_L a$ -   volumetric mass transfer coefficient for chemical absorption in solution, sec^{-1}

B   -   sodium hydroxide concentration in solution   g mole/lit

Q_L -   liquid volumetric flow rate, lit/sec

C^* = p/H_s . equilibrium concentration of carbondioxide in the solution containing sodium hydroxide and sodium carbonate, g mole/lit

p   =   partial pressure of carbon dioxide at interface

H_s -   Henry's law constant for carbon dioxide in the solution.

For instantaneous or very fast chemical reaction in the liquid phase, the carbondioxide concentration in liquid phase can be taken as zero, $C = 0$ and Equation 3.35 can be written as

$$\frac{2\ k_L\ a}{Q_L}\ A\ dz = -\ \frac{dB}{C^*} \qquad \cdot \qquad (3.36)$$

which can be integrated between test section positions 1 and 2 to give

$$(k_L a)_{1-2} = \frac{Q_L}{2\ A\ z}\ \frac{B_1 - B_2}{C^*}\ ; \ \ \text{if}\ C^*\ \text{is constant} \quad (3.37)$$

However, Equation (3.37) is only approximate and can not be used, in general, because C^* can not be considered constant because of its strong dependence on partial pressure of carbondioxide in gas phase, p, and Henry's law constant H_S is also a function of sodiumhydroxide and sodium-carbonate concentrations in solution. The partial pressure of carbondioxide in gas phase changes both due to change in pressure, P, and mole fraction of carbondioxide, y. The mole fraction of carbondioxide in gas phase, y, can be easily expressed as a function of sodiumhydroxide concentration in liquid phase B using the material balance for carbondioxide,

Moles CO_2 absorbed, $G_i\ Y_i - G\ y = \frac{1}{2}\ Q_L\ (B_i - B)$

where $\quad$ G $\quad$ - $\quad$ molar flow rate of gas mixture.

Molar flow rate of gas mixture,

$$G \quad = \quad G_i - \frac{1}{2}\ Q_L\ (B_i - B)$$

Molar flow rate of carbondioxide,

$$G\,y \;=\; G_i\,Y_i \;-\; \tfrac{1}{2}\,Q_L\,(\,B_i \,-\, B\,)$$

Hence the mole fraction of carbondioxide,

$$y \;=\; \frac{G_i\,Y_i \;-\; \tfrac{1}{2}\,Q_L\,(\,B_i \,-\, B\,)}{G_i \;-\; \tfrac{1}{2}\,Q_L\,(\,B_i \,-\, B\,)} \tag{3.38}$$

The pressure P may be expressed easily as a function of z

if a linear variation of the pressure with tube length is assumed,

that is,

$$P \;=\; a' \;-\; bz \tag{3.39}$$

where a' is the pressure at the point from which distance z

is measured and b is the pressure drop per unit length

$(\,\triangle P/\,\triangle L\,)$. This assumption is valid if the hydrodynamic

conditions do not vary significantly with linear position to the

test section.

Using Equations (3.38) and (3.39), we can express C_S^{*}

in measurable quantities

$$C_S^{*} \;=\; \frac{p}{H_S} \;=\; \frac{y\,P}{H_S} \;=\; \frac{G_i\,Y_i - Q_L/2\,(B_i \,-\, B)}{G_i - \dfrac{Q_L}{2}\,(B_i \,-\, B)}\;\frac{a' - bz}{H_S} \tag{3.40}$$

and Equation (3.36) can now be written as,

$$\frac{Q_L}{2}\,dB \;=\; k_L\,a\,A\,dz\,\left(\frac{a' - bz}{H_S}\right)\left(\frac{G_i\,Y_i - Q_L/2\,(B_i \,-\, B)}{G_i - Q_L/2\,(B_i \,-\, B)}\right)$$

or $\dfrac{2\,k_L\,a\,A\,(a' - bz)\,dz}{Q_L} \;=\; \dfrac{H_S\,(\,G_i - Q_L/2\,(B_i \,-\, B)\,)}{G_i\,Y_i - Q_L/2\,(B_i \,-\, B)}\,dB$

$$=\; H_S\,\left(1 + \frac{m_1}{m_2 \,+\, m_3\,B}\right.\;dB \tag{3.41}$$

where constants

$$m_1 = G_i (1 - y_i)$$

$$m_2 = G_i Y_i - \frac{Q_L B_i}{2} \qquad (3.42)$$

and $\qquad m_3 = Q_L / 2$

Theoretically, even at a constant temperature H_s depends on the ionic concentrations of Na^+, OH^- and CO_3^{--} and, therefore, varies with sodiumhydroxide concentration in solution B. If the variation in the value of H_s over the test section due to small changes in sodiumhydroxide and sodiumcarbonate concentrations is not significant, H_s may be assumed constant as H_{sav} and can be evaluated for average concentrations of sodiumhydroxide and sodiumcarbonate between points 1 and 2 using the method described by Danckwerts (115). With the assumption of constancy of H_s, Equation 3.41 on integration gives,

$$\frac{2 k_L a A}{Q_L} \left(a'z - \frac{bz^2}{2} \right) = H_{sav} \left[(B_1 - B_2) + \frac{m_1}{m_3} \ln \frac{m_2 + m_3 B_1}{m_2 + m_3 B_2} \right]$$

$$\therefore k_L a = \frac{Q_L H_{sav}}{2 V \left(a' - \frac{bz}{2} \right)} \left[(B_1 - B_2) + \frac{m_1}{m_2} \ln \right.$$

$$\left. \left(\frac{m_2 + m_3 B_1}{m_2 + m_3 B_2} \right) \right] \qquad (3.43)$$

where

$\qquad V = Az =$ volume of test section between points 1 and 2

$\qquad$ and constants m_1, m_2, m_3 are given by Equation (3.42)

3.3.2 Determination of effective interfacial area, a

The method described in section 3.3.1 gives the value of volumetric liquid phase mass transfer coefficient with chemical reaction, $k_L a$. If the value of k_L, that is, the rate of absorption with chemical reaction can be found theoretically or by calculations the determination of the value of interfacial area can be done as follows :

$$a = \frac{(k_L a)_{experimental}}{(k_L)_{calculated}} \qquad (3.44)$$

Reaction between dissolved carbondioxide A and sodium-hydroxide in solution B may be written as

$$A + z B = p P \qquad (3.45)$$

and since dissolved carbondioxide undergoes a second-order irreversible reaction with dissolved sodiumhydroxide, the rate expression is $r = k_2 AB$ and the variation in time and space of the species A and B is givenby

$$D_A \frac{\delta^2 A}{\delta x^2} = \frac{\delta A}{\delta t} + k_2 AB \qquad (3.46A)$$

$$D_B \frac{\delta^2 B}{\delta x^2} = \frac{\delta B}{\delta t} + z k_2 AB \qquad (3.46 B)$$

where

D_A and D_B are diffusivities of species A and B respectively

k_2 is second order irreversible reaction rate constant

z   is number of moles of reactant B consumed by one

mole of dissolved gas A due to chemical reaction

Equation (3.46)

A   concentration of dissolved gas in liquid phase

B   concentration of reactant B in liquid phase

Analytical and numerical solutions of the above equations

have been discussed by Danckwerts (86) and by Astarita (65).

The effective interfacial area, a, can be calculated in many ways

depending upon the system chosen. Some of the solutions and

methods of estimation of interfacial area are discussed as under.

Analytical, solutions of the differential equations given

by Equation 3.46 A and 3.46 B, is possible under the limited

conditions only, a) for the case of a pseudo-first-order reaction

and/or b) an infinitely fast (instantaneous) irreversible second

order reaction.

i) Danckwerts Method for pseudo first order reaction

Danckwerts (116) presented solution for the pseudo first

order reaction and he obtains the following expression

$$I \equiv \frac{k_L a}{k_L^o a} = \frac{1}{2} e^{\gamma} + \frac{\sqrt{\pi}}{\sqrt{2}} \left(\frac{1}{2} + \gamma \right) \frac{erf \sqrt{\gamma}}{\sqrt{\gamma}} \qquad (3.47)$$

where

I   =   Enhancement factor

γ = $k_2 B_o \theta$

θ =   contact time of fluid element with gas phase.

By carrying out experiments under similar hydrodynamic conditions enhancement factor, I, can be calculated. Knowing the value of I, the value of Υ can be calculated from Equation (3.47). From the value of Υ and the known values of the rate constant k_2 and concentration of B_0 permits the evaluation of θ to be possible. Also, since the penetration theory predicts that

$$k_L^{\,o} = 2 \sqrt{ \left(\frac{\Lambda\, D_A}{\theta} \right) } \qquad (3.48)$$

the individual liquid film mass transfer coefficient, $k_L^{\,o}$ may be calculated and the interfacial area, a, may be evaluated from the relation

$$a = \frac{k_L^{\,o} a}{k_L^{\,o}} = \frac{k_L^{\,o} a}{2 \sqrt{ \left(\frac{\Lambda\, D_A}{\theta} \right) }} \qquad (3.49)$$

where the value of $k_L^{\,o} a$ is obtained from the physical absorption studies.

ii) <u>Method for instantaneous irreversible second order reaction</u>

For the case of an instantaneous irreversible second order reaction, Danckwerts (117) presented a solution for the asymptotic value of I, that is, I_i, for large values of the parameter, $\sqrt{M}$ defined as

$$\sqrt{M} = \sqrt{ \frac{k_2\, B_0\, D_A}{k_L^{\,o}} } \qquad (3.50)$$

which is expressed as the parametric equation

$$I_i = \frac{1}{erf(\sigma)} \qquad (3.51)$$

and $\mathrm{e\,r\,f}\,(\,\delta\,)$ is obtained from

$$q\sqrt{r} = \frac{1 - \mathrm{e\,r\,f}\,(\delta\sqrt{\sqrt{r}})}{\mathrm{erf}\,(\delta)\,\exp\left[\delta^2\left(1 - \frac{1}{r}\right)\right]} \tag{3.52}$$

where

$$q \quad = \quad B_0 / z\,A_i$$

$$r \quad = \quad D_B / D_A$$

$$A_i \quad = \quad \text{concentration of dissolved gas A at}$$

interface in equilibrium with gas at

interface. It is equal to the solubility of

gas when pure A is absorbed.

However, the approximate values of I_i can be calculated using

the penetration - theory solution

$$I_i = 1 + q \quad ; \quad r = 1 \tag{3.53}$$

and $\quad I_i \simeq \dfrac{1}{\sqrt{r}} + q\sqrt{r} \quad ; \quad r \neq 1 \tag{3.54}$

The Equation (3.54) is applicable provided the value of I_i is

much greater than unity. Knowing the value of q and r the

value of I_i can thus be obtained. However q can be calculated

only if A_i is known.

Perry and Pigford (118) have presented a limited number

of numerical solutions for a second order irreversible reaction

of finite speed for $r = 1$ only. Comparison of their results

with the approximate expression proposed by Van Krevelen and

Hoftizer (119), based on the film theory, that is

$$I = \frac{\sqrt{M}\,\sqrt{\left(1 - \dfrac{I - 1}{rq}\right)}}{\tanh\left[\sqrt{M}\,\sqrt{\left(1 - \dfrac{I - 1}{rq}\right)}\right]} \tag{3.55}$$

leads to the approximate expression for the penetration theory
as given below

$$I = \frac{\sqrt{M}\sqrt{(1 - \frac{I - 1}{I_i - 1})}}{\tanh\left[\sqrt{M}\sqrt{(1 - \frac{I - 1}{I_i - 1})}\right]} \tag{3.56}$$

The value of I_i is obtained from Equation (3.51) and (3.52) for
the appropriate values of r and q. From a measured value
of I from physical and chemical absorption experiments under
similar hydrodynamic conditions, the value of $\sqrt{M}$ can be
calculated from Equation (3.56). Knowing the values of $\sqrt{M}$,
k_2, B_o, and D_A one obtains

$$k_L^o = \frac{\sqrt{k_2\ B_o\ D_A}}{M} \tag{3.57}$$

Brian et al (120) have extended the work of Perry
and Pigford (118) for values of r other than unity and a wide
range of I. They have presented corrections to be applied to
the results obtained from Equation (3.56) to obtain a more
accurate solution.

Porter (121) has presented the following expression to
approximate the numerical solutions of Brian et. al.

$$\frac{I - 1}{I_i - 1} = 1 - \exp\left(\frac{\sqrt{M} - 1}{I_i - 1}\right) \tag{3.58}$$

valid only for $\sqrt{M}$ greater than 2.0 and $r = 1.0$ and this
equation can be rearranged to give

$$\sqrt{M} = 1 - (I_i - 1)\ln\left(\frac{I_i - I}{I_i - 1}\right) \tag{3.59}$$

Knowing the values of k_2, B_0, D_A and $\sqrt{M}$, $k_L^{\,0}$ can be calculated from Equation (3.50). The interfacial area, a can now be obtained from this value of $k_L^{\,0}$ and the value of $(k_L^{\,0}\,a)$ obtained from physical absorption experiments.

$$a \quad = \quad \frac{(k_L^{\,0}\,a)_{exp}}{k_L^{\,0}} \qquad (3.60)$$

iii) <u>Method for fast-pseudo-first order reaction</u>

Further simplification of Equation (3.56) is possible if the concentration of dissolved gas in liquid is zero or B_0 value is very large and reaction is fast or $k_L^{\,0}$ is very low the reaction is in pseudo first order regime meeting the conditions (122)

$$3 \quad < \quad \sqrt{M} \quad < \quad \tfrac{1}{2}\,I_i \qquad (3.61)$$

and Equation (3.56) can be approximated by

$$I \quad = \quad \sqrt{M} \qquad (3.62)$$

with good accuracy (error less than 10 percent)

Since $\quad I \quad = \quad k_L / k_L^{\,0}$ and $\sqrt{M} = \dfrac{\sqrt{D_A\,k_2\,B_0}}{k_L^{\,0}}$

Equation (3.62) gives

$$k_L \quad = \quad \sqrt{D_A\,k_2\,B_0} \qquad (3.62)$$

Interfacial area, a, is now calculated from this value of k_L and the measured value of $k_L a$ obtained from the chemical absorption experiments -

$$a \quad = \quad \frac{(k_L a)_{exp}}{\sqrt{(D_A\,k_2\,B_0)}} \qquad (3.63)$$

Therefore evaluation of effective interfacial area can be made provided conditions of Equation (3.61) are satisfied and diffusivity of gas A in the solution used for chemical absorption, D_A, second order reaction rate constant, k_2, and concentration of the reactant in solution, B_o, are known and also when ratio D_B/D_A is close to unity.

This method of calculating the interfacial area is considered superior to those discussed earlier for the obvious reason that the area can be calculated from the chemical absorption experiments alone and hence the inaccuracies of physical absorption experiments do not effect the values of the area. In the present study ratio, D_B/D_A, varies from 1.66 to 1.70 and concentration of sodium hydroxide, B_o, was so chosen that the conditions of Equation (3.61) are always satisfied. The value of D_B/D_A is close to unity and it may be further noted that for $\sqrt{M}$ greater than 5 these values of diffusivity ratio are not likely to effect the accuracy.

The advantage of working in the fast pseudo first order reaction conditions is that the volumetric absorption rate with chemical reaction, $k_L a$, is independent of the liquid film coefficient, k_L^o and hydrodynamically depends solely upon the specific interfacial area. Also when a pseudo first order reaction occurs, $k_L a$, is independent of both constant time and concentration of carbondioxide.

This advantage is responsible for choosing this regime for a number of studies (123) in the field of agitated, packed, and two phase flow mass transfer investigations. Carbondioxide in gas phase and sodiumhydroxide in the liquid phase, system was selected because this is extensively studied and most of the physico-chemical data required for calculating the relevant parameters is available. This system is also useful to chemical industry. Furthermore, with this system it is easy to meet the criteria required to satisfy pseudo first order reaction conditions. The evaluation of physico-chemical data required to calculate, a, for this system is given in the next section.

3.4 PHYSICO-CHEMICAL DATA REQUIRED FOR CHEMICAL MASS TRANSFER CALCULATIONS

3.4.1 Diffusivity D_A :

It is the diffusivity of carbondioxide in the sodium hydroxide solution and depends upon the concentration of sodium hydroxide and temperature of the solution. Correlation used by Wales (95) when altered for units becomes,

$$D_A = 4.736 \times 10^{-7} \times T - 1.2189 \times 10^{-4} - 0.2693 \times 10^{-5} \times N \quad - (3.64)$$

where

D_A - diffusivity in Square cm / sec.

T - temperature in degrees centigrade

N - normality of sodium hydroxide in solution.

3.4.2 Reaction rate constant k_2

Correlation given by Pinsent et. al. (124) and modified by Porter (125) is given as

$$\ln k_2 = 13.635 - \frac{2895.0}{T} + 0.132 N \qquad (3.65)$$

where

k_2 — is in lit / g mole. sec.

T — temperature ^{o}K

N — sodium hydroxide normality in solution

3.4.3 Henry's law constant in solution H_S

It is calculated knowing solution temperature and average concentrations of sodiumhydroxide and sodiumcarbonate between points 1 and 2 by the method described by Danckwerts (115)

$$\log_{10} (H_S / H_W) = \sum (h . G) \qquad (3.66)$$

where H_W is the value of Henry's law constant for carbon dioxide given by the following expression (123)

$$\log_{10} (1 / H_W) = 1140 / T - 5.30 \qquad (3.67)$$

T is temperature in ^{o}K

H_W is in lit. atm / g. mole

G — is the ionic strength of the solution

h — is contribution due to species of positive and negative ions present and species of gas.

$$h_1 = h_{Na} + h_{OH} + h_{CO_2}$$

$$h_2 = h_{Na} + h_{CO_3} + h_{CO_2}$$

$$\text{and} \quad h = h_1 + h_2$$

where h_{CO_2} is a function of solution temperature. Using the values of h_{CO_2} (115) in the temperature range from $15\,^{\circ}C$ to $40\,^{\circ}C$ following expression is developed which could predict h_{CO_2} values within 2 percent of error

$$h_{CO_2} = -1.3417 + 8.44 \times 10^{-3} \times T - 1.3 \times 10^{-5} T^2 \qquad (3.68)$$

where   T   is   in degrees centigrade

so $h_1 = h_{NaOH} = 0.157 + h_{CO_2}$

$h_2 = h_{Na_2CO_3} = 0.112 + h_{CO_2}$

and   term $\sum hG = h_1 N_1 + 6 h_2 N_2$ \qquad (3.69)

where N_1 and N_2 are average normalities of sodium hydroxide and sodiumcarbonate in the solution.

Thus all the physicochemical parameters can be estimated from the solution temperature and concentration of sodiumhydroxide and sodiumcarbonate.

CHAPTER 4

4.1   EXPERIMENTAL SET UP

4.1.1   General

Experiments carried out in the present investigation are divided into three headings :

(i)   Pressure drop measurements

(ii)   Physical absorption

(iii)   Chemical absorption

In all these experiments the experimental set up basically consisted of the following assembly: for the supply of liquid feed at constant flow rate, air supply at constant pressure and flow rate, assembly for carbon dioxide supply at constant pressure and flow rate, arrangement for withdrawing samples at suitable points, sample collection devices, sample analysing instruments and liquid collection and recirculation system. A general discussion of the experimental set up is given in the following sections.

4.1.2   Flow diagram of the experimental set up

An experimental jig was constructed in which all the experiments could be performed with minor alterations. A schematic flow diagram of the jig is given in Fig. 4.1.

The test section was made of perspex tube of 13.5 mm internal diameter and 18.5 mm outside diameter and 5.4 meter in length. It was constructed by three 1.8 meter long sections joined by 75 mm diameter

PHOTO. 1   THE TEST STAND

75

20

1.5

5

23

18.5

18

Front View

25

34

End View

10

22

0.75 Thick

22

12

13.45

70

All dimensions in mm

Tape and Tee

77
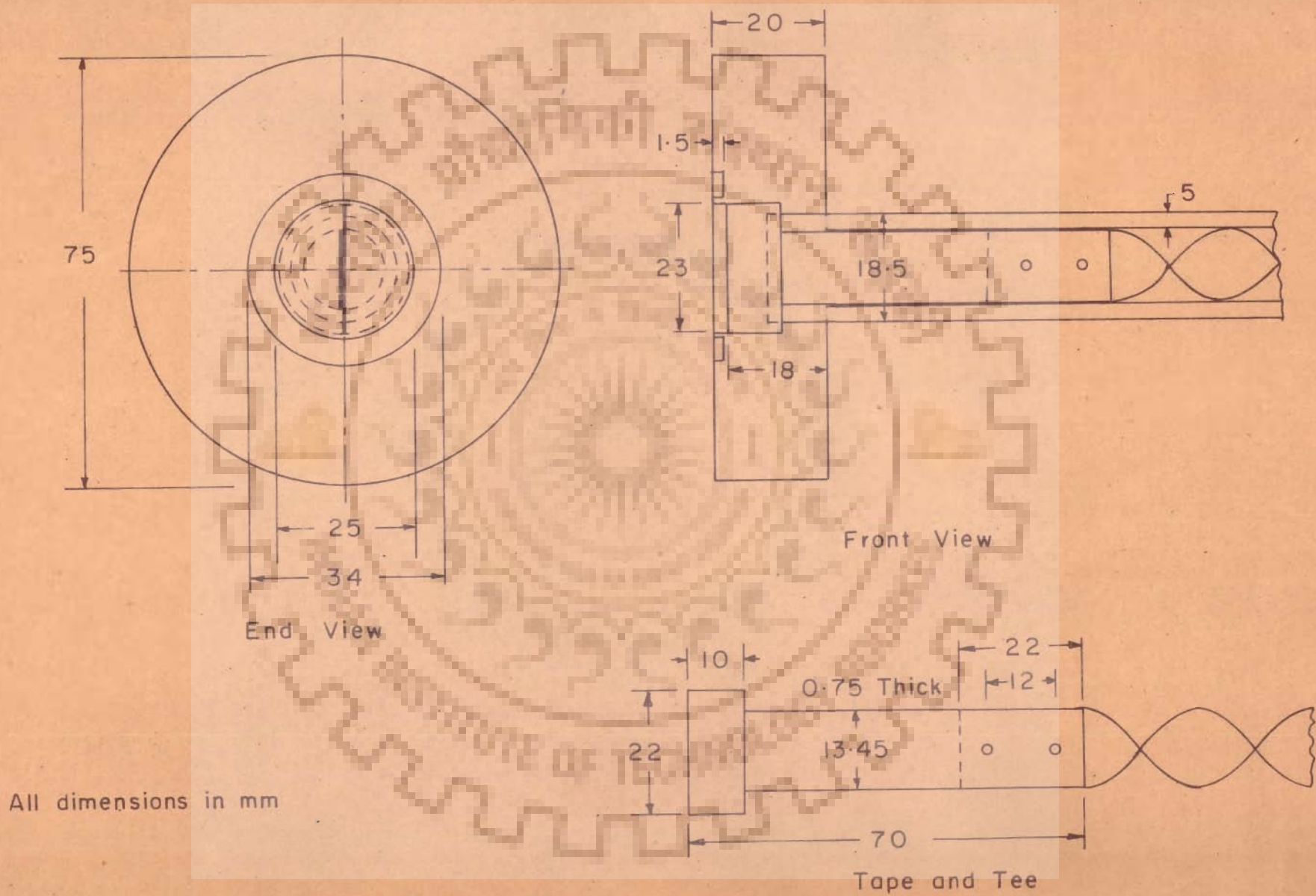
Fig. 4·2 End flange and tape holder

PT - Pressure Tap
ST - Sample Tap
TC - Thermocouple

PT 1   PT 2   PT 3   PT 4

|←550→|←——1152——→|←—635—→|←——1220——→|

TC 1 |←—1106—→|←————1305————→|←——1255——→| TC 2

ST 1 |←————2500————→| ST 2   ST
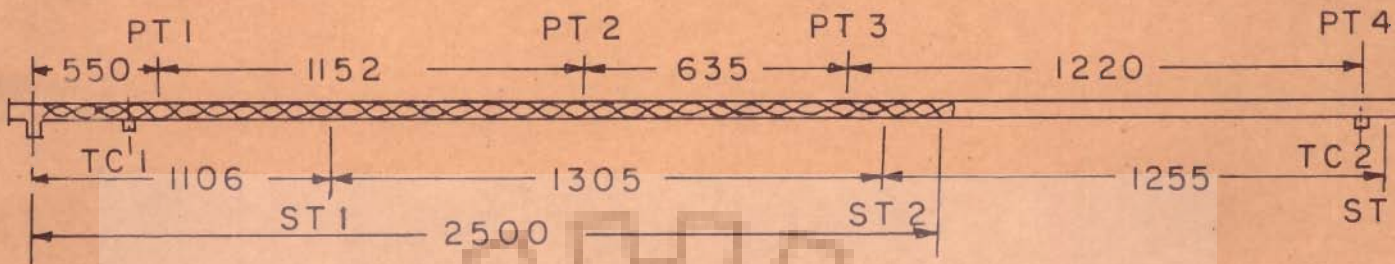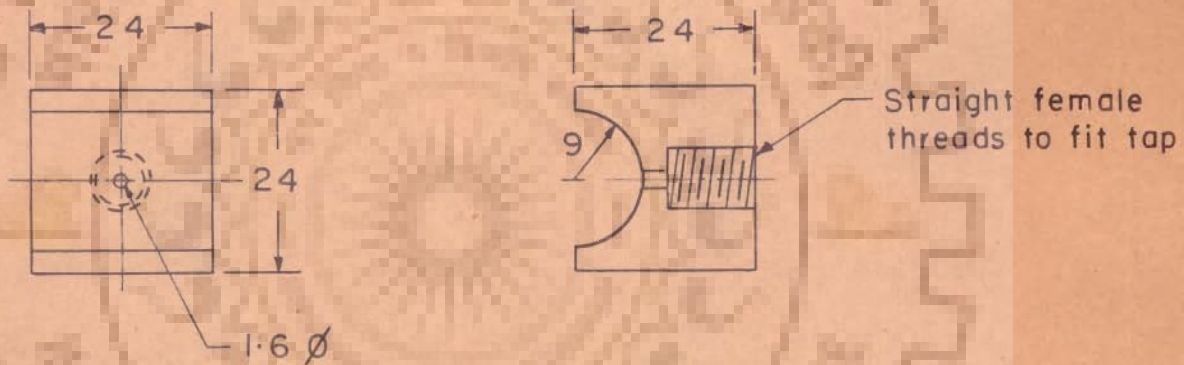
(a) Test Section

(b) Perspex connector for pressure tap

— 24 —

— 24 —

1·6 Ø

24

9

Straight female
threads to fit tap

— 22 —

— 26 —

1·6 Ø

22

9   2

7   4

9

To fit two way
luer lock
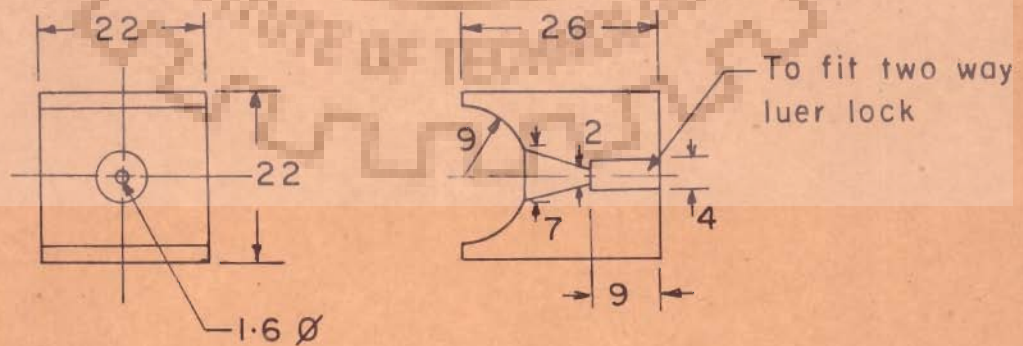
(c) Perspex connector for sample tap

All dimensions in mm

Fig. 4·3 Details of test section

PHOTO. 2   CONTROL PANELS AT INLET SECTION

79
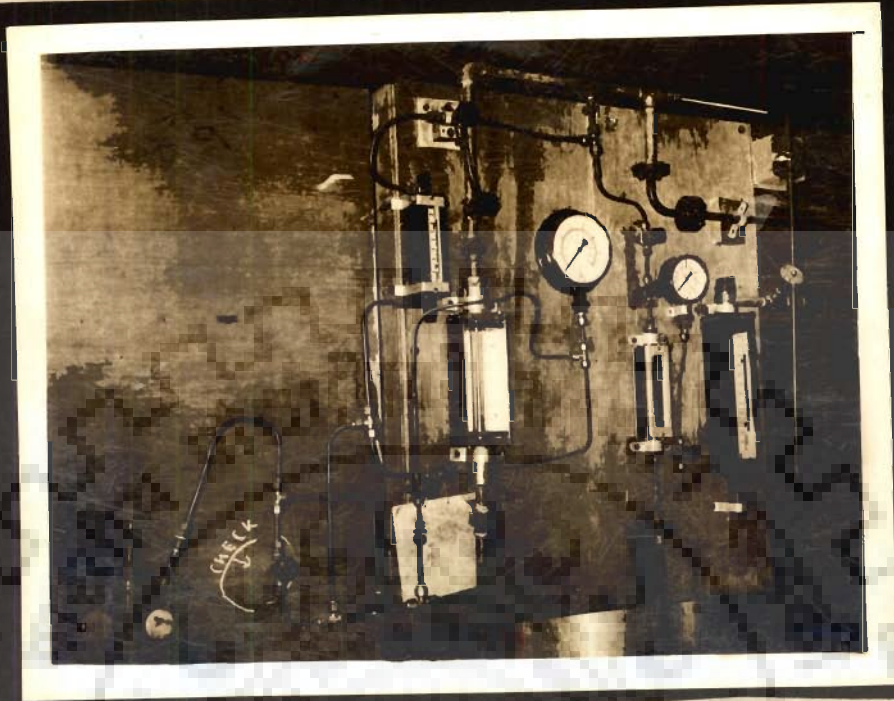
PHOTO. 3   GAS-LIQUID SEPARATOR AND EXIT SECTION
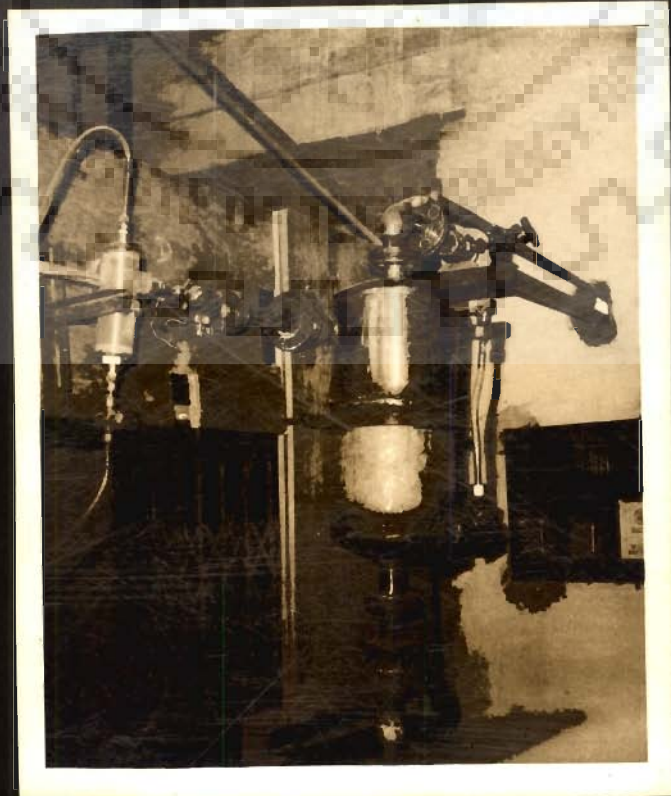
PHOTO. 4   TWISTED TAPE INSERTS
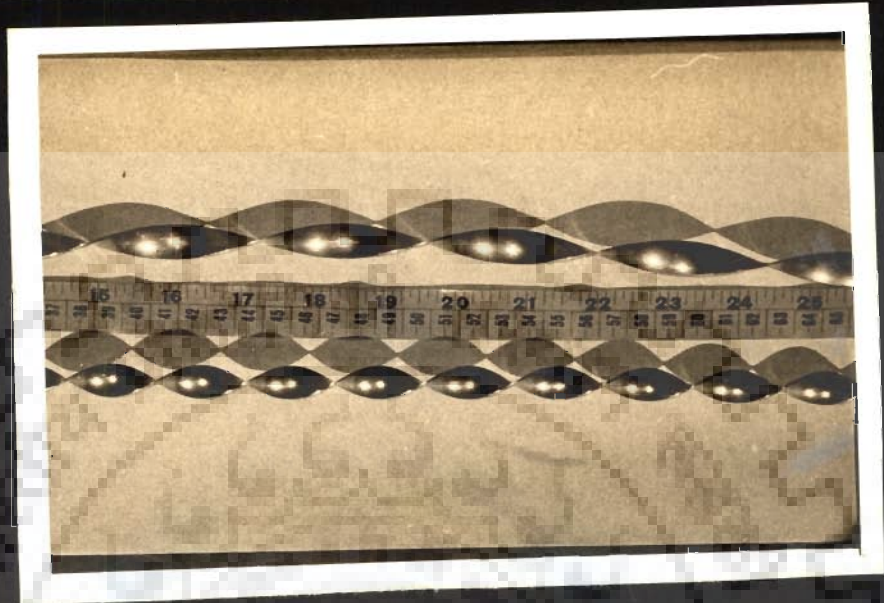
FIG. 4.4   TWISTED TAPE INSERTS
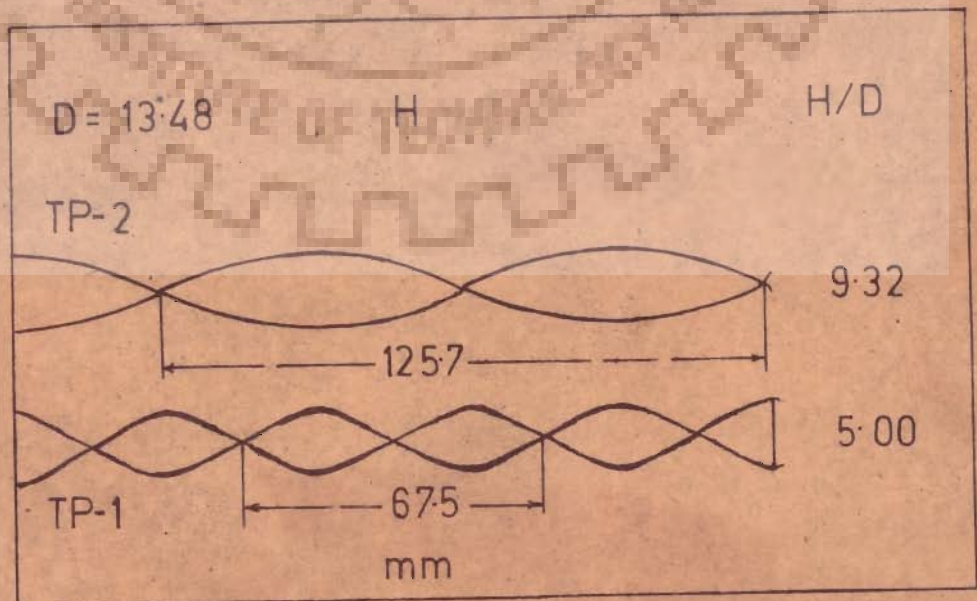
12.5 mm thick perspex end flanges (see Fig. 4.2) with grooves cut

for 25 mm x 30 mm and 3 mm cross sectional diameter teflon

O-ring to make leak proof connections by using four 6 mm diameter

50 mm long bolts with nuts. Compressed air was passed through a

humidifier H and a heat exchanger HE before measuring its flow rate

by means of rotameter R1 (for low flow rates) and R2 (for high flow

rates).

Carbon dioxide obtained from a gas cylinder RV2 at desired

pressure by a double stage static pressure regulator PR2 and its

flow rate was controlled by valves G12, G13. The flow rate of carbon

dioxide was measured by rotameter R3. The rotameters were

calibrated precisely at 35 psia, sufficient to overcome the pressure

drop with twisted tape of smallest pitch ratio 'y' and at the highest

liquid and gas flow rates.

Liquid was pumped from a stainless steel storage tank RV3,

its flow was controlled by valve G20 and measured by the rotameter R4.

The liquid coming from the rotameter R4 was fed at the lower arm of

the gas liquid mixter tee MT. The liquid line with fittings from the

pump P2 to the mixer tee MT was constructed from poly vinyl

chloride (PVC) to prevent the corrosion by caustic solution.

Gas and liquid were introduced in the test-section through

a mixer, which consisted of a perspex tee connector with end flanges

in which gas entered axially as shown in Fig. 4.1. A calming section

0.83 meter long was provided for the gas to eliminate the entrance

effects of the gas mixture before mixing it with liquid in the tee connector

and further length of 1.10 meter was provided for the gas liquid mixture to fully develop the two-phase flow pattern (109) before withdrawing the first sample at sampling tap ST 1.

Three sampling (ST) and four pressure taps (LT) were provided in the test section (see Fig. 4.3). The test section pressure was measured by a pressure gauge PG3. The pressure drop was measured by one meter long manometer M. Mercury was used as manometer fluid. All the pressure tappings were connected to the liquid traps LT1, LT2 and LT3 so as to separate the entrained liquid and to keep only the gas in contact with the manometer fluid.

The exit section (photo 3) consisted of a stainless steel cyclone separator SE to separate the gas and the liquid. The liquid was discharged at the bottom of the separator. It could be either collected in a tank RV4 for recirculation or sent directly into a drain. The test section pressure was controlled by means of three valves G28, G29 and G30 fitted in the gas exhaust line from the separator.

Samples were collected by using syringes of 5 ml capacity which could be attached to the sampling taps ST1, ST2 and ST3 located at various points in the test section, with the help of Luer-lock connector. In order to avoid gas entering the liquid sample collector, a specially manually operated syringe holder was used which permitted a slow and steady withdrawal of liquid by controlled movement of the syringe plunger.

4.1.3 Air Compressor (C)

A single stage reciprocating compressor driven by a 2 H.P. motor and supplied by M/s. Anand Industries Corporation, Kanpur (India) was used for the supply of air. The specifications of the compressor are COMAIR brand, Model SOH 1, No. V600, displacement 9 cubic feet per minute at standard temperature and pressure. The compressor could supply air at a maximum pressure of 300 psig but for the present experiments the cut-off of the compressor was set at 100 psig.

4.1.4 Pressure Regulator (PR1)

The pressure of the air from the compressor was further regulated by a pressure regulator. The regulator was supplied by Shavo Norgren (India) Pvt. Ltd., Bombay. The specifications are 'NORGREN' air pressure regulator type RO2, size 1/2 inch B.S.P.T. with pressure gauge (range 0 to 30 psig or 0 to 2.1 kg/cm^2). For any inlet pressure, the outlet pressure could be adjusted by valve GO and a knob provided on the pressure regulator PR1. The regulator outlet pressure was kept at 25 psig for all the experiments.

4.1.5 Air Humidifier (H)

Consisted of a packed column 75 mm in diameter and 1.10 meter long packed with porcelain raschig rings of 12.5 mm size. Water was sprayed on top of the packings by the pump P1 and the water rate in the humidifier was controlled by valves G3 and G4. The water level in the humidifier was controlled by valve G2 to prevent flooding.

4.1.6   Water Pump (P1)

British Engineers Self Priming Centrifugal Pump, BE No. 115744, Model AO 1210K, capacity 490 gallon per hour, Head 30 to 50 feet drived by GEE Motor, Model B.E.E. No. 6611121, 0.5 H.P., 1425 RPM Single Phase, 230V, AC, 5.9 Amp. The pump assembly was manufactured and supplied by General Electric Works, Calcutta.

4.1.7   Air Heat Exchanger (HE)

Mild steel concentric tube heat exchanger 1.9 meter long having 12.5 mm internal diameter inner tube and 38 mm internal diameter outer tube was used to preheat or precool, if necessary. Condensing steam was used in the annulus as heating medium or cold water could be circulated in the annulus for cooling requirement.

4.1.8   Stainless Steel Feed Pump (P2)

Beresford Self Priming Centrifugal Pump, Type B-2, No.2881, 0.5 H.P. Head 20 psig, Capacity 110 gallon per hour complete with an electric motor of 220 V, single phase AC, was supplied by Modi Industries, Bombay.

4.1.9   Feed Tank Stirrer (S)

G.D. Industrial Stirrer, Remi Kilburn Motor of 0.25 H.P., 220 V. AC with stainless steel 1 inch diameter shaft of 5 feet length and fitted with 8 inches diameter propeller. It had three step pulley to change the stirrer speeds and was supplied by Gordhan Das Desai (P) Ltd., New Delhi.

4.1.10   Gas Rotameter

Two rotameters were used in parallel to cover the entire air flow range upto 5000 liters per hour at N.T.P. and one rotameter was used to measure the carbon dioxide flow rate up to 1000 liters per hour at N.T.P.

4.1.10.1 Rotameter (R1)

For low air flow rates, 1E make rotameter fitted with Brooks glass tube size 6-12-2, Model 652M, No. 2738 was used. Graduations were started from 250 to 4000 with least count of 50. It was supplied by the Blue Star Co., Hyderabad.

4.1.10.2 Rotameter (R2)

For higher air flow rates, RI make rotameter of 1 inch glass tube and tapered S.S. rod having graduations from 750 to 7500 with least count of 50 was used. It was manufactured and supplied by Rota Instrumentation Ltd., Calcutta.

4.1.10.3 Rotameter (R3)

For carbon dioxide IE make rotameter fitted with Brooks tube size 6-15-2, Model 6G2 MV No. 4298 was used. Graduations started from 140 to 1400 with least count of 100. It was manufactured and supplied by the Blue Star Co., Hyderabad.

4.1.11   Liquid Rotameter (R4)

For liquid flow rates, IE make rotameter fitted with Brooks glass tube size R-SM-25-4 BR 1/2-35 G10 Model 84 S14 M No. 1441 having graduation from 1000 to 12000 and a least count of 100 was used.

It was manufactured and supplied by the Blue Star Co., Hyderabad. It was used for all the liquid feeds and for each feed it was calibrated separately.

4.1.12 Pressure Regulator (PR2)

Carbon dioxide cylinders were used for the supply of gas. The outlet pressure of CO_2 was controlled by a two stage pressure regulator. The pressure regulator, GLOOR make, made in Switzerland with two dials one for cylinder pressure 0 to 300 kg/cm^2 and another for outlet pressure 0 to 12 kg/cm^2, was supplied by Indian Engineers, New Delhi. Another similar pressure regulator (not shown in the figure) was used to control the nitrogen gas flow rates, required for analysis and flushing the sample collection bottles.

4.1.13 Pressure Gauge (PG1)

Air rotameters were calibrated at a pressure of 35 psig. A dial type pressure gauge, "FAIR" Model, No. 4052, having calibrations from 0 to 50 psig or 0 to 4 kg/cm^2 was used to measure the air pressure.

4.1.14 Pressure Gauge (PG2)

Carbon dioxide rotameter was also calibrated at a pressure of 35 psig. A dial type pressure gauge, 'PREGA' model, having calibrations from 0 to 50 psig or 0 to 4 kg/cm^2 was used to measure carbon dioxide pressure. It was manufactured and supplied by Precision Industries (India), Delhi.

4.1.15 Pressure Gauge (PG3)

Test section pressure was kept at a constant value of 20 psia for all the runs. The pressure was noted by a dial type 'PREGA' Model pressure gauge, having calibrations from 0 to 30 psig or 0 to 2.3 kg/cm^2. It was manufactured and supplied by Precision Industries (India), Delhi.

4.1.16 Sampling Taps (ST1, ST2, ST3)

Two way stainless steel Luer locks, made in U.S.A., were fixed to the test section with the help of perspex glue for withdrawing liquid samples. The syringe could be attached and stop cock opened when desired.

4.1.17 Liquid Traps (LT1, LT2, LT3)

Liquid traps were made from 50 mm internal diameter 125 mm long perspex tube with a drain valve provided in the bottom to remove the accumulated liquid.

4.1.18 Manometer (M)

Test section pressure drop was measured by a mercury U-tube manometer with 1 meter long arms. Half of the length was filled with mercury.

4.1.19 Gas-Liquid Separator (SE)

A stainless steel cyclone separator, 230 mm diameter and 500 mm long was used. It had a tangential entry and a glass, liquid level indicator with flange connections at the top and the bottom for withdrawal of gas and liquid respectively.

4.1.20   Reservoirs or Storage Tanks

200 litre capacity stainless steel open top cylindrical tanks with lids were used as liquid feed tank (RV3) and liquid discharge collection tank (RV4) and a 200 litre capacity mild steel tank (RV1) was used for water storage, to feed the humidifier. RV2 is a standard carbon dioxide cylinder used for storage and supply of the gas.

4.1.21   Connecting Lines

CL1 - connecting lines used for air from humidifier H upto the valves G6 and G7 consisted of 3/4 inch internal diameter and from valves G6 and G7 to gas mixing tee GT consisted of 1/2 inch internal diameter standard GI pipes.

CL2 - connecting lines used for carbon dioxide from the pressure regulator PR2 upto gas mixing tee GT consisted of flexible copper tubing 1/4 inch internal diameter joined by means of flared and ferrule type brass fittings and brass valves G12, G13, G14, G15 and G16.

CL3 - connecting lines used for liquid inlet consisted of 1/2 inch internal diameter hard PVC piping. It connected outlet of the pump P2 to the gas-liquid mixer tee MT. PVC control valuves G16 and G19 were connected with the help of PVC flanges similar to the flange shown in Fig. 4.2.

CL4 - lines consisted of thick walled flexible transparent polythene tubings of 3/8 inch internal diameter, and were used to connect outlet points of liquid traps LT1 and LT3 to the manometer M and LT2 to

the pressure gauge PG3.

CL5 - lines consisted of copper tubing or fittings as similar to CL2 lines and these connected pressure taps to li quid separation.

4.1.22   Twisted Tape Inserts

Stainless steel sheet 2.5 meters long, 2 meter wide and 0.75 mm thickness was used to cut straight strips 2.5 meters long and 12.5 mm wide. These strips were twisted on a long lathe machine by turning slowly, first from one side and then from the other to get uniform twists. After the twists of desired pitch are obtained, twisted tapes are held tight in the lathe for 24 hours to make the twists stable. Twisted tapes with two pitch ratio 'y' of 5.00 and 9.32 were prepared and were used separately during the experiments.

Tape was held in the test section by rivetting one end to a stainless steel strip of T shape. A groove was cut at the tube edge to hold the Tee strip in position as shown in the Fig. 4.2. The schematic diagram of the twisted tapes used in the experimental work is given in Fig. 4.4 and also shown in photo 4.

4.2   AUXILIARY EQUIPMENT

Besides equipment shown in the experimental set up following auxiliary items were also used during experimentation.

4.2.1   Water Deionizing Plant

Standard demineralizer Model No. AG-200 'O' having normal flow rate 150 lit/hr. and a maximum flow rate 500 lit/hr. was used.

Its capacity was 2600 litres of water per charge with conductivity less than 20 micromhoms at 20°C. Demineralizer was manufactured and supplied by Industrial & Agricultural Engineering Co. Pvt. Ltd., Bombay.

4.2.2   Titration Setup

An Electron Ray Karlfischer's 'THERMONIC' model, potentiometric Titration Equipment was used. It was manufactured by Campbell Electronics and was supplied by Zal-Tex Corporation, Bombay.

The upper part of the cabinet incorporates a Magnetic Stirrer, with a speed regulator, a switch and an Electron Ray Tube. The cabinet is a twin mild steel size 15 inch length x 13-1/4 inch width x 12-1/2 inch height.

The lower part of the cabinet is equipped with a specially designed electronic circuit, in which the amplified potential difference originating between the electrodes in solution interface are transmitted to an Electron-Ray Indicator, which indicates End - Point instantaneously by change in size of Shadow-Angle. Sensitivity control, Ray-Position and Polarizing Switch, are provided on the front panel.

4.2.3   pH Meter

Model CL 41, Toshniwal make pH meter with a glass, combined electrode No. CL 41.05 was used. It had a range from 0 to 14 pH and was supplied by M/s. Toshniwal Brothers Pvt. Ltd., Delhi.

4.2.4   Single Pan Balance

'OWA LABOR' model, type Nr. 707.04 with a range of 0.0001 to 200.0 gm, manufactured by VEB Wagetchnic Rapido Werk, Oschatz, East Germany, and supplied by M/s. K.L. Bhakri, New Delhi was used.

4.2.5   Platform Balance

'AVERY' model balance having a maximum weighing capacity of 1000.0 kg with a least count of 50 gram was used.

4.2.6   Barometer

A 'Fortins Barometer' with a range of 685 to 855 mm Hg and least count of 0.01 mm Hg was used to measure atmospheric pressure.

4.2.7   Stop Watch

'ROCAR' make, antimagnetic, made in Switzerland, having a range 0.1s to 15 minute with a least count of 0.1s was used.

4.2.8   Potentiometer

A portable potentiometer Cat No. PL 52, manufactured and supplied by Toshniwal Brothers, Pvt. Ltd., New Delhi, having range of 0 to 1.8 V and least count of 0.01 mV was used.

4.2.9   Thermocouple Wire

24 gauge Iron Constantan thermocouple was used to measure liquid temperature in the test section.

4.2.10   Viscometer

Oswald type, standard 4-tube glass viscometer No. O was used to measure the viscosity of water and solutions.

4.2.11   Thermometer

Mercury in glass thermometer, made in Germany, having a range of -10° to $110^\circ C$ with a least count of $0.1^\circ C$, was used to measure gas temperature.

4.2.12   Dry Gas Meters

Two gas meters were used for the calibration of gas rotameters. Their specifications are:

4.2.12.1 Dry Gas Meter I

Make UGI (Meters) Ltd., London

Graduations: 1 cu.ft. per revolution.

Capacity: 200 cu.ft. per hour.

4.2.12.2 Dry Gas Meter II

Make UGI (Meters) Ltd., London

Graduations: 2 cu.ft. per revolution.

Capacity: 400 cu.ft. per hour.

4.3   MATERIALS USED

Following chemicals were used for making the solutions for experimental work and analysis:

4.3.1   Hydrochloric Acid

BDH Analytical Reagent Grade was used for analysis and Commercial Grade was used for charging in the demineralizer for regeneration of the resin.

4.3.2   Oxalic Acid

Guaranteed Reagent Grade made by Sarabhai Merk Co., Baroda, was used for analysis.

4.3.3 Sodium Hydroxide

Lab. Reagent, B.P. Grade made by Sarabhai Merk Co., Baroda, was used for experiments and analysis.

4.3.4 Barium Chloride

BDH Lab. Reagent Grade was used for analysis.

4.3.5 Nitrogen Gas

Purified Grade from Modi Gas Co., Modinagar, was used for nitrogen blanket during analysis.

4.3.6 Carbon Dioxide Gas

It was supplied by Modi Distillery, Modinagar.

4.4 EXPERIMENTAL PROCEDURE

For the convenience of presentation this section is divided into the following subsections:

4.4.1 Rotameter calibrations

4.4.2 Thermocouple performance

4.4.3 Pressure drop measurements

4.4.4 Physical absorption or mass transfer without chemical reaction studies

4.4.5 Chemical absorption or mass transfer with chemical reaction studies

4.4.6 Sampling and analysis

Preliminary experimentation was done to find the limitations of the experimental set up (sample analysis procedure) and the reproducibility of the runs.

4.4.1 Rotameter Calibration

The control and measurement of the flow rates was done by the help of four rotameters, one used for liquid feed another used for the carbon dioxide gas and two were used for the humidified air.

4.4.1.1 Liquid Rotameter

For the calibration of liquid rotameter R4, the polyvinyl chloride piping (Fig. 4.1) from rotameter R4 exit to mixer tee MT, was opened at flanges, its outlet direction made downward and the flanges at the rotameter outlet were retightened. The calibrations were made by collecting liquid in a 2 litre measuring cylinder and noting the time. At higher flow rates a plastic bucket was used to collect the liquid and the weight of the liquid was measured in a given time and the weight rate of flow was converted to volumetric rate since its density was determined. Calibration data used in preparing the calibration curves for water and sodium hydroxide are given in appendix A-1 and A-2.

4.4.1.2 Gas Rotameter :

The gas rotameters were calibrated by two U.G.I. - dry gas meters one for low flow range and other for high flow range. Each gas rotameter was provided with an inlet and an outlet pressure control valves. Since the gases are compressible fluids their flow rates vary with pressure. The inlet pressure was kept at a fixed value by controlling both valves manually. The air pressure at rotameter inlet valve was measured by pressure gauge

PG1 by opening the valve fitted in the line connecting the rotameter inlet to pressure gauge. The rotameter reading was set by means of controlling the position of float at different fixed value on the scale and the outlet gas volume was measured by connecting the exit of gas mixing tee GT to the gas meter. The gas meter outlet was open to atmosphere. Time was noted for the fixed volume of the gas flow. The temperature of the gas at the outlet was also measured. These flow rates were then converted to values at the normal temperature and pressure (0° C and 760 mm. Hg.) for convenience. The calibration data used to prepare calibration curves are given in the appendices A-3 and A-4 for air and A-5 for carbon dioxide.

4.4.2   Thermocouple Performance :

Iron - constantan thermocouple measuring junctions were embedded just inside of the inner surface to measure the temperature of flowing gas - liquid mixture by drilling small diameter holes in the test section wall after the inlet tee (TC1) and before the outlet (TC2) as shown in Fig. 4.1. The hole was then sealed using perspex glue after positioning the thermocouple wires to avoid contact with each other. The tip of thermocouple measuring junction was coated with thin film of araldite adhesive to prevent corrosion by flowing liquid. The cold junction kept in ice was connected to portable potentiometer. In order to compare the temperature readings standard mercury in glass thermometer of

$0.1\,^{\mathrm{o}}C$ least count was used and thermocouple and thermometer readings were found to be within $0.2\,^{\mathrm{o}}C$.

4.4.3 Pressure and Pressure Drop Measurements :

The procedure of pressure drop measurements was the same for all gas-liquid systems. The gas and liquid flow rates and test section pressure were adjusted at desired values. Pressure tappings were made at four points on the test section as shown in Fig. 4.4. Fig. 4.4 also shows perspex connector used for fixing sample and pressure taps. In case of empty tube runs since pressure drop is low the manometer arms were joined to tappings PT1 & PT4 so as to have longer test section length for measuring pressure drop accurately. In this case test section pressure was measured at tapping PT3. Tapping PT2 was not used and was kept closed.

To measure the pressure drop of the test section with twisted tapes, since the pressure drop is much higher, manometer arms were joined to tappings PT1 & PT3 and the test section pressure was measured at point PT2. In this case tapping PT4 was kept closed. It may be noted that the length of the twisted tape is more than the distance from inlet to tapping point PT3. Thick polythene flexible tubing was used as the connecting line CL4 from the pressure tapping, and each section contained a liquid trap LT so as to arrest any liquid and avoid its contact with manometer fluid (mercury) or pressure gauge. These are shown in Fig. 4.1. Pressure fluctuations were dampened by partially

closing the valves in the manometer lines. All the lines were
carefully tested for any leaks at twice the operating pressure in
the test section before starting the experimental runs.

4.4.4   Physical Absorption :

The physical absorption experiments were done using
pure carbon dioxide in 20 and 43.85 percent concentration in air
as the gas phase while the liquid phase was distilled or deionized
water. The gas phase resistance in this system is insignificantly
small as compared to liquid phase resistance and, therefore,
the volumetric liquid phase mass transfer coefficient $k_L^o a$ can
be determined. Theoretically, the use of pure carbon dioxide
would be preferable but because of limited supply of the carbon
dioxide and the problem of gas freezing in the pressure regulator,
eventhough hot air blower was used to prevent freezing, at high
gas flow rate, it was decided to use mixtures of carbon dioxide
and air in these experiments. 20 percent CO_2 gas mixture was
used for all experiments except those of lowest gas flow rate,
570 litre/hour, where 43.85 percent carbon dioxide gas mixture
was used. The air used was humidified at room temperature by
means of passing it through a countercurrent packed column
humidifier to reduce the water evaporation in the test section
from liquid phase to gas phase as far as possible.

The sample collecting bottles were rinsed with deionized
water, dried, flushed with N_2 gas and were closed using snap -
on plastic caps. 4.0 ml. NaOH solution (N/50) was introduced

in each bottle using a 5 ml. glass syringe and these bottles were
stored in a tightly covered box, flushed with N_2, to prevent
absorption of atmospheric carbon dioxide till they were taken
for collecting the liquid samples.

The liquid samples were withdrawn with a 5.0 ml. syringe.
The movement of the plunger was controlled by a screw operated
device to help uniform and slow withdrawal of liquid sample from
sampling taps. This was found necessary to prevent the entrain-
ment of gas bubbles in the liquid sample. The syringe was rinsed
with test section liquid atleast twice. If any gas bubble appeared in
the liquid in the syringe, the sample was rejected and liquid sample
was withdrawn again. 4.0 ml. of liquid sample was injected into
the sample bottle. Atleast three liquid samples were collected at
each tap for analysis. After collecting the samples, the bottles
were stored for two hours in the nitrogen flushed box for completion
of the reaction between sodium hydroxide and absorbed carbon dioxide.

4.4.5 Chemical Absorption :

The experimental procedure in the chemical absorption
runs was the same as in the physical absorption experiments.
Carbon dioxide - humidified air mixtures were used as the gas
phase and 2N sodium hydroxide solution was used as the liquid
phase. Since large quantity of liquid was required, 50 to 200 litres
for each run, it was considered desirable to recirculate the
solution till sodium hydroxide concentration was dropped to 0.5

normal. The density and viscosity of liquid feed for each run was measured at the start of the run.

Sodium hydroxide solution was prepared in a stainless steel tank equipped with a stirrer and cooling coils. Sodium hydroxide was weighed separately and dissolved in a measured quantity of deionized water in the tank. This solution was stirred and cooled by tap water flowing through the cooling coils.

The liquid rotameter was calibrated for each sodium hydroxide solution. Nearly 5 ml. of the liquid samples were withdrawn and injected in the sample bottles which were prepared as in the case of the physical absorption runs but without adding any sodium hydroxide solution initially. In addition to withdrawing samples from each tap, one sample of sodium hydroxide feed solution from the feed tank was also taken to find its concentration. 1.0 ml. of the liquid sample from the sample bottle using 2.0 ml. glass syringe was withdrawn and added to 100 ml. conical glass stoppered flask flushed with nitrogen. Three such samples were prepared for analysis of each liquid sample.

4.4.6   Sampling and Analysis :

A.   Physical Absorption

B.   Chemical Absorption

4.4.6.1 Physical Absorption :

Before starting the experiment a set of 100 ml. glass bottles with snap-on plastic caps were cleaned and prepared for the liquid samples. The bottles were purged with Nitrogen gas

and approximately 20.0 ml. of distilled water and 4.0 ml. of 0.02 N sodium hydroxide solution were added to each bottle. The bottles were again purged with nitrogen gas and caps were closed. These bottles were kept in a tightly covered box until required. The box was also purged with nitrogen gas.

Liquid samples of 4.0 ml. each were withdrawn and added into the bottles which were then stored in the box in nitrogen atmosphere. To ensure that all dissolved carbon dioxide was converted to sodium carbonate the sample bottles were kept in the box for nearly two hours prior to titration (85) with 0.02 N hydrochloric acid using pH meter for determining the unreacted sodium hydroxide concentration. The solution was kept under nitrogen blanket while titrating, to prevent the reaction of atmosphere.

4.4.6.2 Chemical Absorption :

In this case the sample was analysed for determining the concentration of sodium hydroxide and sodium carbonate as described below :

a)   The withdrawn sample was added to an excess of 0.5 N $BaCl_2$ solution which precipitated all the carbonate formed during the reaction of carbon dioxide with sodium hydroxide solution in the test section. The bottles were heated to $70^{\circ}C$ in an oven and kept for about one hour in order to complete the precipitation. The solution after precipitation of $BaCO_3$ was anslysed for

unreacted sodium hydroxide. The total alkali in solution was determined by titrating the solution directly with 0.10 N hydrochloric acid using phenolphthalein solution as indicator. The amount of carbon dioxide absorbed was determined from the stoichiometry. The details of analysis are given by Vogel (110).

CHAPTER 5

OBSERVATIONS AND CALCULATIONS

5.1 EXPERIMENTAL DATA

Experimental runs were taken following the procedure as outlined in Chapter 4. Physical absorption runs were taken with air-carbondioxide mixture containing 20 per cent carbon dioxide and 80 per cent humidified air for all runs except those taken at the lowest gas flow rate where 43.85 per cent carbondioxide and 56.15 percent humidified air mixture was used. The liquid phase consisted of deionized or distilled water with conductivity less than 5 micro mhos.

Gas and liquid flow rates were controlled and measured by the help of precalibrated rotameters. The test section pressure was maintained at 20 psia and measured at point PT3 for empty tube runs and at point PT2 for runs with twisted tape inserts. The pressure drop was measured in millimetres of mercury and the distance between the two points, BL, over which the pressure drop was measured, was also recorded. The fluid mixture temperature was noted at points TC1 and TC2 and the difference between inlet and outlet positions was never found to be more than 0.1°C for physical absorption experiments. Average temperature was also recorded. Three samples drawn at each sampling tap were analysed and volume of the standard hydrochloric acid, average of the three samples, required to neutralize sodium hydroxide solution was noted. Concentration of the carbon dioxide

in liquid sample was calculated from these volume and normality

of hydrochloric acid following the procedure described in

Appendix G.

Experimental data for physical absorption runs is given

in Appendix B. Table B 1 consists of the data for the runs taken

in empty tube, Table B 2 and Table B 3 consist of the data taken

with twisted tape inserts TP-1 (H/D = 5.00) and TP-2 (H/D = 9.32)

respectively. Fraction of the carbondioxide at the inlet,

designated by F, is also reported in each of these tables. This

was calculated from measured values of the flow rates of each

stream, that is, air and carbondioxide. The following values are

reported in tables B 1, B 2 and B 3 for each of the runs :

D   -   internal diameter of the pipe, cm

AL1   -   distance between inlet and ST1, cm

AL2   -   distance between ST1 and ST2, cm

AL3   -   distance between inlet and ST2, cm

BL   -   distance between points where pressure drop DELP

                is measured, cm

CL1   -   distance of the point where test section pressure PT

                is recorded from inlet, cm

CL2   -   distance between test section pressure point and

                sampling tap ST1, cm

CL3   -   distance between test section pressure point and

                sampling tap ST2, cm

BR   -   breadth of the twisted tape insert, cm

W1   -   width or thickness of the twisted tape insert, cm

RUN   -   sequence of the experimental run

Q_L -   liquid flow rate, lit/hr.

Q_G -   Gas flow rate at N.T.P., lit/hr.

PT   -   test section pressure, psia

X   -   normality of the hydrochloric acid

T   -   average fluid temperature, ^{o}C

B0   -   Volume of standard hydrochloric acid required to

           neutralize 4 ml sodium hydroxide solution taken in

           sample collector, ml

S1   -   volume of the hydrochloric acid required to neutralize

           4 ml sodium hydroxide solution plus 4 ml liquid

           sample at point ST1, ml

S2   -   above for sample at point ST2, ml

F   -   fraction of carbondioxide gas at the inlet

DELP -   pressure drop between two pressure taps, mm Hg

           Chemical absorption runs were taken under conditions

of identical flow rates of gas mixture and liquid but in this case

the liquid feed consisted of sodium hydroxide solution in deionized

water and its concentration at inlet varied from 2N to 0.5N sodium

hydroxide. In chemical absorption runs the temperature difference

between points TC1 and TC2 was higher because of the exothermic

reaction between carbondioxide and sodium hydroxide but the

this difference was never found to be more than $4^{o}C$. The test

section temperature was recorded as the average of these two readings.

The experimental data for chemical absorption is given in appendix C. Table C 1 consists of empty tube runs. Tables C 2 and C3 consist of the runs taken with twisted tape inserts TP-1 and TP-2 respectively. In the chemical absorption runs the feed solution was analysed separately for total alkali and the sodium hydroxide concentrations. The following values are reported in tables C 1, C 2, and C 3 for each of the runs :

B0   -   volume of standard hydrochloric acid consumed to neutralize total alkali in 1 ml feed solution, ml

B1   -   volume of the acid consumed after the addition of excess bariumchloride solution in 1 ml feed solution, ml

S1   -   volume of the acid consumed after the addition of excess bariumchloride solution in 1 ml of liquid sample collected at point ST1, ml

S2   -   volume of the acid consumed after the addition of excess bariumchloride solution in 1 ml of liquid sample collected at point ST2, ml

remaining terms are similar to those explained in physical absorption experimental data.

The concentrations of sodium carbonate and sodium hydroxide present in each sample were calculated from the

volume and the normality values following the procedure described in Section 4.4.6.2.

5.2 PRELIMINARY EXPERIMENTATION

Preliminary investigations were carried out in order to standardize the set-up and the solutions. They also helped to determine the experimental limitations and to finalize the concentration of the sodium hydroxide solution needed for the collection of the liquid samples for physical absorption experiments. The normality of hydrochloric acid was chosen so as to give sufficient volume when titrated against the sodium hydroxide solution in order to ensure a reasonable volume difference for accurate estimation of the carbondioxide absorbed. Standardization of the hydrochloric acid was done by titrating against the standard sodium hydroxide solution which itself was standardized by titrating against the standard oxalic acid solution. Two to four litres of standard hydrochloric acid was prepared at a time for the analysis.

Liquid and gas flow rate limits were decided on the following basis :

i)   The lowest gas flow rate was determined so as to give slow slugs as observed visually and resulting in sufficient absorption of carbondioxide for accurate analysis in the liquid samples. Since at the lowest flow rate of 570 lit/hr. of gas mixture the amount of carbondioxide absorbed was observed to be very low, it was found necessary to increase the percentage

of carbondioxide at the inlet to 43.85. At other flow rates the carbondioxide concentration at inlet was kept at 20.0 per cent.

ii)   Highest gas flow rate was determined so as to obtain a free flow of carbondioxide gas without freezing at the cylinder outlet or pressure regulator or in the inlet connecting lines. Although a hot air blower and a 1000 watt radiator were used to prevent the freezing at the regulator and its outlet, it was not possible to get carbondioxide flow rate in excess of 1200 lit/hr. Accordingly, carbondioxide flow rate of 1000 lit/hr. was chosen as the higher limit and thus resulting in 4000 lit/hr. as the upper limit for air flow rate or 5000 lit/hr. was the maximum flow rate of the gas mixture.

iii)   The lowest liquid flow rate was selected so as to satisfy the slug flow regime in the two phase flow. Below 50 lit/hr. of the liquid flow rate it was observed visually that the flow becomes stratified or wavy. Accordingly, the lower limit for the liquid flow rate was set at 70 lit/hr.

iv)   The highest value of liquid flow rate was limited by the maximum volumetric capacity of the liquid feed pump P2 to feed the caustic soda solution at constant flow rate for highest pressure drop condition. The maximum liquid flow rate which could be obtained was limited to 410 lit/hr. in the present experimental set up with twisted tape insert of smaller pitch ratio (H/D = 5.00) and highest gas flow rate. Hence the maximum liquid flow rate was set at 350 lit/hr. to be on safe side.

Test section pressure was aimed at a value just above the atmospheric pressure so as to overcome the maximum frictional pressure drop under experimental conditions. Maximum pressure drop was observed at the highest liquid and gas flow rates with twisted tape insert of smaller pitch ratio. Thus, the test section pressure was kept at a value of about 20 psia which was slightly more than the maximum pressure drop encountered.

Inlet gas mixture had to be kept at a pressure higher than the test section pressure to ensure the gas-liquid mixture flow towards outlet direction only. All the gas rotameters were thus calibrated and kept at 35 psia pressure at the rotameter inlet.

5.3 RANGE OF PARAMETERS STUDIED

The experiments were carried out using empty tube and twisted tape inserts of two different pitch ratios. The parameters and their range of variation is given below :

Carbondioxide percentage 43.85 at the lowest gas rate of 570 lit/hr. and 20.0 at other gas flow rates.

Gas flow rate, lit/hr.	-	570	2000	3500	5000
Liquid flow rate, lit/hr.	-	70	140 210 280		350
Pitch ratio H/D	-	∞	9.32	5.00	

For physical absorption studies a set of 20 runs was taken for each of the twisted tape inserts and for the empty tube. Identical set of runs were taken for chemical absorption studies.

For chemical absorption runs the density and viscosity of the feed solution were also measured for use in subsequent calculation and correlation.

5.4 EXPERIMENTAL RUN NUMBERS

In order to facilitate the identification of different types of experimental runs following numbering system was used :

	Empty tube	TP-1	TP-2
Physical absorption runs;	1000	1100	1200
Physical absorption repeated runs;	4000	4100	4200
Chemical absorption runs;	2000	2100	2200
Chemical absorption repeated runs;	5000	5100	5200

Thus from the run number itself it is possible to identify the condition for the given run.

5.5 EXPERIMENTAL RESULTS

5.5.1 Physical Absorption

Data reported in Tables B 1, B 2 and B 3 were used as input to the computer program given in Appendix F Program F.1. IBM 1620 was employed to calculate the experimental results. Empty tube results are listed in Table B 4. The results for twisted tape inserts TP-1 and TP-2 are listed in Tables B 5 and B 6 respectively. The following values are reported in Tables B 4, B 5 and B 6 for each of the runs with column headings defined as follows :

Run No.   -   number of the run

TS   -   average test section temperature, ^{o}K

PTS   -   pressure in test section, kN/m^{2}

VLO   - V_{SL} superficial liquid velocity, m/sec

VGO   - V_{SG} superficial gas velocity, m/sec

(Note :- VGO has been corrected for the amount of gas absorbed

and pressure drop in the test section)

PL   - $\triangle P/\triangle L$ pressure drop per unit length of

the test section, kN/m^{3}

EDPJ   -   Jepsen energy dissipation parameter, $kN/m^{2}/sec$

KLOA   = k_{L}^{o} a, volumetric liquid phase physical mass

transfer coefficient, /sec

(1 is calculated between inlet and ST1, 2 is calculated between

ST1 and ST2 and 3 is calculated between inlet and ST2)

FABS   -   fraction of carbondioxide absorbed upto point ST1

and upto point ST2.

Superficial gas velocity VGO is a function of pressure,
temperature and molar flow rate and varies from point to point
in the test section. The values reported are corrected for
pressure, temperature and fraction of carbondioxide absorbed.
The average value between two points ST1 and ST2 of the test
section are reported in these tables.

The Jepsen's energy dissipation parameter EDPJ is
calculated using the calculated superficial velocities VLO, VGO

in the test section and pressure drop per unit length, PL, in the test section.

Three values of volumetric liquid mass transfer coefficients are reported, $(k_L^o a)_1$ - between inlet and sample tap ST1, $(k_L^o a)_2$ - between taps ST1 and ST2 and $(k_L^o a)_3$ - between inlet and ST2. Since the $(k_L^o a)_1$ and $(k_L^o a)_3$ values are affected by the conditions in mixer tee and in the inlet section of the tube where fully developed slug flow conditions do not exist, for correlations only the values of $(k_L^o a)_2$ are used. It is to be noted that the sampling tap ST1 is located after a distance of about 85 tube diameter and the distance between ST1 and ST2 is 100 to 200 tube diameter, it is expected, as observed visually, that fully developed slug flow conditions exist.

In the last two columns fraction of carbondioxide absorbed between inlet and ST1 and between inlet and ST2 are also tabulated. These values indicate the extent of absorption and are used in correcting the superficial gas velocity due to absorption of carbondioxide in the test section.

Reliability criteria for not using a run for correlation of $k_L^o a$ was chosen somewhat arbitrarily. If the values of $(k_L^o a)_1$ and $(k_L^o a)_2$ differed by less than 50 per cent, the measurements during the run were considered satisfactory and if the above criteria was not met then these runs were not used for the correlation purposes. Runs not satisfying the

reliability criteria are marked with astericks. This criteria was considered useful to discriminate runs with unusual entrance effects and errors in experimental measurements. For pressure drop correlations, however, all the runs were used since no such discriminating criteria for pressure drop measurements was available and all the runs were considered reliable as far as pressure drop measurements are concerned.

5.5.2 Chemical Absorption

The data reported in Appendix C, Tables C 1, C 2 and C 3 was used as input and computer program used to calculate interfacial area and other quantities is given in Appendix F, Program F.2. Empty tube results are listed in Table C 4 and the calculated results for twisted tape inserts TP-1 and TP-2 results are given in Table C 5 and C 6 respectively. The columns headings are defined as follows :

Run   =   number of the runs

TS   -   average test section temperature, ^{o}K

PTS   -   pressure in test section, $k N/m^2$

VLO   = V_{SL} - superficial liquid velocity, m/sec

VGO   = V_{SG} - corrected superficial gas velocity, m/sec

PL   - $\Delta P/\Delta L$ pressure drop per unit length of the test section, kN/m^3

EDPJ   -   Jepsen energy dissipation parameter, $kN/m^2/sec$

EDPB   -   Banerjee energy parameter, N/sec

SURF   =   a, - effective gas, liquid interfacial area m^2/m^3

FABS   -   fraction of carbondioxide absorbed.

Just like physical absorption, for chemical absorption also effective interfacial area is calculated for three zones of the tube and are tabulated as : $(SURF)_1$ - between inlet and sample tap ST1, $(SURF)_2$ - between sample taps ST1 and ST2 and $(SURF)_3$ - between inlet and sample tap ST2.

Reliability criteria for selecting a run for correlations involving interfacial area was - if the values of $(SURF)_1$ and $(SURF)_2$ differed by less than 50 per cent the run was considered satisfactory. Runs not satisfying this criteria are marked with astericks.

5.5.3 Reproducibility of Data

Experimental runs both for physical and chemical absorption, were repeated under the similar conditions either to check the reproducibility of the data for some random conditions or when the initial run failed to satisfy the reliability criteria. Reproducibility of the runs as measured from the computed results was not very good and in some cases the two runs under identical flow conditions resulted in the variation of k_L^o a or a to as high a value as 80 per cent. This variation may be attributed to, some extent to experimental or analytical errors but largely it is due to inherent scatter existing in the two phase gas liquid system in the slug flow regime. Similar data scatter is also observed in experimental

results of other workers discussed earlier in Chapter 2. and
more specifically in the experimental results reported by
Gregory and Scott (99) and Zarnett (107).

5.6 RESULTS AND CORRELATING PARAMETERS

5.6.1 Area creation parameter

Kasturi and Stepanek (102) found that the area
creation rate or the rate at which the interfacial surface is
created, defined as

$$ACRET = Q_L . SURF / E_L \quad (m^2/sec) \quad (5.1)$$

correlates most satisfactorily with the pressure drop.
Therefore values of this parameter are also calculated by using
Program F.10 and are reported in Table E.1, Appendix E.
The values of the volume occupied by liquid, E_L are calculated
using Hughmark k_H factor and are also reported in that table
as ALFAL.

5.6.2 Liquid Film Mass Transfer Coefficient

In most of the experimental results reported in
literature, it appears that the criteria used for similarity or
hydrodynamic similarity was chosen as the idential superficial
gas and liquid velocities either at the inlet or in the test section
for physical and chemical absorption runs so as to calculate
k_L^o from k_L^o a (physical absorption) and a (chemical
absorption) values. However, the author has not seen any
specific criteria in the published literature. It is felt that the
criteria of identical superficial gas and liquid velocities at inlet

for chemical and physical absorption experiments have little

meaning because the gas velocity in the test section for chemical

absorption runs will be significantly different due to the difference

in absorption rate and pressure drop even when the inlet

conditions were same as that in physical absorption run. The

criteria of identical velocities in the test section is also not

considered satisfactory because the condition of hydrodynamic

similarity is normally characterized by Reynolds number and

not velocities. Accordingly, identical two phase Reynolds

number, Re_{TP}, is chosen as a criteria for hydrodynamic

similarity for physical and chemical absorption runs. This

necessitated to correlate interfacial area, a, with Re_{TP} and

use this correlation to determine a at Re_{TP} value of the

physical absorption run and then obtain k_L^o by dividing k_L^o a

with a. k_L^o experimental, identified as KLOEX and calculated

by this method are given in Tables E.2, E.3 and E.4,

Appendix E, for empty tube, TP-1 (H/D = 5.00) and

TP-2 (H/D = 9.32) respectively. The units of k_L^o are

meters per second. In the third column are the values of k_L^o,

identified as KLOB calculated using Banerjee's (84) equation

given by

$$(k_L^o)_B = (D_A \frac{2.25 \pi V_{LO}}{2 Q_L} \frac{D_P}{4 \rho_L} \frac{\Delta P}{\Delta L})^{\frac{1}{2}} \qquad (5.2)$$

and in the fourth column are k_L^o values, designated as KLOK,

calculated using Kasturi-Stepanᵊ (103) equation –

$$(k_L^o)_{KS} = 0.25 \ Sc_L^{-\frac{1}{2}} \ Pe_L \ Eu_L \tag{5.3}$$

where

Sc_L = liquid Schmidt number $\left(\dfrac{\mu_L}{\rho_L D_A} \right)$

Pe_L = liquid Peclet number $(V_L \ D_P \ / D_A)$

Eu_L = liquid Euler number $\left(\dfrac{\triangle P}{\triangle L} \dfrac{D_P}{\rho_L \ v_L^2} \right)$

In the fifth column are the values of experimental liquid phase

Sherwood number calculated by

$$Sh_{exp} = \frac{(k_L^o)_{exp} \ D_P}{D_A} \tag{5.4}$$

In all cases hydraulic diameter D_H is used for correlations as

defined below -

$$D_H = \frac{4 \ x \ \text{cross sectional area for flow}}{\text{wetted perimeter}} \tag{5.5}$$

In the case of empty tube hydraulic diameter D_H becomes

identical to pipe diameter D_P. The values of liquid phase

Schmidt, Peclet and Euler numbers are also given in

Tables E.2, E.3 and E.4.

5.7 LINEAR REGRESSION ANALYSIS

Most of the data is correlated in the following form

$$Y_{pred} = Bo \ (X)^{B_1} \tag{5.6}$$

which is linearized by taking logarithm and each pair of

experimental X and Y is converted to LOG X and LOG Y for

linear regression. Using the method of least squares the values

of constants Bo and B_1 are calculated. Details of this method
are discussed by Himmelblau (114) 95 per cent confidence limit
is found by using, t, distribution for the number of data sets,
N, and function P (t) from the standard tables. The per cent
standard error is calculated by the relation

$$\text{per cent std. error} = \sqrt{\left[\frac{(PDEV)^2}{N-2}\right]} \qquad (5.7)$$

where
$$PDEV = \left(\frac{Y - Y_{pred}}{Y_{pred}}\right) \times 100$$

and Y_{pred} is the value of Y predicted for experimental X
value using Equation (5.7).

The computations were performed using IBM 1620
computer and the Program F.8 listed in Appendix F. This
program was used for regression analysis of the correlations
after making the necessary modifications in the input format
and value of N and P (t) in accordance with the data used.

CHAPTER 6

RESULTS AND DISCUSSIONS

6.1.1   Experimental Pressure Drops

Pressure drop per unit length is plotted against superficial gas velocity, V_{GO}, with superficial liquid velocity, V_{LO} as parameter in Figures 6.1, 6.2 and 6.3 for empty tube, twisted tape inserts TP-1 (H/D = 5.00) and TP-2 (H/D = 9.32) respectively. The continuous lines represent chemical absorption runs and dashed lines are for physical absorption runs.

As can be observed in these figures, pressure drop increases with an increase in superficial velocities V_{GO} and V_{LO}. Pressure drop also increases with decrease in pitch ratio, y, for given values of V_{GO} and V_{LO}. It is obvious that at higher fluid velocities frictional losses increase and thus an increase in pressure drop is expected. Furthermore, it is noticed that at the same gas and liquid superficial velocities chemical absorption values for pressure drop are higher than the values obtained in physical absorption. This is due to higher viscosity of sodium hydroxide solution, used as liquid phase in the chemical absorption experiments, which results in lower Reynolds number and higher value of friction factor giving higher pressure drop at same gas and liquid velocities.

Higher pressure drops are observed as the pitch ratio, y, is decreased. Pressure losses increase due to increased vortex mixing
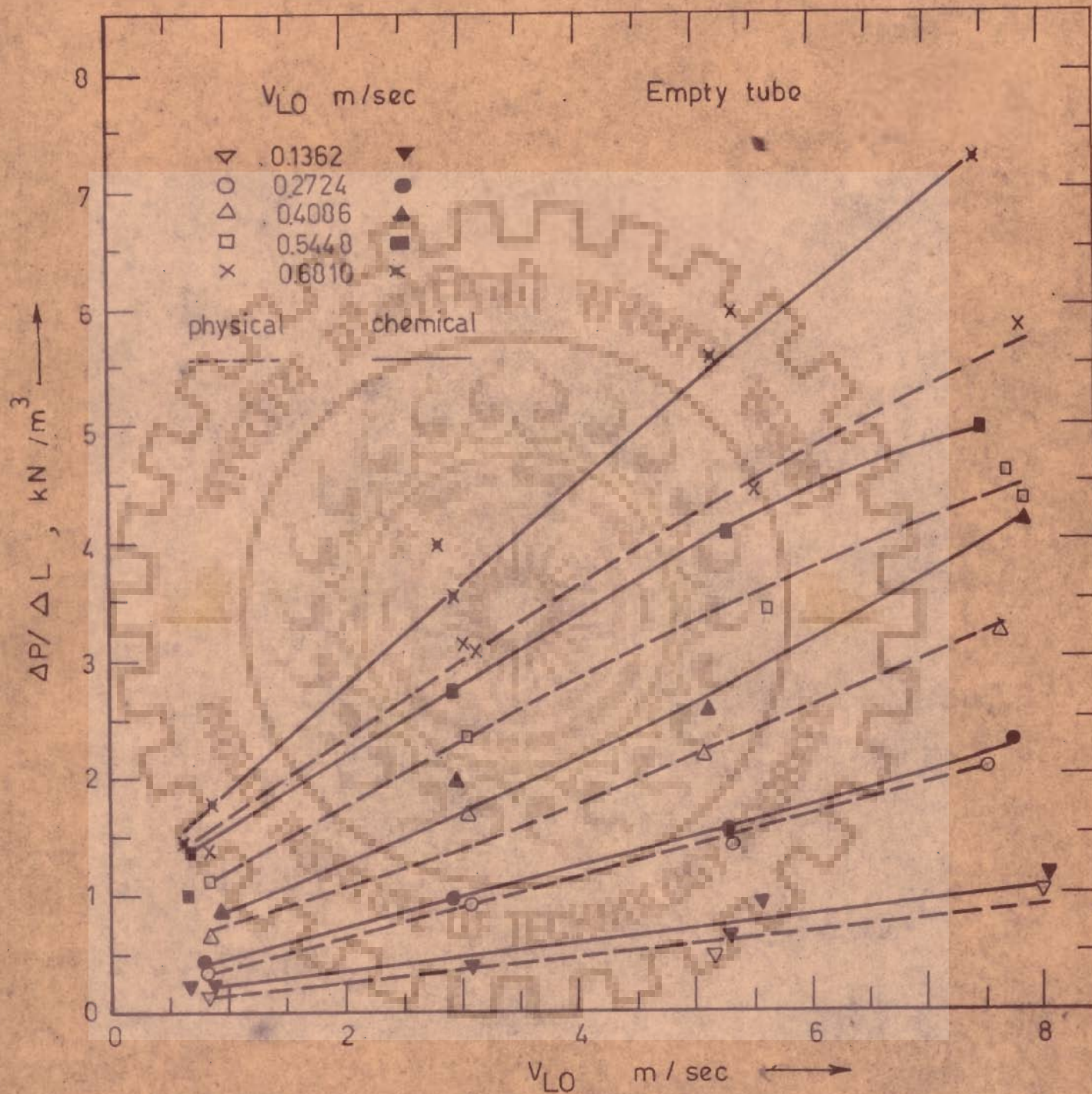
Fig 6.1   Pressure drop vs superficial gas velocity
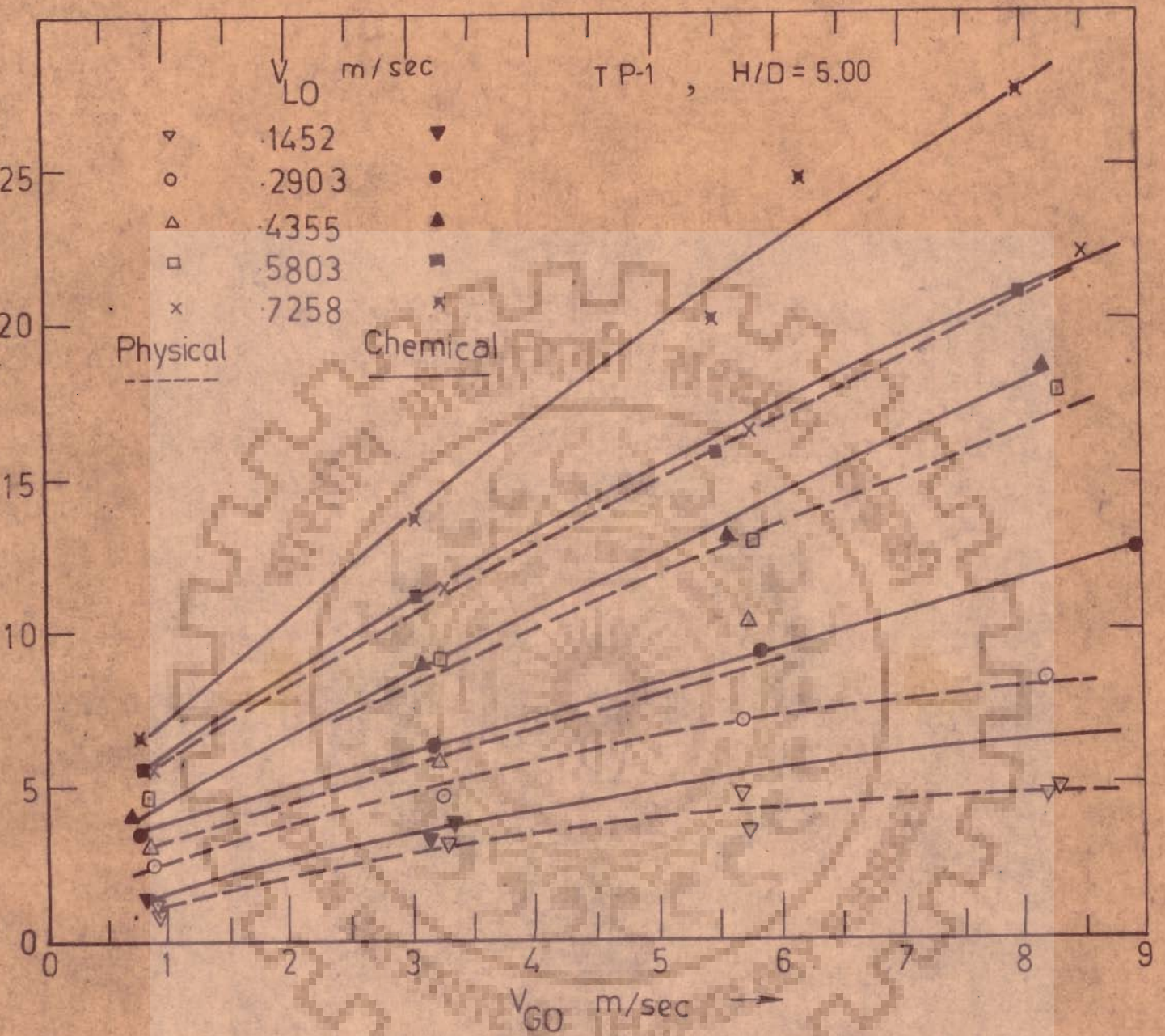
Fig. 6.2 Pressure drop vs superficial gas velocity
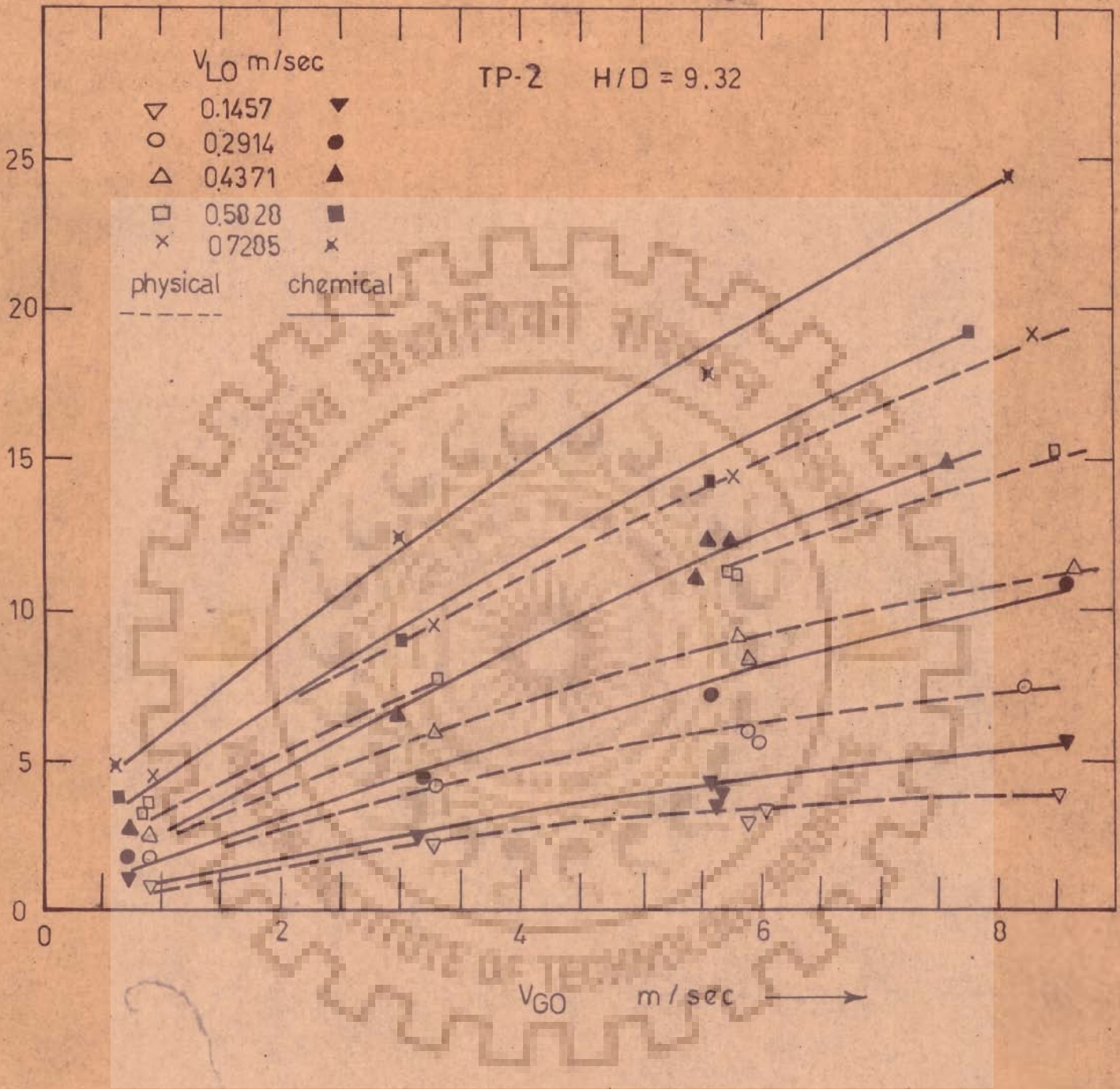
Fig.6.3   Pressure drop vs superficial gas velocity
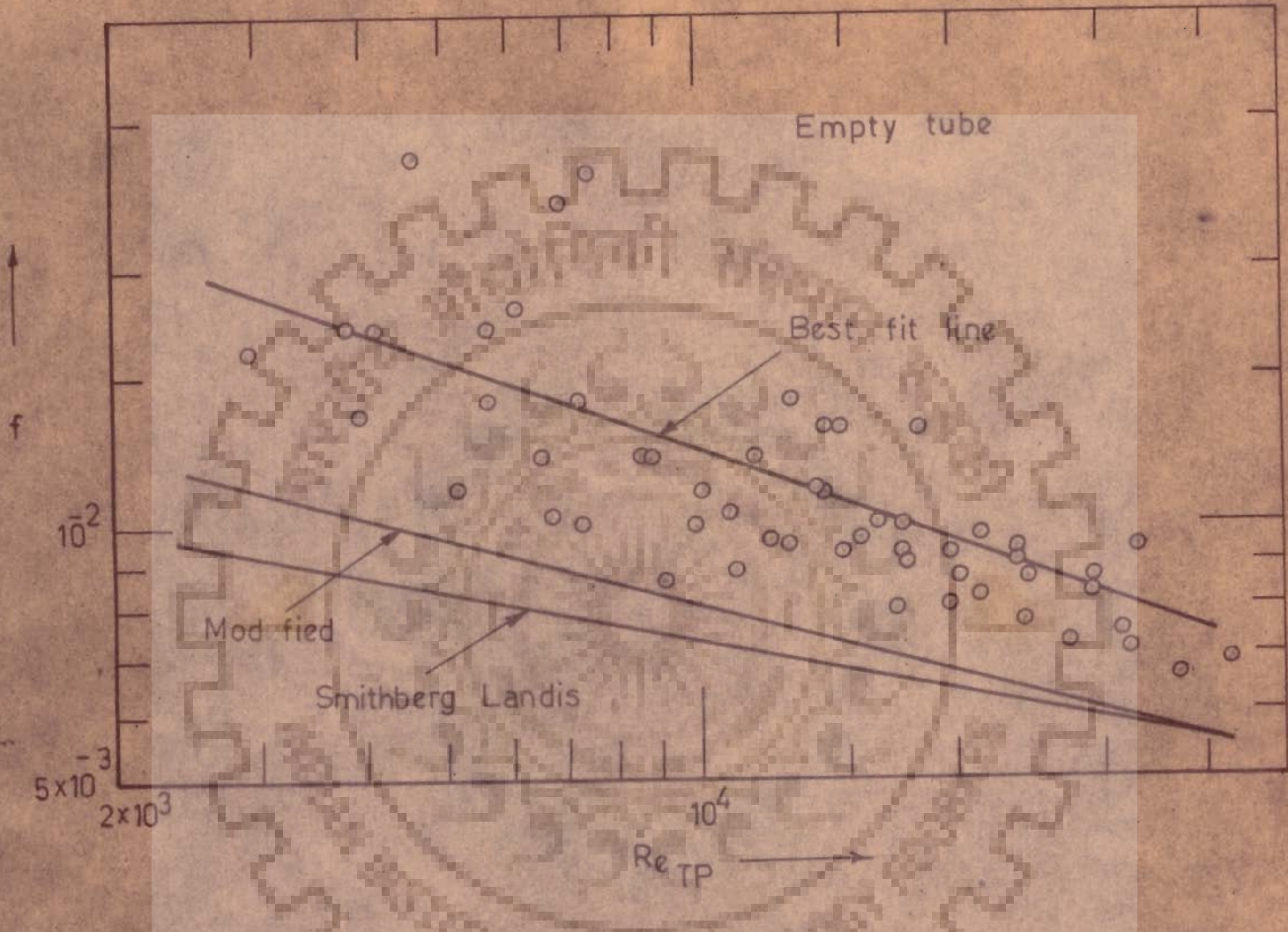
Fig. 6.4 Friction factor vs two phase Reynolds number
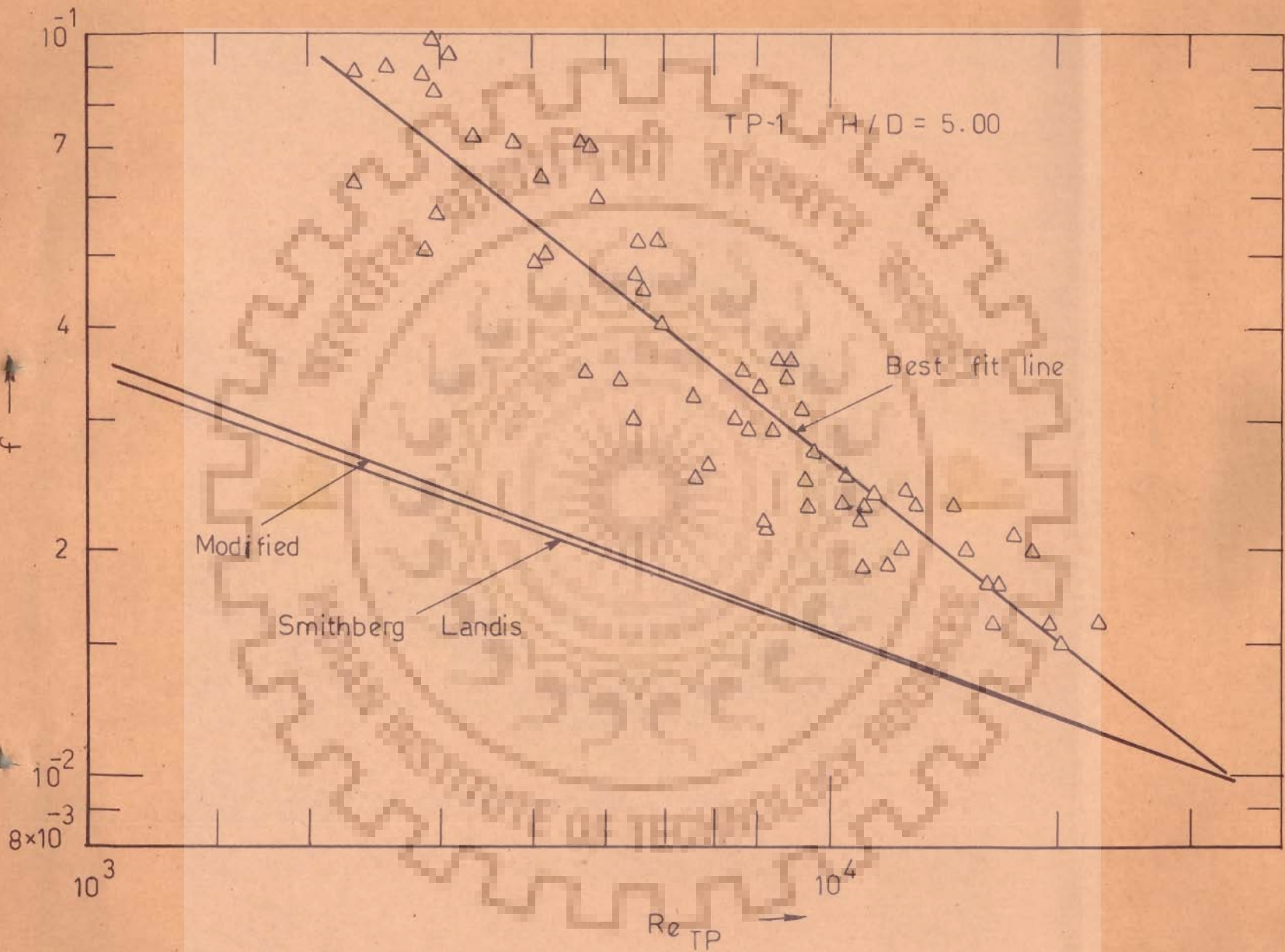
Fig. 6.5   Friction   factor   vs   two - phase   Reynolds   number
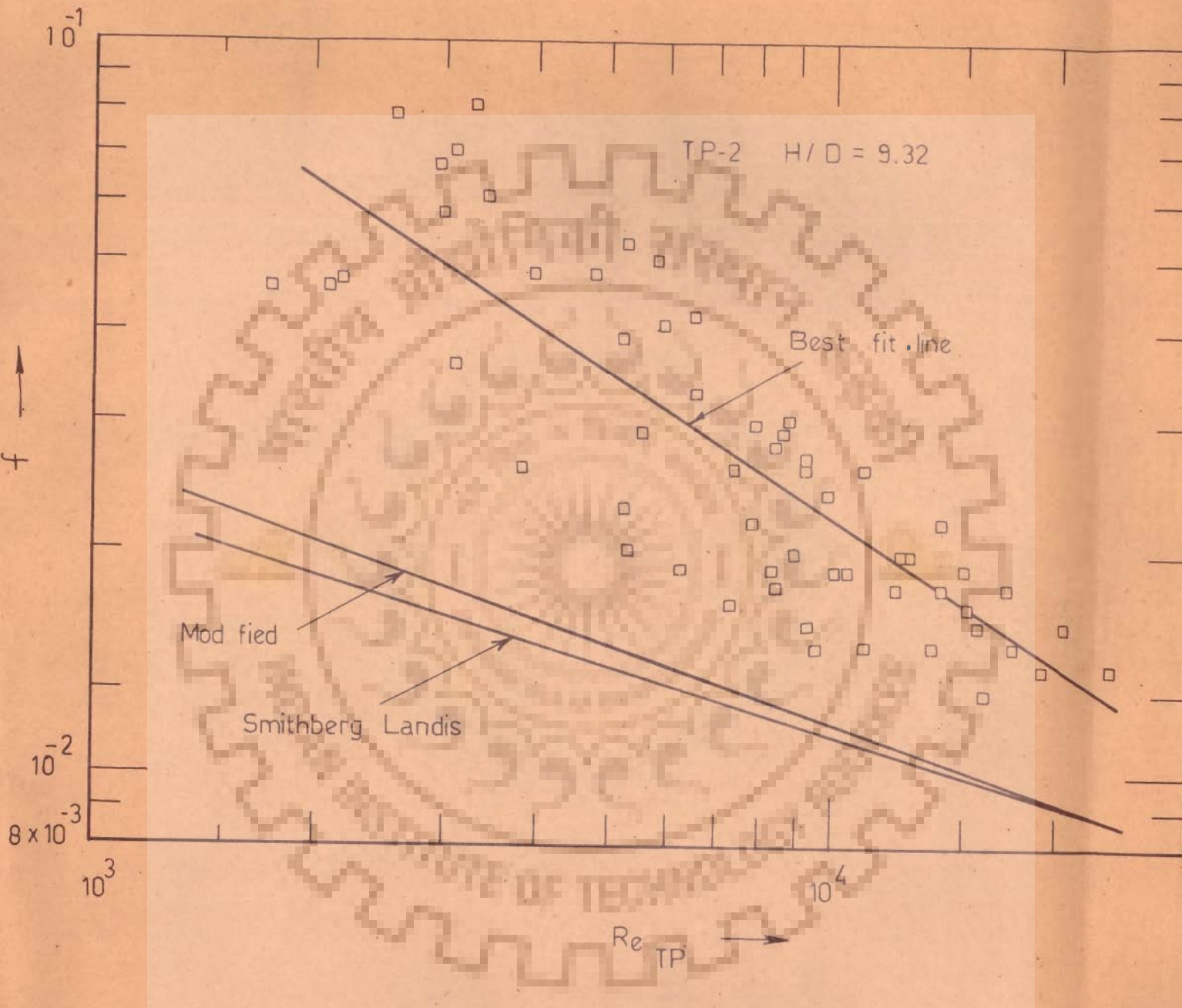
Fig. 6.6 Friction factor vs two phase Reynolds number

as a result of more intense swirling motion of the fluids and also due to increase in the tangential velocity caused by longer path travelled by the fluids, at smaller pitch ratio of the twisted tape insert, in the same period for any specified value of flow rate.

It is further observed, Fig. 6.1 that the data points in the case of empty tube results do not fall on a smooth curve probably due to the larger fluctuations observed during pressure drop measurements when gas and liquid are flowing in empty tube in slug flow regime. The pressure drop fluctuations were considerably smaller for tubes fitted with twisted tape inserts probably due to the pressure of liquid at the tube wall all the time as a result of the centrifugal force in swirling flow. Therefore, data in Figs. 6.2 and 6.3 lie closer to smooth curves and show lesser scatter.

6.1.2   Friction Factor Correlations

Normally the friction factor is correlated with Reynolds number and these correlations are used to calculate the pressure drop knowing pipe geometry, fluid velocities and physical properties like viscosity and density. In the present study fluid consisted of two phases, hence the two phase Reynolds number, Re_{TP}, is used for correlations, which is calculated by the method discussed in section 3.1.2.

Friction factors, f, are plotted against two phase Reynolds numbers in Figs. 6.4, 6.5 and 6.6 for empty tube, tube with twisted tape insert TP-1 (H/D = 5.00) and TP-2 (H/D = 9.32) respectively. The calculated values of two phase, superficial gas and superficial liquid Reynolds numbers, Re_{TP}, Re_{SG} and Re_{SL}, are :

	Re$_{TP}$	Re$_{SG}$	Re$_{SL}$
Empty tube	2925-42860	913-10086	1368-12215
TP-1	2295-17720	650-6457	804-7148
TP-2	1730-23593	558-6180	819-7311

Experimental friction factor is calculated from the experimental pressure drop value for two phase slug flow:

$$f_{exp} = \frac{g_c \, D_H}{2 \, V_L^2 \, \rho_L} \left(\frac{\Delta P}{\Delta L} \right)_{exp} \qquad (6.1)$$

where ρ_L is liquid density, V_L is actual liquid velocity that is superficial liquid velocity, V_{LO}, divided by volume fraction occupied by the liquid, E_L.

Each figure has three lines; one for friction factor calculated by Smithberg-Landis Equation 3.2, f_{SL}, one for values, f_{cal}, calculated using modified friction factor correlation, equation 3.13 developed in the present study using two phase Reynolds number, Re$_{TP}$, and another for best fit line through experimental friction factor, f_{exp} and Re$_{TP}$ values. The equation of the best fit line for f_{exp} and friction factor calculated using modified equation, f_{cal}, are

Empty tube: $\qquad (f)_{pred} = 9.94 \, (f_{cal})^{1.390} \qquad (6.2)$

TP-1 (H/D = 5.00): $\qquad (f)_{pred} = 194.1 \, (f_{cal})^{2.134} \qquad (6.3)$

TP-2 (H/D = 9.32): $\qquad (f)_{pred} = 102.4 \, (f_{cal})^{1.900} \qquad (6.4)$

Observing Figs. 6.4, 6.5 and 6.6 it is quite clear that the proposed friction factor correlation is a definite improvement over that given by Smithberg and Landis especially at Reynolds number less than 10^4. For Reynolds number greater than 10^4 the friction factor values predicted by Smithberg-Landis equation and modified friction factor correlation approach each other. Thus, the proposed correlation, Equation 3.13, has a wider range of applicability for the Reynolds number values of 2×10^3 to 4×10^6 as discussed in section 3.1.1. The scatter of data points in Fig. 6.4, for empty tube runs is mainly due to error caused by fluctuations which were observed while measuring the experimental pressure drop. Furthermore, it is clear from Equations 6.2, 6.3 and 6.4 and Figs. 6.4, 6.5 and 6.6 that the f_{exp} varies more steeply with two phase Reynolds number than predicted by modified correlation and this steepness increases with decrease in pitch ratio, y. Since the friction factor values are less than unity the decrease in its value due to higher exponent to which it is raised is to be compensated by increased value of the pre-exponential factor. Thus for the empty tube, corresponding to pitch ratio y equal to infinity, the exponent is 1.390 and the pre-exponential factor is 9.94 while for TP-1, y = 5.0, the exponent is 2.134 and pre-exponential factor is 194.1.

In two phase gas liquid flow in horizontal pipes operating under slug flow regime it is well known (109) that the gas moves at much higher velocities than the liquid and liquid slugs also move at a greater velocity than the average velocity used in calculations. The experimental pressure

drop is actually due to flow of gas and liquid both and not due to the flow of liquid alone. Further, the pressure drop due to the liquid slug moving at higher velocity will be considerably more as compared to that predicted from liquid velocity calculated using average volume fraction occupied by liquid. In view of the reasons given above, it is evident that the value of f_{exp} as calculated by Equation 6.1 will be higher than f_{cal}, predicted by the modified friction factor equation.

A careful examination of Figs. 6.4, 6.5 and 6.6 bring out more salient features which may need some explanation. Firstly, the difference between f_{exp} and f_{cal} increases as the Reynolds number decreases for any given flow geometry. Secondly, this difference at any given Reynolds number also increases as the pitch ratio, y, decreases. It may be recalled that the modified friction factor correlation Equation 3.13, is obtained from Smithberg-Landis Equation 3.1 by modifying only the wall friction term to improve its applicability to lower Reynolds number range. The other terms which account for losses due to vortex mixing and tangential flow were obtained by theoretical analysis of the single phase flow only. In two phase gas-liquid flow the vortex mixing creates two more complications: (i) the intra phase momentum transfer between two fluids of widely different density and (ii) the problem related to interfacial area, that is, coalescence of bubbles and formation of new bubbles. Both these factors result in additional pressure drop due to energy losses and are not accommodated in the derivation. At high Reynolds number the contribution of these factors in pressure drop may be small as compared to the total pressure

drop but at low Reynolds number their contribution may become significant. Thus, larger difference between f_{exp} and f_{cal} is observed at low Reynolds number for any flow geometry. Also when the twist pitch ratio, y, decreases, the intensity of swirling increases and the above two factors contribute more to pressure drop due to increased vortex mixing. This explains why the difference between f_{exp} and f_{cal} increases with decreasing pitch ratio of the twisted tape insert.

It is possible to make better prediction of pressure drop using f_{pred} from the correlations given by Equations 6.2, 6.3 and 6.4. However, the above equations have no theoretical basis and no generalization is possible to predict the values of exponents and pre-exponential factor for different geometry of twisted tapes. Therefore, it was considered more appropriate to calculate pressure drop per unit flow length, $\Delta P/\Delta L$, using either Hughmark method (section 3.1.2) or Lockhart-Martinelli method (section 3.1.3) and then develop correlation of the form,

$$(\Delta P/ \Delta L)_{pred} = a \; (\Delta P/ \Delta L)_{cal}^{b} \qquad (6.5)$$

for better prediction of the experimental pressure drop. This correlating procedure was found more satisfactory and is discussed in the following sections.

6.1.3 Pressure Drop Correlation - Hughmark Method

Fig. 6.7 shows a plot of the experimental pressure drop values $(\Delta P/ \Delta L)_{exp}$ as a function of the pressure drop values calculated by Hughmark's correlation, $(\Delta P/\Delta L)_{H}$, using the method
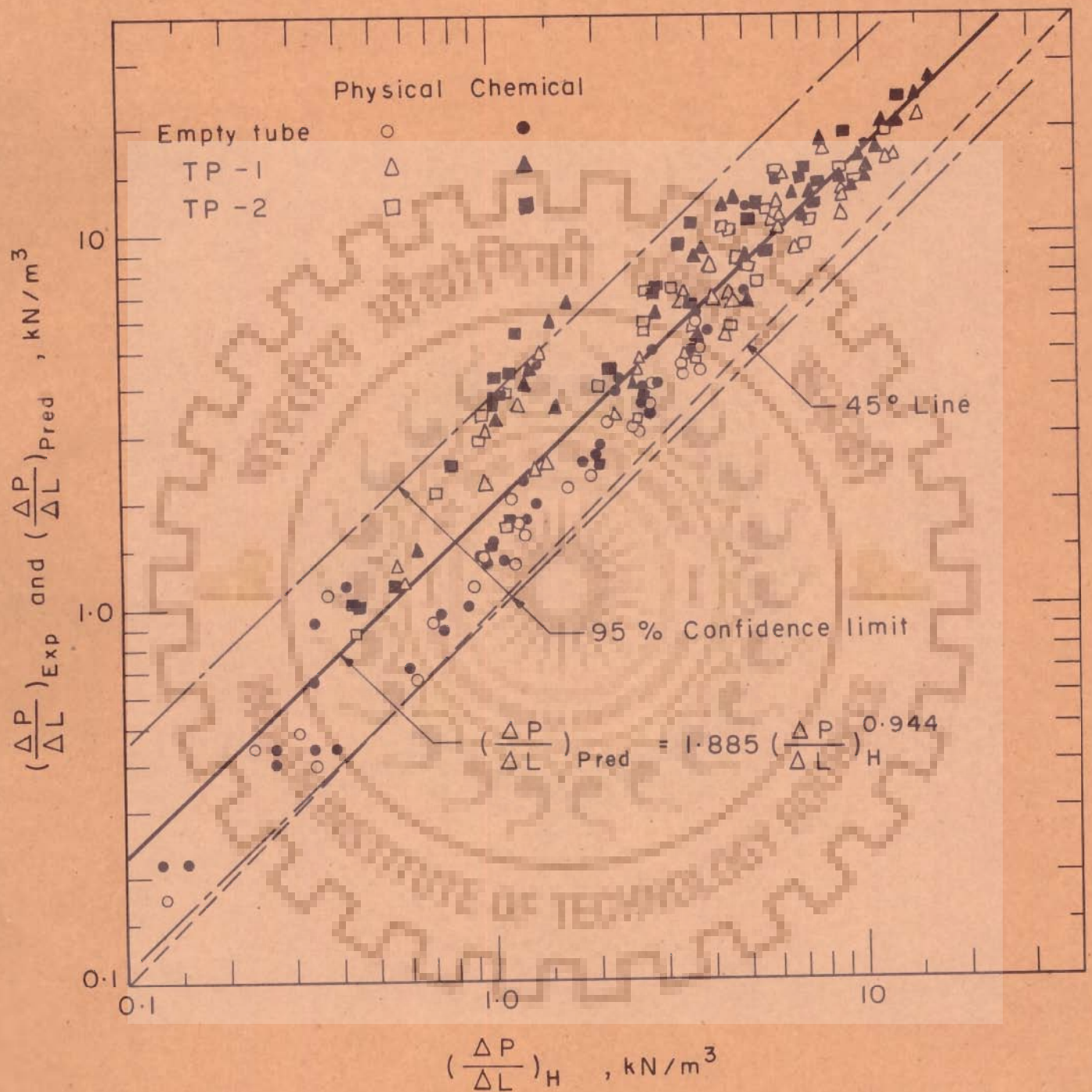
Fig. 6·7 Experimental pressure drop $(\frac{\Delta P}{\Delta L})_{Exp}$ against pressure drop $(\frac{\Delta P}{\Delta L})_H$ predicted by Hughmark

discussed earlier in section 3.1.2. The figure also shows the 45° line, that is, $(\Delta P/\Delta L)_{exp} = (\Delta P/\Delta L)_{H}$, to clearly indicate the deviation, the 95 percent confidence limits, and the best fit line. The equation of the best fit line is given by $(\Delta P/\Delta L)_{pred} = 1.885 (\Delta P/\Delta L)_{H}^{0.944}$, standard error $\pm$ 39.4 %

$$(6.6)$$

From Fig. 6.7, it is clear that no separate trends are exhibited by the values obtained for physical absorption runs or chemical absorption runs or for runs taken in empty tube or in tubes with twisted tape inserts. It is further noticed that the Hughmark correlation using modified friction factor, f_{cal}, underpredicts the pressure drop observed experimentally by 4 to 78 percent with an average value of 37.7 percent.

Gregory and Scott (35) reported similar correlations using empty tube given as,

$$(\Delta P/\Delta L)_{pred} = 1.236 (\Delta P/\Delta L)_{H}^{0.96} ; \text{ sd } 22\%$$

$$(6.7)$$

for the physical absorption case and

$$(\Delta P/\Delta L)_{pred} = 1.144 (\Delta P/\Delta L)_{H}^{1.02} ; \text{ sd } 19\% \quad (6.8)$$

for the chemical absorption case. Their pressure drop values are in mm Hg/m whereas that given in Equation 6.6 are in kN/m^{3}.

The correlation obtained in the present study, Equation 6.6, compares well with those reported by Gregory and Scott as shown by Equations 6.7 and 6.8, especially when we compare the values of exponents. The values of the pre-exponential factors depend upon the units used to express the pressure drop and as such direct comparison
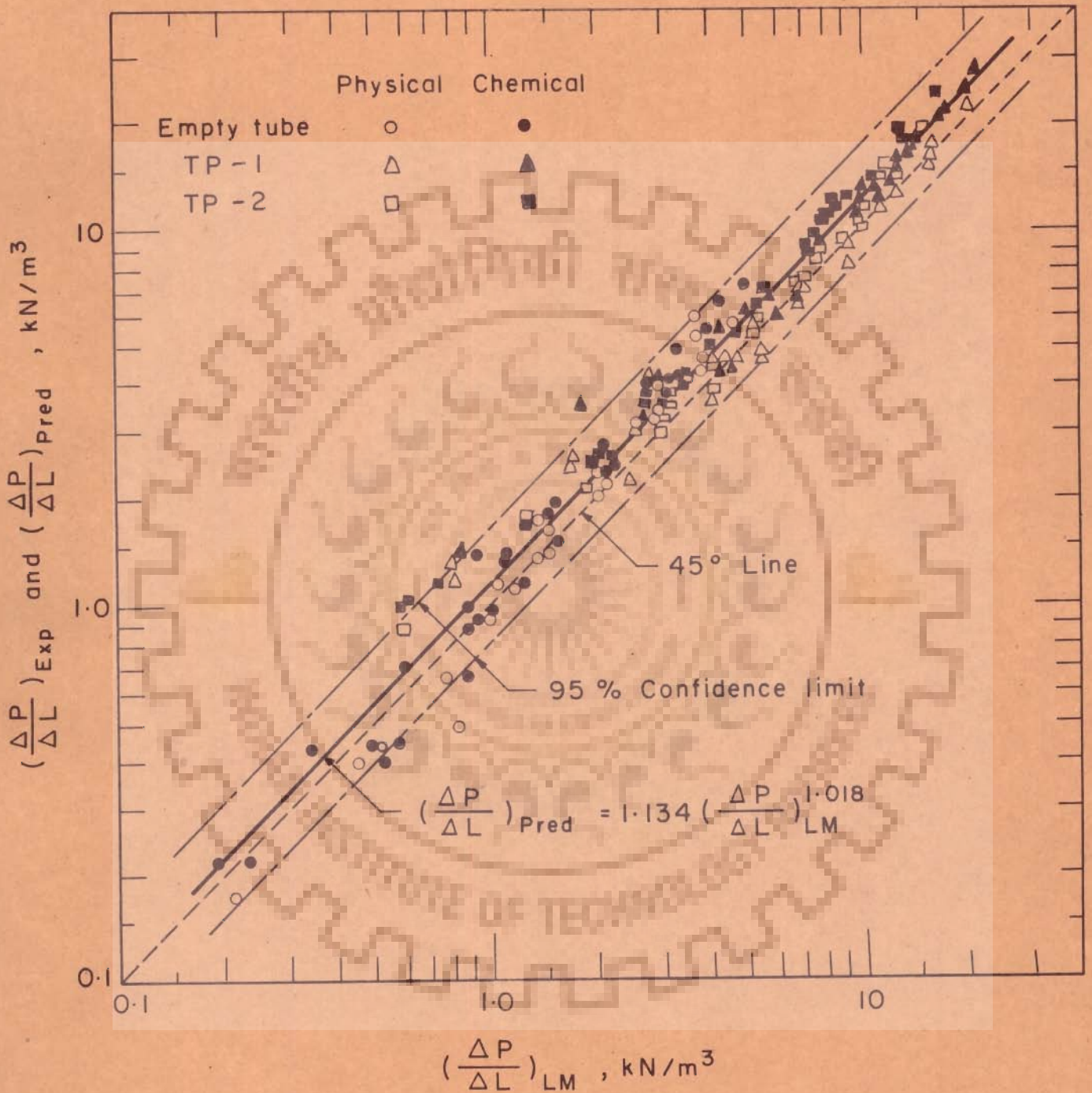
Fig. 6·8 Experimental pressure drop $(\frac{\Delta P}{\Delta L})_{Exp}$ against pressure drop $(\frac{\Delta P}{\Delta L})_{LM}$ predicted by Lockhart-Martinelli

is not feasible. The standard error for correlation given by Equation 6.6 appears to be higher than the values of standard deviation reported by Gregory and Scott (35) but exact comparison is difficult because they have not indicated how they have defined the standard deviation. But the correlation given by Equation 6.6 even with higher percent standard error has a wider applicability because it is based on all experimental results taken for physical and chemical absorption and with and without twisted tape inserts.

Gregory and Scott also observed that Hughmark method under-predicts the pressure drop on an average of 22 and 15 percent in the case of physical and chemical absorption experiments respectively.

6.1.4   Pressure Drop Correlation - Lockhart-Martinelli Method

Fig. 6.8 shows a plot of all experimental pressure drop $(\triangle P/\triangle L)_{exp}$ values as a function of pressure drop values calculated by Lockhart-Martinelli correlation, $(\triangle P/\triangle L)_{LM}$ using the method discussed in section 3.1.3. The figure also shows the 45° line, the 95 percent confidence limit, and the best fit line. The equation of the best fit line is given by

$$(\triangle P/\triangle L)_{pred} = 1.134 \; (\triangle P/\triangle L)_{LM}^{1.018} \; , \text{ standard error } \pm 17.9 \text{ \%}$$

$$(6.9)$$

It is observed in Fig. 6.8 that 20 percent of the data points are overpredicted while 80 percent of the data points are underpredicted. It is further noticed that the overprediction is mostly for the data points obtained for flow in the tube without inserts and the underprediction is for

thefl ow in thet ube with twisted tape inserts. The overall under-
prediction was found to be 11.3 %. However the points are so close
to 45° line that separate correlations were considered unnecessary and
a single best fit line is drawn, Equation 6.9. The values of the exponent
and pre-exponential factor are quite close to unity. A comparison of
Figs. 6.7 and 6.8 shows that Lockhart-Martinelli's method is much
better than Hughmark's method.

Gregory and Scott (35) presented their result s on gas liquid slug
flow in horizontal tube without inserts in the form of Lockhart-Martinelli
parameters ϕ_L and X. They observed that this method gave better
estimates of the pressure drop than the Hughmark correlation which
predicts values slightly lower than those found experimentally. They
have also used Equation 3.5 for estimating the value of friction factor
for estimating the single phase pressure drops to calculate Lockhart-
Martinelli parameters. It may be recalled that the modified friction
factor correlation Equation 3.13 reduces to Equation 3.5 for the
empty tube, that is, when pitch ratio H/D is infinity.

Narasimhamurty and Varaprasad (52) used Smithberg-Landis
simplified Equation 3.2 to calculate single phase pressure drop and
Lockhart-Martinelli method to calculate two-phase pressure drop in
the horizontal tube with twisted tape inserts. They also reported the
results in the form of parameters ϕ_L and X for various air and
water flow rates for three pitch ratios, y, 3.75, 5.00 and 7.50. The
superficial liquid and gas Reynolds number ranges from 1.005 x 10^4 to

4.215×10^4 and 4.44×10^3 to 5.151×10^4 respectively. They found that the use of Lockhart-Martinelli with Smithberg-Landis correlation Equation 3.2 , for friction factor gave pressure drop values with a maximum of underprediction of 32.0 percent to a maximum overprediction of 7.0 percent and an overall underprediction of 11.6 percent as compared to their experimental pressure drop values. Closer examination of their experimental conditions reveals two facts; (i) the twisted tape inserts were 20.0 millimetrewide while the internal diameter of the test section pipe was 25.54 millimetre, (ii) superficial gas and liquid Reynolds numbers were at a relatively higher range. Since the twisted tape did not fit tightly the liquid near the tube wall has only axial flow because of the gap between the tube wall and twisted tape and the pressure drop comparatively lower than that found for swirling flows in tightly fitted twisted tapes. This explains why the standard error in the present study is slightly higher as compared to those reported by Narasimhamurty and Varprasad. It may also be noted that the lowest value of superficial gas and liquid Reynolds number are much higher in the case of Narasimhamurty and Varaprasad as compared to the present study, 4440 as compared to 558 for Re_{SG} and 10050 as compared to 804 for Re_{SL}, the use of simplified Smithberg-Landis equation can be considered adequate to predict the frictional loss.

Zarnett (107) who used rifled tubes in two phase flow also plotted his data in the form of Lockhart-Martinelli parameters ϕ_L and ϕ_G and X. Experimental values of ϕ are found to lie slightly below the values given by

Lockhart-Martinelli correlation, indicating that Lockhart-Martinelli correlation overpredicts the pressure drop by 20 to 40 percent for two phase flow in rifled tube.

Duckler et.al. (127) used 5000 data points obtained in various experimental investigations and compared various available correlations to predict the pressure drop in two-phase gas liquid flow systems. They also found that the Lockhart-Martinelli correlation predicted the pressure drop values closest to the experimental pressure drop values. The average deviation was found to be lowest, 10 percent, in the case of 1.0 inch diameter pipe and highest, 47.5 percent, in the case of 3.5 inch diameter pipe with an overall average of 25 percent considering all sizes of the pipes from 1.0 inch to 5.0 inch internal diameter.

The reason of Lockhart-Martinelli method predictions being closest to experimental pressure drop value as compared to other available methods in two phase gas liquid flow systems appears to be that its parameter X consists of the ratio of the pressure drop values at superficial fluid velocities. Thus, X is proportional to the ratio f_{SL}/f_{SG} and any inherent error caused caused in predicting single phase friction factor values due to inadequacy of the correlation used is likely to cancel out and the error in the calculated values of X are likely to be very small. This will mean that the computed value of the Lockhart-Martinelli parameter ϕ_G or ϕ_L will not be effected. It is also to be noted that the two phase Reynolds number values depend upon the estimated values of volume fraction occupied by liquid and as such the value of Re_{TP} are less reliable as compared to the values of Reynolds

number Re_{SG} and Re_{SL} based on superficial gas and liquid velocities.

Accordingly, it is felt that Lockhart-Martinelli method using modified friction factor correlation, Equation 3.13 gives most accurate prediction for two phase pressure drop and further improvements in the predicted values can be made by using Equation 6.9 which correlates $(\triangle P/\triangle L)_{pred}$ with $(\triangle P/\triangle L)_{LM}$.

6.2.1 Volumetric Liquid Phase Mass Transfer Coefficient

The volumetric liquid phase mass transfer coefficients were calculated from the experimental values by the method discussed in Section 3.2. The values of volumetric liquid phase mass transfer coefficient, $k_L^o a$, are plotted against the superficial gas velocity, V_{GO}, with superficial liquid velocity, V_{LO}, as parameter in Figures 6.9, 6.10 and 6.11 for the case of empty tube and tube with twisted tape inserts TP-1 (H/D = 5.00) and TP-2 (H/D = 9.32) respectively. From Figures 6.9, 6.10 and 6.11 it is clear that the volumetric liquid mass transfer coefficient $k_L^o a$ increases with an increase in superficial gas and liquid velocities. Further, it is also observed that $k_L^o a$ increases with increase in twist pitch ratio y. For the case of data in tube with twisted tape inserts. Figures 6.10 and 6.11, the values of $k_L^o a$ could not be obtained at low liquid superficial velocities of 0.145 and 0.29 m/sec and above the superficial gas velocity of 6.0 m/sec because the concentration of carbondioxide in liquid phase was found to be a value close to saturation even at the first
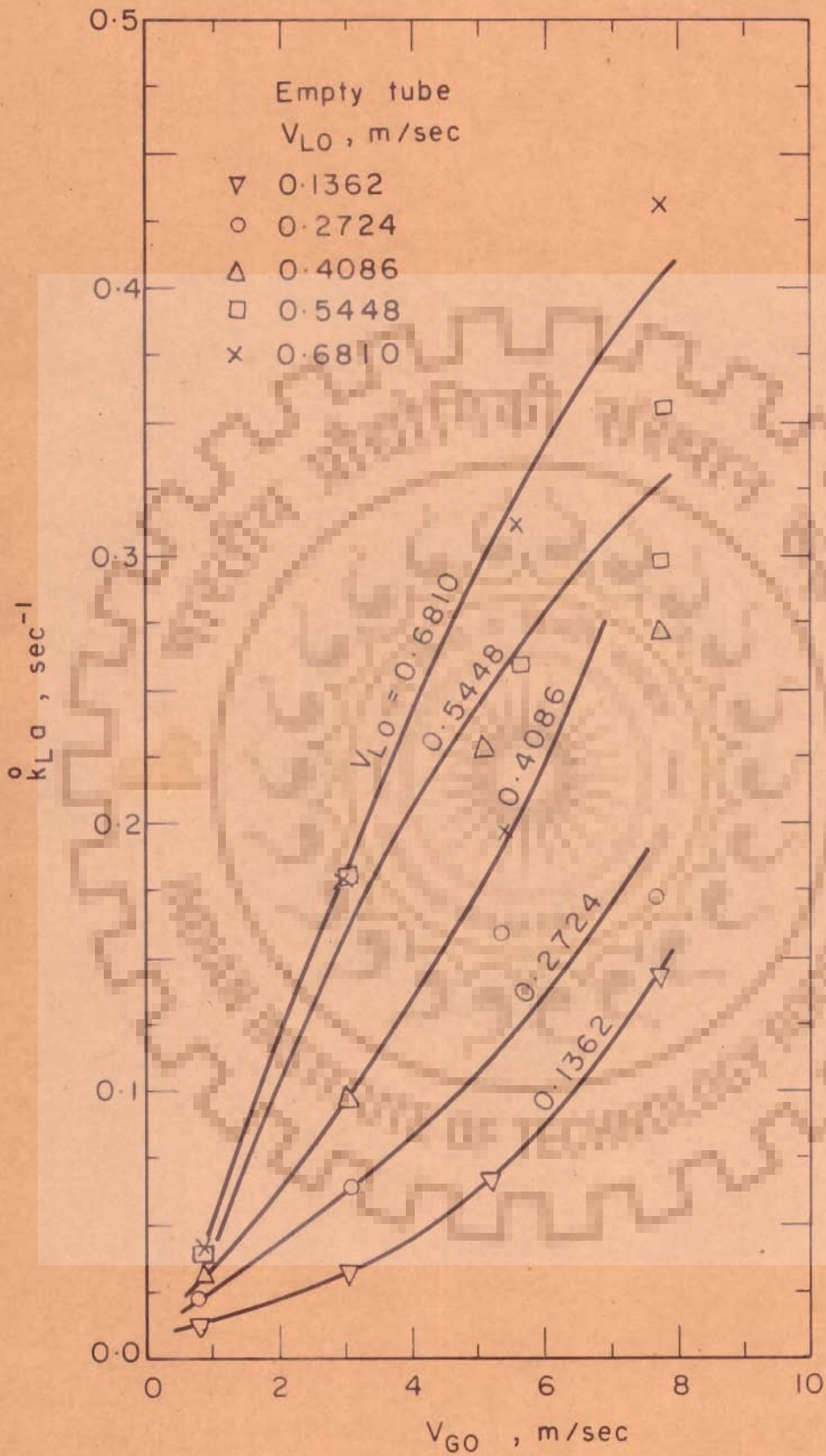
Fig. 6·9 $\overset{o}{k}_L a$ vs superficial gas velocity
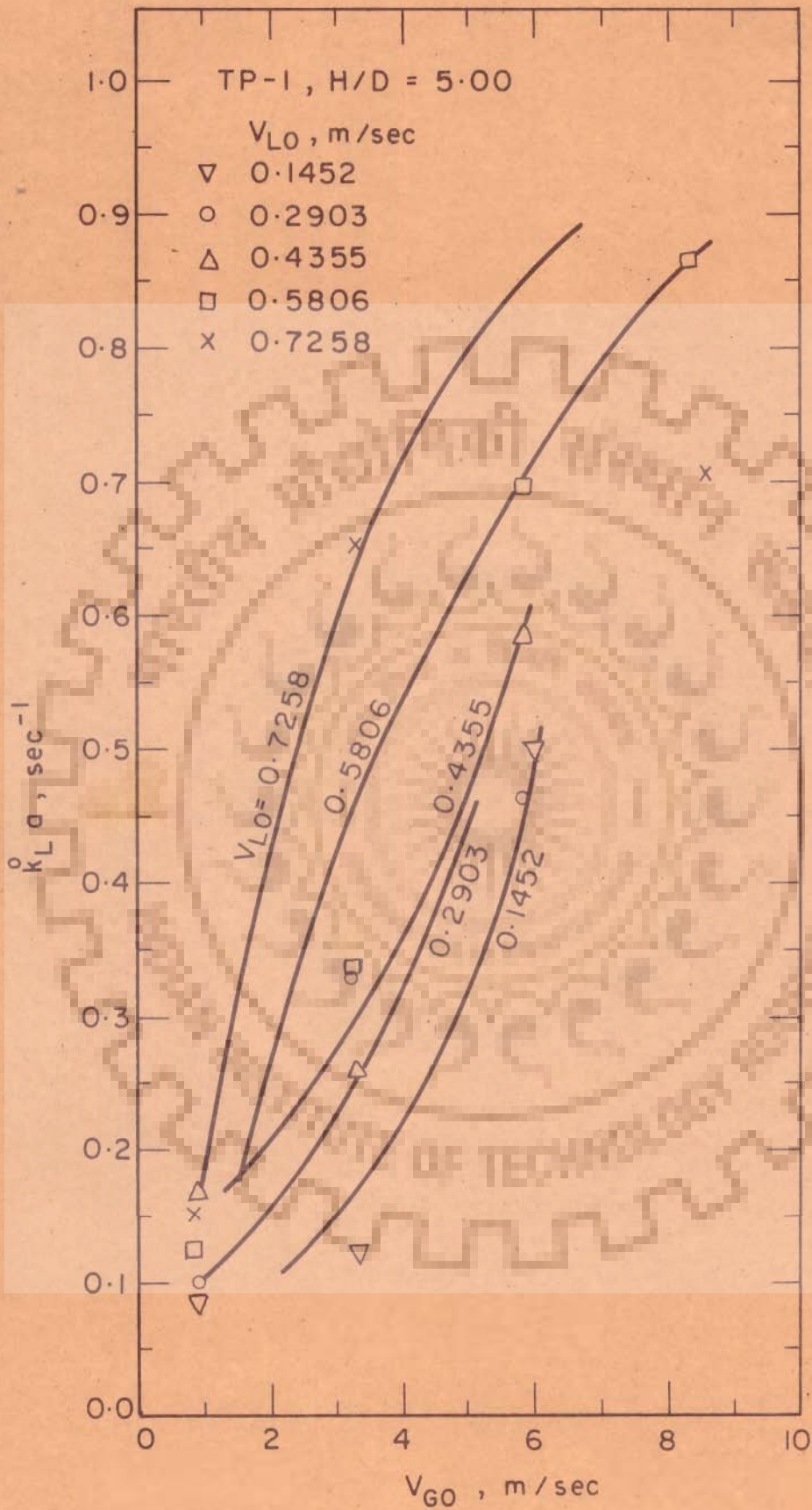
Fig. 6·10 $\overset{o}{k}_L a$ vs superficial gas velocity
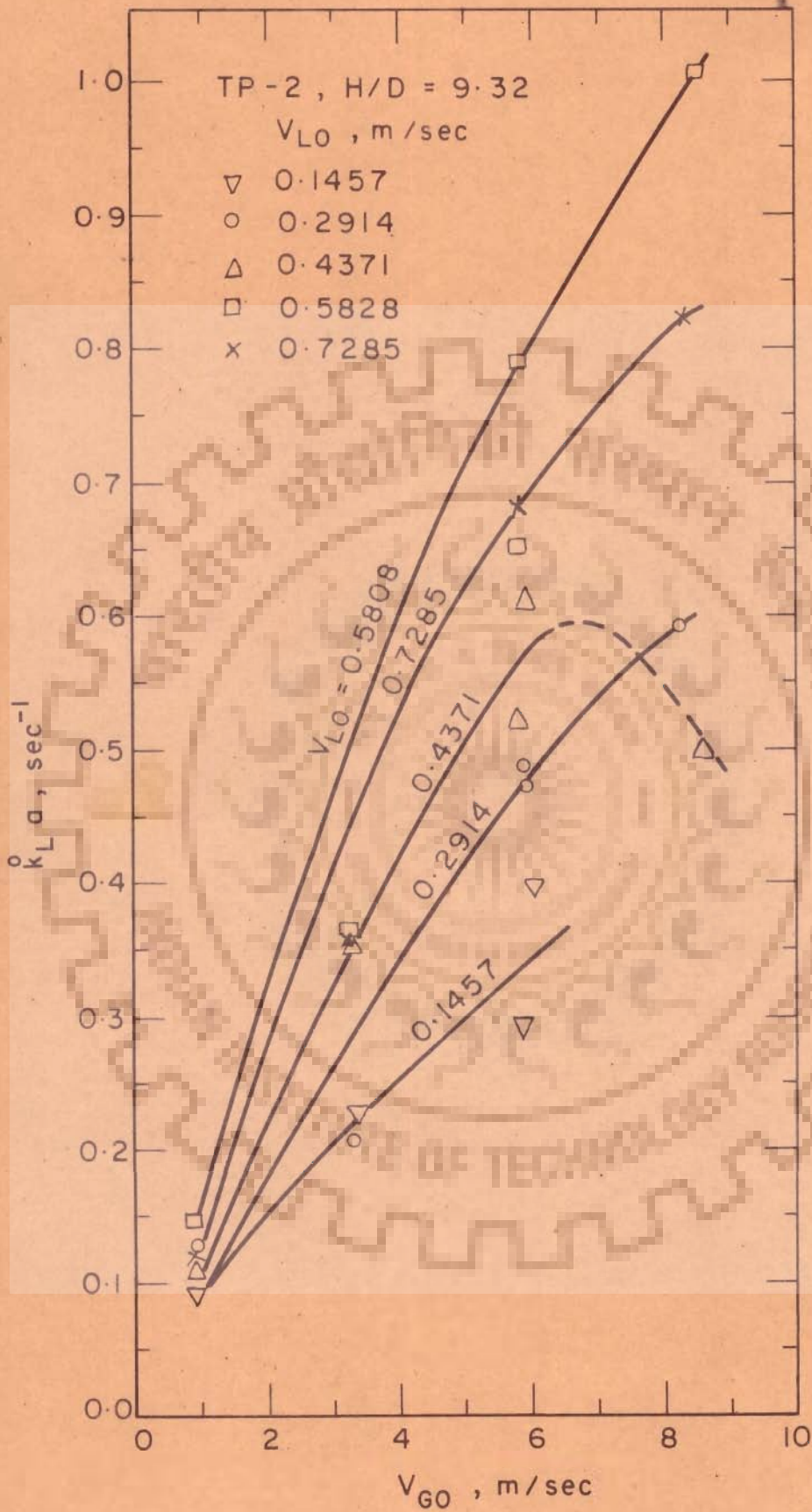
Fig. 6·11 $\overset{o}{k}_L a$ vs superficial gas velocity

sampling point ST1 and accurate determination of $k_L^O a$ was not possible.

A closer examination of these figures shows that for any gas and liquid velocities there is a large increase in the value of $k_L^O a$ if twisted tape inserts are used inside the tubes, but no significant effect appears to exist in the values of $k_L^O a$ for tube with twisted tape insert TP-1, Figure 6.10, and twisted tape insert TP-2, Figure 6.11. Although the difference in the pitch ratio of these tapes is quite large but the difference in $k_L^O a$ values is not at all significant. This means that a change in the flow pattern from axial flow to swirling flow, due to the presence of twisted tapes, increases the mass transfer coefficient $k_L^O a$, but the intensity of swirls due to the difference in pitch ratio does not affect $k_L^O a$ to a significant extent. However, the saturation in the liquid phase reaches at a higher value of superficial liquid velocities when the pitch ratio, y, is low.

The volumetric liquid phase mass transfer coefficient, $k_L^O a$, appears to have a maximum when plotted against the superficial gas velocity V_{GO} for different values of superficial liquid velocity V_{LO}. It is also observed that the maxima lie at different values of V_{GO} at different values of V_{LO} which can be observed in Figure 6.11. In the present study maximum superficial gas velocity V_{GO} was limited to about 10.0 m/sec; hence all the curves in Figures 6.9, 6.10 and 6.11 do not show this maximum. Furthermore, at lower liquid flow rates the

liquid phase reaches saturation condition at first sample tap ST1

and it becomes rather difficult to obtain precise value of $k_L^o a$

at higher superficial gas velocities.

The experimental data is limited and fairly large scatter

is observed in these figures. Similar scatter in the data is also

found in the experimental results of Gregory and Scott (35) for

two phase gas liquid horizontal flow in the slug flow regime and

hence they have not given any plot similar to Figures 6.9, 6.10

and 6.11. Kasturi and Stepanek (103) have plotted their $k_L^o a$

values in a similar manner and obtained smooth curves with

little scatter for their data, but they worked mostly in vertical

annular flow regime and hence it may not be fully appropriate

to compare the results of present investigation with those of

Kasturi and Stepanek.

6.2.2 $\underline{k_L^o a \text{ correlation with two phase Reynolds number } Re_{TP}}$

Figures 6.12 and 6.13 show a plot of volumetric

liquid phase mass transfer coefficient, $k_L^o a$, as a function of

two phase Reynolds number, Re_{TP}, for the case of empty tube

and tube with twisted tape inserts TP-1 (H/D = 5.00) and

TP-2 (H/D = 9.32). From Figure 6.13 it is clear that the

points for twisted tapes TP-1 and TP-2 intermix and separate

figures are not necessary since they do not exhibit separate trend.

In each of the figures two lines of $\pm$ 95 percent confidence limits

and also the best fit line are shown. The equation of the best fit
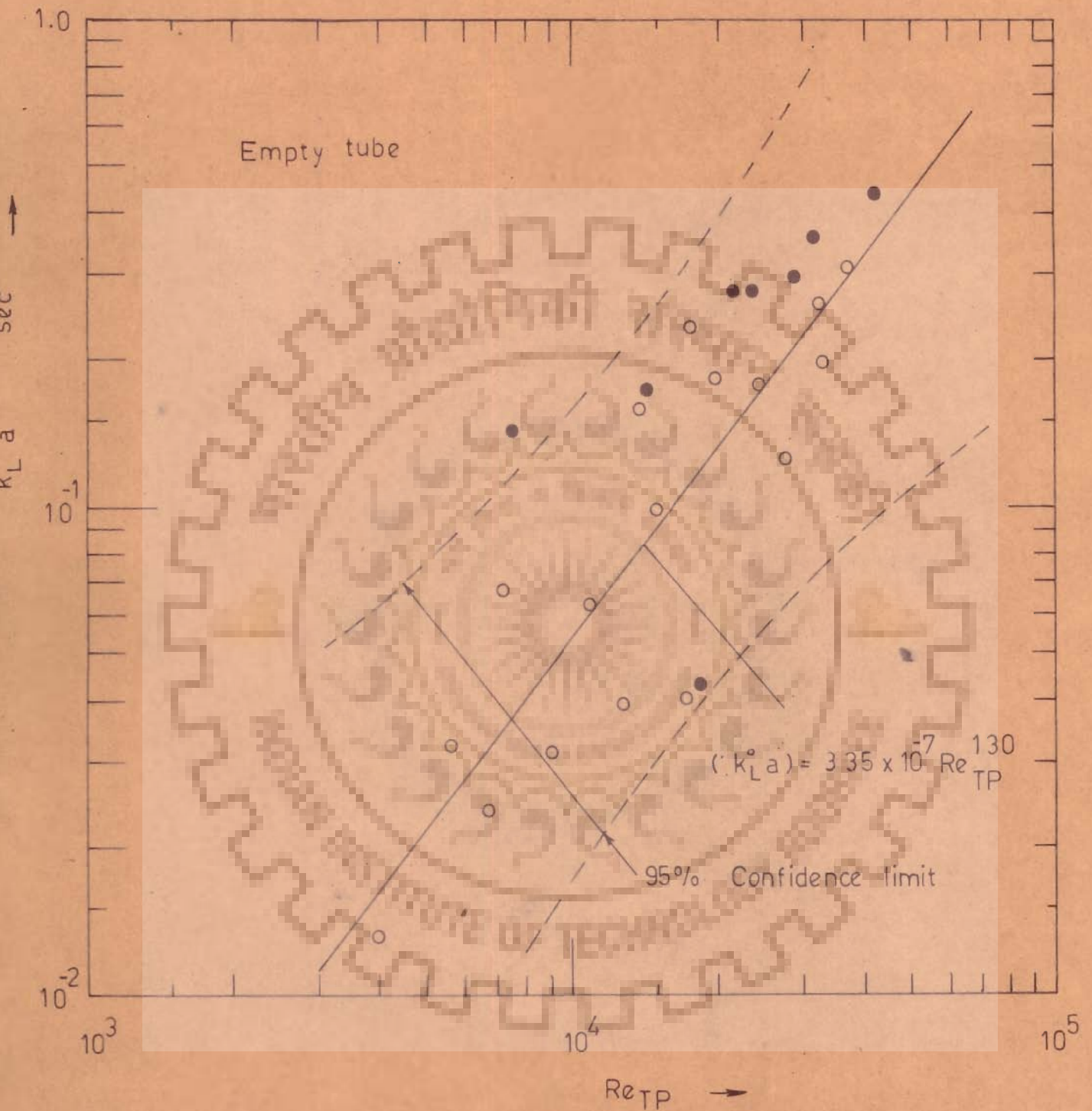
Fig.6.12 $k_L^\circ a$ vs two phase Reynolds number

(dark points not used for correlation)
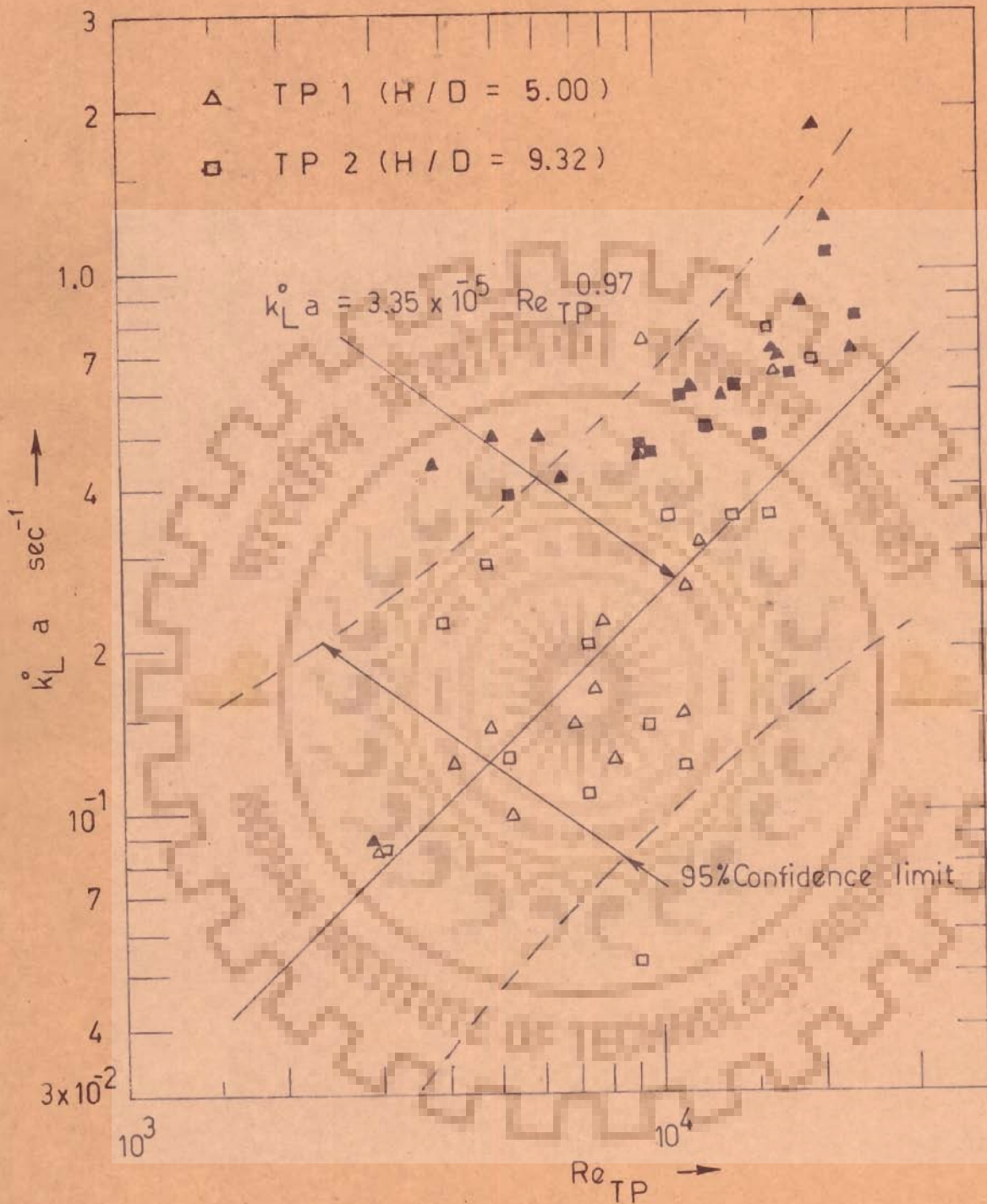
Fig. 6.13 k^o_L a vs two phase Reynolds number
(dark points not used for correlation)

line are given as

Empty tube :

$$(k_L^{\,o}a)_{pred} = 3.35 \times 10^{-7} (Re_{TP})^{1.30} \text{ ; standard error}$$
$$\pm 52.7\% \qquad (6.10)$$

Tube with twisted tape inserts TP-1 and TP-2 :

$$(k_L^{\,o}a)_{pred} = 3.35 \times 10^{-5} (Re_{TP})^{0.97} \text{ ; standard error}$$
$$\pm 48.6\% \qquad (6.11)$$

where $k_L^{\,o}a$ is in sec^{-1}

The values of volumetric liquid phase mass transfer coefficient, $k_L^{\,o}a$, which do not satisfy the reliability criteria as discussed in the section 5.5.1 are also shown in the figures for comparison and establishing the trend. It is observed that most of the data points lie within the 95 percent confidence limits but the scatter and the percentage standard error are quite large. The scatter may be largely due to the two factors, firstly the experimental errors involved in analysing the liquid samples and in measuring the values of gas and liquid flow rates and secondly in the method of estimating two phase Reynolds number, Re_{TP}. The two phase Reynolds number, Re_{TP} is calculated using actual average liquid velocity, V_L, which is based on the estimate of the volume fraction occupied by liquid, E_L, and involves greater uncertainties as discussed in section 3.1.2. It is also possible that Re_{TP} may not be a very satisfactory correlating parameter. However, these correlations between $k_L^{\,o}a$ and Re_{TP} are useful to calculate the liquid phase mass transfer coefficient $k_L^{\,o}$ since

146

Re_{TP} is chosen as a criteria for hydrodynamic similarity. These correlations enable to find the value of $k_L{}^o a$ at the Re_{TP} value equal to that used in chemical absorption experiments used to determine the interfacial area. However, the large scatter from the best fit line makes the usefulness of these relations somewhat uncertain for estimating liquid phase mass transfer coefficient $k_L{}^o$. This aspect is discussed in greater detail in section 6.4.1.

6.2.3 $k_L{}^o a$ correlation with experimental pressure drop

Values of the volumetric liquid phase mass transfer coefficient, $k_L{}^o a$, are shown plotted against the test section pressure drop per unit length in Figure 6.14 for all the experimental measurements. The figure shows that the difference in the trend for empty tube and tube fitted with twisted tape inserts is practically insigificant and the scatter in the data points is relatively large therefore, separate plots and correlations were not considered necessary. The equation of the best fit line is given by :

$$(k_L{}^o a)_{pred} = 0.0647 (\triangle P/ \triangle L)^{0.825} ; \text{ standard error}$$

$$\pm 41.4 \% \qquad (6.12)$$

where $k_L{}^o a$ is in sec^{-1} and $(\triangle P/\triangle L)$ is in kN/m^3. .
In the same figure 95 percent confidence limit lines and data points not satisfying the reliability criteria are also shown. Considerable scatter in the experimental data is observed, but this method of correlation is much better than correlation with
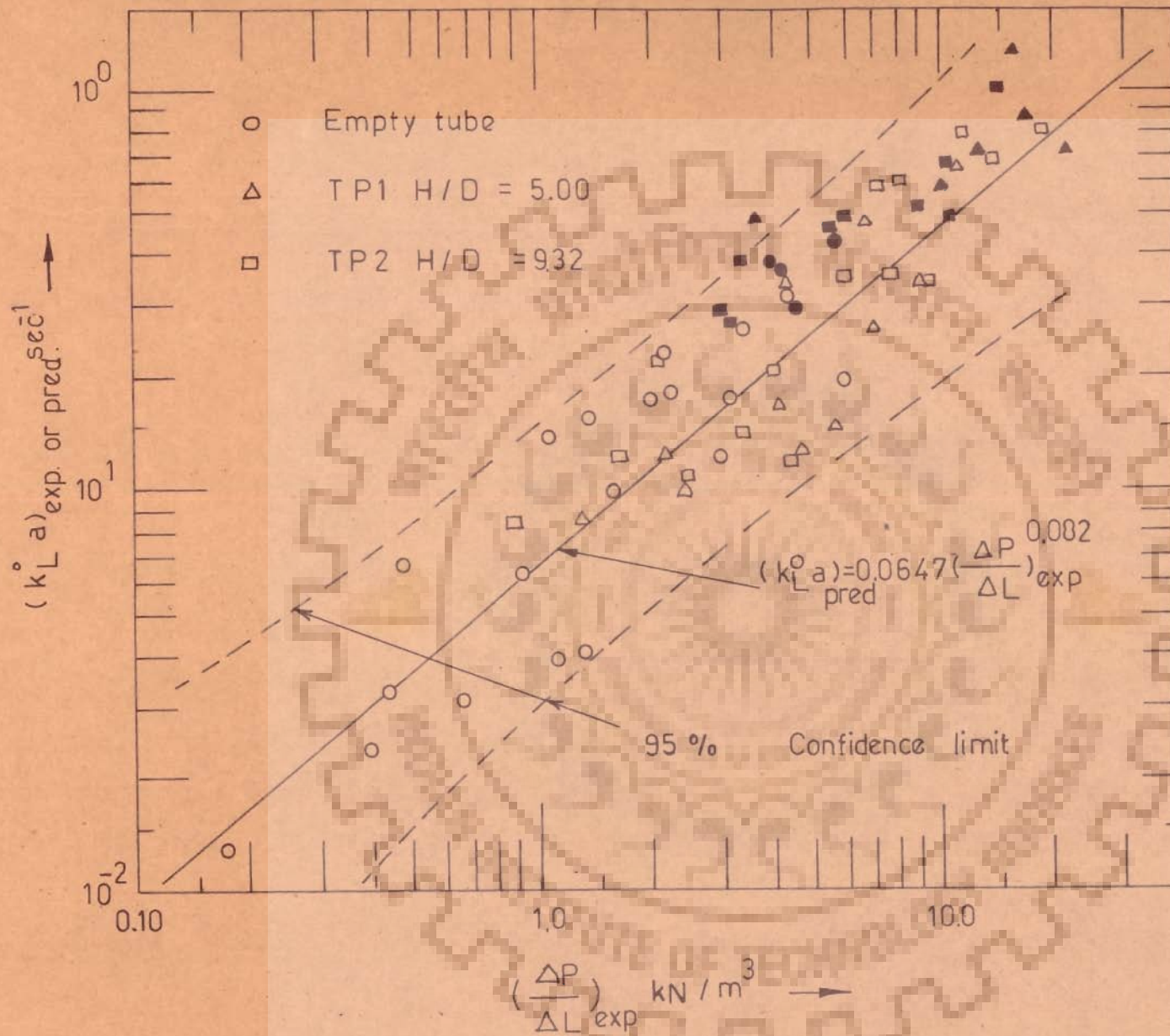
Fig. 6.14 $k_L^o\,a$ vs experimental pressure drop

(dark points not used for correlation)

The axes of the figure read:

Y-axis: $(k_L^o\,a)_{exp.\ or\ pred.}\ sec^{-1}$

X-axis: $(\dfrac{\Delta P}{\Delta L})_{exp}$ kN/m^3

Legend:
- ○ Empty tube
- △ TP1 H/D = 5.00
- □ TP2 H/D = 9.32

$(k_L^o\,a)_{pred} = 0.0647\,(\dfrac{\Delta P}{\Delta L})_{exp}^{0.082}$

95 % Confidence limit

Re_{TP} in view of the smaller value of standard error and the applicability of one correlation to all data points with and without twisted inserts.

Gregory and Scott (35) also correlated their $k_L^o a$ values with the experimental pressure drop values in empty tube for gas - liquid cocurrent slug flow conditions. They found the equation of the best fit line for their experimental data as given by :

$$(k_L^o a)_{pred} = 11.39 (\triangle P/\triangle L)^{1.346} ; \text{ standard deviation}$$
$$49.6\% \qquad (6.13)$$

where $k_L^o a$ is in hr^{-1} and $(\triangle P/\triangle L)$ is in mm Hg/m

A comparison of Equations 6.12 and 6.13 shows that the data of the present study has lesser amount of standard error indicating that the scatter is somewhat less. Also it is observed that the experimental $k_L^o a$ values of Gregory and Scott increase more steeply with an increase in the value of pressure drop as compared to that observed in the present study. The direct comparison of the pre-exponential factors of Equations 6.12 and 6.13 is not possible because of the difference in units. When Equation 6.13 is reduced to the same units as used in Equation 6.12, the value of pre-exponential factor becomes 0.0474 which compares well with the value of 0.0647 found in this study. It will be useful to mention that the superficial liquid and gas velocity ranges used by Gregory and Scott are from 0.22 to 0.775 m/sec for V_{LO} and from 1.125 to 6.82 m/sec for V_{GO} while in the present study

the range is from 0.136 to 0.728 m/sec for V_{LO} and from 0.65

to 10.0 m/sec for V_{GO}. Gregory and Scott used larger pipe

(19 mm internal diameter) as compared to that used in the present

study (13.5 mm internal diameter).

6.2.4   <u>$k_L^o a$ correlation with Jepsen's energy dissipation</u>

<u>parameter for empty tube</u>

In Figure 6.15 all the values of $k_L^o a$ obtained in empty

tube and in tube with twisted tape insert TP-1 and TP-2 are

shown plotted against Jepsen's energy dissipation parameter.

The equation of the best fit line is given by

$$(k_L^o a)_{pred} = 0.0434 (\epsilon_J)^{0.611} ; \text{ standard error}$$

$$\pm 34.1 \% \qquad (6.14)$$

where $k_L^o a$ is in sec^{-1} and $\epsilon_J = (V_{LO} + V_{GO}) (\Delta P/ \Delta L)_{exp}$

is in kN/m^2 sec..

In the same figure two lines for 95 percent confidence limit are

also shown. A closer examination of Figure 6.15 reveals that

different trends exist in the data points for empty tube and those

for the tube with twisted tape inserts. This indicates that

separate correlations for empty tube and for twisted tape

inerts are desirable.

Figure 6.16 shows the values of $k_L^o a$ plotted against

Jepsen's energy dissipation parameter ϵ_J for the experimental

data points in empty tube and the equation of best fit line is found

to be
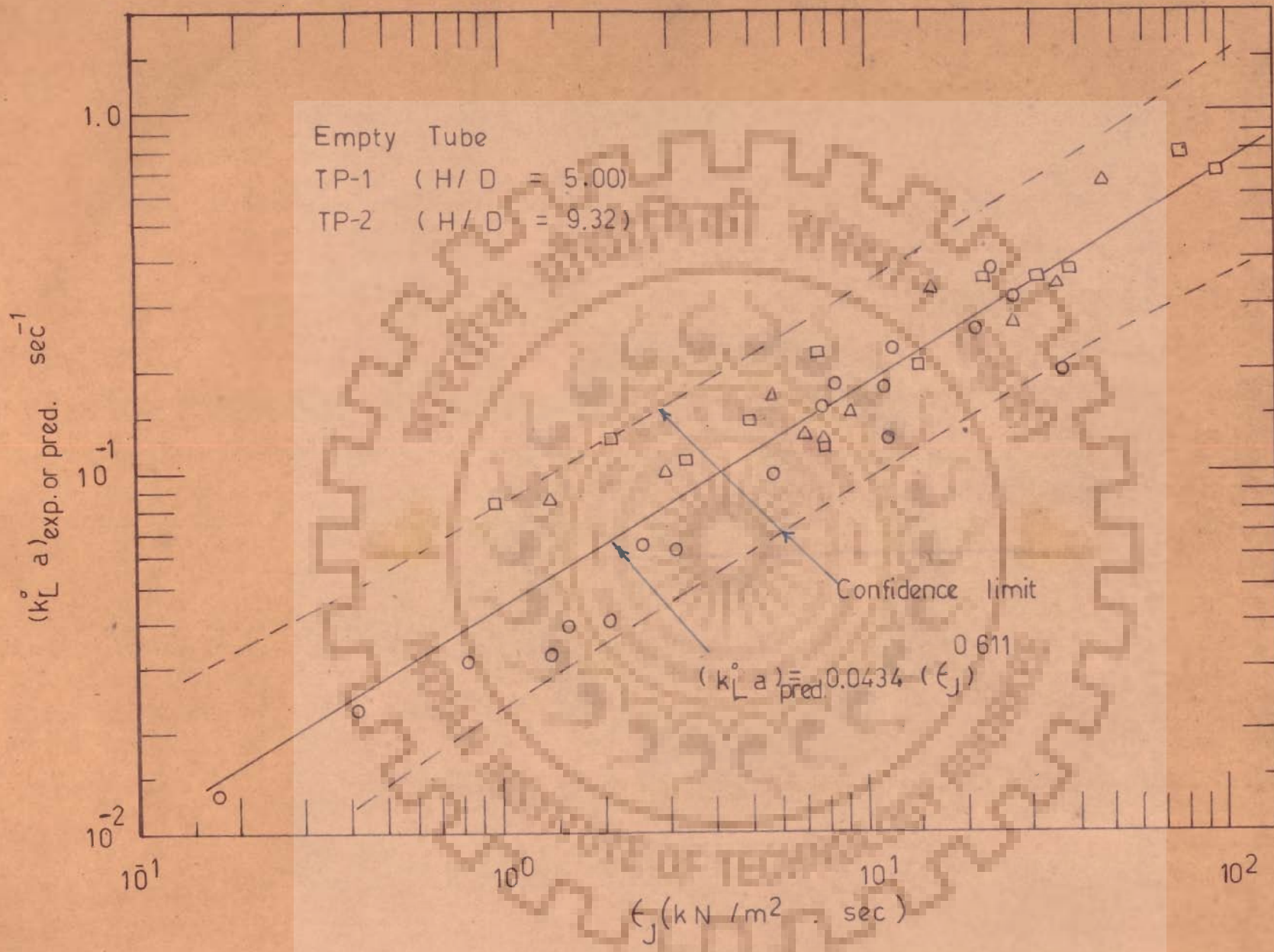
Fig. 6.15 $k_L^o\,a$ vs   Uepsens   dissipation   parameter
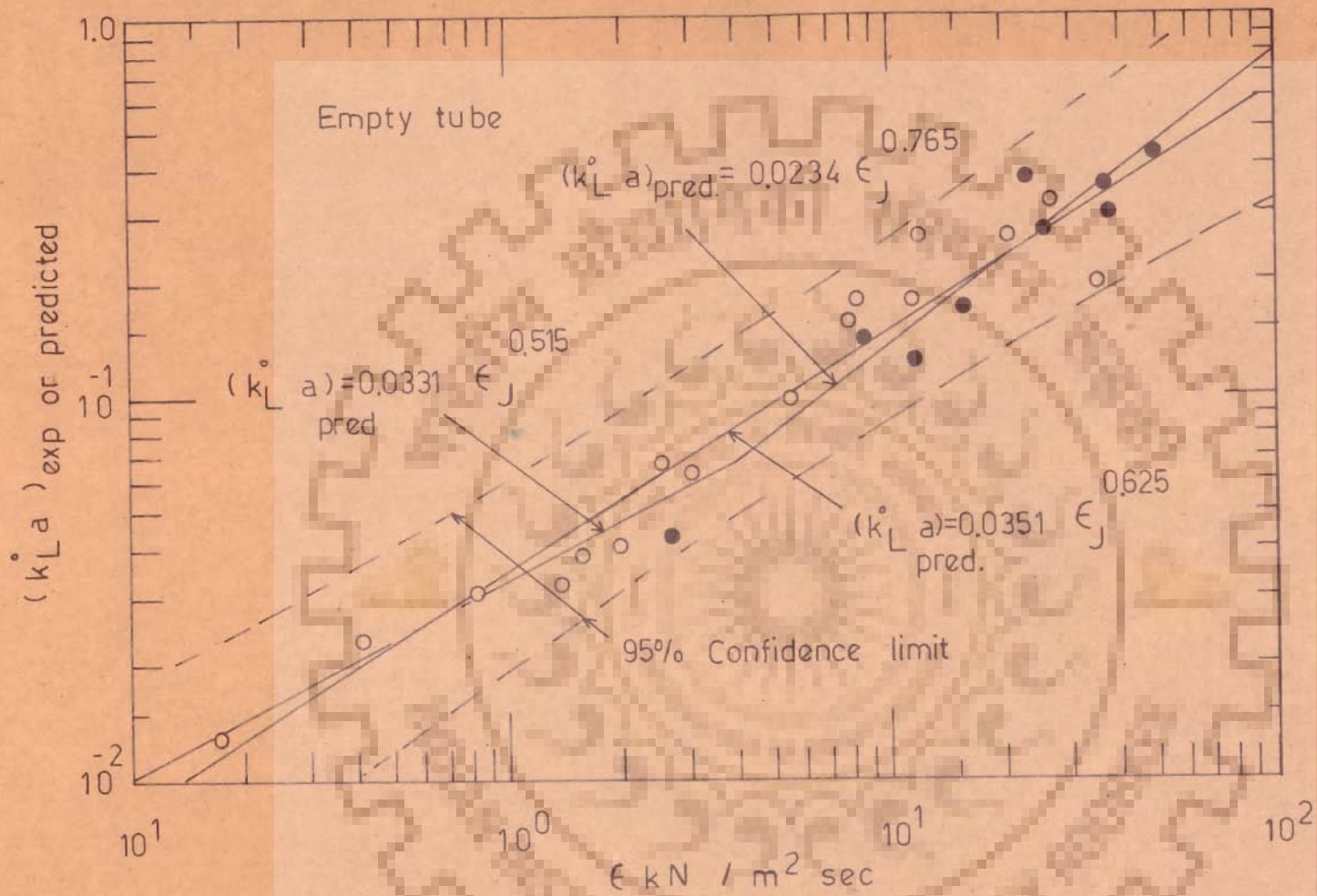
Fig. 6.16 $k_L^o a$ vs Jepson's energy dissipation parameter

$$(k_L{}^{o}a)_{pred} = 0.0351 (\epsilon_J)^{0.625} \; ; \; standard \; error$$

$$\pm \; 23.1 \, \% \qquad\qquad (6.15)$$

The two lines of 95 percent confidence limits and the points which do not meet the reliability criteria are also shown. It is observed that the values of $k_L{}^{o}a$ are well within 95 percent confidence limits even for points not satisfying the reliability criteria. It is also observed in Figure 6.16 that the data exhibit a change of slope at ϵ_J value close to 4.0. The two lines of best fit are given by the expressions :

For ϵ_J less than or equal to 4.0 kN/m^2 sec,

$$(k_L{}^{o}a)_{pred} = 0.0331 (\epsilon_J)^{0.515} \; ; \; standard \; error$$

$$\pm \; 15.8 \, \% \qquad\qquad (6.16)$$

For ϵ_J greater than 4.0 kN/m^2 sec,

$$(k_L{}^{o}a)_{pred} = 0.0234 (\epsilon_J)^{0.765} \; ; \; standard \; error$$

$$\pm \; 38.4 \, \% \qquad\qquad (6.17)$$

It is worthwhile to mention at this stage that the value of percent standard error increases as the number of data points, N, becomes less because of the definition, Equation 5.7. Square of percent deviation is summed for N data points but this sum is devided by (N - 2), since fitting of two constant equation is desired, and then the square root is taken to estimate the percent standard error. Number of data points used for obtaining correlations given by Equations 6.14, 6.15, 6.16 and 6.17 are 38, 16, 8 and 8 respectively. Thus the correlation given by Equation 6.15 is definitely better than that given by Equation 6.14

and similarly the correlation given by Equation 6.16 is definitely

better than that given by Equation 6.15 because the standard error

is lesser inspite of lesser number of data points. However, the

standard error of Equation 6.17 is very high as compared to

that of Equation 6.15 and the difference can not be explained

simply on the basis of the number of data points, that is, 8 as

against 16. Examination of Figure 6.16 reveals that such a high

value of the standard error in Equation 6.17 is due to one point

which lies very much below the best fit line. If this point is

neglected much better fit can be obtained that there is no

a priori justification to neglect that point.

   It may also be noted that allowing a free fit of the data

corresponding to ϵ_J value higher than 4.0 the two lines, given

by Equation 6.16 and the best fit line for the data for ϵ_J

greater than 4.0 did not intersect at point ϵ_J equal to 4.0.

The correlation given by Equation 6.17 was obtained by

specifying the value of intercept corresponding to that obtained

from Equation 6.16 at ϵ_J equal to 4.0 and determining the

best value of slope only to minimize the sum of the square of

error for the eight points having ϵ_J value greater than 4.0.

In order to test the suitability of Equation 6.17 the data points

not satisfying the reliability criteria are also shown in Figure 6.16

and fortunately these points, eight in number, fall quite close to

the best fit line given by Equation 6.17. Therefore, Equation 6.17

is considered satisfactory.

Similar correlations between volumetric liquid phase mass transfer coefficient $k_L{}^oa$ and Jepsen's energy dissipation parameter are also reported by other investigators, of which those reported by Jepsen (83), Gregory and Scott (35) and Zarnett (107) are relevant to the present investigation.

Jepsen has correlated his data as :

For ϵ_J less than 0.05 atm/sec or 5.07 kN/m^2 sec.

$$k_L{}^oa \, D_p{}^{0.68} / (D_A{}^{0.50} \, \sigma^{0.50} \, \mu_L{}^{0.05}) = 3.47 \, (\epsilon_J)^{0.40}$$

$$\cdots \quad (6.18)$$

For $_J$ greater than or equal to 0.05 atm/sec

$$k_L{}^oa / (D_A{}^{0.50} \, \sigma^{0.50} \, \mu_L{}^{0.05}) = 18.75 \, (\epsilon_J)^{0.79} \quad (6.19)$$

where $k_L{}^oa$ is in sec^{-1}

D_p — pipe diameter, in.

μ_L — liquid viscosity, cp.

σ — surface tension, dynes/cm

D_A — gas diffusivity, cm^2/sec

ϵ_J is in atm/sec

Gregory and Scott have correlated their data (for 0.75 inch ID pipe) as :

For ϵ_J less than 0.05 atm/sec.

$$k_L{}^oa = 0.48 \, a \, (\epsilon_J)^{0.722}, \text{ standard deviation } 25.1\% \quad (6.20)$$

For ϵ_J equal or greater than 0.05 atm/sec.

$$k_L{}^oa = 1.874 \, (\epsilon_J)^{1.153}, \text{ standard deviation } 27.9\% \quad (6.21)$$

where $k_L{}^oa$ is in sec^{-1} and ϵ_J is in atm/sec. They have

obtained separate correlations for ϵ_J values less than 0.05 atm/sec and greater than 0.05 atm/sec even though it is reported by them that data exhibit a change of slope at ϵ_J close to 0.04 atm/sec or 4.05 kN/m^2 sec.

Zarnett has correlated his data for 0.719 inch internal diameter pipe as :

$$k_L^{\,o} a = 0.0915 \, (\epsilon_J)^{0.413} \qquad \ldots \qquad (6.22)$$

where $k_L^{\,o} a$ is in sec^{-1} and ϵ_J is in atm/sec. The range of parameters used by Zarnett is such that ϵ_J values are always less than 0.05 atm/sec and hence he correlated his data satisfactorily by a single correlation.

A comparison of the various correlations proposed for physical absorption data obtained in empty tube shows that the correlations obtained in the present study Equations 6.16, 6.17 and Figure 6.16 are quite good with a change in slope at ϵ_J equal to 4.0 KN/m^2 sec and corresponds well with the observations of Jepsen, Gregory Scott and Zarnett.

As pointed out earlier, the comparison of pre-exponential factor is not possible unless the correlations are converted to similar form with identical units for $k_L^{\,o} a$ and ϵ_J. Further, Jepsen has observed that the value of $k_L^{\,o} a$ depends on pipe diameter, D_p, as $D_p^{-0.68}$ if ϵ_J is less than 0.05 atm/sec and $k_L^{\,o} a$ is independent of D_p for ϵ_J equal or greater than 0.05 atm/sec. For proper comparison all the correlations between $k_L^{\,o} a$, expressed in sec^{-1}, and ϵ_J,

expressed in kN/m^2 sec, are written below for 13.5 millimetre internal diameter pipe -

Jepsen

$$k_L{}^o a = 0.0458 \, \epsilon_J{}^{0.4} \qquad \text{for} \quad \epsilon_J < 5.07 \qquad (6.18A)$$

$$k_L{}^o a = 0.0266 \, \epsilon_J{}^{0.79} \qquad \text{for} \quad \epsilon_J \geq 5.07 \qquad (6.19A)$$

Gregory and Scott

$$k_L{}^o a = 0.0228 \, \epsilon_J{}^{0.722} \qquad \text{for} \quad \epsilon_J < 5.07 \qquad (6.20A)$$

$$k_L{}^o a = 0.00925 \, \epsilon_J{}^{1.153} \qquad \text{for} \quad \epsilon_J \geq 5.07 \qquad (6.21A)$$

Zarnett

$$k_L{}^o a = 0.0179 \, \epsilon_J{}^{0.413} \qquad \text{for} \quad \epsilon_J < 5.07 \qquad (6.22A)$$

Present Study

$$k_L{}^o a = 0.0331 \, \epsilon_J{}^{0.515} \qquad \text{for} \quad \epsilon_J \leq 4.0 \qquad (6.16)$$

$$k_L{}^o a = 0.0234 \, \epsilon_J{}^{0.765} \qquad \text{for} \quad \epsilon_J \geq 4.0 \qquad (6.17)$$

The exponent in Equation 6.16 for ϵ_J less than 4.0 kN/m^2 sec is 0.515 which corresponds well with the values of 0.40 and 0.413 reported by Jepsen and Zarnett respectively, but the value of 0.722 for the exponent reported by Gregory and Scott is somewhat higher. Similarly the value of 0.765 for the exponent for ϵ_J greater than 4.0 kN/m^2 sec compares well with the values of 0.79 reported by Jepsen but the value of 1.153 reported for the exponent by Gregory and Scott is somewhat higher. For lower values of ϵ_J less than 4.0 kN/m^2 sec the value of 0.0331 in Equation 6.16 is less than the value of 0.0458 obtained for Jepsen correlation but it is greater than the values of 0.0228 and 0.0179 obtained respectively for Gregory Scott and Zarnett correlations.

For higher value of ϵ_J the value of 0.0234 for pre-exponential factor lies close to the value of 0.0266 for Jepsen correlation but much higher than the value of 0.00935 for Gregory and Scott correlation. It appears that higher values of exponents are responsible for lower values of pre-exponential factor in Gregory and Scott correlations. From above comparison it is clear that the correlations obtained in the present investigation for empty tube are quite close to those reported by Jepsen.

It is difficult to put forward any satisfactory reasoning to explain the change in slope at energy dissipation parameter ϵ_J, value of 4.0 to 5.0 kN/m^2 sec and may be attributed to some unknown change in the hydrodynamic conditions.

6.2.5 $k_L^o a$ correlation with Jepsen's energy disspation

parameter for tube with twisted tape inserts

Figure 6.15 also shows that there is no significant difference in the data obtained in tube with twisted tape insert TP-1 and TP-2 to necessitate separate correlations for different tapes. Figure 6.17 shows the values of $k_L^o a$ plotted against Jepsen's energy dissipation parameter for the data obtained in tube fitted with twisted tape inserts TP-1 (H/D = 5.00) and also TP-2 (H/D = 9.32). The equation of the best fit line is given by

$$(k_L^o a)_{pred} = 0.0645 (\epsilon_J)^{0.503} ; \text{ standard error}$$
$$\pm 25.1 \% \qquad (6.23)$$
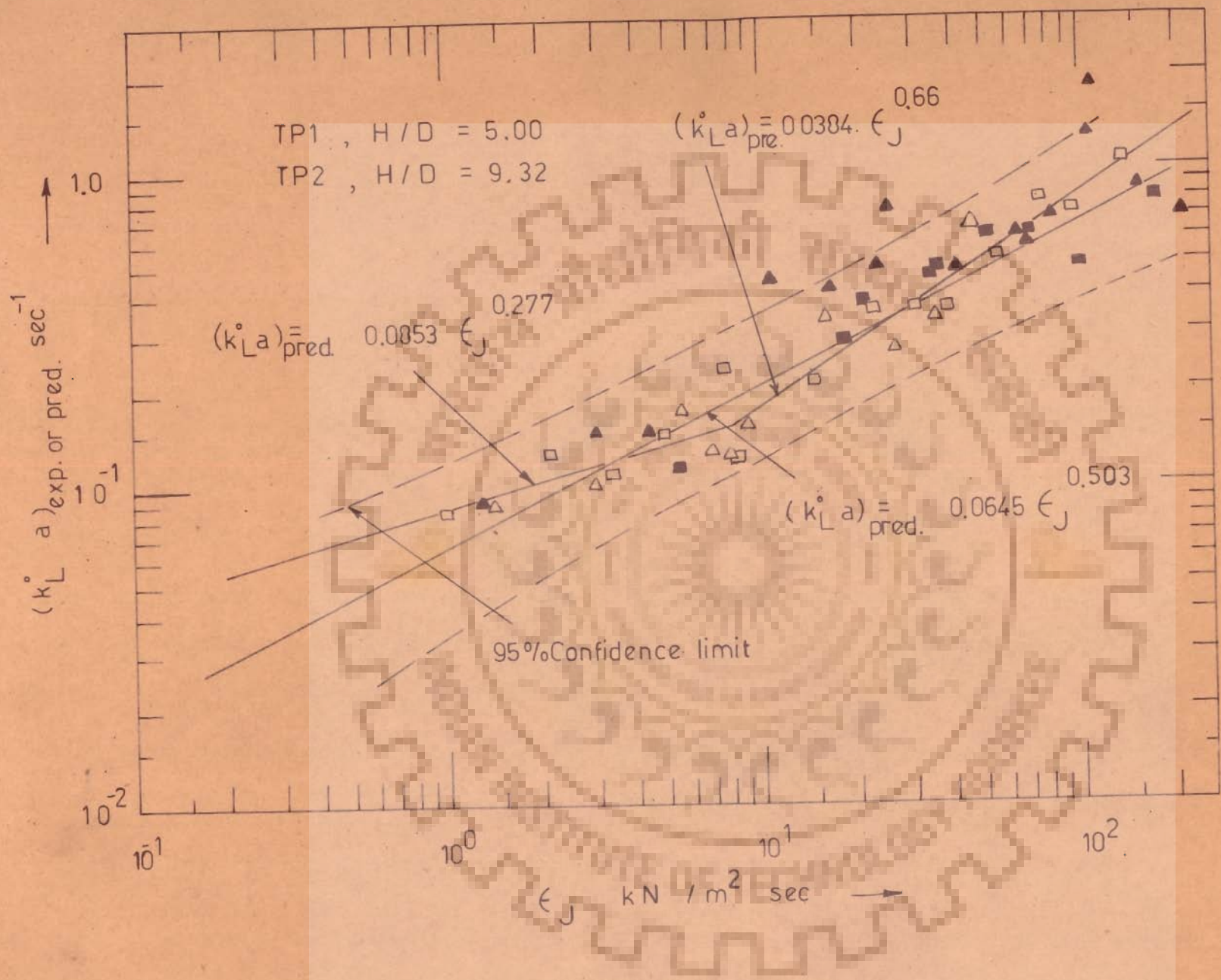
Fig.6.17 $k_L^\circ a$ vs Jepsons energy dissipation parameter
(dark points not used for correlation)

The following labels appear within the figure:

TP1 , H/D = 5.00
TP2 , H/D = 9.32

$(k_L^\circ a)_{pre.} = 0.0384 \cdot \epsilon_J^{0.66}$

$(k_L^\circ a)_{pred.} = 0.0853 \, \epsilon_J^{0.277}$

$(k_L^\circ a)_{pred.} = 0.0645 \, \epsilon_J^{0.503}$

95% Confidence limit

$(k_L^\circ a)_{exp.\ or\ pred.}\ sec^{-1}$

ϵ_J kN / m^2 sec

where $k_L^o a$ is in sec^{-1} and ϵ_J is in kN/m^2 sec.

Similar to Figure 6.16 the data exhibit a change of slope but at ϵ_J value closer to 8.0 kN/m^2 sec for this case. For the data in tube fitted with twisted tape insert TP-1 and TP-2 two lines of best fit are given by the expressions :

For ϵ_J less than or equal to 8.0 kN/m^2 sec

$$(k_L^o a)_{pred} = 0.0853 (\epsilon_J)^{0.277}, \text{ standard error}$$
$$\pm 23.6 \% \qquad (6.24)$$

For ϵ_J equal or greater than 8.0 kN/m^2 sec

$$(k_L^o a)_{pred} = 0.0384 (\epsilon_J)^{0.660}, \text{ standard error}$$
$$\pm 22.7 \% \qquad (6.25)$$

where $k_L^o a$ is in sec^{-1} and ϵ_J is in kN/m^2 sec.

Standard errors of correlations given by Equation 6.24 and 6.25 are less than that of Equation 6.23 inspite of lesser number of data points and Equations 6.24 and 6.25 definitely correlate the data better. It is to be noted that free fit was allowed for 11 data points corresponding to ϵ_J values greater than 8.0 kN/m^2 sec to obtain Equation 6.25 and then specifying the value of $k_L^o a$ from this equation at ϵ_J equal to 8.0 kN/m^2 sec as the intercept for determining the best slope to minimize the sum of the squares of error for the 11 data points having ϵ_J value less than 8.0 kN/m^2 sec to give Equation 6.24. However, the standard error of both equations is quite close to each other and is less than that of Equation 6.23.

No mass transfer studies are reported in the literature
for tubes with twisted tape inserts. It is, therefore, not possible
to compare the results obtained in the present investigation but
an estimate can be made by comparing the correlation given by
Zarnett (107) who carried out experiments on the absorption of
carbondioxide from CO_2 - N_2 mixture in aqueous diethanol amine
(DEA) solutions in rifled tubes. He used internal spiral ribs to
generate the swirling flow and to investigate the effect of swirl
intensity on volumetric mass transfer coefficient and interfacial
area. The swirl intensity was varied by changing the pitch,
ratio, y, of the spiral ribs.

Zarnett (107) correlated his data for rifled tube 0.719 inch
internal diameter pipe with 1/8 inch high spiral ribs of pitch ratio
1.57 and 2.79, and gave the following expressions :

$$k_L^o a \simeq 0.275 \, \epsilon_J^{0.413} , \quad \text{for } \epsilon_J < 0.04 \qquad (6.26)$$

where $k_L^o a$ is in sec^{-1} and ϵ_J is in atm/sec. He also
observed, in conformity with the observation in the present
investigation, that the data for both pitch ratio can be satisfactorily
correlated by a single correlation. He has claimed that the main
effect of the rifled tube is to cause the gas to move away from the
tube wall and flow in the central core. In his case it is probable
that the core may not have any swirl flow, a situation not possible
if twisted tapes are used. If it is assumed that even for rifled tube,
the dependence of $k_L^o a$ on tube diameter, D_p, remains the same
as reported by Jepsen for smooth tubes, Equations 6.18 and 6.19,

then Equation 6.26 can be written for 13.5 milimetre internal

diameter pipe with ϵ_J expressed in kN/m^2 sec for comparison

with the results of present investigation

Zarnett

$$k_L^o a \quad 0.0502 \; \epsilon_J^{0.413}, \quad \text{for} \quad \epsilon_J < 4.05 \; \frac{kN}{m^2 \, sec} \qquad (6.26A)$$

Present Study

$$k_L^o a = 0.0853 \; \epsilon_J^{0.277}, \quad \text{for} \quad \epsilon_J \leq 8.0 \; \frac{kN}{m^2 \, sec} \qquad (6.24)$$

$$k_L^o a = 0.0384 \; \epsilon_J^{0.660}, \quad \text{for} \quad \epsilon_J \geq 8.0 \; \frac{kN}{m^2 \, sec} \qquad (6.25)$$

From the above equations, it is clear that the value of exponent

obtained in the present study is smaller than that obtained by

Zarnett for his correlation for values of ϵ_J less about

4.0 kN/m^2 sec. However, the value of pre-exponential factor

obtained in the present study is nearly seventy percent more than

that found in Zarnett's correlation.

Comparison of correlations, for $k_L^o a$ at ϵ_J less than

4.0 kN/m^2 sec, for smooth tube Equation 6.16, rifled tube,

Equation 6.26A and tube with twisted tape insert, Equation 6.24

reveals that as the flow becomes increasingly swirling the

pre-exponential factor increases but the exponent decreases.

This indicates that at low values of ϵ_J twisted tapes will give

higher value of $k_L^o a$ and as the value of ϵ_J increases, the

use oe twisted tapes become less and less advantageous. A

comparison of Figures 6.16, for empty tube, and 6.17 for

twisted tapes also reveals that the values of $k_L^o a$ are increased

substantially at lower values of ϵ_J by using tubes with twisted tape

inserts. However the effect of twisted tape inserts on the increase

in $k_L^o a$ values becomes less significant as the value of ϵ_J

increases. This is clearly seen from the following values of

effectiveness factor, $Ek_L^o a$ is

ϵ_J, kN/m^2 sec	0.1	0.4	1	4	10	40	100	147
$Ek_L^o a \dfrac{(k_L^o a)_{\text{with tape}}}{(k_L^o a)_{\text{empty tube}}}$	4.45	3.29	2.42	1.68	1.33	1.19	1.02	1.00

Therefore, the use of twisted tapes is advantageous at lower

energy dissipation values or in other words at lower flow ranges of

the gas and liquid phases. The higher values of $k_L^o a$ may possibly

be due to two reasons : either the individual liquid phase mass

transfer coefficient, k_L^o, is enhanced or the effective interfacial

area, a, is increased due to increased interfacial turbulence. This

behaviour can be explained as follows. At low values of ϵ_J the

presence of swirling flow aids in the mixing of two phases which

results increased mass transfer rates probably both due to increase

in interfacial area and interfacial turbulence due to mixing and the

use of twisted tape is advantageous. But at high values of ϵ_J the

intensity of swirl flow is so large that most of the gas flows in the

central core while liquid flows near the wall. This type of

situation is unlikely to occur in empty tube. Consequently, the use

of twisted tape at very high values of ϵ_J is likely to retard the

mass transfer rate probably due to lesser surface area as well as lesser interfacial turbulence due to mixing as compared to empty tube.

6.2.6 Volumetric liquid phase mass transfer modulus

From a practical point of view, it is more important to study the effect of the presence of twisted tape insert on volumetric liquid phase mass transfer coefficient per unit pressure drop per unit length, that is

$$KLAMOD = \frac{k_L^o a}{(\Delta P/\Delta L)} \text{ in } \frac{m^3}{kN. \text{ sec}} \tag{6.27}$$

The computed values of KLAMOD are given in Table E.5, Appendix E., along with other measured and calculated parameters, for empty tube and in tube with twisted tape inserts. A careful examination of the tabulated values indicates that no simple correlation can be found to satisfactorily correlate the values of KLAMOD with any other single parameter.

The values of KLAMOD are plotted as a function of superficial liquid velocity for two values of superficial gas velocity for empty tube and tube with twisted tape inserts, TP-1 and TP-2, in Figure 6.18. From the figure it can be observed that for any tube geometry KLAMOD decreases with increasing liquid velocity at a given value of gas velocity and it increases with gas velocity at a given liquid velocity. At low gas velocity the decrease in the value of KLAMOD is very rapid with increase in superficial liquid velocity, V_{LO}, but at higher V_{GO}, superficial gas velocity, the

decrease in the value is not as steep as at lower value of super-
facial gas velocity V_{GO}.

It can also be observed that the curve for twisted tape
insert, TP-2 (H/D = 9.32), always lies above the curves for empty
tube and twisted tape insert, TP-1 (H/D = 5.00), in the entire range
of V_{LO} at lowest gas velocity but the three curves approach close
to each other at high liquid velocity. Further, the curve for twisted
tape TP-2 for higher gas velocity is always above the curve for
twisted tape TP-1, but the curve for TP-2 lies above the curve for
empty tube at V_{LO} lower than approximately 0.40 m/sec and it lies
below the empty tube curve for higher liquid velocities. It is, therefore,
clear that if KLAMOD or the modulus of $k_L^o a$ is the criteria
used for designing the absorber, then the use of twisted tape with
very small pitch ratio is always undesirable because increase in
the pressure drop is much more significant than the increase in
$k_L^o a$. At lower gas velocities it appears that superimposition
of mild swirl flow may be of advantage at superficial liquid velocity
upto about 0.8 m/sec but at higher gas velocity the advantage may
be restricted to much lower liquid velocity.

6.3.1 The Effective Interfacial Area, a.

The effective interfacial surface area between the gas and
the liquid were calculated from the chemical absorption experiments by
the method discussed in sections 3.3 and 3.4. The values of inter-
facial surface area, a, are plotted against the superficial
gas velocity, V_{GO}, with superficial liquid velocity, V_{LO} ,
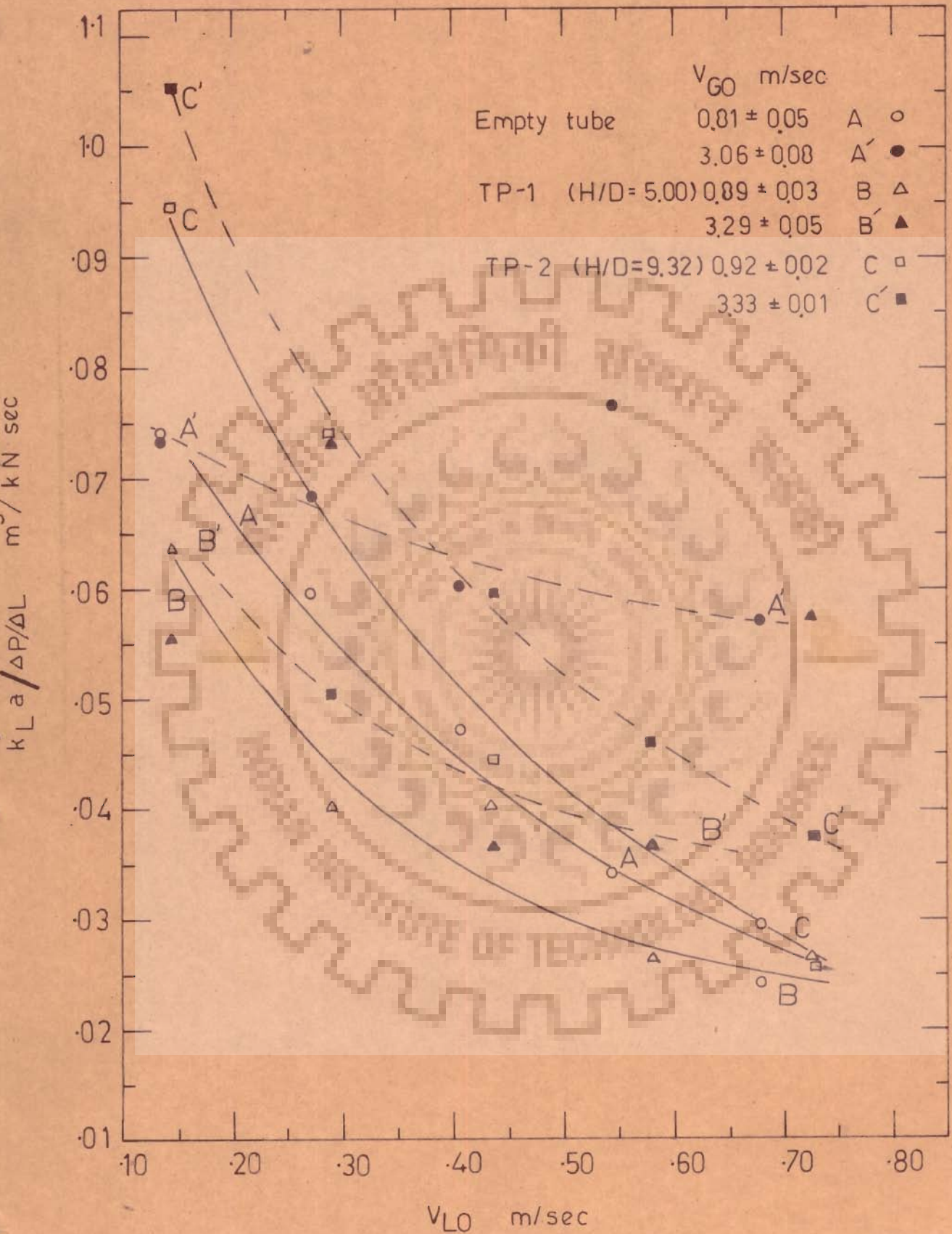
Fig.6.18 Volumetric mass transfer modulus(KLAMOD) vs superficial liquid velocity

as parameters in Figs. 6.19, 6.20 and 6.21 for empty tube and tube

with twisted tape inserts TP-1 (H/D = 5.00) and TP-2 (H/D = 9.32)

respectively. From these figures, it appears that in general the

interfacial area increases with an increase in superficial gas velocity

and decrease in the pitch ratio, y. However, the difference in inter-

facial area is only marginal for two tapes of different pitch ratio but

these values are 1.5 to 4.0 times the values obtained in empty tube.

It is observed in Fig. 6.19 that for flow in empty tube the values

of interfacial area increases initially with an increase in superficial

liquid velocity, V_{LO}, upto a value of 0.41 m/sec but further increase in

V_{LO} decreases the interfacial area. Similar trends are also observed

in Figs. 6.20 and 6.21 where higher values of interfacial area are

obtained for superficial liquid velocity, V_{LO}, value of approximately

0.44 m/sec.

For empty tube, Fig. 6.19, the curves are nearly straight lines

and they tend to diverge at higher gas velocities. For twisted tape inserts,

Figs. 6.20 and 6.21, most of the curves show a rapid increase in the

value of interfacial area initially as the value of superficial gas velocity,

V_{GO}, increases but it is observed that this rate of increase in inter-

facial area decreases with further increase in the superficial gas

velocity. It is also observed that for twisted tape inserts the effect of

increasing the liquid velocity even at lower gas velocity has a pronounced

effect, while most of the curves for different liquid velocities tend to

approach an interfacial area value of about 100 m^2/m^3, at a liquid

velocity of about 1.0 m/sec.
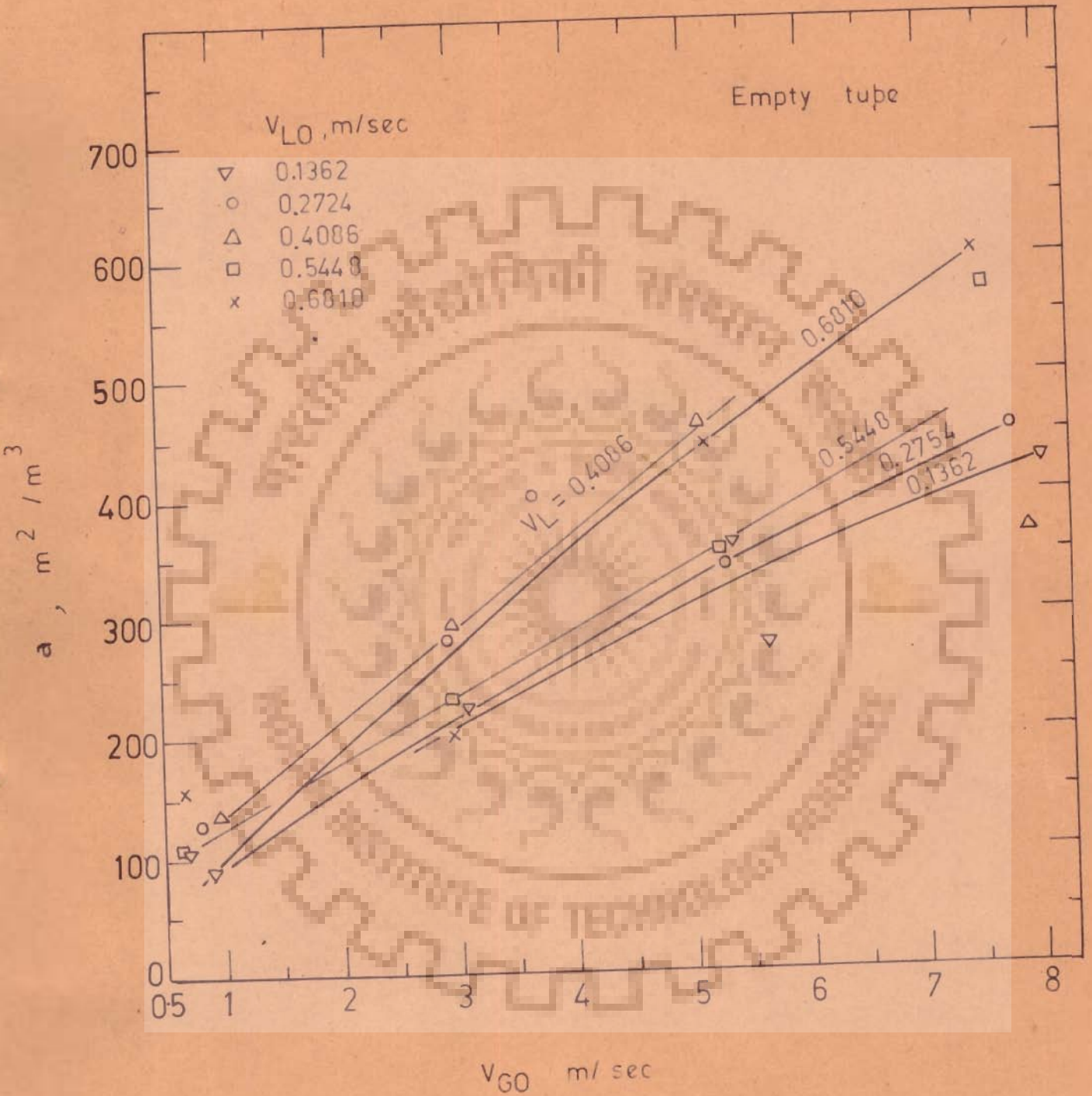
Fig.6.19 Interfacial area vs superficial gas velocity
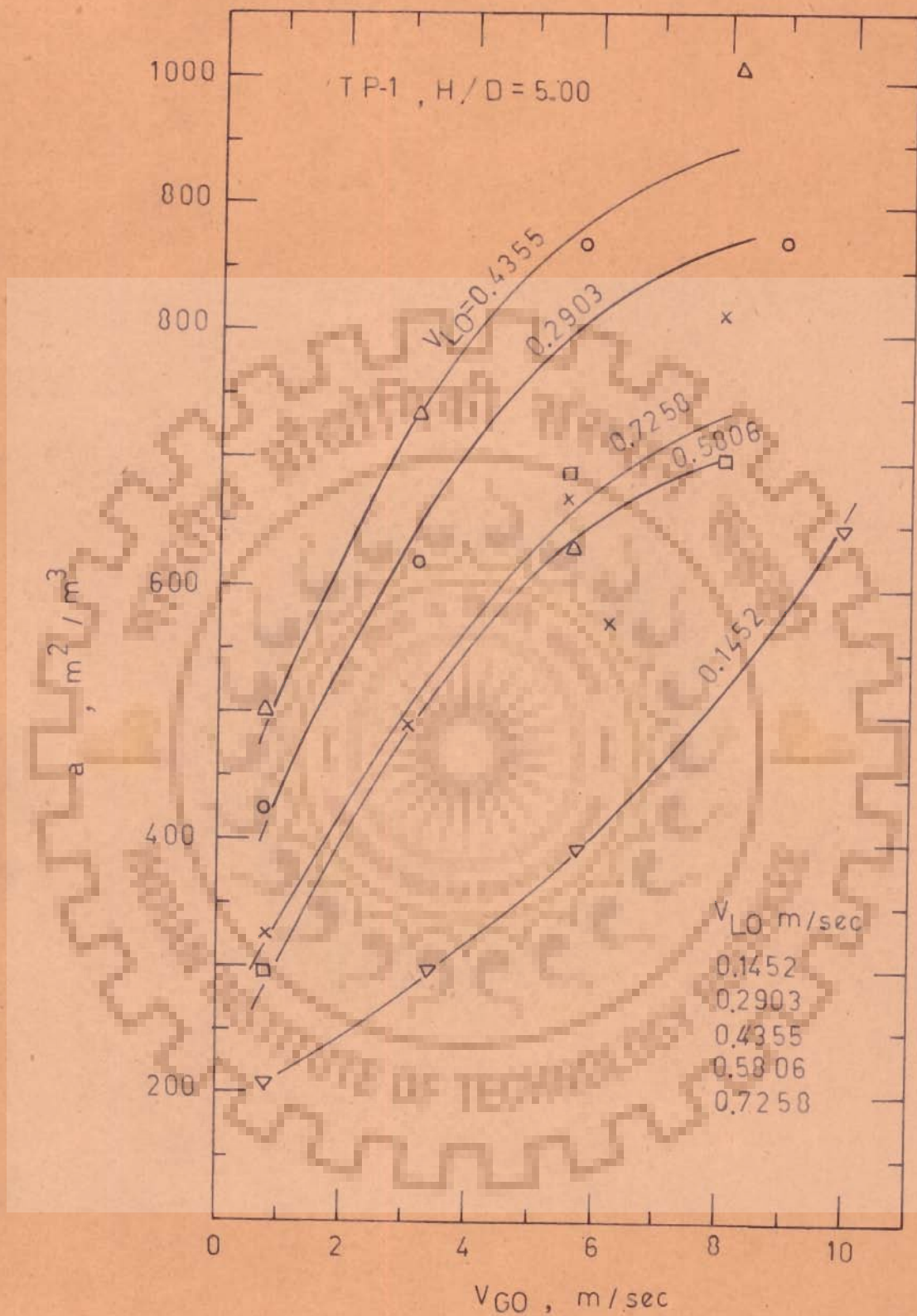
Fig 6.20 Interfacial area vs superficial gas velocity
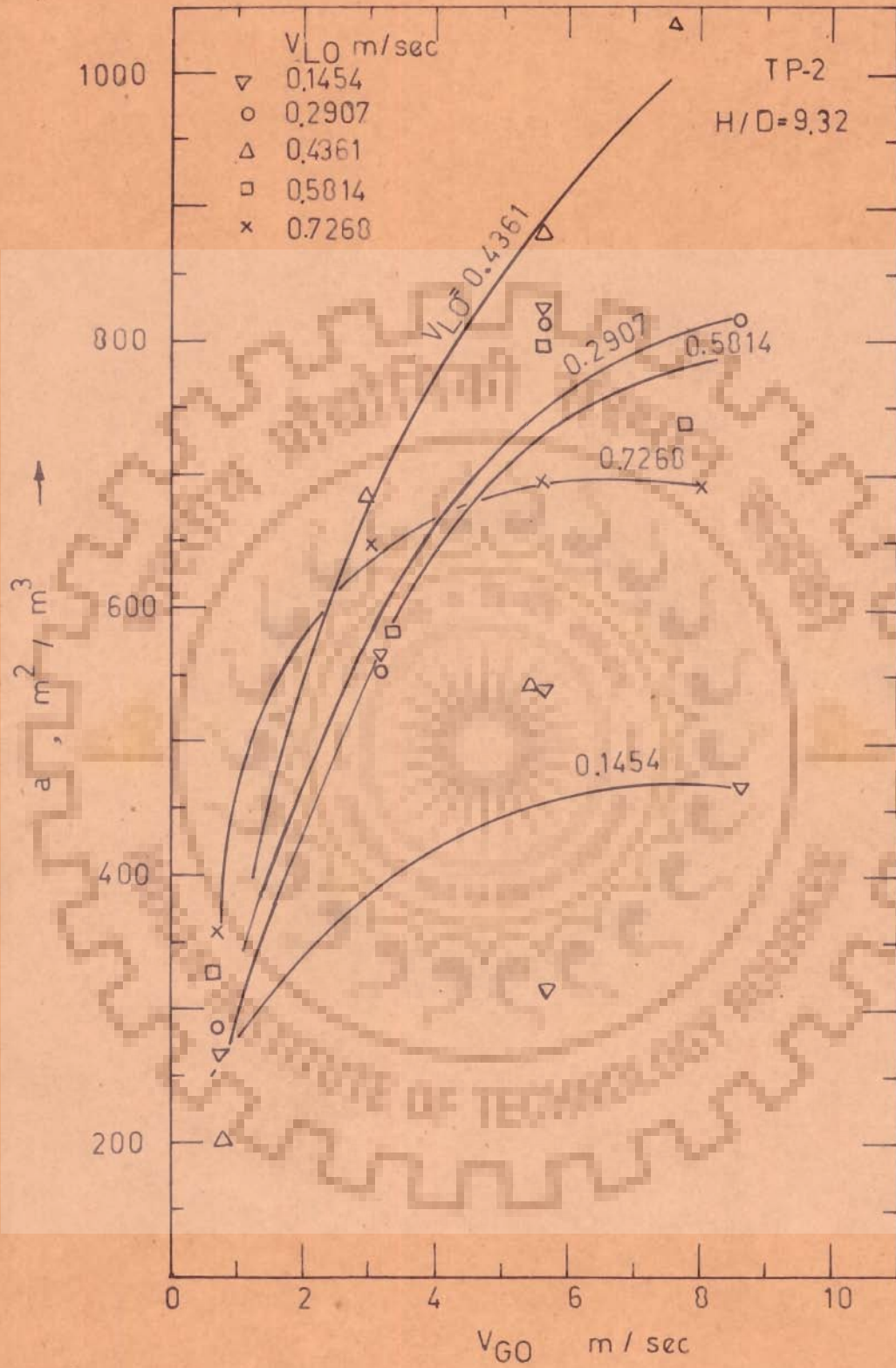
Fig 6.21 Interfacial area vs superficial gas velocity

It is interesting to observe that for gas-liquid slug flow in horizontal pipes, at any gas velocity, largest interfacial area is observed for liquid velocity close to 0.4 m/sec for all tube geometries. Some unascertained hydrodynamic factors may be responsible for this behaviour and further experimentation may be needed to establish the reasons precisely.

Large scatter is also observed from the values reported by Gregory and Scott (35) and it is comparable to our results as presented in Fig. 6.19 for chemical absorption in empty tube. It can be observed from their results that interfacial area increases both with the increase in gas and liquid velocities and no maximum in interfacial area is reported either for liquid or gas velocity. Wales (95) reported his results for interfacial area in two-phase annular and dispersed flow regimes using horizontal pipe of 1.0 inch internal diameter. He plotted the interfacial area against mass flow rate of the gas with liquid mass flow rate as a parameter. It is observed from his results that the interfacial area rises with the increase in gas and liquid mass flow rates.

Kasturi and Stepanek (102) reported interfacial area in cocurrent gas liquid flow in vertical tubes using the same gas and liquid system as used in the present study. They reported that for any liquid velocity interfacial area increases with the gas velocity reaches a maximum value then decreases with further increase in V_{GO}. They argued that with an increase in gas velocity, the liquid becomes more dispersed but, at the same time, the liquid hold up decreases. At lower gas velocities, increased dispersion is dominant, while beyond a certain

gas velocity the liquid hold up becomes the controlling factor and the

reduction in interfacial area values may be attributed to the decreasing

liquid content at higher gas velocities. They further argued that the

interfacial area must be zero when no gas is flowing in the pipe and may

approach zero again at very high gas flow rates when the liquid holdup

tends to approach zero. Kasturi and Stepanek did not observe that the

interfacial area, at any gas velocity, reaches a maximum with increase

in liquid velocity and then starts decreasing. However, the maximum

liquid velocity used by them is limited to about 0.5 m/sec and they

investigated annular and annular-mist flow regimes in a vertical pipe.

6.3.2   Interfacial Area Correlation with two phase Reynolds number Re_{TP}

Interfacial surface area, a, is plotted against two phase

Reynolds number, Re_{TP}, in Figs. 6.22 and 6.23 for the case of empty

tube and for the tube with twisted tape inserts TP-1 (H/D = 5.00) and

TP-2 (H/D = 9.32) respectively. Again it was not considered necessary

to have separate plots for each tape. These correlations are similar

to the ones described for Figs. 6.12 and 6.13 in section 6.2.2 for

volumetric liquid phase mass transfer coefficient, $k_L^o a$, except that

the scatter is relatively less. The equations of the best fit lines are

given as:

Empty tube ;

$$(a)_{pred} = 1.132 \ (Re_{TP})^{0.591} \ ; \ \text{standard error} \pm 47.3 \ \% \tag{6.28}$$

Twisted tape inserts TP-1 and TP-2 ;

$$(a)_{pred} = 33.7 \ (Re_{TP})^{0.323} \ ; \ \text{standard error} \pm 39.2 \ \% \tag{6.29}$$

where , a, is in m^2/m^3 .

Empty tube

$(a)_{Pred.} = 1.132 \ Re^{0.591}$

95 % Confidence limit

$a \ m^2/m^3 \longrightarrow$

Re_{TP}
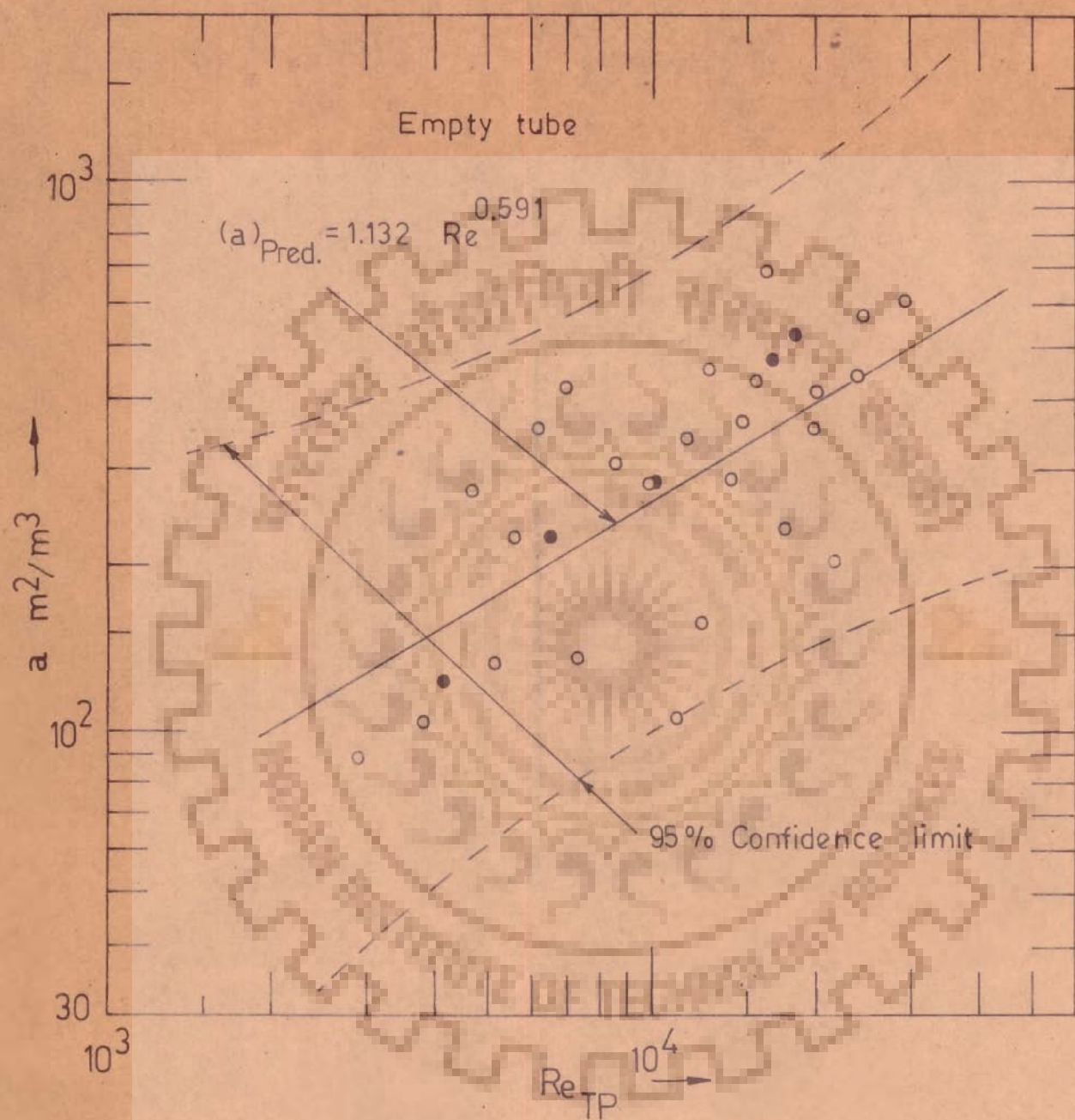
Fig 6.22 Interfacial area vs two phase Reynolds number
(Dark points not used for correlation)
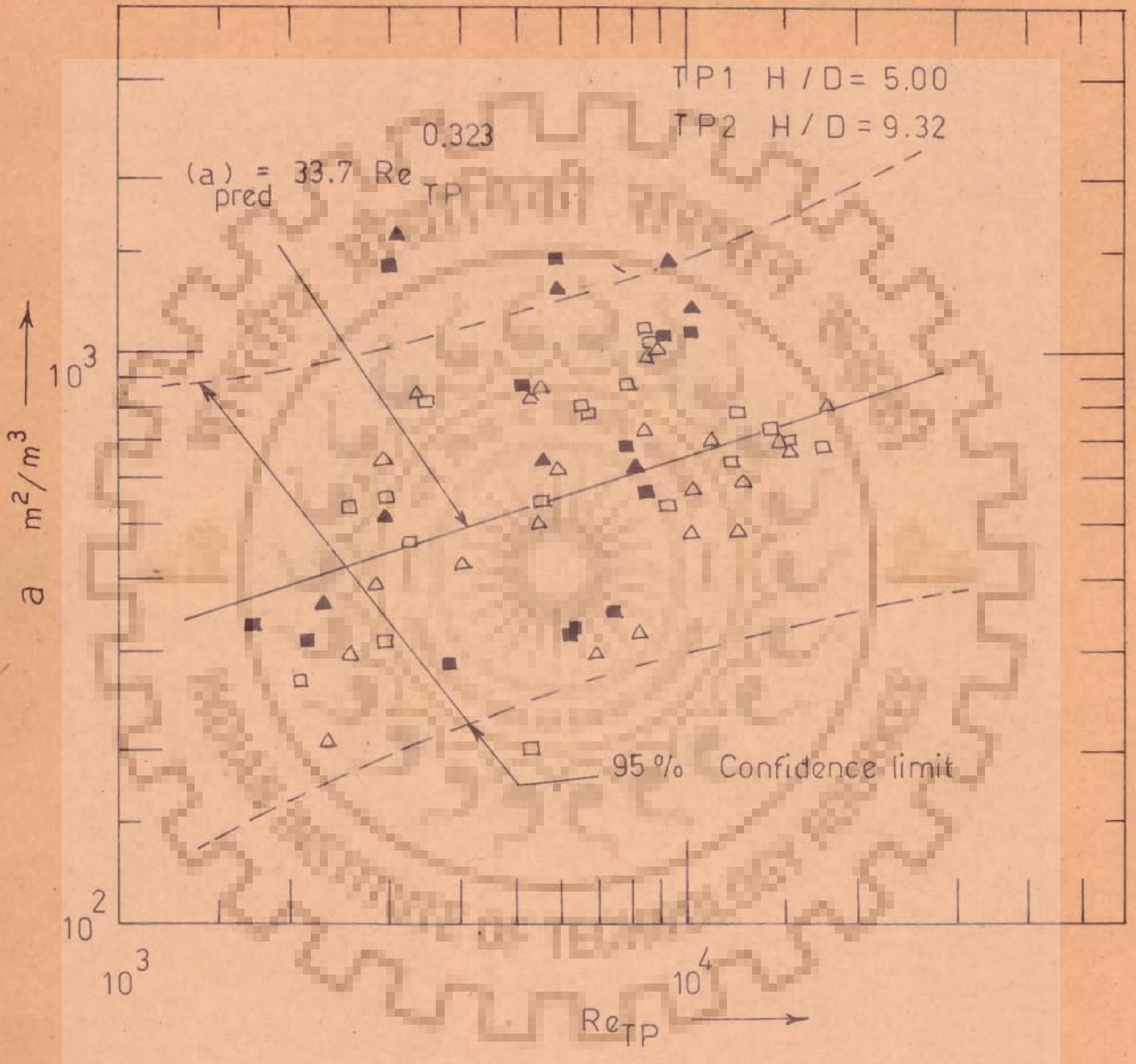
Fig. 6.23 Interacial area vs two phase Reynolds number
(dark points not used for correlation)

Dark points are the values of interfacial surface area data which do not satisfy the reliability criteria as discussed in section. The correlations given by Equations 6.28 and 6.29 have 5 to 10 percent lower value for the standard error as compared to those obtained for k_L^o a and Re_{TP} correlations. However, the scatter is still very large and Re_{TP} can not be considered as a satisfactory correlating parameter. The usefulness of these correlations lies in the fact that the value of interfacial area, a, can be calculated at the Re_{TP} value equal to that used in physical absorption studies used to obtain volumetric mass transfer coefficient k_L^o a. This aspect is discussed in section 6.4.1.

Figs. 6.22 and 6.23 indicate that the interfacial area increases as the two phase Reynolds number is increased, interfacial area increases more steeply with increase in the two phase Reynolds number for flow in empty tube (exponent 0.591) as compared to flow in tube with twisted tape inserts (exponent 0.323) and the presence of twisted tape increases the value of interfacial area to nearly four times at Re_{TP} equal to 2000 and to nearly two times at Re_{TP} equal to 20,000.

6.3.3   Interfacial area correlation with Banerjee's energy dissipation parameter

The values of effective interfacial area are shown in Fig. 6.24 against Banerjee's energy dissipation parameter ϵ_B. Equation of the best fit line for all the data points satisfying the reliability criteria is given by

$$(a)_{pred} = 655.4 \, (\epsilon_B)^{0.259} \; ; \text{ standard error } \pm 48.8 \% \qquad (6.30)$$

where $\epsilon_B = Q_L \, (\frac{\Delta P}{\Delta L})$ in N/sec.
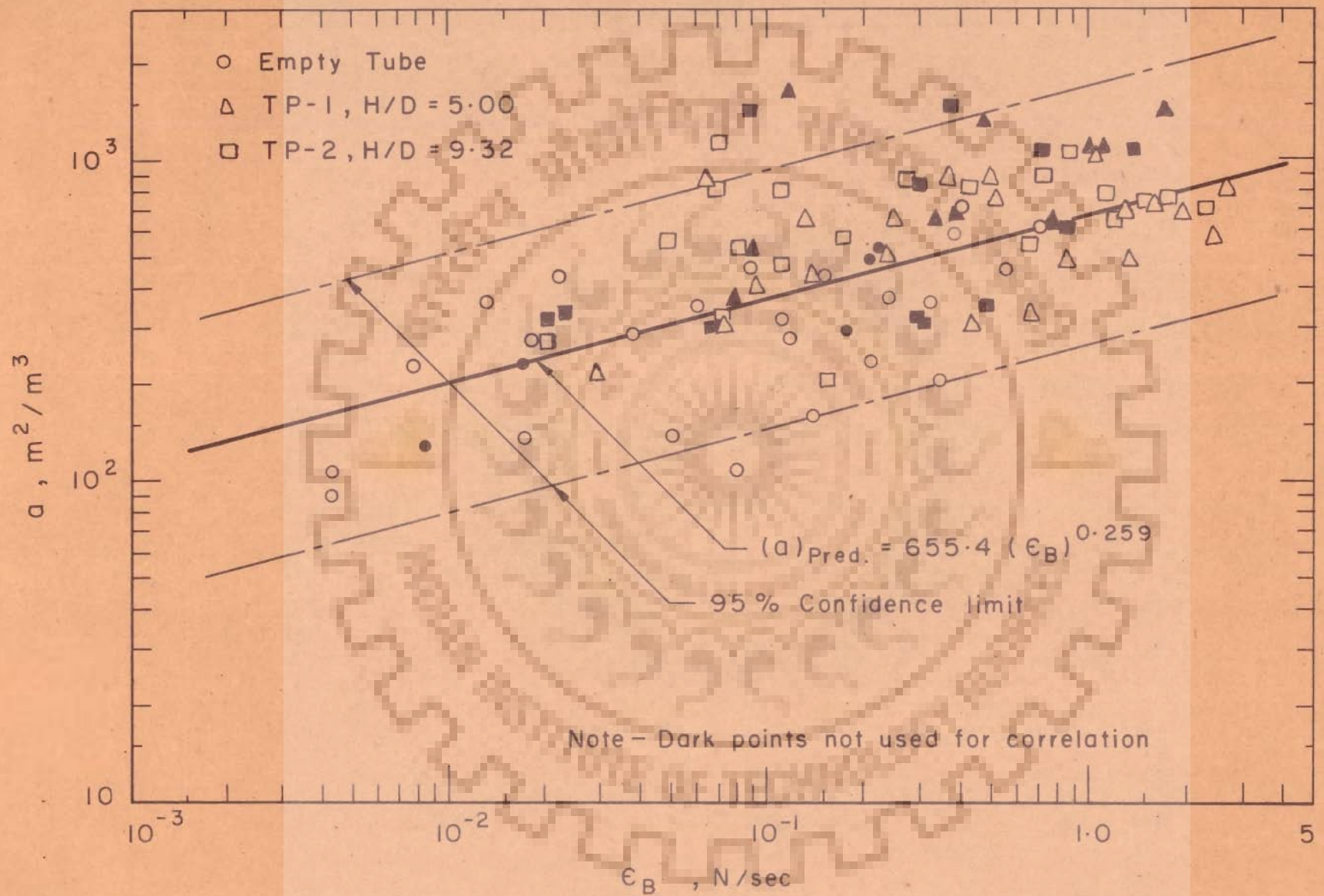
Fig. 6·24 Interfacial area vs Banerjee's energy dissipation parameter

Also shown, with dark points, in the same figure are values which do not satisfy the reliability criteria. Scatter in the data points is large and can be reduced to some extent if the data for the empty tube and tube with twisted tape inserts are correlated separately. The equations of the best fit lines for the empty tube and tube with twisted tape inserts are given by

Empty tube

$$(a)_{pred} = 499.3 \, (\epsilon_B)^{0.233} \; ; \text{standard error} \pm 48. \; \% \qquad (6.31)$$

Tube with twisted tapes TP-1 and TP-2

$$(a)_{pred} = 680.0 \, (\epsilon_B)^{0.166} \; ; \text{standard error} \pm 38.7 \, \% \qquad (6.32)$$

Separate correlations show some marginal improvement but the values of standard errors are still quite high. Strangely, the exponents in Equations 6.31 and 6.32 are both lower than that in Equation 6.30.

Standard errors of Equations 6.31 and 6.32 are high and close to those for correlations of, a, with Re_{TP}, Equations 6.28 and 6.29. It, therefore, appears that Banerjee energy dissipation parameter is also not very satisfactory correlating parameters.

Gregory and Scott (35) also correlated their data with parameter ϵ_B and the equation of best fit line is given as

$$a = 2.039 \, (\epsilon_B)^{0.241} \; ; \text{standard deviation} \; 31.2 \, \% \qquad (6.33)$$

where $a = cm^2/cm^3$ and $\epsilon_B = J/m.sec$

For proper comparison Equation 6.33 is rearranged in the units used in present study to give

$$a = 203.9 \, (\epsilon_B)^{0.241} \qquad (6.33A)$$

where a is in m^2/m^3 and ϵ_B is in N/sec.

A comparison of empty tube data correlation given by Equation 6.31 with that of Gregory and Scott, Equation 6.33A, shows that the value of 0.233 for the exponent obtained in present study is quite close to the value of 0.241 obtained by Gregory and Scott, however the value of pre-exponential factor is nearly 2.5 times that obtained by Gregory and Scott. Thus, the interfacial area values obtained in the present study are nearly 2.5 times larger than those given by Gregory and Scott. For their correlations, Gregory and Scott obtained 31.2 percent standard deviation which, if calculated in the similar manner as done in the present study Equation 5.7 and section 5.7, is about 17 percent lower than that obtained in the present investigation.

Kasturi and Stepanek (102) also plotted their data of interfacial area against Banerjee's energy dissipation parameter ϵ_B on log-log coordinates and found this correlation to be satisfactory but they have not reported the equation for the best fit line.

6.3.4 Interfacial area correlation with Jepsen's energy dissipation parameter

Fig. 6.25 shows a plot of interfacial surface area, a, against Jepsen's energy dissipation parameter. Equation of the best fit line for all the data points satisfying the reliability criteria is given by

$$(a)_{pred} = 184.8 \, (\epsilon_J)^{0.303} \quad ; \text{ standard error} \pm 34.4 \, \% \qquad (6.34)$$

where, a, is in m^2/m^3 and ϵ_J is in $kN/m^2 \cdot sec$

$$(a)_{Pred.} = 184 \cdot 8 \, (\epsilon_J)^{0 \cdot 303}$$

95 % Confidence limit

○ Empty Tube
△ TP-1 , H/D = 5·00
□ TP-2 , H/D = 9·32

a , m^2/m^3

ϵ_J , kN/m^2 sec
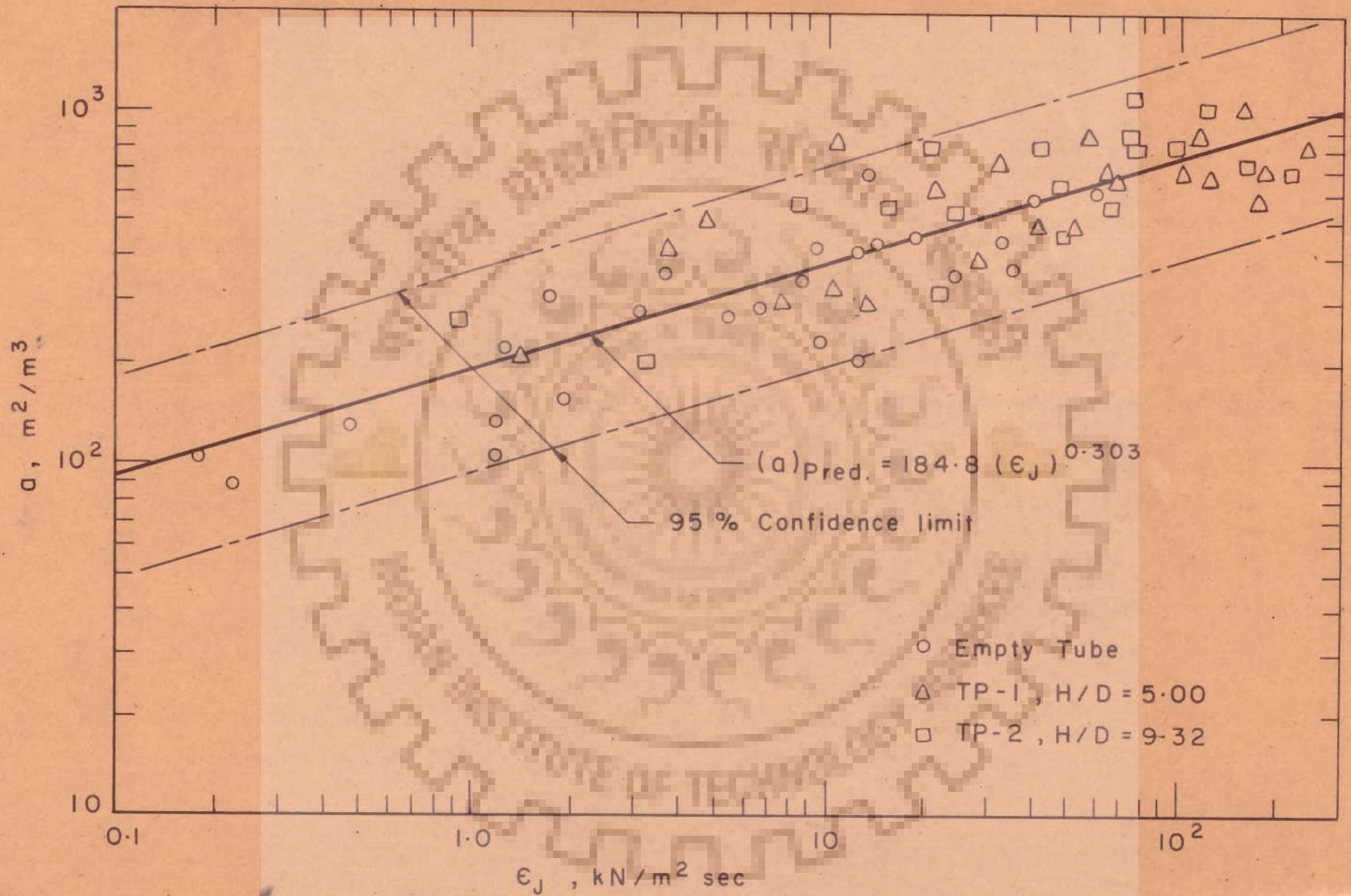
Fig. 6·25 Interfacial area vs Jepsen's energy dissipation parameter ϵ_J
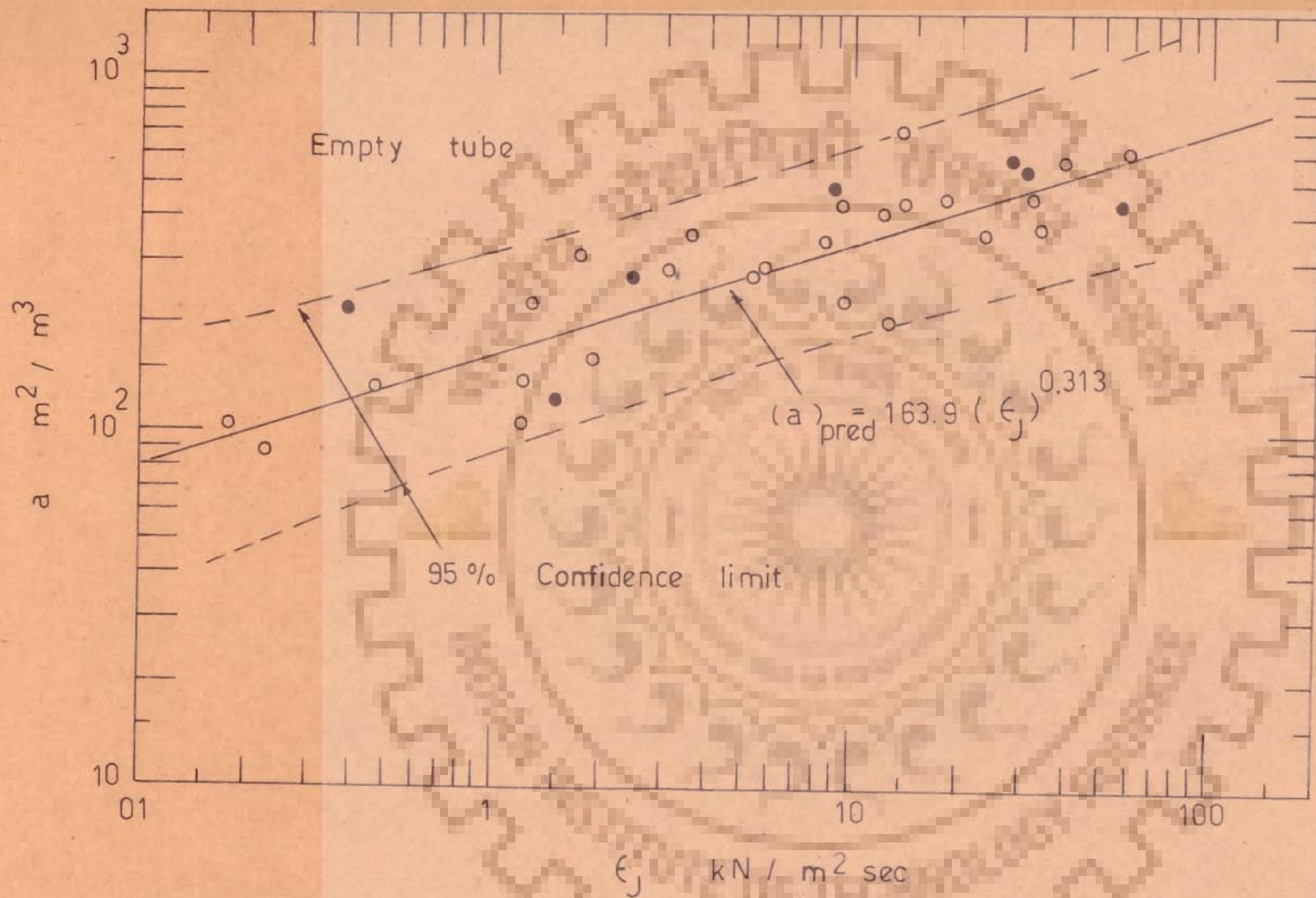
Fig. 6.26   Interfacial area vs Jepsens energy dissipation parameter
(dark points not used for correlation)
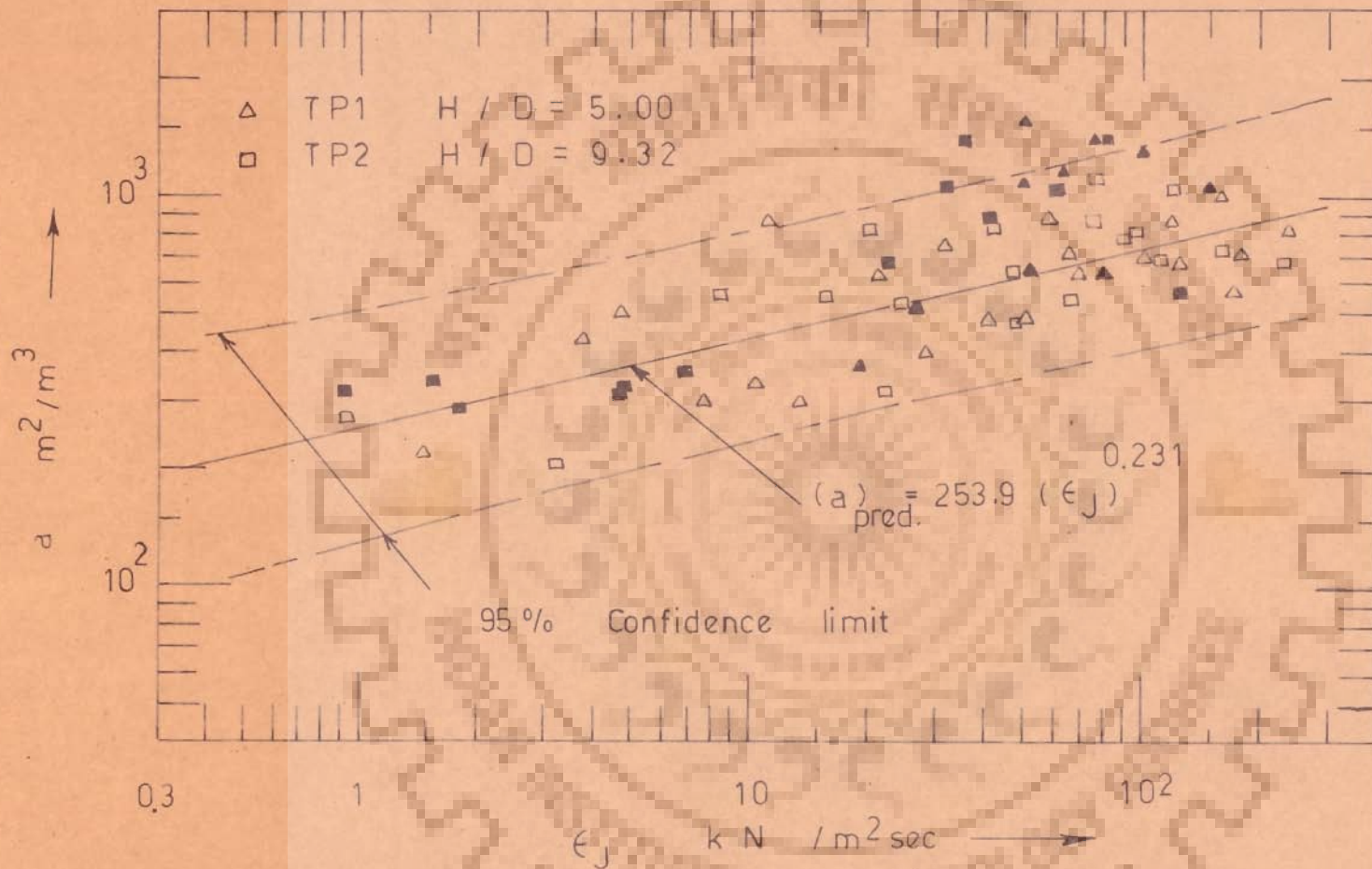
Fig. 6.27 Interfacial area vs Jepsens energy dissipation parameter
(dark points not used for correlation)

The examination of Fig. 6.25 reveals that different trends exist

for the data in empty tube and in the tube with twisted tape inserts.

This indicates that separate correlations for empty tube and for tube

with twisted tape inserts are desirable. Figs. 6.26 and 6.27 show plots

of interfacial area, a, against Jepsen's energy dissipation parameter

for the data in empty tube and the data in tube with twisted tape inserts

respectively. The equations of best fit lines are found to be:

Empty tube:

$$(a)_{pred} = 163.9 \, (\epsilon_J)^{0.313} \; ; \text{standard error} \pm 31.0 \, \% \qquad (6.35)$$

Tube with twisted tape inserts TP-1 and TP-2:

$$(a)_{pred} = 253.9 \, (\epsilon_J)^{0.231} \; ; \text{standard error} \pm 31.2 \, \% \qquad (6.36)$$

Lines of 95 percent confidence limits and the points which do not

satisfy the reliability criteria for the value of, a, are also shown. It is

observed that although the points not satisfying the reliability criteria

were not considered in finding the correlation, these points also lie

within 95 percent confidence limits. The standard error of separate

correlations is reduced by over three percent as compared to the

correlation given by Equation 6.34.

Similar correlations between interfacial area and Jepsen's energy

dissipation parameter are also reported by other investigators and those

relevant to the present investigation are given below:

Gregory and Scott (35) have suggested the following correlation:

$$a = 3.273 \, (\epsilon_J)^{0.313} \text{; standard deviation 25.2 \%} \qquad (6.37)$$

where a is in cm^2/cm^3 and ϵ_J is in atm/sec and for comparison in terms of the units used in this investigation Equation 6.37 becomes,

$$a = 77.2 \, (\epsilon_J)^{0.313} \qquad (6.37A)$$

where, a, is in m^2/m^3 and ϵ_J is in kN/m^2 sec.

Zarnett (107) has correlated his empty tube data by,

$$a = b_0 \, (\epsilon_J)^{0.413} \qquad (6.38)$$

where, a, is in cm^2/cm^3 and ϵ_J is in atm/sec. The value of constant b_0 for empty tube was observed by Zarnett to depend upon the concentration of diethyl amine (DEA) and the values reported by him are 7.92 and 12.04 for 4.5 and 9.5 percent diethyl amine in solution respectively. Zarnett's correlations are rearranged in the units used in this study for proper comparison to give

$$a = 118.2 \, (\epsilon_J)^{0.413} \text{ for 4.5\% DEA solution} \qquad (6.38A)$$

$$a = 179.0 \, (\epsilon_J)^{0.413} \text{ for 9.5 \% DEA solution} \qquad (6.38B)$$

where, a, is in m^2/m^3 and ϵ_J is in kN/m^2.sec

Kasturi and Stepanek (102) have given a figure correlating interfacial area with Jepsen's energy dissipation parameter on log-log coordinates and found considerable scatter and have not reported the equation for the best fit line.

A comparison of various correlations proposed for interfacial area with Jepsen's energy dissipation parameter in empty tube shows that

the correlation obtained in the present study Equation 6.35 and Fig. 6.26
is quite good and exponent with a value of 0.313 is same as that reported
by Gregory and Scott, Equation 6.37A, and reasonably close to a value
0.413 reported by Zarnett. However, it is observed that the values of
interfacial area obtained in the present investigation are somewhat
higher than the value of 163.9 for pre-exponential factor in Equation 6.35
is more than twice the value reported by Gregory and Scott, Equation
6.37A. The values of pre-exponential factor obtained for Zarnett for his
correlations are 1.5 to 2.3 times the value reported by Gregory and
Scott and are closer to the value obtained in the present investigation.
Kasturi and Stepanek also reported their values of interfacial area to
be higher as compared to those reported by Gregory and Scott. It may
be noted that the data of Kasturi and Stepanek was taken in a vertical
tube operating in the annular or annular-mist flow regime while Gregory
and Scott and the present study were carried out in a horizontal tube in
the slug flow regime.

In the absence of any reported studies for interfacial area in
tubes fitted with twisted tape inserts, only an estimate can be obtained by
comparing equation 6.36 with that reported by Zarnett (107) for rifled
tubes. Zarnett has correlated his data for rifled tube by

$$a = 9.56 \, (\epsilon_J)^{0.413} \tag{6.39}$$

where, a, is in cm^2/cm^3 and ϵ_J is in atm/sec.

Expressing in units used in the present study,

$$a = 142.2 \, (\epsilon_J)^{0.413} \tag{6.39A}$$

where, a, is in m^2/m^3 and $\in_J$ is in kN/m^2 sec.

Interfacial area values reported by Zarnett are more strongly dependent

on the energy dissipation parameter since the value of exponent

reported by him is 0.413 as compared to a value of 0.231 obtained in the

present study. It is to be noted that even for the volumetric mass

transfer coefficient correlations, Equation 6.11 , it was observed that

the exponent for twisted tapes is less than that for empty tube. Accordingly

the exponent value of 0.231 for twisted tapes as compared to a value of

0.313 for empty tube appears reasonable. The presence of swirl flow

throughout the test section in the present study is probably responsible

for lower value of exponent and higher value of pre-exponential factor as

compared to those obtained by Zarnett in rifled tubes in which the

swirl flow appear to exist close to the tube wall only. Zarnett has also

found that he could correlate his data satisfactorily by a single correlation

for his rifled tubes of different pitch ratio. The present investigation

also confirmed this observation.

Comparing Figs. 6.26 and 6.27 to observe the effect of twisted

tape inserts on interfacial area, it is noticed that the presence of twisted

tape insert is more useful at lower energy dissipation parameter and

becomes less significant as the value of $\in_J$ increases. This is clearly

seen from the following values of area effectiveness factor E_a, that is,

$$\Big[(a) \quad \text{twisted tape}\Big]\Big/\Big[(a) \quad \text{empty tube}\Big]:$$

ϵ_J in kN/m^2 sec							
0.1	0.4	1	4	10	40	100	210
1.96	1.67	1.525	1.40	1.28	1.126	1.073	1.00

Ea

It is, therefore, clear that the use of twisted tape inserts increases the value of interfacial significantly at lower values of energy dissipation parameter, ϵ_J, but for ϵ_J values greater than about 100, the gain in area due to the twisted tapes over empty tube is extremely small. It may be recalled that same values of ϵ_J for twisted tapes and for empty tube do not imply same pressure drop and it can be seen quite easily that for twisted tapes the pressure drop will be much larger and superficial velocities smaller as compared to empty tube. The effect of twisted tapes on interfacial area is similar to that observed for volumetric liquid phase mass transfer coefficient. More discussion about this aspect is given in sections 6.4.5 and 6.5.

6.3.5   Volume fraction occupied by liquid, E_L

The volume fraction occupied by liquid, E_L, is calculated from the superficial fluid velocities and Hughmark factor, K_H, following the method discussed in section 2.1.2. Calculated values of volume fraction occupied by liquid, E_L, are plotted against superficial gas velocity, V_{GO}, with superficial liquid velocity, V_{LO}, as parameter for experimental conditions in empty tube, Fig. 6.28, twisted tape insert TP-1 (H/D = 5.00), Fig. 6.29 and TP-2 (H/D = 9.32) Fig. 6.30.
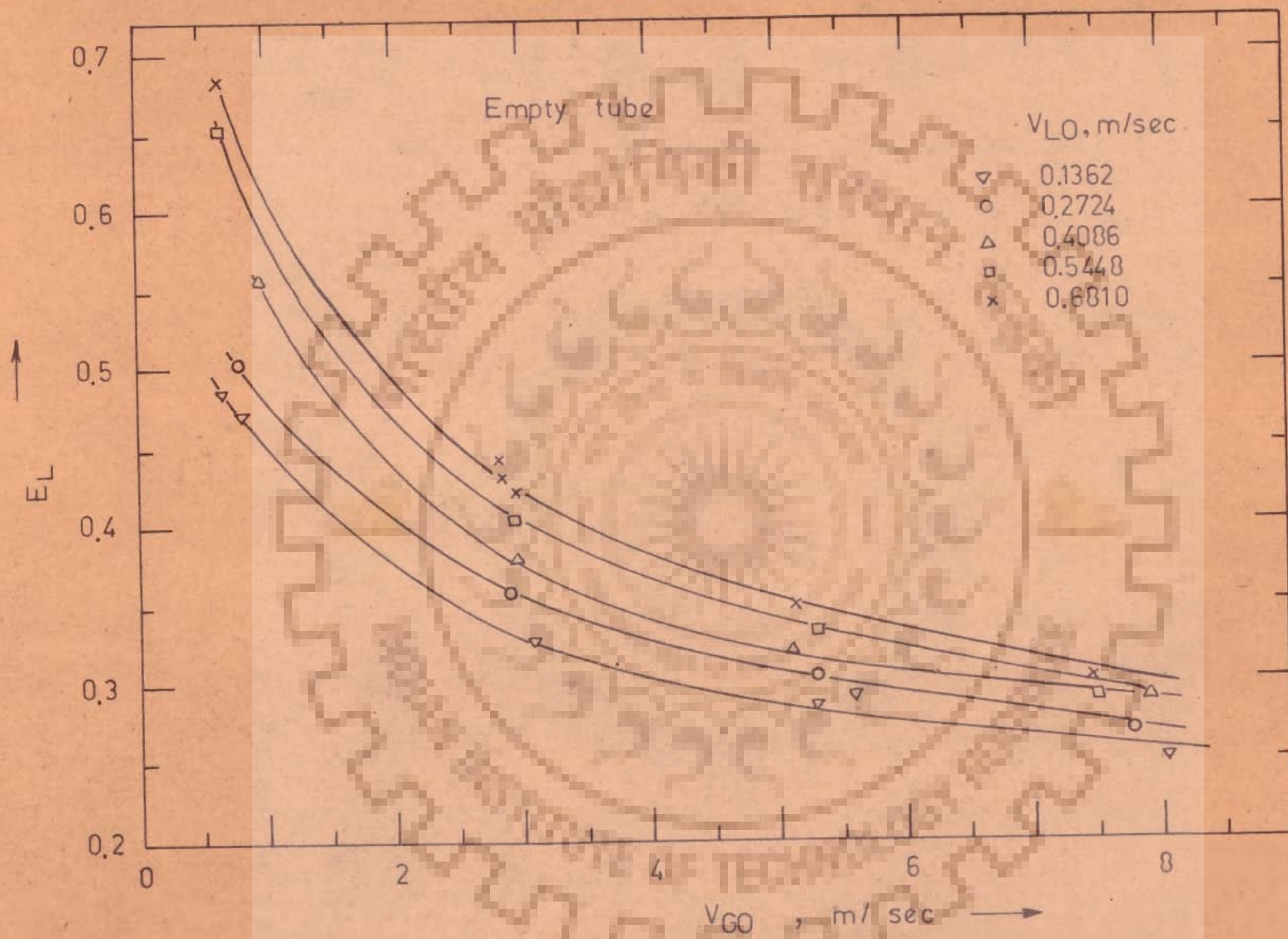
Fig. 6.28   Liquid   fraction E_L vs   superficial   gas   velocity
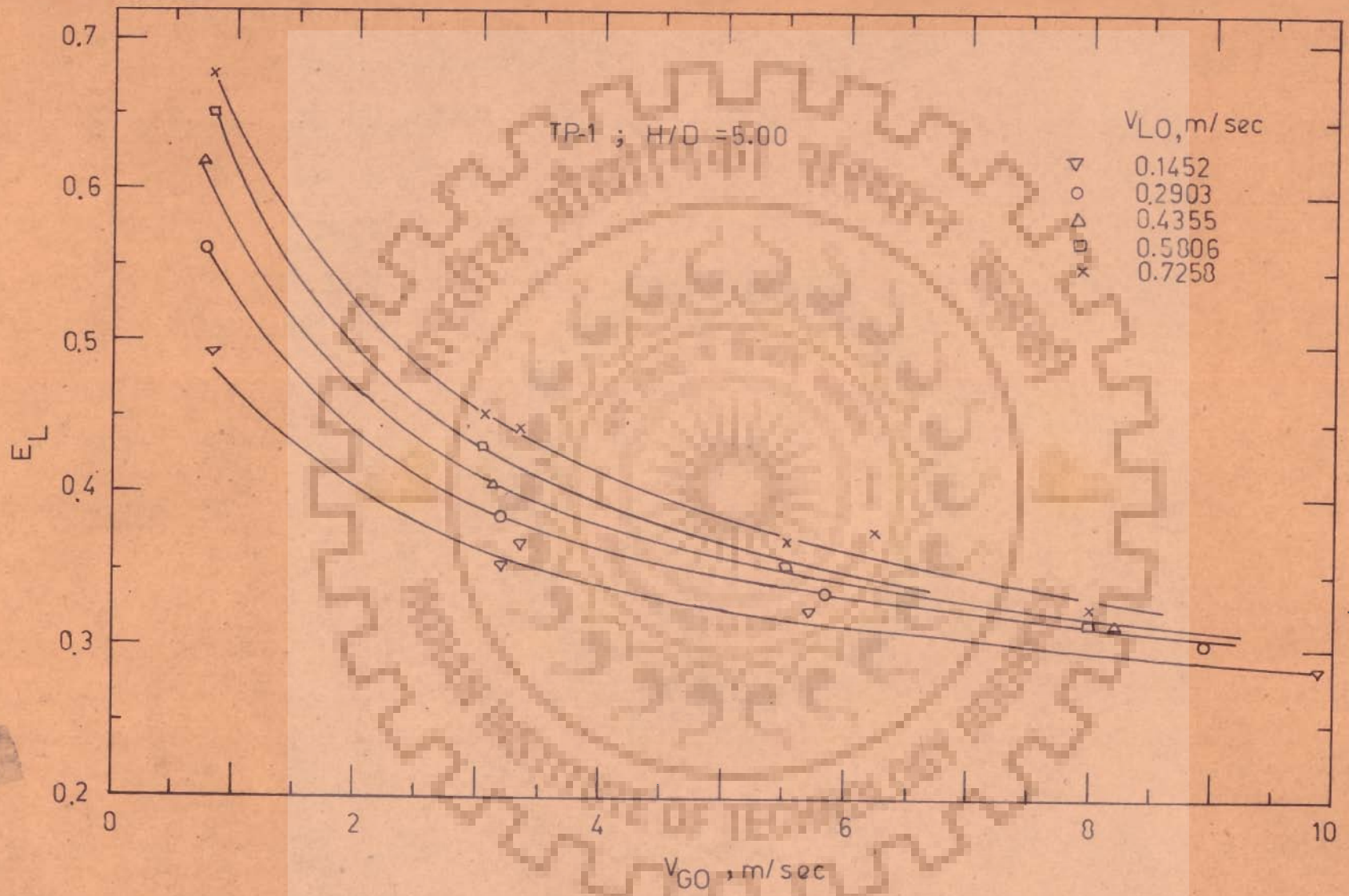
Fig.6.29   Liquid   fraction E_L vs   superficial   gas   velocity
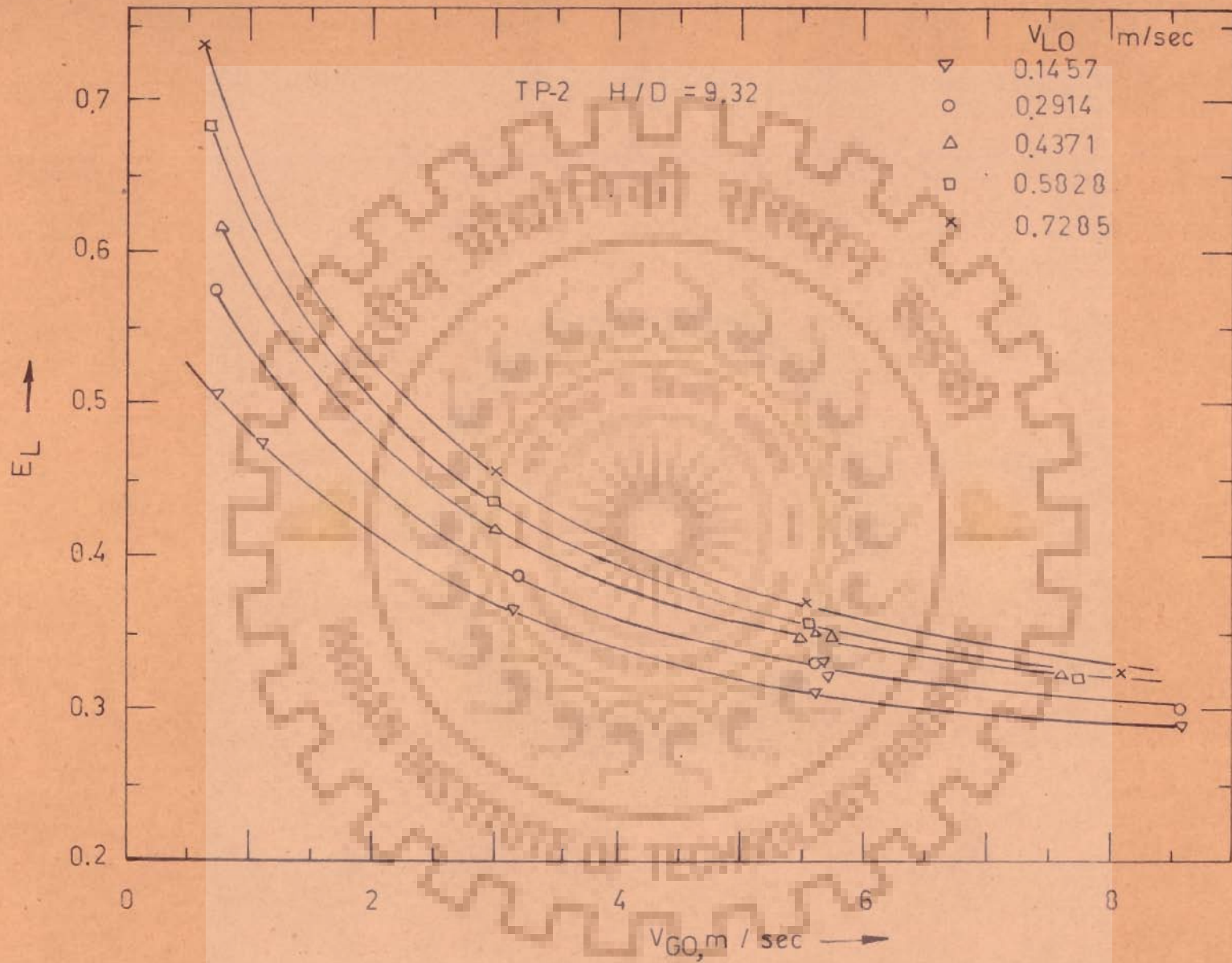
Fig. 6.30 Liquid fraction E_L vs superficial gas velocity

From these figures it is clear that the value of E_L decreases with increase in the value of the superficial gas velocity, V_{GO}, and the value of E_L increases as the superficial liquid velocity V_{LO} is increased. The value of E_L changes very rapidly at low gas velocity and the curves tend to flatten at high gas velocity. Further, at low gas velocity the effect of change in liquid velocity on E_L is more as compared to that at high gas velocity. As expected, the value of E_L depends upon V_{LO}, V_{GO}, density and viscosity of liquid and not on the pitch ratio, y. A small difference in the values of E_L is entirely due to the differences in fluid velocities and liquid density and viscosity.

Kasturi and Stepanek (102) measured the values of E_L in vertical tube operating in the annular flow regime. A comparison of Fig. 6.28 with that reported by Kasturi and Stepanek shows a similarity in the trends, although it is noticed that the values of E_L obtained by Hughmark factor, K_H, and used in the present investigation are slightly higher, especially at low gas velocity, than those reported by Kasturi and Stepanek for vertical flow in the annular flow regime.

These values of volume fraction occupied by liquid, E_L, are used in calculating the actual liquid velocities to estimate the value of two phase Reynolds number, Re_{TP}, as discussed in section 3.1.2. These E_L values are also used to calculate the area creation parameter which is discussed in the next section.

6.3.6 Rate of area creation correlation with pressure drop

Fig. 6.31 shows a plot of area creation rate, a term first used by Kasturi and Stepanek (102), for empty tube. Equation of the best fit line for the data points satisfying the reliability criteria is given by

$$\left(\frac{a \, Q_L}{E_L} \right)_{pred} = 0.0224 \left(\frac{\triangle P}{\triangle L} \right)^{1.034} ; \text{ standard error} + 32.3 \%$$

(6.40)

where $\dfrac{a \, Q_L}{E_L}$ is area creation rate, m^2/sec and

$\dfrac{\triangle P}{\triangle L}$ is in kN/m^3

A similar correlation proposed by Kasturi and Stepanek for their data is

$$\left(\frac{a \, Q_L}{E_L} \right) = 0.226 \left(\frac{\triangle P}{\triangle L} \right)^{1.07}$$

(6.41)

where $\dfrac{a \, Q_L}{E_L}$ is in cm^2/sec and $\dfrac{\triangle P}{\triangle L}$ is in N/m^3

which can be written in the units used in this work

$$\left(\frac{a \, Q_L}{E_L} \right) = 0.036 \left(\frac{\triangle P}{\triangle L} \right)^{1.07}$$

(6.41A)

where $\left(\dfrac{a \, Q_L}{E_L} \right.$ is in m^2/sec and $\dfrac{\triangle P}{\triangle L}$ is in kN/m^3

A comparison of Equations 6.40 and 6.41A shows that the values of exponent obtained in the present study are quite close but the value of pre-exponential factor is only about sixty percent of the value reported by Kasturi and Stepanek. It, therefore, appears that for same pressure drop nearly sixty percent more area is created in vertical annular flow than horizontal slug flow.
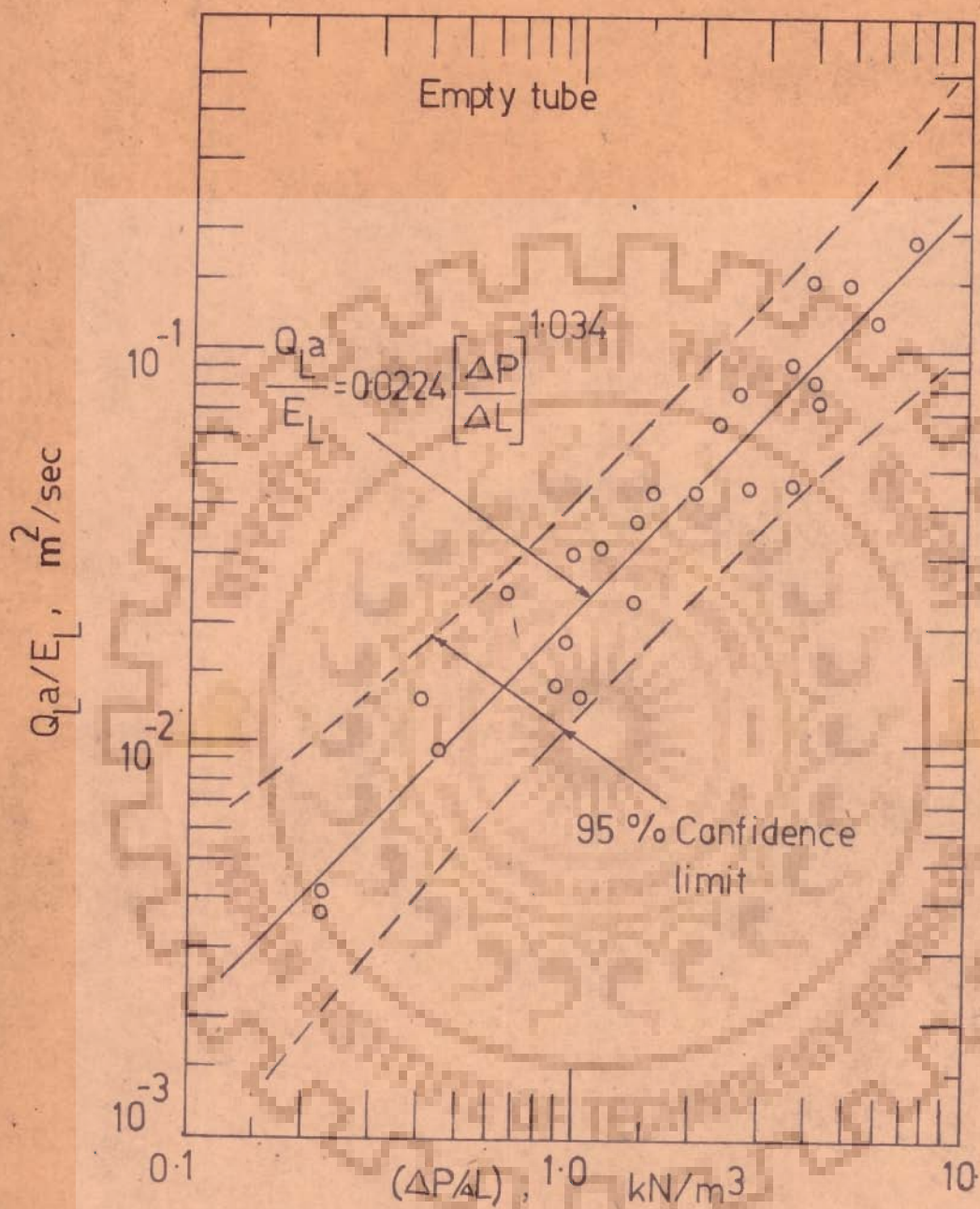
Fig. 6·31 Area creation rate versus

pressure drop

The plot shows $Q_L a / E_L$, m^2/sec versus $\Delta P/\Delta L$, kN/m^3 with data series:

TP-1 △

TP-2 □

$$\frac{Q_L a}{E_L} = 0.00778 \left[\frac{\Delta P}{\Delta L}\right]^{1.064}$$

95% Confidence limit
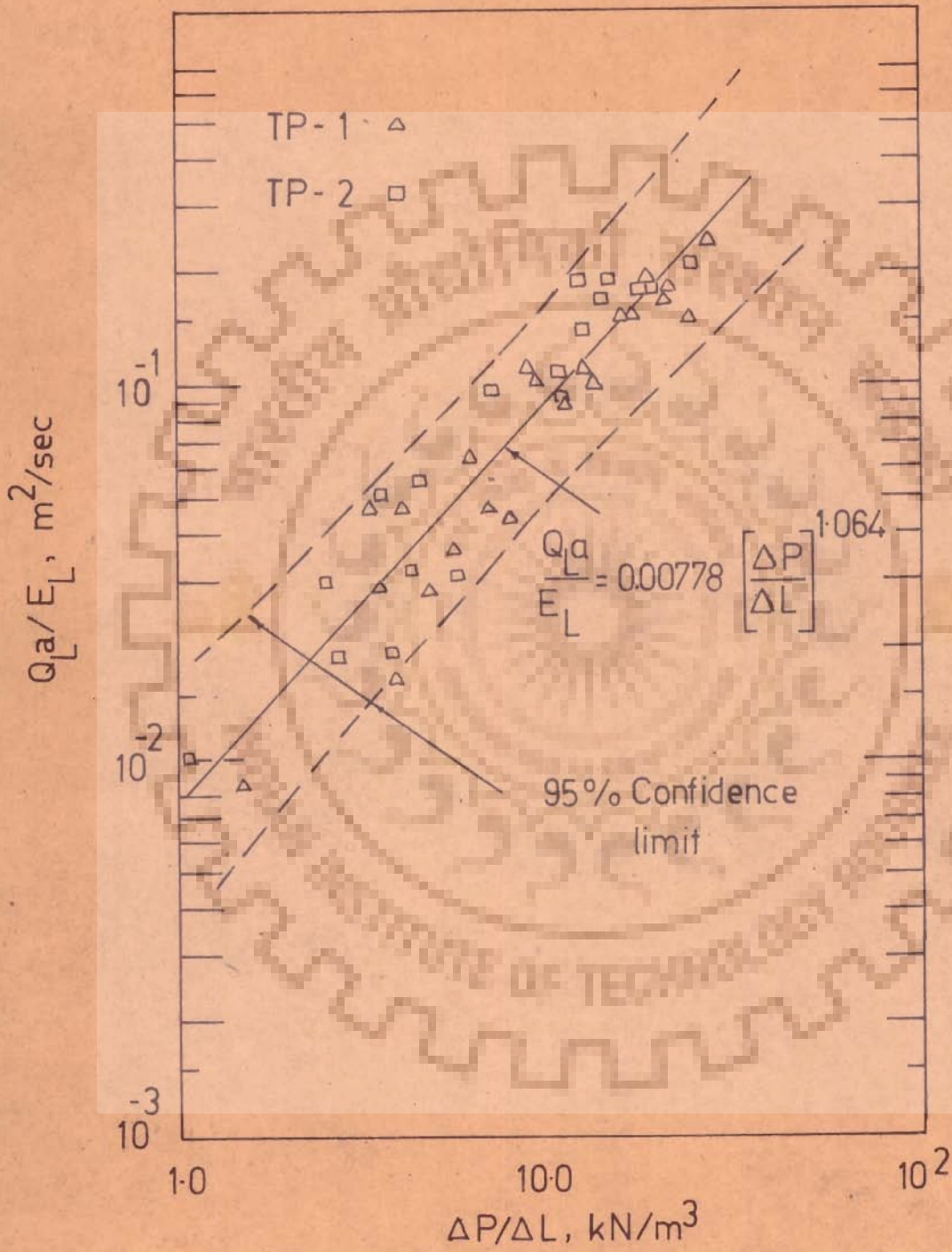
Fig. 6.32 Area creation rate versus pressure drop

Kasturi and Stepanek (102) also reported that the accuracy of Equation 6.41 is better, in predicting the interfacial area values, than the correlation relating interfacial area with Banerjee's energy dissipation parameter, ϵ_B, or Jepsens energy dissipation parameter, ϵ_J. A comparison for different forms of correlations for interfacial area, Equations 6.31, 6.35 and 6.40 shows that the correlation with Jepsen's energy dissipation parameter gives the minimum standard error, 31.0 %, and is only slightly better than the correlation between area creation parameter and the pressure drop as suggested by Kasturi and Stepanek (102). The Banerjee's energy dissipation parameter correlates the data most unsatisfactorily.

Data for area creation rate and experimental pressure drop values obtained in tube with twisted tape inserts TP-1 and TP-2 is shown in Fig. 6.32. Equation of the best fit line is

$$\left(\frac{a \, Q_L}{E_L} \right)_{pred} = 0.00778 \left(\frac{\Delta P}{\Delta L} \right)^{1.064} ; \text{ standard error } \pm 32.8 \, \%$$

$$(6.42)$$

The value of exponent 1.064 for tube with twisted tape inserts as compared to the value of 1.034 for empty tube are quite close to each other but the value of pre-exponential factor for empty tube is nearly three times that for the tube with twisted tape inserts.

From the above discussion it can be concluded that for gas-liquid horizontal flow in slug flow regime either the interfacial area may be correlated by Jepsen's energy dissipation parameter or the area creation rate may be correlated to pressure drop with nearly the same

accuracy. Correlation with Jepsen's energy dissipation parameter is advantageous because the volumetric mass transfer coefficient, $k_L^o a$, can also be correlated with the help of this parameter. But correlation of area creation rate parameter with pressure drop provides better physical picture and has some other advantage as discussed in the next section.

6.3.7 Area modulus and area creation rate modulus

From a practical point of view it is important to study the effect of the presence of twisted tape inserts on interfacial area per unit pressure drop per unit length that is,

$$\text{Area modulus} = M_a = a / (\Delta P/\Delta L), \text{ m}^2/\text{kN} \qquad (6.43)$$

The computed values of area modulus are given in Table E.6, Appendix E, along with other measured and calculated parameters for empty tube and twisted tape inserts. Fig. 6.33 shows a plot of area modulus values plotted against superficial liquid velocity with superficial gas velocity as a parameter for some selected data points for empty tube and twisted tape inserts TP-1 and TP-2. From the figure it is observed that for any tube geometry the value of area modulus decreases with increase in superficial gas and liquid velocities. It is also observed that initial decrease in area modulus with V_{LO} is quite rapid upto a V_{LO} value of 0.4 m/sec and the effect of difference in pitch ratio is practically negligible. An interesting feature is also revealed that for any value of fluid velocity area modulus has a maximum value for the empty tube. It is due to the fact that although the interfacial area increases in the tube
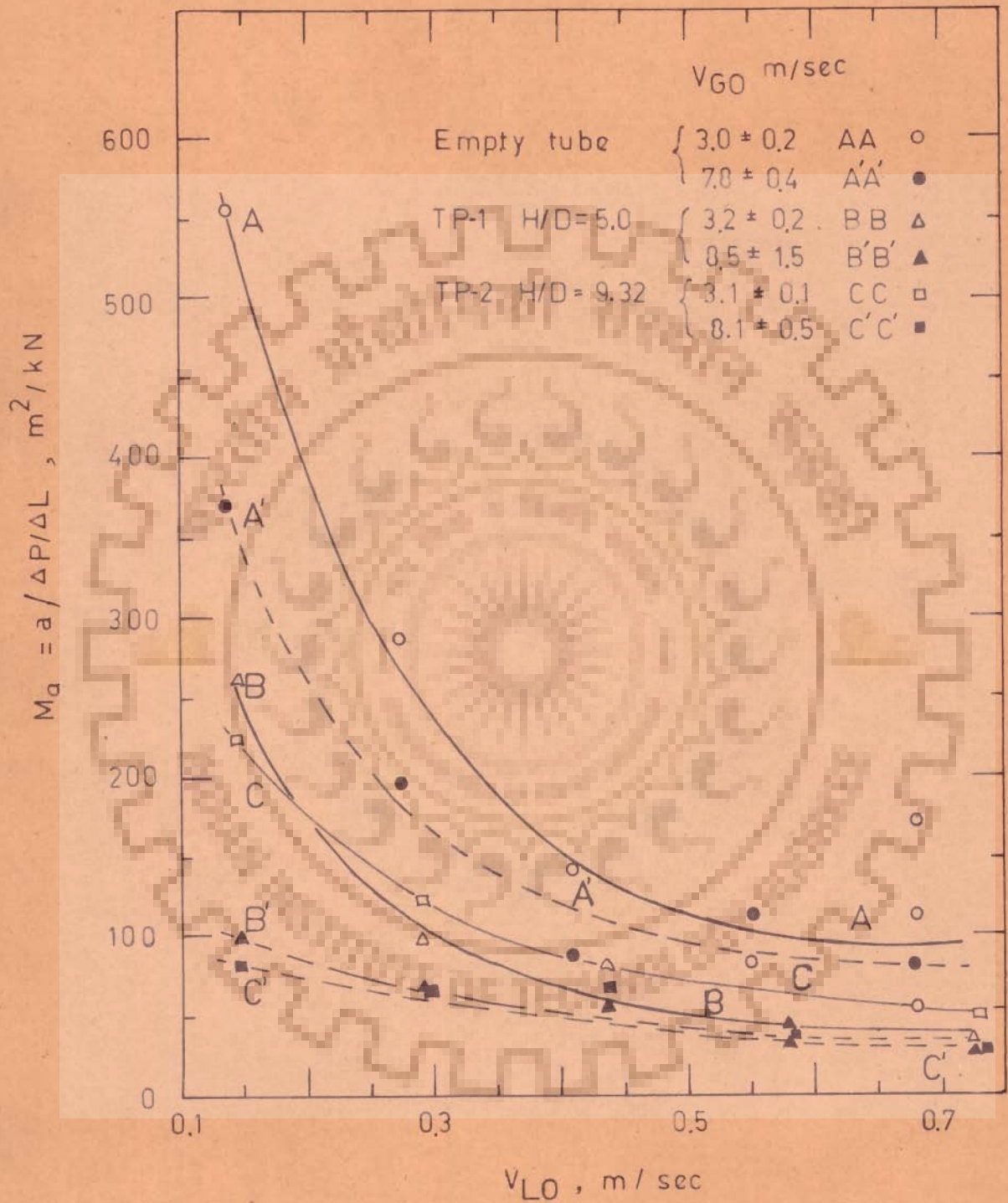
Fig 6.33 Area modulus vs superficial liquid velocity

with twisted tape inserts but the increase in the pressure drop value is even more and hence the value of area modulus for twisted tape becomes lower than the value in the empty tube. Furthermore, it is observed that at higher values of the superficial liquid velocity the difference in area modulus between different geometries and the superficial gas velocities is very much decreased.

It is, therefore, clear that if area modulus M_a, a $/(\Delta P/\Delta L)$, is the criteria used for designing the absorbers then the use of twisted tape is always undesirable because for a given pressure drop much more interfacial area can be obtained in empty tube by using higher velocities than by creating swirl flow at lower flow rates with the help of twisted tape inserts.

As with area modulus Ma, area creation rate modulus M_{ac}, (a. Q_L/E_L)/($\Delta P/\Delta L$), may have a greater practical utility and can quite easily be obtained from area creation rate correlations, Equations 6.40 and 6.42 as follows:

Empty tube:

$$M_{ac} = \frac{(a\, Q_L/E_L)}{(\Delta P/\Delta L)} = 0.0224 \left(\frac{\Delta P}{\Delta L}\right)^{0.034} \simeq 0.0224 \qquad (6.44)$$

Tube with twisted tape inserts TP-1 and TP-2 :

$$M_{ac} = \frac{(a\, Q_L/E_L)}{(\Delta P/\Delta L)} = 0.00778 \left(\frac{\Delta P}{\Delta L}\right)^{0.064} \simeq 0.00778 \qquad (6.45)$$

where M_{ac} is in $(m^2/sec)/(kN/m^3)$ and $\dfrac{\Delta P}{\Delta L}$ is in $\dfrac{kN}{m^3}$.

Because of the very low values of exponents in Equation 6.44 and 6.45 the effect of pressure drop per unit length may be considered insignificant and the area creation rate modulus, M_{ac} , may be assumed to have nearly constant values independent of pressure drop. Thus, it can be safely stated that the area creation rate per unit pressure drop per unit length have values close to 0.0224 and 0.00778 $(m^2/sec)/(kN/m^3)$ for empty tube and tube with twisted tape respectively. This provides a good approximation for estimating the value of interfacial area and clearly indicates that the empty tubes are nearly three times more efficient if the area creation rate modulus is the controlling design criteria.

6.4.1   Liquid phase mass transfer coefficient k_L^o

The values of the individual liquid phase or liquid side mass transfer coefficient k_L^o were evaluated by dividing the values of volumetric mass transfer coefficient, $k_L^o a$, by the values of interfacial surface area, a, under the same hydrodynamics conditions.

In the section 5.6.2 it has been pointed out that the proper similarity criteria for hydrodynamic similarity is the identity of the two-phase Reynolds number for physical and chemical absorption experiments. Some of the difficulties in using this criteria are already discussed earlier and can be summarised as:

(i) error in estimating the value of Re_{TP} due to inaccurate estimation of the volume fraction occupied by liquid, E_L, which is used to calculate the actual liquid velocity V_L, that is, $V_L = V_{LO}/E_L$, and (ii) relatively large values of standard error for the correlation of interfacial area with Re_{TP} ,

that is 47.3 and 39.2 percent for empty tube and tube with twisted

tape inserts respectively (section 6.3.2). But inspite of these

inaccuracies it was still considered better to use this procedure

for estimating liquid phase mass transfer coefficient, k_L^o ,

because identity of Re_{TP} is an accepted and most suitable criteria

for hydrodynamic similarity and also the curves showing interfacial

area as a function of superficial gas velocity with superficial liquid

velocity as a parameter have large scatter. Figure 6.19, 6.20 and

6.21, and cannot be considered more accurate than the correlation

of interfacial area with Re_{TP}.

It was also possible to calculate the value of $k_L^o a$ at the same

Re_{TP} at which interfacial area, a, was found and then compute the

value of k_L^o from this estimated value of $k_L^o a$ and measured value

of the interfacial area, a. However, this method was not followed

because of two reasons; (i) the correlations of $k_L^o a$ with Re_{TP} have

5 to 10 percent higher standard error, Equations 6.10 and 6.11 as

compared to the correlations for interfacial area with Re_{TP} ,

Equations 6.28 and 6.29, and (ii) the basic measurements to

estimate volumetric mass transfer coefficients were carried out

in the physical absorption studies and not in the chemical

absorption studies which were used exclusively to estimate the

interfacial area.

Figure 6.34 shows the plot of liquid phase mass transfer

coefficient, k_L^o , as a function of Jepsen's energy dissipation

parameter for all the experimental data, obtained in empty tube
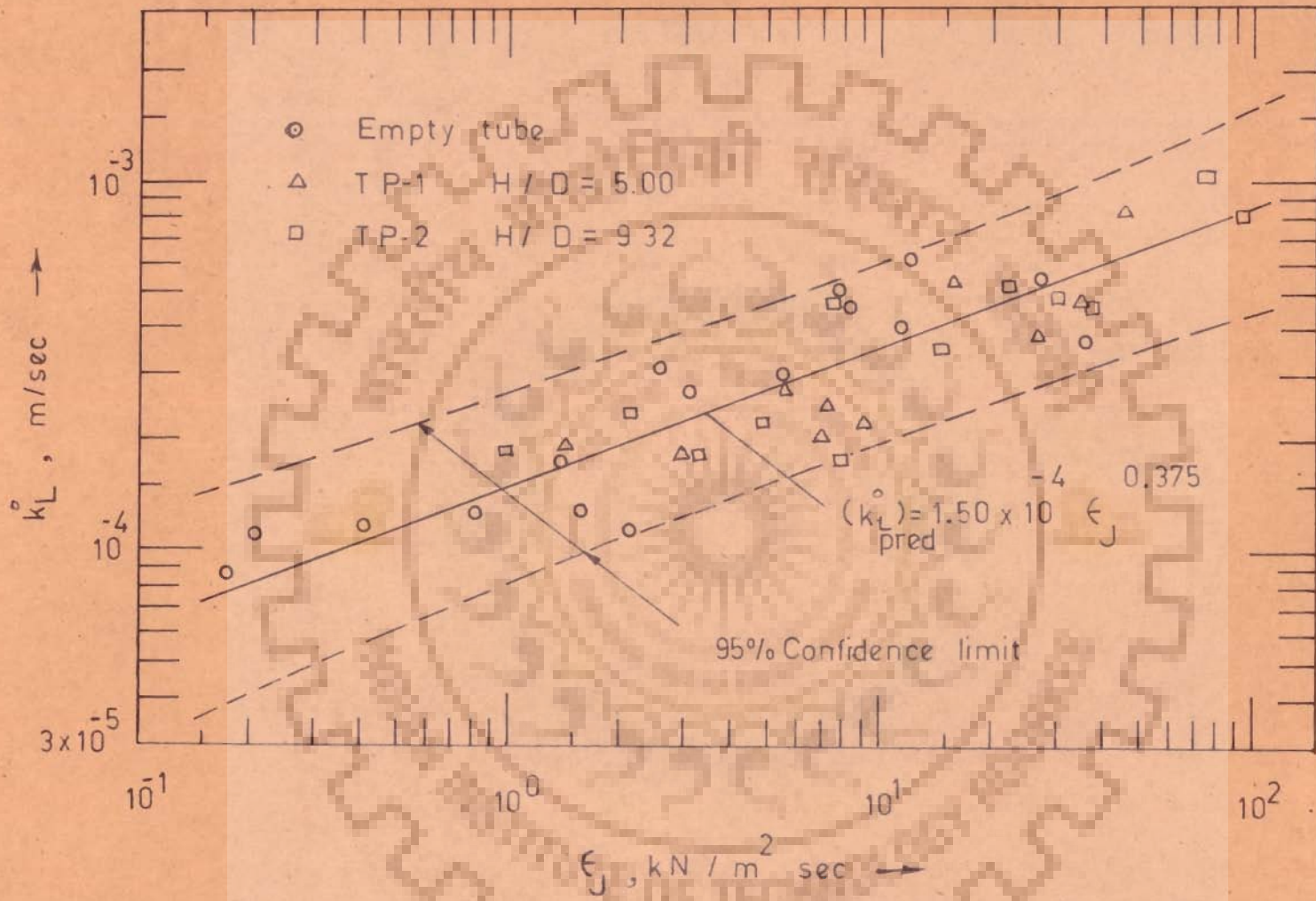
Fig.6.34 Liquid phase mass transfer coefficient k_L° vs Jepsens energy dissipation parameter ϵ_J

$(k_L^\circ)_{pred} = 1.50 \times 10^{-4} \epsilon_J^{0.375}$

95% Confidence limit

Empty tube

T P-1   H / D = 5.00

T P-2   H / D = 9.32

k_L° , m/sec

ϵ_J , kN / m^2 sec
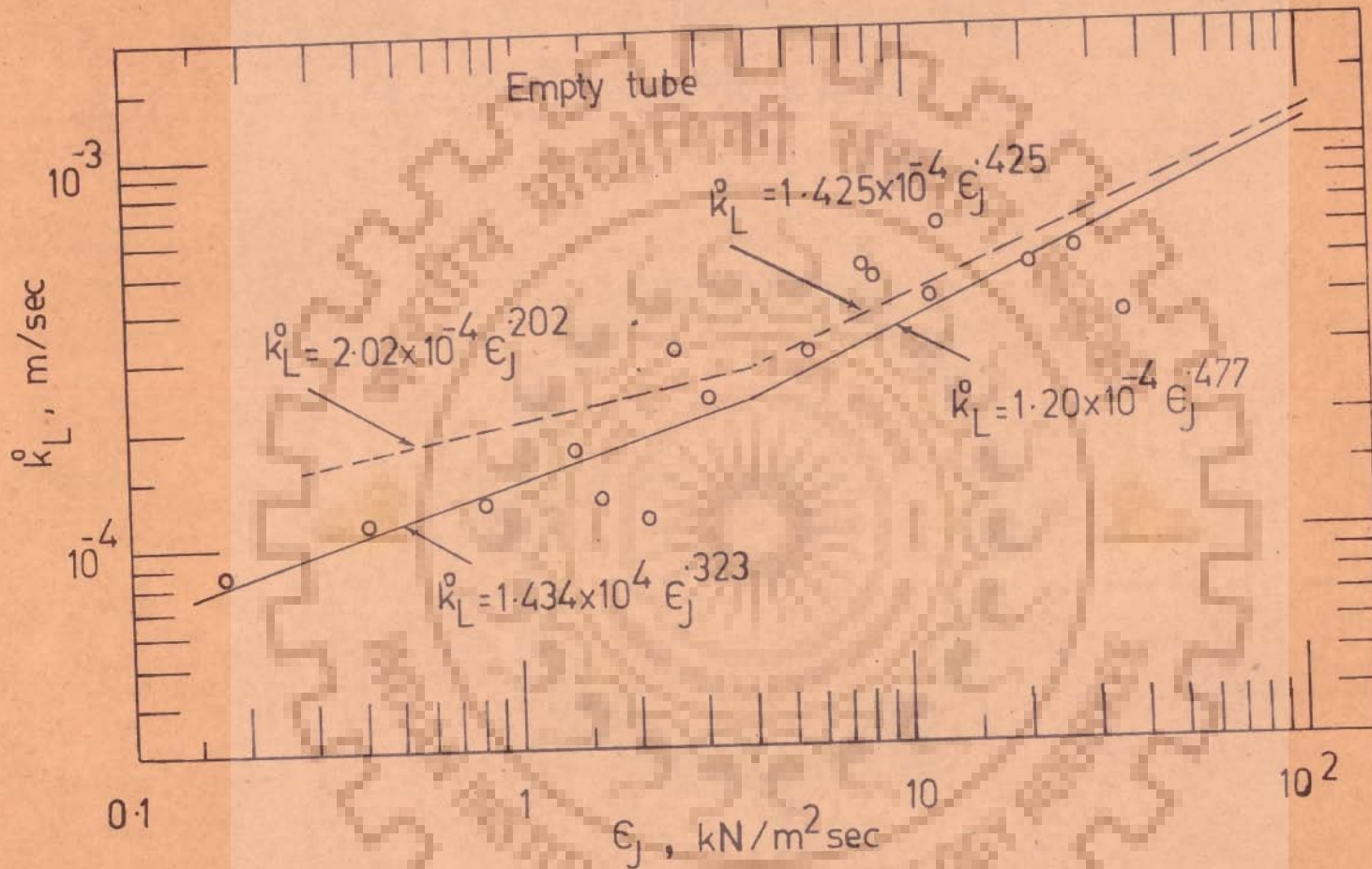
Fig. 6·35 Liquid phase mass transfer coefficient $\overset{\circ}{k}_L$ versus Jepsen's energy dissipation parameter ϵ_j
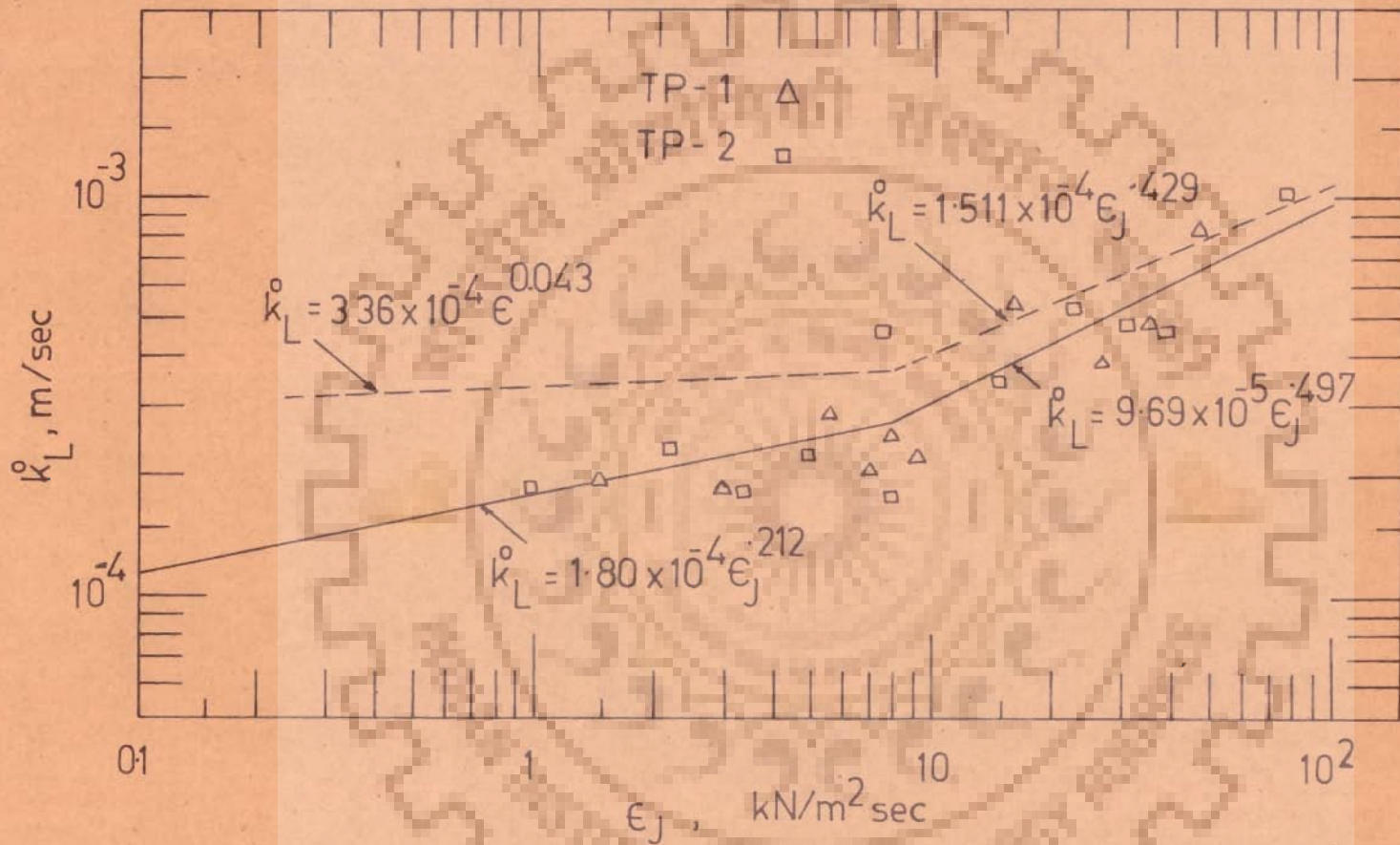
Fig. 6.36 Liquid phase mass transfer coefficient $\overset{o}{k_L}$ versus Jepsen's energy dissipation parameter ϵ_J

and in tube with twisted tape inserts TP-1 (H/D = 5.00) and TP-2 (H/D = 9.32), which satisfy the reliability criteria for the values of $k_L{}^o a$. The equation of the best fit line is given by the following expression : $(k_L{}^o)_{pred} = 1.500 \times 10^{-4} (\epsilon_J)^{0.375}$;

$$\text{standard error} \pm 28.8\,\% \qquad\qquad (6.46)$$

where $k_L{}^o$ is in m/sec and ϵ_J is in $kN/m^2 sec$. Also shown are two lines of 95 percent confidence limits. An observation of the Fig. 6.34 shows that all the data points lie within 95 percent confidence limits and the value of 28.8 percent for the standard error of Equation 6.46 appears to be very good considering the indirect procedure used for the calculation of the value of liquid phase mass transfer coefficient, $k_L{}^o$.

It has been pointed out in section 6.2.4 that the correlation of volumetric coefficient, $k_L{}^o a$, with ϵ_J changes its slope at a value of approximately 4.0 kN/m^2 sec. Fig. 6.35 shows the value of $k_L{}^o$ plotted against Jepsen's energy dissipation parameter for the results obtained in empty tube. Following the procedure as discussed in section 6.2.4, the following correlations are obtained:

Empty tube ; ϵ_J less than 4.0 kN/m^2 sec,

$$(k_L{}^o)_{pred} = 1.434 \times 10^{-4} (\epsilon_J)^{0.323} ;$$

$$\text{standard error} \pm 31.5\,\% \qquad\qquad (6.47)$$

ϵ_J equal to or greater than 4.0 kN/m^2. sec.

$$(k_L{}^o)_{pred} = 1.200 \times 10^{-4} (\epsilon_J)^{0.477} ;$$

$$\text{standard error} \pm 44.6\,\% \qquad\qquad (6.48)$$

Contrary to expectations, the value standard error for the

correlation given by Equation 6.46 is less than the value obtained

for correlations given by Equations 6.47 and 6.48. It shows that

there is no improvement in the correlation by considering the

limited data individually for empty tube separately for ϵ_J values

less and more than 4.0 kN/m^2. sec. Also shown in Figure 6.35

are the lines obtained when identity of Jepsen's energy dissipation

parameter, ϵ_J, is used as similarity criteria. These

correlations are obtained simply by deviding equations expressing

$k_L^o a$ as a function of ϵ_J, Equations 6.16 and 6.17 by the

equation expressing interfacial area as a function of $_J$.

These correlations are given as :

$$(k_L^o)_{pred} = 2.024 \times 10^{-4} (\epsilon_J)^{0.202} ; \text{ for } \epsilon_J \leq 4.0 \quad (6.49)$$

$$(k_L^o)_{pred} = 1.425 \times 10^{-4} (\epsilon_J)^{0.452}; \text{ for } \epsilon_J \geq 4.0 \quad (6.50)$$

It is important to note that there is absolutely no basis for

using ϵ_J as a similarity criteria, and Equations 6.49 and 6.50

are only shown for comparison purpose in order to show that the

lines given by Equations 6.49 and 6.50 are much different that the

best fit lines given by Equations 6.47 and 6.48 for the values

obtained by using proper similarity criteria of Re_{TP} .

Figure 6.36 shows a similar plot of k_L^o as a function of

energy dissipation parameter, ϵ_J, for the values obtained in

tube with twisted tape inserts TP-1 and TP-2 using Re_{TP} as the

criteria for similarity. The equation of best fit lines are given

as :

<u>Tube with twisted tape inserts</u> TP-1 and TP-2

ϵ_J less than or equal to 8.0 kN/m^2 sec.

$$(k_L^o)_{pred} = 1.800 \times 10^{-4} (\epsilon_J)^{0.212} \; ;$$

and $\qquad\qquad$ standard error $\pm$ 30.1% $\qquad$ (6.51)

$$(k_L^o)_{pred} = 9.693 \times 10^{-5} (\epsilon_J)^{0.497} \; ;$$

for $\epsilon_J \geq 8.0$ $\qquad$ standard error $\pm$ 23.1% $\qquad$ (6.52)

A comparison of these equations with the Equation 6.46 for all data points shows improvement in standard error for ϵ_J greater than 8.0 only. The value of exponent in Equation 6.46 is in between the value for the exponents in Equations 6.51 and 6.52. Also shown in Figure 6.36 are the lines obtained by using Jepsen's energy dissipation parameter as the similarity criteria following the procedure similar to that discussed earlier. The equations of these lines are :

$$(k_L^o)_{pred} = 3.360 \times 10^{-4} (\epsilon_J)^{0.046} \; ; \quad \epsilon_J \leq 8.0 \qquad (6.53)$$

$$(k_L^o)_{pred} = 1.511 \times 10^{-4} (\epsilon_J)^{0.429} \; ; \quad \epsilon_J \geq 8.0 \qquad (6.54)$$

As observed in Figure 6.35 for empty tube once again it is observed in Figure 6.36 that the lines given by Equations 6.53 and 6.54 lie quite away from the best fit lines given by Equations 6.51 and 6.52 for the values of k_L^o obtained by using proper similarity criteria of two phase Reynolds number, Re_{TP}.

Kasturi and Stepanck (103) have also correlated k_L^o with Jepsen's energy dissipation parameter and reported that 20 percent of the data differs from the best fit line by a factor of

more than $(1.5)^{+1}$ but have not reported the correlation for the best fit line.

6.4.2 Banerjee Model Prediction

The values of liquid phase mass transfer coefficient, k_L^o, are calculated using Equation 5.3 proposed by Banerjee (84) section 5.6.2, from the experimental data. Values calculated in this way are designated as $(k_L^o)_B$. Figures 6.37 and 6.38 show the values of $(k_L^o)_{exp}$, calculated from the experimental data as described in section 6.4.1 as a function of $(k_L^o)_B$. Also shown in these figures is the 45 degree line, about which the points should lie when the experimental values are close to values predicted by Banerjee correlation. As observed from these figures the difference between $(k_L^o)_{exp}$ and $(k_L^o)_B$ is very large and the ratio $(k_L^o)_{exp} / (k_L^o)_B$ increases sharply with the increase in $(k_L^o)_{exp}$ values. The lines of best fit are given by the expressions :

For empty tube :

$$(k_L^o)_{pred} = 686.6 (k_L^o)_B^{1.7} ;$$

$$\text{standard error} \pm 49.4\% \qquad (6.55)$$

For tube with twisted tape inserts TP-1 and TP-2

$$(k_L^o)_{pred} = 6.835 \times 10^4 (k_L^o)_B^{1.929} ;$$

$$\text{standard error} \pm 46.3\% \qquad (6.56)$$

Large values of standard errors and large values of exponents and pre-exponential factors indicate that the correlation proposed by Banerjee for the calculation of the liquid phase mass transfer
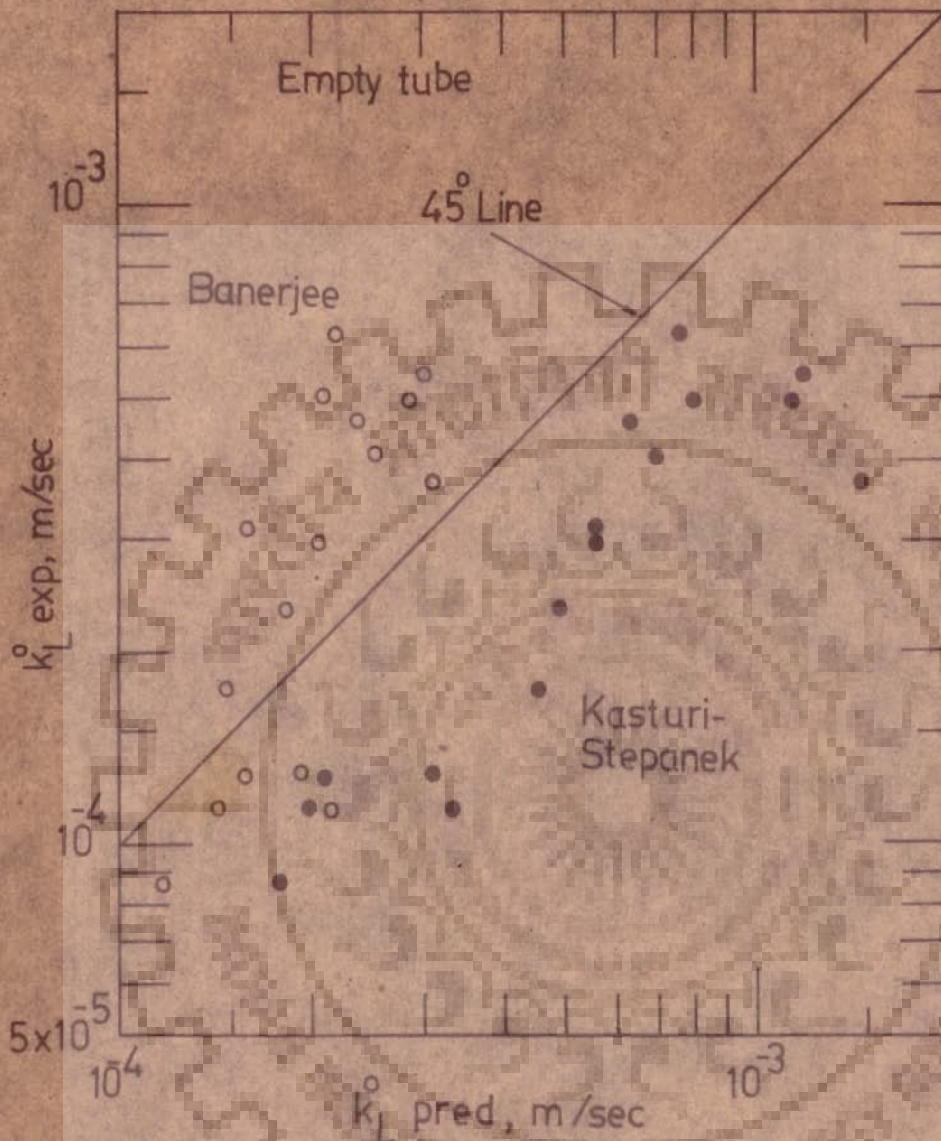
Fig. 6. 37 Individual mass transfer coeficient
vs predicted values

Fig. 6·38 Individual mass transfer coefficient
vs predicted values

coefficients is not very satisfactory.

It may be recalled that Banerjee (84) proposed his model for annular flow regime but the present investigations were carried out in the slug flow regime. In the case of slug flow the liquid film is thick and the holdup values vary with slug size and, therefore, a model suitable for annular flow may not be applicable.

Gregory and Scott (35) reported the following expression for the line of best fit ;

$$k_L^o = 3.127 (k_L^o)_B - 0.050 \qquad (6.57)$$

where k_L^o is in cm/sec and $(k_L^o)_B$ is the value predicted by Banerjee model. They further observed that the values prediced by Equation 6.57 were also not very accurate and experimental values of mass transfer coefficient, $(k_L^o)_{exp}$, show a considerable scatter around the best fit line of Equation 6.57.

Kasturi and Stepanek (103) in their investigation for vertical annular and annular-mist gas-liquid flow also observed that the values predicted by Banerjee formula, Equation 5.3, differ from the experimental values by a factor ranging. from 1.5 to 2.0.

6.4.3   Kasturi - Stepanek Model Prediction

On the basis of the penetration theory and the rate of momentum transfer at the gas-liquid interface Kasturi and Stepanek (103) correlated the liquid phase mass transfer coefficient, k_L^o, in terms of the dimensionless groups and suggested that

$$Sh_L = 0.25 \; Sc_L^{-\frac{1}{2}} \; Pe_L \; Eu_L \qquad (6.58)$$

This correlation is rearranged for the prediction of k_L^o,

Equation 5.4 in section 5.6.2. Equation 5.4 is used to calculate

the values of liquid phase mass transfer coefficient and these

values are designated as $(k_L^o)_{KS}$. Figure 6.37 and 6.38 also

show these values and invariably all points lie below the 45 degree

line indicating that the correlation proposed by Kasturi and

Stepanck overpredicts the value of the liquid phase mass transfer

coefficient. Instead of developing a correlation between experimental

value of k_L^o and $(k_L^o)_{KS}$ it was considered better to obtain the

correlation in dimensionless form. Figure 6.39 shows a plot of

experimental values of Sherwood number against the correlating

group, $(Sh_L)_{cal} = Eu_L \, Pe_L \, (Sc_L)^{-\frac{1}{2}}$, for the data obtained in

empty tube. The equation of the best fit line is given by,

$$(Sh_L)_{pred} = 0.194 \, (Sh_L)_{cal}^{0.954} \; ;$$

standard error $\pm 31.0\%$ (6.59)

where

$$(Sh_L)_{pred} = (k_L^o)_{exp} \, D_P / D_A \quad \text{and}$$

$$(Sh_L)_{cal} = Eu_L \, Pe_L / (Sc_L)^{\frac{1}{2}}$$

In the Equation 6.59 the value of the exponent is very close to unity.

Since Kasturi and Stepanek from theoretical considerations

established that the exponent should be unity, the best value of

pre-exponent factor was found using exponent as unity and the

following expression is obtained ;

$$(Sh_L)_{pred} = 0.1243 \, (Sh_L)_{cal} \; ;$$

standard error $\pm 30.5\%$ (6.60)
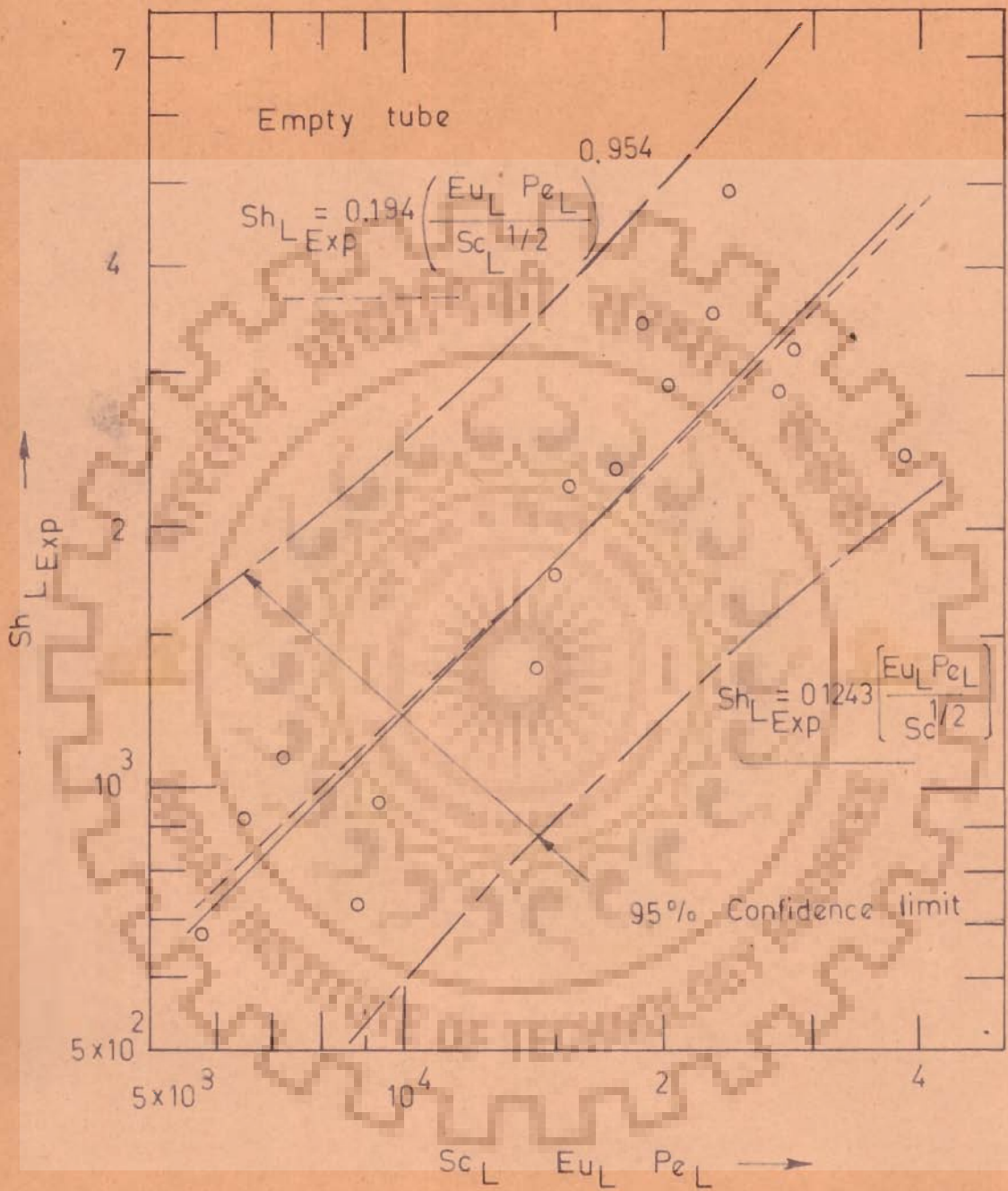
Fig.6.39 Experimental values of Sherwood number against correlating group
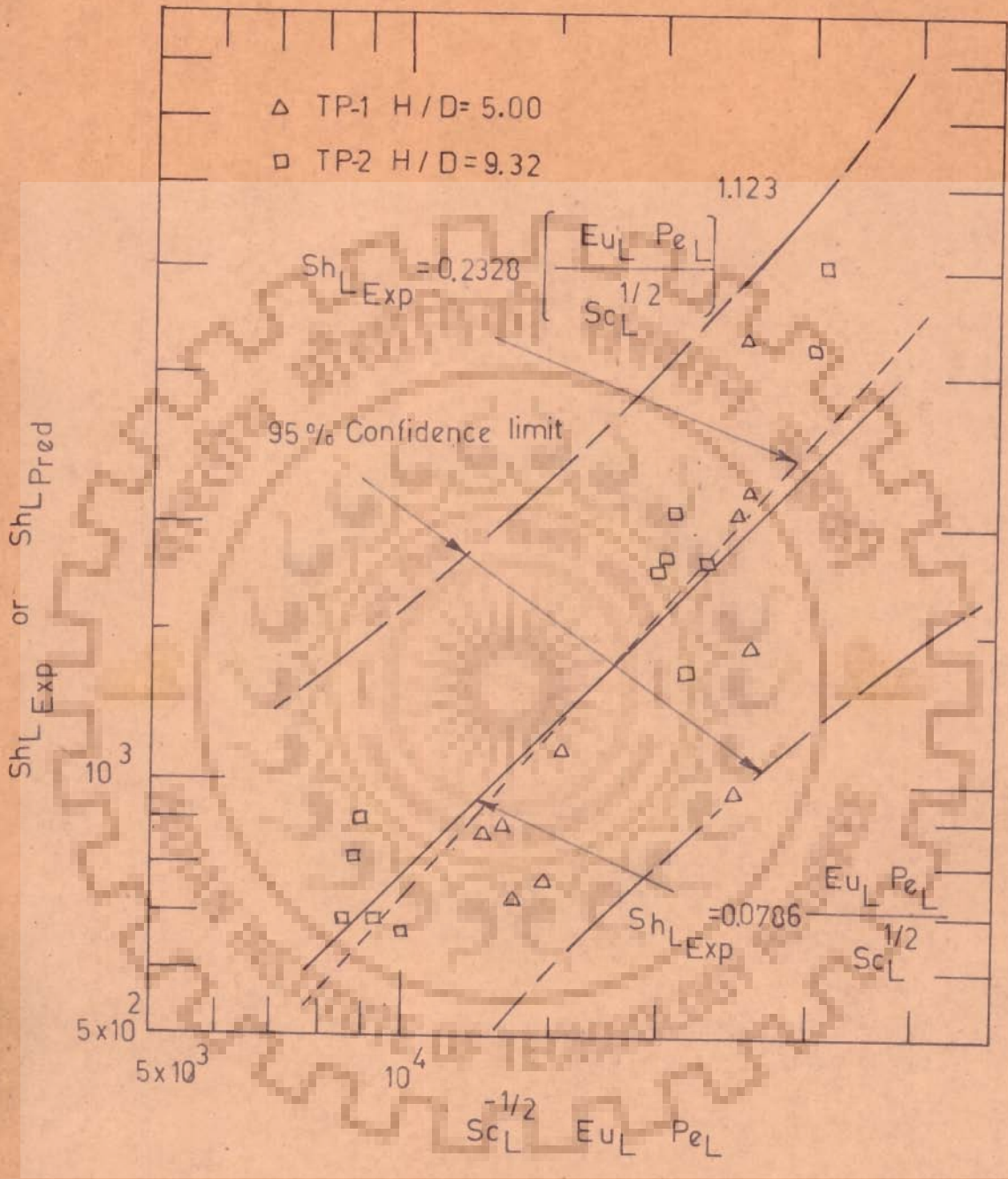
Fig. 6.40 Experimental values of Sherwood number agains correlating group

This slightly lower value of the standard error for Equation 6.60 as compared to best fit line, Equation 6.59, may appear surprizing but actually the total sum of the squares of error for correlation given by Equation 6.60 is slightly more than that for the correlation given by Equation 6.59. The definition of the standard error requires that the sum of the squares of error in the Equation 6.59 is devided by 14 (since the number of data points is 16 and arbitrary constants are 2) while that in case of Equation 6.60 is to be devided by 15 (since arbitrary constant is only one). Since the sum of squares of error for Equation 6.59 is only slightly less than that for Equation 6.60 this resulted in slightly higher value of the standard error for Equation 6.59 as compared to that for Equation 6.60. From the above discussion it is clear that the error is rather insensitive to the value of the exponent in the region 0.95 to 1.0. Equation 6.60 is preferable due to its simplicity and theoretical basis as compared to Equation 6.59.

A comparison of Equation 6.60 with that proposed by Kasturi and Stepanek, Equation 6.58, reveals that the pre-exponential factor value of 0.1243 obtained in the present investigation is about 50 percent of the value of 0.25 given by Kasturi and Stepanck and this difference may be due to the difference in the hydrodynamic conditions for slug and annular flow.

Figure 6.40 shows a similar plot of experimental values of Sherwood number against the correlating group, $(Sh_L)_{cal}$, for the

data obtained in tube with twisted tape inserts TP-1 and TP-2. The equation of the best fit line is given as,

$$(Sh_L)_{pred} = 0.0238 \, (Sh_L)_{cal}^{1.123} \; ;$$

$$\text{standard error} \pm 29.4\% \qquad (6.61)$$

Also shown in the figure are best fit line and lines of 95 percent confidence limits. It is observed in Equation 6.61 that the value of exponent is close to unity. Following expression correlates the data best when the value of the exponent is taken as unity :

$$(Sh_L)_{pred} = 0.07863 \, (Sh_L)_{cal} \; ;$$

$$\text{standard error} \pm 31.2\% \qquad (6.62)$$

It is observed that the values of the pre-exponential factor in Equations 6.61 and 6.62 are much less than the value for empty tube runs, Equation 6.60. This is due to the fact that the pressure drop per unit length is very high in the tube with twisted tape inserts, due to the superposition of swirl flow, so that the Euler number, $(Eu)_L$, values are quite high and the value of k_L^o has not increased comensurate to pressure drop. The Equation 6.62 is again preferred as compared to Equation 6.61 using the same arguments as advanced for empty tube.

6.4.4   Lamont and Scott Model Prediction

Lamont and Scott (97) studied the mass transfer from bubbles in cocurrent horizontal flow and successfully correlated their data in terms of dimensionless groups such as Sherwood, Reynolds and Schmidt numbers. Lamont and Scott have correlated their data by the following expression :

$$(Sh_B / Sc^{1/3}) = 9.3 (Re_B)^{1/2} \qquad (6.63)$$

Where B stands for bubble values and they have also reported $k_L{}^o$ values correlated to Reynolds number by,

$$k_L{}^o = 0.030 \, Re^{0.49} \qquad \pm 18\% \qquad (6.64)$$

where $k_L{}^o$ is in cm/min.

Figure 6.41 shows a similar plot of experimental Sherwood number divided by (Schmidt number)$^{1/3}$ plotted as a function of the two phase Reynolds number, Re_{TP}, for all the data obtained in empty tube and in tube with twisted tape inserts. The equation of the best fit line is given by the following expression :

$$((Sh_L)_{exp} / Sc_L^{1/3})_{pred} = 0.5342 (Re_{TP})^{0.642} ;$$

$$\text{standard error} \pm 49.01\% \qquad (6.65)$$

In view of the large value of standard error for the above correlation for all the data points it was desirable to obtain separate correlation for empty tube and twisted tapes. The following correlations are obtained:

Empty tube

$$((Sh_L)_{exp} / Sc_L^{1/3})_{pred} = 0.4147 (Re_{TP})^{0.667} ;$$

$$\text{standard error} \pm 53.0\% \qquad (6.66)$$

Tube with twisted tape inserts

$$((Sh_L)_{exp} / Sc_L^{1/3})_{pred} = 0.5203 (Re_{TP})^{0.647} ;$$

$$\text{standard error} \pm 48.6\% \qquad (6.67)$$

Comparing Equations 6.66 and 6.67 with Equation 6.65 it is observed that there is no significant improvement in the correlation by considering separate equations for empty tube and twisted tape
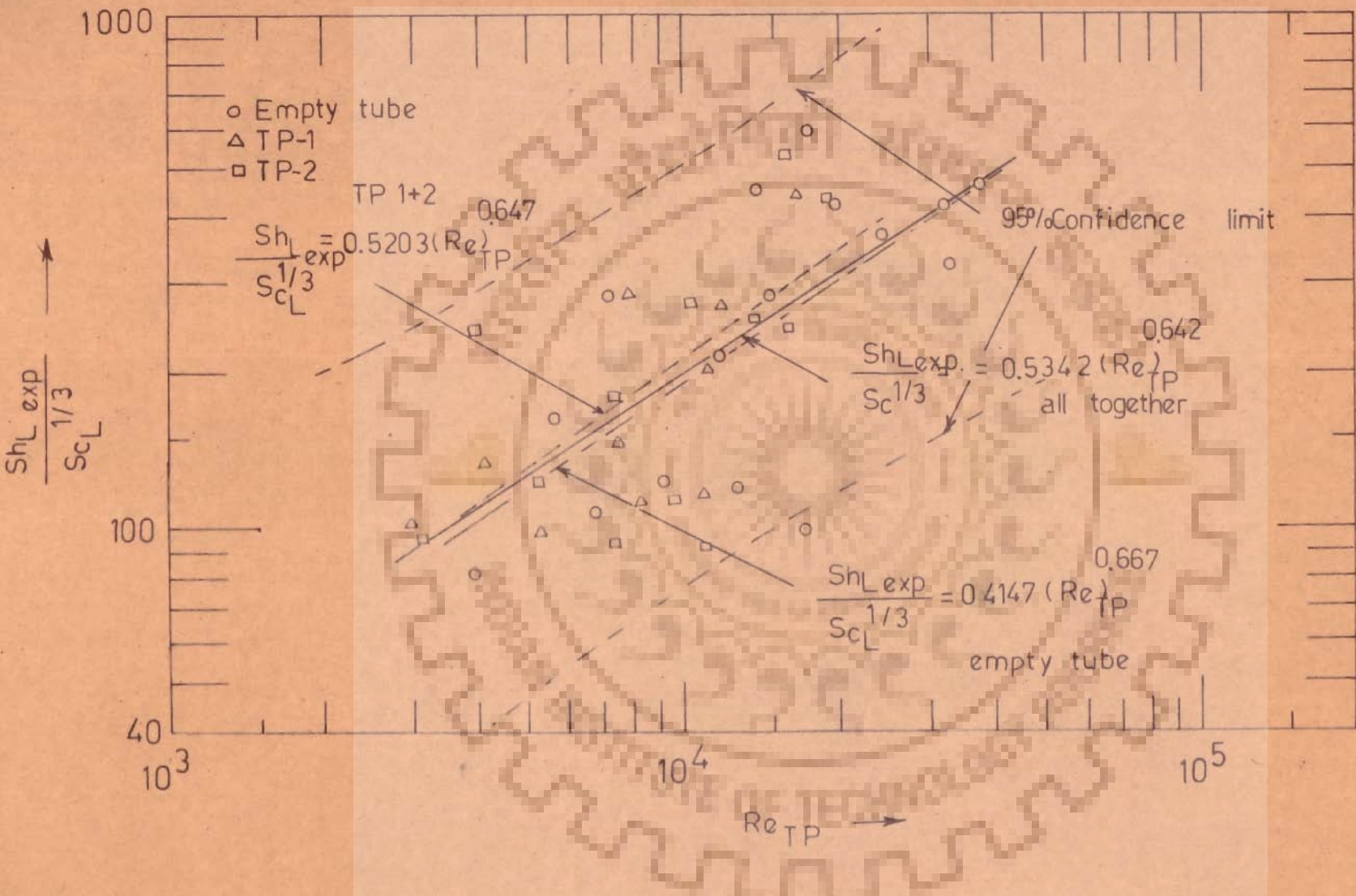
Fig.6.41 $\mathrm{Sh_L\, exp}\, /\, \mathrm{Sc_L^{1/3}}$ vs two phase Reynolds number

inserts. Hence it is concluded that the correlation group proposed by Lamont and Scott is not very successful in predicting the value of the individual liquid phase mass transfer coefficient k_L^o. In view of poor accuracy of these correlations and also because the correlations of $k_L^o a$, and, a, with Re_{TP} are not very accurate, Equations 6.10, 6.11 and Equations 6.28, 6.29, it was not considered useful to correlate liquid phase mass transfer coefficient, k_L^o, with two phase Reynolds number, Re_{TP}.

6.4.5 Comparison of Models to predict Liquid Phase Mass Transfer coefficient k_L^o

The basic aim of various models lies in their utility to estimate the value of liquid phase mass transfer coefficient, k_L^o, for a specific geometry under particular hydrodynamic conditions of gas-liquid flow. The estimated value can be used for the design purposes or to provide a better theoretical understanding of the mass transfer process. In general, it is desired that from some simple known parameters like fluid properties and flow velocities, the model should be able to predict reasonable estimates of the mass transfer coefficient. Hence the analogy between mass transfer and momentum transfer is utilised and models are developed in terms of dimensionless groups or some other parameters which can be easily and accurately determined.

Jepsen was able to correlate the volumetric mass transfer coefficient, $k_L^o a$, successfully with a term ϵ_J which is

defined by him as a type of two phase frictional energy dissipation per unit volume of the test section. In the present study it has been used to correlate, a, $k_L{}^o$a and $k_L{}^o$. Similarly Banerjee model is based on relating the mass transfer coefficient to the difference between the wave and surface velocities where as the model proposed by Kasturi and Stepanek for $k_L{}^o$ is based on the analogy between momentum and mass transfer. The values of constants in the models of Banerjee and Kasturi and Stepanek were determined using the experimental data obtained in gas-liquid annular flow. Model proposed by Lamont and Scott was basically developed for two phase bubble flow considering the spherical geometry of bubbles.

The experimental data and calculated results obtained in the present study were used to find out an estimate for the value of liquid phase mass transfer coefficient using different models and these values were then correlated with the experimental results. In the previous sections correlations based on Jepsen's energy dissipation parameter, Banerjee, Kasturi-Stepanek and Lamont and Scott methods have been subjected to a detailed analysis to compare the experimentally obtained values of $k_L{}^o$ and the values predicted by these correlations.

It is clearly seen from the above discussion that Jepsen's energy dissipation parameter correlation based on all the data points, Equation 6 gives the minimum value of the standard error closely followed by Kasturi and Stepanek. Hence either of these

correlations can be used for estimation purposes. Correlation based on Jepsen energy dissipation parameter requires the knowledge of only pressure drop per unit length of the test section and superficial liquid and gas velocities while that based on Kasturi and Stepanck method requires the knowledge of diffusivity of gas in liquid, pipe diameter, viscosity and density of the liquid also. In order to estimate the value of pressure drop per unit length, the Lockhart - Martinelli method may be used. Hence it may be concluded that correlation based on Jepsen's energy parameter is preferable from practical point of view for estimating the value of k_L^o for gas liquid slug flow in horizontal pipes, even though it has little theoretical basis. The correlation based on Kasturi and Stepanek method has a better theoretical basis and can also be used with nearly equal accuracy.

The effective use of twisted tape inserts for enhancing the liquid phase mass transfer coefficient, k_L^o, is limited to lower values of ϵ_J which can be easily seen from the following values of the ratio, $E_{k_L^o} = (k_L^o)_{twisted\ tape} / (k_L^o)_{empty\ tube}$ calculated from Equations 6.47, 6.48 and 6.53, 6.54 for different values of ϵ_J.

$\epsilon_J = kN/m^2\ sec$	0.1	0.4	1	4	4.6	10	40	100
$E_{k_L^o}$	1.72	1.43	1.27	1.09	1.0	0.88	0.89	0.90

It is, therefore, clear that the use of twisted tape inserts increases the value of liquid phase mass transfer coefficient at lower values of energy dissipation parameter, ϵ_J, but for values greater than $\epsilon_J = 4.6$ kN/m^2 sec the use of twisted tapes is disadvantageous and the value of liquid phase mass transfer coefficient is observed to be less than that for empty tube at same ϵ_J. This effect is similar to those observed for $E_{k_L^O a}$ and E_a.

6.5 PERFORMANCE COMPARISON FOR TWO PHASE MASS TRANSFER WITH AND WITHOUT TWISTED TAPES

The effect of the use of twisted tapes on the volumetric mass transfer coefficient, $E_{k_L^O a} = (k_L^O a)_{TT} / (k_L^O a)_{ET}$, $E_a = a_{TT} / a_{ET}$ and individual liquid phase mass transfer coefficient, $E_{k_L^O} = (k_L^O)_{TT} / (k_L^O)_{ET}$ at different values of Jepsen's energy dissipation parameter, is already discussed in respective sections. The effect of the use of twisted tapes on mass transfer modulus, $M_{k_L^O a} = k_L^O a / (\Delta P / \Delta L)$, and area modulus, $M_a = a / (\Delta P / \Delta L)$, at different values of superficial velocity, V_{LO}, and superficial gas velocity, V_{GO}, has also been discussed earlier.

It may be noted that the Jepsen's energy dissipation parameter ϵ_J, defined as $(\Delta P / \Delta L) (V_{LO} + V_{GO})$, does not characterize the two-phase flow condition uniquely but has been found to be a satisfactory correlating parameter of $k_L^O a$, a, and k_L^O. It also does not provide any information about the exact value of two-

phase pressure drop. However, large values of ϵ_J normally imply large values of pressure drop. If, for a specific design requirement when absorber volume is the controlling factor, highest mass transfer rates are desirable irrespective of the magnitude of the pressure drop then the use of twisted tapes of lower pitch ratio for largest value of ϵ_J is recommended for which the effectiveness factor $E_{k_L^o a}$ is greater than unity, that is $\epsilon_J = 147$ kN/m^{2}sec. If the pressure drop is the controlling factor then the flow conditions are to be so chosen that the value of mass transfer modulus $M_{k_L^o a}$ is the highest.

In order to complete the discussion, the values of various effectiveness factors, $E_{k_L^o a}$, E_a and $E_{k_L^o}$ are plotted as a function of ϵ_J in Figure 6.42. From the figure it can be observed that for ϵ_J values less than about 5.0 kN/m^{2}sec the values of all effectiveness factors are greater than unity but the values are highest at the lowest value of ϵ_J. At ϵ_J greater than 4.6 kN/m^{2}sec the use of twisted tape is disadvantageous as far as the liquid phase mass transfer coefficient, k_L^o, is concerned since $E_{k_L^o}$ becomes less than unity. Similarly the use of twisted tapes become disadvantageous at ϵ_J value of 147 kN/m^{2}sec as far as the volumetric liquid phase mass transfer coefficient is concerned since $E_{k_L^o a}$ becomes less than unity even though E_a at this value of ϵ_J is still greater than unity. At ϵ_J values greater than 210. kN/m^{2}sec the use of twisted tapes becomes disadvantageous from all three considerations, that is, $k_L^o a$, a,
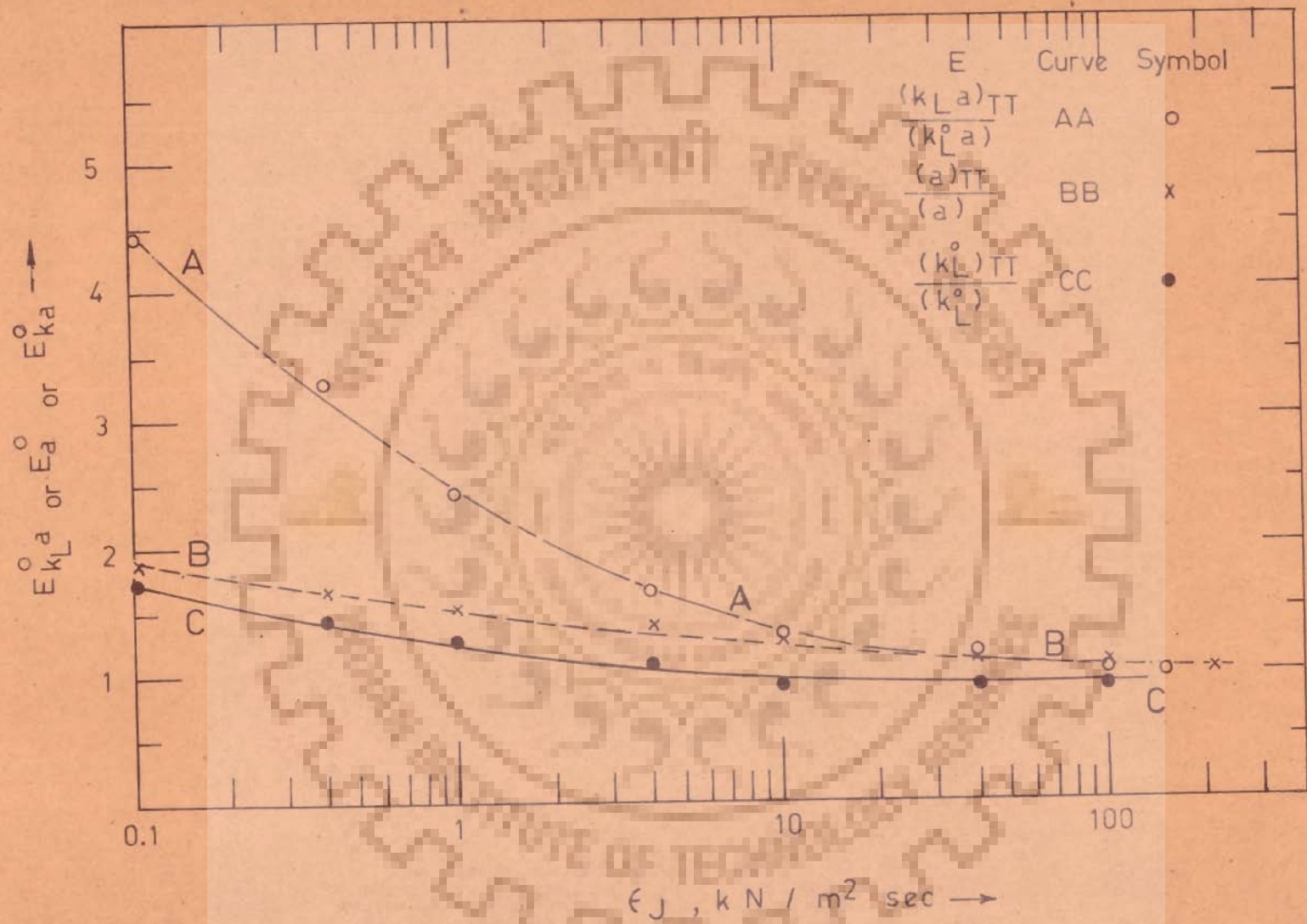
Fig. 6.42   Twisted tape effectiveness vs Jepsen energy dissipation parameter

and k_L^o. It may also be recalled that $E_{k_L^o a}$ is not equal to the multiplication product of $E_{k_L^o}$ and E_a since the condition of similarity used for physical and chemical absorption is the same two-phase Reynolds number and not the same Jepsen's energy dissipation parameter.
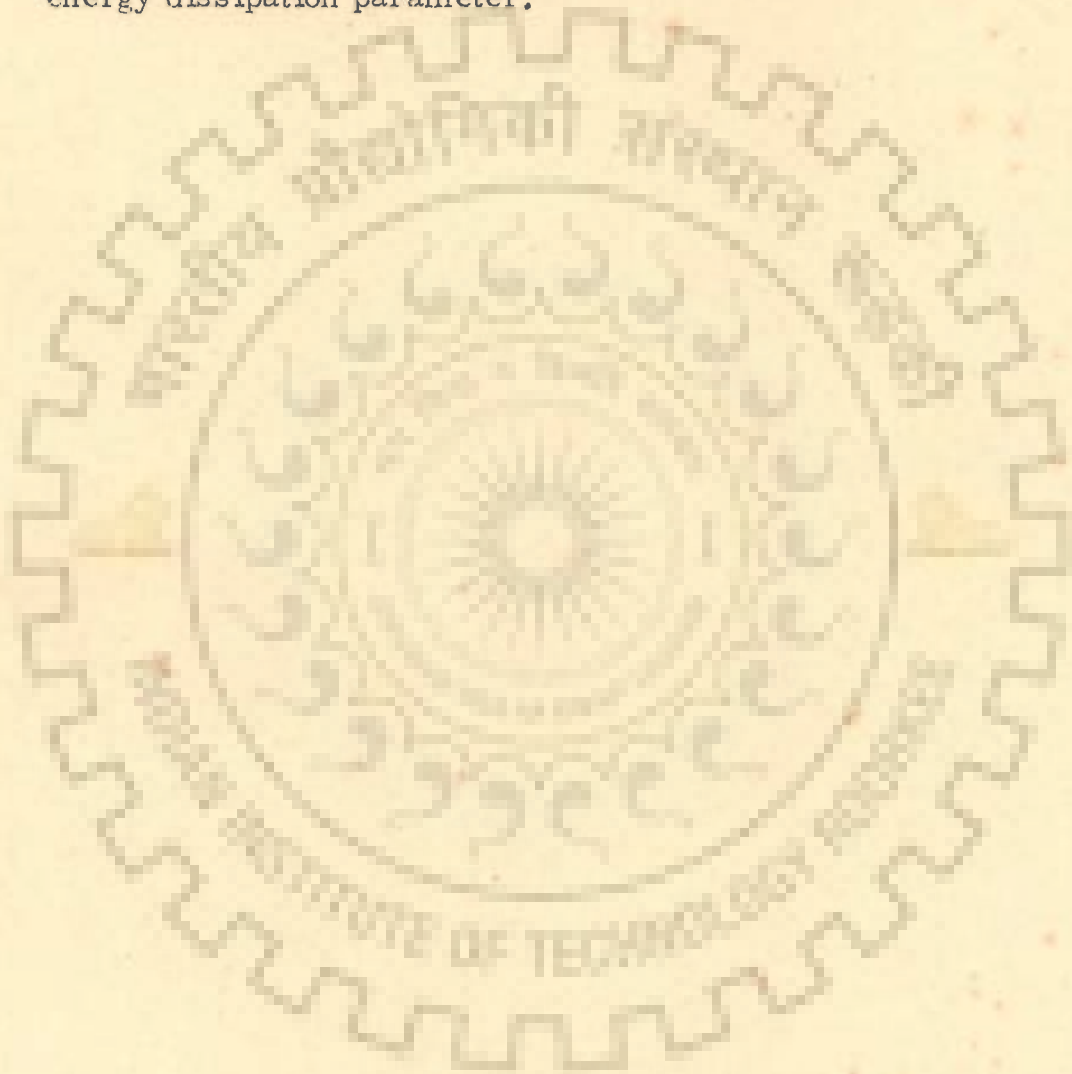
CHAPTER 7

CONCLUSIONS AND RECOMMENDATIONS

Pressure drop and mass transfer with and without chemical reaction have been studied for two-phase gas-liquid systems in slug flow regime flowing horizontally in smooth tube and in tube with twisted tape insert having pitch ratio, H/D, value of 5.00 and 9.32 for 360 degree twist. The gas phase consisted of 20 and 43.8 percent carbondioxide in humidified air and the liquid phase consisted of deionized water for physical absorption and 0.5 to 2.0 normal sodium hydroxide solution in deionized water for chemical absorption experiments.

The major conclusions and recommendations are given below :

7.1   CONCLUSIONS

7.1.1   Pressure Drop, ($\Delta P/\Delta L$)

i)   Pressure drop per unit length increases with gas and liquid superficial velocities and also with decrease in pitch ratio, H/D.

ii)   Single phase pressure drop can be calculated from the fluid velocity and physical properties knowing the friction factor. The friction factor can be determined for smooth tube or tube with twisted tape inserts in the Reynolds number range of 2.1×10^3 to 3×10^6 more accurately by the following expression :

$$f = 0.0014 + \left[0.125 + 2.51 \, (H/D - 0.5)^{-1.07} \right] Re^{-n}$$

where

$$n = 0.32 \left[1.0 + 0.65 \, (D/H)^{0.5} \right]$$

$H/D =$ pitch ratio for 360 degree twist

$$Re = D_H \cdot V \cdot \rho / \mu$$

$$D_H = \text{hydraulic diameter} = \frac{4 \cdot \text{cross sectional area}}{\text{wet perimeter}}$$

iii) Pressure drop in two-phase gas-liquid flow can be calculated from the single phase pressure drop values most accurately by the use of Lockhart-Martinelli correlations using the above correlations for single phase friction factor values. However, this method predicted two phase pressure drop values with an average under-prediction of 11.3 percent as compared to the experimental pressure drop values. For more accurate prediction of the two-phase pressure drop values the experimental pressure drop values are correlated with the value predicted by Lockhart - Martinelli method and the use of the following relationship is recommended :

$$(\Delta P/\Delta L) = 1.134 \, (\Delta P/\Delta L)_{LM}^{1.018} \, ;$$

$$\text{standard error} = 17.9 \, \%$$

where

$(\Delta P/\Delta L) =$ predicted two-phase pressure drop, kN/m^3

$(\Delta P/\Delta L)_{LM} =$ two-phase pressure drop estimated by Lockhart-Martinelli method, kN/m^3

iv) Two-phase gas-liquid pressure drop can also be predicted using the above correlation for the friction factor and two-phase Reynolds number by the method of Hughmark. However, this

method under-predicted all the experimental values with an average
under-prediction of 37.7 percent as compared to the experimental
pressure drop values. For more accurate prediction of the two-
phase pressure drop values the experimental pressure drop
values are correlated with the values predicted by Hughmark
method and the use of the following relationship is recommended :

$$(\triangle P / \triangle L) = 1.885 \, (\triangle P / \triangle L)_H^{0.944} \, ;$$

$$\text{standard error} = 39.4 \%$$

where

$(\triangle P / \triangle L)$ = predicted two-phase pressure drop, kN/m^3.

$(\triangle P / \triangle L)_H$ = two-phase pressure drop estimated by Hughmark method, kN/m^3.

7.1.2 <u>Volumetric Liquid Mass Transfer Coefficient, $k_L^o a$</u>.

i) $k_L^o a$ increased with an increase in superficial gas and
liquid velocities.

ii) $k_L^o a$ also increases with decrease in twist pitch ratio y,
(H/D for 360 degrees).

iii) With an increase in two-phase Reynolds number, $k_L^o a$
increases more for flow in empty tube as compared to the flow in
tube with twisted tape inserts.

iv) The volumetric liquid mass transfer coefficient can be
best correlated using Jepsen's energy dissipation parameter,

ϵ_J , as :

<u>Empty tube</u> :

for ϵ_J less than or equal to $4.0 \text{ kN/m}^2\text{sec}$,

$k_L{}^o a = 0.0331 (\epsilon_J)^{0.515}$; standard error $= 15.8\%$

for $\;_J$ equal to or greater than $4.0 \text{ kN/m}^2 \text{ sec}$,

$k_L{}^o a = 0.0234 (\epsilon_J)^{0.765}$; standard error $= 38.4\%$

where $k_L{}^c a$ is in sec^{-1} and ϵ_J is in $\text{kN/m}^2 \text{ sec}$

<u>Tube with twisted tape inserts</u> :

for ϵ_J less than or equal to 8.0

$k_L{}^o a = 0.0853 (\epsilon_J)^{0.277}$; standard error $= 23.6\%$

for ϵ_J equal to or greater than 8.0

$k_L{}^o a = 0.0384 (\epsilon_J)^{0.660}$; standard error $= 22.7\%$

v)   If mass transfer modulus, $M_{k_L{}^o a}$, that is volumetric

liquid phase mass transfer coefficient per unit pressure drop per

unit length or $k_L{}^o a / (\Delta P/\Delta L)$, is the criteria for designing

the absorbers then the use of twisted tape inserts with very small

pitch ratio are always undesirable since their values of $M_{k_L{}^o a}$

are always low.

vi)   At lower gas velocities the twisted tape with larger pitch

ratio ($H/D = 9.32$) is advantageous at superficial liquid velocity

upto 0.8 m/sec but at higher gas velocity the advantage is

restricted to much lower liquid velocity.

vii)   Effectiveness factor $E_{k_L{}^o a}$, that is, the ratio of volumetric

liquid mass transfer coefficient with twisted tapes and without

twisted tape or $(k_L{}^o a)_{\text{twisted tape}} / (k_L{}^o a)_{\text{empty tube}}$, decreases

with increase in ϵ_J and becomes unity at a value of ϵ_J equal to

147.0 k N/m^{2}sec. However, only for ϵ_J values less than

5.0 k N/m^2 sec it is found that value of $E_{k_L}{}^o{}_a$ is more than 1.5.

7.1.3 Effective interfacial area, a

i)   In general the interfacial area increases with an increase

in superficial gas velocity and decrease in the pitch ratio.

ii)   Interfacial area increases initially with an increase in

superficial liquid velocity upto a value of approximately 0.4 m/sec

but further increase in superficial liquid velocity decreases the

interfacial area.

iii)   The effect of difference in pitch ratio (H/D value of 5.00

and 9.32) is only marginal but the values of interfacial area are

1.5 to 4.0 times the value obtained in empty tube.

iv)   With an increase in two-phase Reynolds number interfacial

area increases more steeply for flow in empty tube as compared

to flow in tube with twisted tape inserts.

v)   The effective interfacial area can be correlated most

satisfactorily in terms of Jepsen's energy dissipation parameter

as :

Empty tube

a = 163.9 (ϵ_J)$^{0.313}$; standard error = 31.0 %

Tube with twisted tape inserts

a = 253.9 (ϵ_J)$^{0.231}$; standard error = 31.2 %

where a is in m^2/m^3 and ϵ_J is in kN/m^2 sec

vi)   The effective interfacial area can be correlated with equal

success using the area creation rate parameter of Kasturi and

Stepanek and the pressure drop as follows :

Empty tube

$$\frac{a\, Q_L}{E_L} = 0.0224\, (\triangle P/\triangle L)^{1.034} \quad ; \text{ standard error } = 32.3\%$$

Tube with twisted tape inserts

$$\frac{a\, Q_L}{E_L} = 0.00778\, (\triangle P/\triangle L)^{1.064} \quad ; \text{ standard error } = 32.8\%$$

where $\dfrac{a\, Q_L}{E_L}$ is rate of area creation m^2 / sec.

vii)   If area modulus, M_a , that is, effective interfacial area

per unit pressure drop per unit length, $a/\, (\triangle P/\triangle L)$, is the

criteria for designing the absorber then the presence of twisted

tape is always undesirable because for a given pressure drop

much more interfacial area can be obtained in empty tube by using

higher velocities than by superimposing swirl flow with the help of

twisted tape inserts at lower flow rates. Area modulus is related

to pressure drop by :

Empty tube

$$M_a = \frac{a\, Q_L / E_L}{(\triangle P/\triangle L)} = 0.0224\, (\triangle P/\triangle L)^{0.034} \simeq 0.0224$$

Tube with twisted tape inserts

$$M_a = \frac{a\, Q_L / E_L}{(\triangle P/\triangle L)} = 0.00778\, (\triangle P/\triangle L)^{0.064} \simeq 0.00778$$

viii)   Effectiveness factor, E_a , that is, the ratio of interfacial

area with twisted tapes and without twisted tape, decreases with

increase in ϵ_J and becomes unity for a value of ϵ_J equal to

$210.0 \, \text{kN/m}^2 \text{sec}$. However, only for ϵ_J values less than

$1.0 \, \text{kN/m}^2 \text{sec}$ it is found that the value of E_a is more than 1.5.

7.1.4 Liquid Phase Mass Transfer Coefficient, $k_L{}^o$

i) Liquid phase mass transfer coefficient increases with an

increase in superficial gas velocity and decrease in the pitch

ratio.

ii) Liquid phase mass transfer coefficient can be correlated

for empty tube and tube with twisted tape inserts most satisfactorily

in terms of Jepsen's energy dissipation parameter as :

$$k_L{}^o = 1.500 \times 10^{-4} \, (\epsilon_J)^{0.375} \; ; \text{standard error} = 28.8 \, \%$$

iii) Dimensionless group correlations can also be used to

calculate the liquid phase mass transfer coefficient. The

experimental data are best correlated by :

Empty tube :

$$Sh_L = 0.1243 \, Pe_L \, Eu_L \, Sc_L^{-\frac{1}{2}} \; ; \text{standard error} = 30.5\%$$

Tube with twisted tape inserts

$$Sh_L = 0.07863 \, Pe_L \, Eu_L \, Sc_L^{-\frac{1}{2}} \; ; \text{standard error} = 31.2\%$$

where Sh_L, Pe_L, Eu_L and Sc_L are liquid phase Sherwood,

Peclet, Euler and Schmidt numbers respectively.

iv) Effectiveness factor, $E_{k_L}{}^o$, that is, the ratio of liquid

phase mass transfer coefficient with twisted tapes and without

twisted tape, decreases with increase in ϵ_J and becomes unity

for a value of ϵ_J equal to $4.6 \, \text{kN/m}^2 \text{sec}$ but from the practical

point of view $E_{k_L}{}^o$ is substantial at ϵ_J less than $3.0 \, \text{kN/m}^2 \text{sec}$.

7.2   RECOMMENDATIONS

1.   Only two pitch ratios (H/D = 5.00 and 9.32) were studied in the present investigations, it is, therefore, recommended that the mass transfer studies are carried out on other pitch ratios, especially with larger values of H/D , so as to have a better understanding of the effect of swirling flow on the transfer coefficients and interfacial area.

2.   In place of a long continuous twisted tape, investigations with tapes of shorter lengths placed inter-mittently be also carried out. It may also be desirable to study the effect of twisted tapes made out of perforated sheet strips. It is expected that they may give good mass transfer rates without excessive pressure losses.

3.   In order to understand the effect of liquid phase physical properties, studies on mass transfer may be carried out by varying liquid phase viscosity, density and surface tension.

4.   Investigations may be carried out by varying the liquid and gas flow rates over a broader range to check the validity of correlations at lower and higher ranges of flow rates. It may be recalled that the twisted tape inserts are more efficient at lower flow rates.

5.   Effect of the presence of twisted tape on the gas phase mass transfer rates be investigated since it is observed that the increase in gas flow rates does not increase the pressure drop to that extent as in the case of liquid. Therefore, it may be

possible to obtain higher mass transfer rates without excessive pressure drop especially for systems where gas phase mass transfer rates may control the overall mass transfer rates.

6.   It is necessary to identify and develop suitable parameter to classify the gas-liquid flow regimes when swirl flow is superimposed on axial flow.

APPENDIX A   CALIBRATION DATA
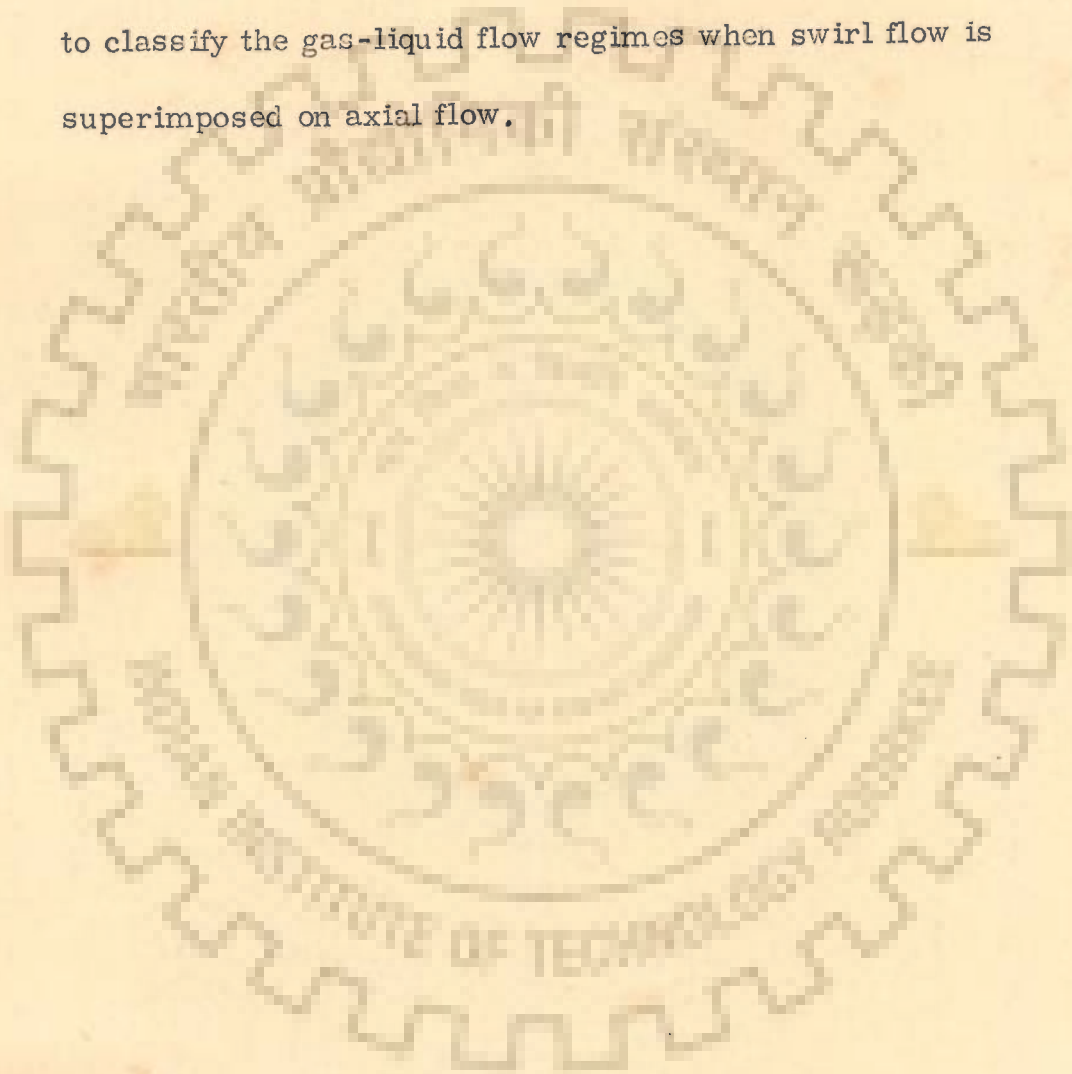
TABLE A.1

I & E LIQUID ROTAMETER CALIBRATION
(Deionized Water)

Water Temp. = 31.5°C

No.	Time sec.	Volume litre	Rotameter Reading	Flow Rate lit/hr
1	313.8	3.70	1000	42.5
2	212.1	2.50	1000	42.5
3	184.8	4.10	2000	80.0
4	117.4	3.75	3000	115.0
5	108.8	4.50	4000	149.0
6	111.7	5.75	5000	185.5
7	83.7	5.10	6000	219.5
8	87.8	6.15	7000	250.0
9	85.8	6.90	8000	289.5
10	63.6	5.73	9000	324.0
11	60.2	6.05	10,000	362.0
12	63.6	6.95	11,000	393.5
13	52.5	6.25	12,000	428.5

TABLE A.2

I & E LIQUID ROTAMETER CALIBRATION
(2N NaOH Solution)

Density = 1.10 gm/ml (kg/lit.)

Liquid Temp. = 30.4°C

No.	Time sec.	Volume litre	Rotameter Reading	Flow Rate lit/hr
1	122.60	1.195	1000	35.25
2	70.60	1.345	2000	68.60
3	69.30	1.995	3000	103.80
4	55.10	1.830	3500	119.75
5	45.65	1.937	4500	152.70
6	34.30	1.945	6000	204.10
7	27.10	1.920	7500	255.00
8	23.50	1.980	9000	303.50
9	19.50	1.918	10,500	354.10

TABLE A.3

I & E AIR ROTAMETER CALIBRATION

Atmospheric Pressure   =   736.0 mm Hg.

Inlet Pressure   =   35.0 psia

No.	Time sec.	Volume cu.ft.	Temp. °C	Rotameter Reading	Flow Rate lit/hr, N.T.P.
1	89.1	0.3	17.5	250	312.
2	101.4	0.4	17.5	300	366.
3	112.0	0.5	17.4	350	414.
4	161.9	1.0	15.4	450	576.
5	153.9	1.0	15.4	500	606.
6	108.4	1.0	15.6	750	858.
7	84.0	1.0	15.3	1000	1110.
8	138.0	2.0	15.6	1250	1351.
9	117.0	2.0	15.6	1500	1592.
10	129.2	2.5	15.6	1750	1802.
11	92.7	2.0	15.7	2000	2030.
12	84.3	2.0	17.2	2250	2202.
13	77.5	2.0	17.1	2500	2395.
14	66.0	2.0	15.4	3000	2825.
15	60.4	2.0	17.2	3250	3075.
16	56.8	2.0	17.2	3500	3270.

TABLE A.4

RI AIR ROTAMETER CALIBRATION

Atmospheric Pressure = 737.50 mm Hg

Inlet Pressure   = 35.0 psia

No	Time sec.	Volume cu.ft.	Temp. $^{\circ}C$	Rotameter Reading	Flow Rate lit/hr. N.T.P.
1	78.2	2.0	15.4	1300	2385.
2	101.7	3.0	15.5	1500	2750.
3	88.2	3.0	15.2	1750	3165.
4	93.1	3.5	15.4	2000	3510.
5	87.3	3.5	15.4	2200	3735.
6	93.3	4.0	15.4	2500	4000.
7	874	4.0	15.3	2750	4270.
8	102.9	5.0	15.2	3000	4535.
9	98.7	5.0	15.2	3250	4770.
10	90.7	5.0	15.2	3500	5140.
11	104.0	6.0	15.2	3750	5375.
12	69.4	4.0	15.2	3750	5375.
13	82.5	5.0	15.2	4000	5650.
14	94.9	6.0	15.2	4250	5890.
15	120.7	8.0	15.2	4500	6180.
16	114.2	8.0	15.2	4750	6525.

TABLE A.5

I & E CO_2 ROTAMETER CALIBRATION

Atmospheric Pressure = 737.50 mm Hg.

Inlet Pressure = 35.0 psia

SNo.	Time sec.	Volume cu.ft.	Temp. ^{O}C	Rotameter Reading	Flow Rate lit/hr, N.T.P.
1	103.0	0.20	17.9	100	179.7
2	93.5	0.20	16.2	100	199.0
3	106.0	0.30	16.3	150	263.5
4	116.4	0.40	16.3	200	320.0
5	106.0	0.50	17.2	300	434.0
6	84.6	0.54	16.2	450	594.0
7	64.3	0.50	16.2	550	728.
8	76.4	0.60	16.4	550	734.0
9.	61.8	0.50	18.2	600	749.0
10	83.0	0.70	16.4	650	784.0
11	87.9	0.80	17.0	700	837.5
12	102.2	1.00	16.2	750	911.0
13	83.1	0.90	16.7	850	995.0
14	87.2	1.00	16.4	950	1068.
15	99.7	1.20	16.4	1000	1120.
16	81.8	1.00	15.6	1050	1138.

EXPERIMENTAL DATA EMPTY TUBE

D CM	AL1 CM	AL2 CM	AL3 CM	BL CM	CL1 CM	CL2 CM	CL3 CM
1.348	110.6	256.0	366.5	300.7	233.7	123.2	132.8

RUN NO.	QL LIT/HR	QG LIT/HR	PT PSIA	X	T DEG C	BO ML	S1 ML	S2 ML	F CO2	DELP MM HG
1014	70.0	570.0	20.30	.02065	19.80	5.70	5.10	4.25	.4385	4.
1015	140.0	570.0	22.23	.02065	19.50	5.46	5.06	4.16	.4385	9.
1016	210.0	570.0	19.73	.02065	17.40	5.79	5.22	4.51	.4385	15.
1017	280.0	570.0	20.00	.02000	22.20	6.00	5.54	4.93	.4385	26.
1018	350.0	570.0	20.00	.02020	27.60	5.74	5.28	4.84	.4385	40.
1019	70.0	2000.0	20.00	.02130	20.00	5.72	5.25	4.57	.2000	10.
1020	140.0	2000.0	20.00	.02130	21.60	5.74	5.24	4.64	.2000	21.
1021	210.0	2000.0	20.00	.02130	20.40	5.80	5.30	4.67	.2000	37.
1022	280.0	2000.0	20.00	.02130	22.00	5.80	5.26	4.58	.2000	53.
1023	350.0	2000.0	20.10	.02000	23.80	5.44	5.01	4.36	.2000	71.
1024	70.0	3500.0	21.00	.02000	24.00	6.00	5.12	4.36	.2000	11.
1025	140.0	3500.0	20.30	.02000	24.20	5.93	5.13	4.33	.2000	32.
1026	210.0	3500.0	21.00	.02000	20.60	5.81	5.00	4.04	.2000	50.
1027	280.0	3500.0	20.00	.02000	21.80	5.98	5.18	4.31	.2000	90.
1028	350.0	3500.0	20.30	.02000	27.70	5.40	4.70	4.23	.2000	135.
1029	70.0	5000.0	20.00	.02000	21.20	5.67	4.26	3.41	.2000	25.
1030	140.	5000.	20.	.020	21.2	5.82	4.78	3.66	.20	46.
1031	210.	5000.	20.	.020	22.8	5.89	4.85	3.99	.20	73.
1032	280.	5000.	20.	.020	24.6	5.87	5.0	3.99	.20	104.
4001	350.0	570.0	20.56	.02030	27.60	6.27	5.92	5.47	.4385	31.
4002	350.0	2000.0	19.76	.02030	28.00	6.27	5.82	5.42	.2000	70.
4003	350.0	3500.0	19.96	.02010	32.00	6.06	5.67	4.98	.2000	100.
4004	280.0	3500.0	19.65	.02010	33.00	6.16	5.68	5.07	.2000	77.
4005	350.0	5000.0	20.25	.02010	33.00	6.16	5.39	4.44	.2000	131.
4006	280.0	5000.0	19.76	.02030	27.80	6.27	5.40	4.70	.2000	98.

EXPERIMENTAL DATA TP-1 (H/D= 5.00)

D CM	AL1 CM	AL2 CM	AL3 CM	BL CM	CL1 CM	CL2 CM	CL3 CM	BR CM	WI CM
1.348	110.6	131.5	242.1	178.7	170.2	59.7	70.8	1.175	.075

RUN NO.	QL LIT/HR	QG LIT/HR	PT PSIA	X	T DEG C	BO ML	S1 ML	S2 ML	F CO2	DELP MM HG
1103	70.0	570.0	20.00	.02016	25.60	5.70	3.16	2.54	.4385	16.
1104	140.0	570.0	20.00	.02016	23.60	5.80	3.88	3.02	.4385	34.
1105	210.0	570.0	20.00	.02016	24.30	5.57	3.81	3.18	.4385	45.
1106	280.0	570.0	20.00	.02016	23.50	5.80	4.68	4.05	.4385	64.
1107	350.0	570.0	19.95	.02016	28.30	5.96	5.03	4.50	.4385	76.
1108	70.0	2000.0	19.95	.02016	24.20	5.69	3.93	3.52	.2000	41.
1109	140.0	2000.0	19.95	.02016	22.00	6.35	4.80	4.37	.2000	63.
1110	210.0	2000.0	20.00	.02016	21.80	6.61	5.41	4.89	.2000	91.
1111	280.0	2000.0	20.00	.02016	22.00	6.61	5.58	5.18	.2000	123.
1112	350.0	2000.0	19.95	.02016	27.80	5.99	5.03	4.69	.2000	153.
1113	70.0	3500.0	20.00	.02016	22.10	6.32	4.28	4.12	.2000	48.
1114	140.0	3500.0	20.00	.02016	21.60	6.00	4.03	3.74	.2000	95.
1115	210.0	3500.0	19.97	.02016	23.20	5.95	4.41	4.03	.2000	138.
1116	280.0	3500.0	19.95	.02016	27.10	6.08	4.76	4.46	.2000	221.
1117	350.0	3500.0	20.00	.02016	27.00	5.73	4.11	3.77	.2000	65.
1118	70.0	5000.0	19.96	.02016	24.40	6.20	4.01	3.90	.2000	113.
1119	140.0	5000.0	20.04	.02016	22.80	6.16	4.21	4.03	.2000	64.
1120	70.0	5000.0	20.00	.02016	23.30	5.88	4.79	4.77	.1000	18.
4101	70.0	570.0	20.09	.01928	27.25	5.23	3.23	2.31	.4385	33.
4102	140.0	570.0	20.09	.01928	27.50	5.23	3.84	3.04	.4385	56.
4103	210.0	570.0	19.90	.01928	28.50	6.44	5.37	4.45	.4385	30.
4104	70.0	2000.0	20.10	.01928	28.00	6.44	5.18	4.89	.2000	60.
4105	140.0	2000.0	20.42	.01928	28.50	6.57	5.52	5.06	.2000	95.
4106	210.0	2000.0	20.02	.01928	29.00	6.57	5.64	5.29	.2000	219.
4107	350.0	3500.0	19.68	.01928	28.50	6.51	5.77	5.11	.2000	297.
4108	350.0	5000.0	19.58	.01928	28.00	6.51	5.26	4.92	.2000	178.
4109	280.0	3500.0	19.95	.01928	28.00	6.54	5.21	4.95	.2000	237.
4110	280.0	5000.0	20.12	.01928	27.80	6.25	4.73	4.60	.2000	137.
4111	210.0	3500.0	20.12	.01928	28.00	6.25	4.86	4.66	.2000	90.
4112	140.0	3500.0	20.12	.01928	28.00	6.25	4.78	4.56	.2000	49.
4113	70.0	3500.0	19.32	.01928	28.40	6.25	4.63	4.46	.2000	

EXPERIMENTAL DATA Tp-2 (H/D= 9.32)

D CM	AL1 CM	AL2 CM	AL3 CM	BL CM	CL1 CM	CL2 CM	CL3 CM	BR CM	WI CM
1.348	110.6	131.5	242.1	178.7	170.2	59.7	70.8	1.242	.075

RUN NO.	QL LIT/HR	QG LIT/HR	PT PSIA	X	T DEG C	BO ML	S1 ML	S2 ML	F CO2	DELP MM HG
1201	70.0	570.0	20.00	.02020	29.50	6.24	4.64	3.72	.4385	12.
1202	140.0	570.0	20.00	.02020	28.00	5.78	4.77	3.73	.4385	23.
1203	210.0	570.0	20.01	.02020	28.60	6.18	5.36	4.66	.4385	33.
1204	280.0	570.0	20.01	.02020	29.10	6.18	5.50	5.19	.4385	49.
1205	350.0	570.0	20.00	.02020	29.50	6.24	5.60	5.10	.4385	64.
1206	70.0	2000.0	20.02	.02020	27.00	6.14	4.93	4.55	.2000	29.
1207	140.0	2000.0	20.02	.02020	26.90	6.14	5.19	4.78	.2000	55.
1208	210.0	2000.0	20.02	.02020	26.85	6.14	5.21	4.78	.2000	80.
1209	280.0	2000.0	20.00	.02020	28.40	6.30	5.59	5.15	.2000	104.
1210	350.0	2000.0	20.00	.02020	27.70	6.30	5.68	5.25	.2000	128.
1211	70.0	3500.0	20.00	.02020	28.70	5.91	4.46	4.13	.2000	40.
1212	140.0	3500.0	20.00	.02020	29.30	5.91	4.55	4.21	.2000	80.
1213	210.0	3500.0	20.00	.02020	26.60	5.99	4.69	4.36	.2000	121.
1214	280.0	3500.0	20.00	.02020	26.70	6.10	5.00	4.62	.2000	160.
1215	350.0	3500.0	20.00	.02020	27.10	6.10	5.12	4.73	.2000	195.
4201	280.0	570.0	20.38	.01928	30.60	6.24	5.26	4.63	.4385	45.
4202	280.0	3500.0	20.38	.01928	30.60	6.24	5.03	4.51	.2000	151.
4203	210.0	3500.0	20.04	.01928	31.40	7.32	6.05	5.67	.2000	112.
4204	140.0	3500.0	19.84	.01928	31.80	7.32	6.02	5.62	.2000	75.
4205	70.0	3500.0	19.64	.01928	32.20	7.32	5.88	5.61	.2000	46.
4206	350.0	5000.0	20.44	.01928	30.50	7.26	5.98	5.81	.2000	257.
4207	280.0	5000.0	20.01	.01928	32.00	7.30	5.88	5.70	.2000	205.
4208	210.0	5000.0	19.54	.01928	30.30	7.26	6.06	5.60	.2000	151.
4209	140.0	5000.0	20.61	.01928	32.20	7.30	5.85	5.20	.2000	100.
4210	70.0	5000.0	20.01	.01928	32.20	7.30	5.52	4.70	.2000	52.

EXPERIMENTAL RESULTS EMPTY TUBE

RUN NO.	TS DEG K	PTS KN/M2	VLO M/SEC	VGO M/SEC	PL KN/M3	EDPJ KN/M2/SEC	KLOA /SEC			FABS	
							1	2	3	2	3
1014	293.0	140.0	.1362	.8486	.177	.175	.0174	.0131	.0144	.019	.047
1015	292.7	153.3	.2724	.7666	.399	.415	.0203	.0238	.0228	.026	.084
1016	290.6	136.0	.4086	.8442	.665	.833	.0472	.0315	.0363	.055	.124
1017	295.4	137.8	.5448	.8444	1.153	1.601	.0555	.0393	.0443	.058	.134
1018	300.8	137.8	.6810	.8554	1.773	2.725	.0828	.0429	.0553	.073	.143
1019	293.2	137.9	.1362	3.0588	.443	1.417	.0333	.0327	.0329	.010	.024
1020	294.8	137.9	.2724	3.0658	.931	3.108	.0755	.0638	.0675	.021	.046
1021	293.6	137.8	.4086	3.0432	1.640	5.663	.1081	.0989	.1021	.031	.071
1022	295.2	137.8	.5448	3.0467	2.350	8.440	.1666	.1805	.1775	.045	.102
1023	297.0	138.4	.6810	3.0505	3.148	11.747	.1551	.1799	.1733	.042	.106
1024	297.2	144.8	.1362	5.1704	.488	2.588	.0730	.0675	.0694	.010	.018
1025	297.4	139.9	.2724	5.3403	1.419	7.963	.1341	.1598	.1532	.018	.036
1026	293.8	144.7	.4086	5.0842	2.217	12.177	.1691	.2304	.2135	.027	.059
1027	295.0	137.7	.5448	5.3508	3.990	23.525	.2418	.3766	.3420	.036	.075
1028	300.9	139.7	.6810	5.3840	5.986	36.302	.3045	.1970	.2387	.039	.066
1029	294.4	137.8	.1362	7.6839	1.108	8.668	.1434	0.0000	0.0000	.011	.018
1030	294.4	137.8	.2724	7.6698	2.040	16.198	.1720	0.0000	0.0000	.016	.034
1031	296.0	137.7	.4086	7.7000	3.237	26.245	.2730	0.0000	0.0000	.024	.045
1032	297.8	137.7	.5448	7.7373	4.611	38.189	.2981	0.0000	0.0000	.027	.059
4001	300.8	141.7	.6810	.8382	1.374	2.088	.0605	.0406	.0467	.056	.127
4002	301.2	136.1	.6810	3.1529	3.104	11.899	.1960	.1243	.1478	.045	.085
4003	305.2	137.4	.6810	5.5634	4.434	27.686	.1796	.3113	.2729	.022	.061
4004	306.2	135.3	.5448	5.6747	3.414	21.233	.1967	.2600	.2434	.022	.049
4005	306.2	139.3	.6810	7.8510	5.808	49.555	.4303	0.0000	0.0000	.030	.068
4006	301.0	136.0	.5448	7.9216	4.345	36.787	.3556	0.0000	0.0000	.028	.050

EXPERIMENTAL RESULTS TP-1 (H/D= 5.00)

RUN NO.	TS DEG K	PTS KN/M2	VLO M/SEC	VGO M/SEC	PL KN/M3	EDPJ KN/M2/SEC	KLOA /SEC 1	2	3	FABS 2	3
1103	298.8	137.8	.1452	.9128	1.194	1.263	.1452	.0882	.1155	.080	.100
1104	296.8	137.8	.2903	.8830	2.537	2.976	.1705	.1430	.1573	.121	.176
1105	297.5	137.7	.4355	.8653	3.357	4.367	.2373	.1466	.1911	.167	.227
1106	296.7	137.6	.5806	.8698	4.775	6.926	.1679	.1265	.1470	.142	.221
1107	301.5	137.2	.7258	.8833	5.670	9.124	.1984	.1512	.1749	.147	.231
1108	297.4	137.4	.1452	3.3040	3.059	10.550	.4429	0.0000	0.0000	.035	.043
1109	295.2	137.3	.2903	3.2612	4.700	16.693	.4149	0.0000	0.0000	.061	.078
1110	295.0	137.5	.4355	3.2425	6.789	24.971	.3598	.7540	.6002	.071	.102
1111	295.2	137.4	.5806	3.2408	9.177	35.068	.3742	.3377	.3701	.081	.113
1112	301.0	136.9	.7258	3.3061	11.415	46.023	.5427	.6516	.6470	.095	.128
1113	295.3	137.7	.1452	5.7451	3.581	21.094	0.0000	0.0000	0.0000	.023	.025
1114	294.8	137.5	.2903	5.7160	7.088	42.571	0.0000	0.0000	0.0000	.044	.051
1115	296.4	137.1	.4355	5.7506	10.296	63.690	.6055	0.0000	0.0000	.052	.065
1116	300.3	136.8	.5806	5.8293	12.982	83.210	.7172	0.0000	0.0000	.060	.073
1117	300.2	137.0	.7258	5.7800	16.488	107.269	1.8399	0.0000	0.0000	.091	.111
1118	297.6	137.3	.1452	8.3024	4.849	40.966	0.0000	0.0000	0.0000	.017	.018
1119	296.0	137.7	.2903	8.2126	8.431	71.685	0.0000	0.0000	0.0000	.031	.034
1120	296.5	137.6	.1452	8.2699	4.775	40.181	0.0000	0.0000	0.0000	.017	.018
4101	300.4	138.4	.1452	.9204	1.343	1.431	.0963	.0856	.0911	.060	.088
4102	300.7	138.4	.2903	.9074	2.462	2.949	.1185	.0994	.1088	.084	.132
4103	301.7	137.0	.4355	.9068	4.178	5.608	.1335	.1691	.1535	.097	.181
4104	301.2	138.5	.1452	3.3283	2.238	7.774	.1691	.1243	.1485	.024	.029
4105	301.7	140.5	.2903	3.2700	4.476	15.938	.2389	.3283	.2948	.040	.057
4106	302.2	137.6	.4355	3.3349	7.088	26.723	.3061	.2617	.2926	.053	.073
4107	301.7	134.8	.7258	5.9558	16.339	109.170	.3345	1.2363	.8392	.040	.076
4108	301.2	133.8	.7258	8.5656	22.158	205.880	.7020	0.0000	0.0000	.047	.060
4109	301.2	136.8	.5806	5.8514	13.280	85.417	.6948	0.0000	0.0000	.057	.069
4110	301.0	137.7	.5806	8.3227	17.682	157.428	.8630	0.0000	0.0000	.046	.050
4111	301.2	138.2	.4355	5.8119	10.221	63.855	.5805	0.0000	0.0000	.045	.052
4112	301.2	138.3	.2903	5.8203	6.715	41.031	.4628	0.0000	0.0000	.032	.036
4113	301.6	133.0	.1452	6.0815	3.656	22.763	.4971	0.0000	0.0000	.017	.019

EXPERIMENTAL RESULTS   TP-2 (H/D= 9.32)

RUN NO.	TS DEG K	PTS KN/ M2	VLO M/ SEC	VGO M/ SEC	PL KN/ M3	EDPJ KN/M2/ SEC	KLOA /SEC 1	2	3	FABS 2	3
1201	302.7	137.8	.1457	.9386	.895	.971	.0827	.0846	.0840	.051	.080
1202	301.2	137.8	.2914	.9209	1.716	2.080	.0868	.1272	.1088	.064	.130
1203	301.8	137.8	.4371	.9166	2.462	3.333	.1039	.1097	.1073	.078	.144
1204	302.3	137.8	.5828	.9208	3.656	5.497	.1131	.0562	.0829	.086	.125
1205	302.7	137.6	.7285	.9080	4.775	7.814	.1334	.1227	.1282	.101	.181
1206	300.2	137.9	.1457	3.3422	2.164	7.546	.1632	.2274	.2027	.024	.031
1207	300.1	137.8	.2914	3.3316	4.103	14.866	.2108	.2070	.2129	.038	.054
1208	300.0	137.7	.4371	3.3185	5.969	22.416	.3036	.3548	.3404	.055	.081
1209	301.6	137.5	.5828	3.3376	7.759	30.419	.2886	.3570	.3317	.056	.091
1210	300.9	137.4	.7285	3.3262	9.550	38.721	.2903	.3583	.3324	.061	.104
1211	301.9	137.7	.1457	5.9010	2.984	18.045	.2922	0.0000	0.0000	.016	.020
1212	302.5	137.6	.2914	5.9004	5.969	36.956	.4859	0.0000	0.0000	.031	.038
1213	299.8	137.4	.4371	5.8371	9.027	56.640	.5203	0.0000	0.0000	.044	.055
1214	299.9	137.2	.5828	5.8357	11.937	76.619	.4927	.7874	.7195	.050	.067
1215	300.3	137.1	.7285	5.8401	14.548	95.563	.5086	.6812	.6539	.055	.077
4201	303.8	140.3	.5828	.8872	3.357	4.935	.1707	.1458	.1582	.119	.195
4202	303.8	139.9	.5828	5.7933	11.266	71.831	.6517	0.0000	0.0000	.052	.075
4203	304.6	137.7	.4371	5.9200	8.356	53.120	.6102	0.0000	0.0000	.041	.053
4204	305.0	136.5	.2914	5.9990	5.596	35.198	.4684	0.0000	0.0000	.028	.037
4205	305.4	135.2	.1457	6.0816	3.432	21.372	.3950	0.0000	0.0000	.016	.018
4206	303.7	139.9	.7285	8.2949	19.174	173.015	.8186	0.0000	0.0000	.048	.055
4207	305.2	137.1	.5828	8.5132	15.294	139.119	1.0733	0.0000	0.0000	.043	.048
4208	303.5	134.1	.4371	8.6794	11.266	102.703	.4965	0.0000	0.0000	.027	.038
4209	305.4	141.7	.2914	8.2753	7.461	63.913	.5920	0.0000	0.0000	.022	.032
4210	305.4	137.7	.1457	8.5294	3.880	33.656	0.0000	0.0000	0.0000	.013	.020

APPENDIX C.

TABLE C.1

EXPERIMENTAL DATA EMPTY TUBE

D CM	AL1 CM	AL2 CM	AL3 CM	BL CM	CL1 CM	CL2 CM	CL3 CM	BR CM	WI CM
1.348	110.5	256.0	366.5	300.7	233.7	123.2	132.8		

RUN NO.	QL LIT/HR	QG LIT/HR	PT PSIA	X	T DEG C	BO ML	B1 ML	S1 ML	S2 ML	F CO2	DELP MM HG
2009	70.0	570.0	20.00	.09620	32.10	21.20	20.39	19.19	17.85	.4385	5.
2010	140.0	570.0	20.00	.09620	32.10	21.20	20.39	19.36	18.57	.4385	10.
2012	280.0	570.0	20.00	.09620	32.10	21.80	21.05	20.79	20.39	.4385	23.
2013	350.0	570.0	18.90	.09620	32.50	21.80	21.05	20.80	20.45	.4385	32.
2014	70.0	2000.0	19.10	.09620	32.71	20.92	19.96	18.89	17.32	.2000	9.
2015	140.0	2000.0	19.80	.09625	31.50	20.31	18.20	17.85	16.85	.2000	22.
2016	210.0	2000.0	19.60	.09625	31.60	20.31	18.20	17.81	17.19	.2000	45.
2017	280.0	2000.0	19.80	.09620	30.90	20.73	18.94	18.66	18.24	.2000	62.
2018	350.0	2000.0	20.00	.09620	32.40	20.73	18.94	18.68	18.38	.2000	80.
2019	70.0	3500.0	20.00	.09625	31.20	16.81	11.62	10.85	9.12	.2000	15.
2020	140.0	3500.0	20.00	.09625	31.20	16.81	11.62	11.03	10.17	.2000	35.
2021	210.0	3500.0	20.00	.09625	27.90	19.10	15.78	15.38	14.51	.2000	58.
2022	280.0	3500.0	19.62	.09625	28.10	18.46	14.45	14.17	13.65	.2000	92.
2023	350.0	3500.0	20.00	.09625	28.80	18.46	14.45	14.22	13.70	.2000	126.
2024	70.0	5000.0	19.03	.09800	30.00	16.16	10.68	9.93	8.11	.2000	26.
2025	140.0	5000.0	19.63	.09800	29.50	16.16	10.68	10.19	9.13	.2000	52.
2026	210.0	5000.0	20.03	.09800	29.60	16.16	10.68	10.40	9.53	.2000	87.
2027	280.0	5000.0	20.00	.09625	31.20	17.61	13.09	12.71	11.89	.2000	112.
2028	350.0	5000.0	20.00	.09625	31.20	17.61	13.09	12.62	11.98	.2000	164.
2029	280.0	2000.0	20.00	.09625	30.20	19.40	16.55	16.30	15.66	.2000	61.
2030	350.0	2000.0	20.00	.09625	30.40	19.40	16.55	16.25	15.83	.2000	80.
5001	70.0	570.0	17.70	.09710	21.90	17.90	11.52	11.21	10.56	.4385	5.
5002	210.0	570.0	15.70	.09710	21.60	17.90	11.52	11.39	11.10	.4385	20.
5004	70.0	2000.0	18.35	.09710	22.93	16.73	10.45	10.03	9.59	.2000	10.
5005	70.0	3500.0	18.66	.09710	22.40	16.21	10.02	9.54	8.79	.4385	10.
5008	140.0	570.0	18.97	.09640	23.93	16.53	9.46	9.26	8.84	.4385	32.
5009	280.0	570.0	18.77	.09640	24.20	16.53	9.46	9.23	8.99	.4385	41.
5010	350.0	570.0	19.37	.09640	24.47	16.53	9.46	9.32	8.80	.20	90.
5011	350.	2000.	20.17	.0964	24.93	16.12	9.40	9.21	8.70	.20	94.
5012	210.	5000.	19.27	.0964	24.47	16.12	9.40	9.17			

EXPERIMENTAL DATA Tp-1 (H/D= 5.00)   TABLE C.2

D CM	AL1 CM	AL2 CM	AL3 CM	BL CM	CL1 CM	CL2 CM	CL3 CM		
1.348	110.5	130.5	241.	178.7	170.2	59.7	70.8	1.175	.075

RUN NO.	QL LIT/HR	QG LIT/HR	PT PSIA	X	T DEG C	BO ML	B1 ML	S1 ML	S2 ML	F CO2	DELP MM HG.
2107	70.0	570.0	20.01	.09800	31.30	15.02	8.58	7.97	7.15	.4385	20.
2108	140.0	570.0	19.10	.09800	30.90	15.02	8.58	7.77	7.30	.4385	47.
2109	210.0	570.0	19.81	.09800	30.70	15.02	8.58	7.98	7.65	.4385	54.
2110	280.0	570.0	20.00	.09800	30.70	14.41	7.45	7.14	6.92	.4385	75.
2111	350.0	570.0	19.60	.09800	30.80	14.41	7.45	7.21	7.02	.4385	92.
2112	70.0	2000.0	20.00	.09800	31.40	13.38	6.70	5.57	4.49	.2000	44.
2113	140.0	2000.0	20.10	.09800	31.40	13.38	6.70	6.01	5.57	.2000	84.
2114	210.0	2000.0	20.30	.09800	31.50	13.38	6.70	6.14	5.81	.2000	119.
2115	280.0	2000.0	20.10	.09800	30.50	21.88	21.72	21.08	20.77	.2000	149.
2116	350.0	2000.0	20.10	.09800	30.50	21.88	21.72	21.16	20.93	.2000	182.
2117	70.0	3500.0	19.73	.09508	28.10	15.00	8.67	8.25	7.20	.2000	60.
2118	140.0	3500.0	20.43	.09508	28.30	15.00	8.67	8.42	7.72	.2000	118.
2119	210.0	3500.0	20.43	.09508	28.60	15.00	8.67	8.43	7.97	.2000	176.
2120	280.0	3500.0	19.83	.09800	30.40	21.30	20.62	20.00	19.40	.2000	225.
2121	350.0	3500.0	19.93	.09800	30.60	21.30	20.62	20.07	19.61	.2000	270.
2122	70.0	5000.0	19.65	.09508	27.10	14.19	7.75	7.42	4.83	.2000	80.
2123	140.0	5000.0	20.05	.09508	26.90	14.19	7.75	7.47	6.27	.2000	162.
2124	210.0	5000.0	20.15	.09503	27.10	14.19	7.75	7.51	6.83	.2000	236.
2125	280.0	5000.0	20.11	.09800	31.90	20.33	18.79	17.96	17.35	.2000	280.
2126	350.0	5000.0	20.01	.09800	31.90	20.33	18.79	18.12	17.56	.2000	366.
5101	70.0	2000.0	14.13	.09508	19.40	13.18	5.48	4.82	4.54	.2000	55.
5102	350.0	2000.0	17.13	.09508	20.40	13.18	5.48	4.89	4.75	.2000	235.
5103	350.0	3500.0	17.96	.09710	18.50	19.87	13.49	13.34	13.16	.2000	331.
5104	70.0	5000.0	16.23	.09508	21.33	21.09	15.17	13.86	12.93	.2000	91.
5105	140.0	5000.0	17.83	.09508	21.33	21.09	15.17	14.28	13.58	.2000	170.
5106	70.0	2000.0	19.24	.09640	25.90	15.74	9.35	8.77	8.24	.2000	51.
5107	350.0	2000.0	19.14	.09640	26.00	15.74	9.35	9.02	8.72	.2000	64.
5108	70.0	3500.0	19.98	.09640	25.60	15.55	8.96	8.26	7.66	.2000	125.
5109	140.0	3500.0	19.18	.09640	25.73	15.55	8.96	8.35	7.66	.2000	125.
5110	210.0	5000.0	19.68	.09640	26.13	15.55	8.96	8.34	7.78	.2000	248.
5111	280.0	2000.0	19.88	.09640	27.17	13.47	7.02	6.67	6.31	.2000	177.
5112	350.0	2000.0	18.88	.09640	27.67	13.47	7.02	6.79	6.58	.2000	211.

TABLE C.3

EXPERIMENTAL DATA TP-2 (H/D= 9.32)

D CM	AL1 CM	AL2 CM	AL3 CM	BL CM	CL1 CM	CL2 CM	CL3 CM	BR CM	WI CM
1.348	110.5	130.5	241.	178.7	170.2	59.7	70.8	1.242	.075

RUN NO.	QL LIT/HR	QG LIT/HR	PT PSIA	X	T DEG C	BO ML	B1 ML	S1 ML	S2 ML	F CO2	DELP MM HG
2201	70.0	570.0	20.00	.09508	32.95	20.19	16.64	15.74	14.15	.4385	14.
2202	140.0	570.0	20.00	.09508	32.35	20.19	16.64	16.14	15.38	.4385	24.
2203	210.0	570.0	20.10	.09508	32.20	20.19	16.64	16.26	15.87	.4385	36.
2204	280.0	570.0	19.83	.09508	30.70	16.70	11.48	11.06	10.57	.4385	51.
2205	350.0	570.0	20.13	.09508	30.80	16.70	11.48	11.11	10.73	.4385	67.
2206	70.0	2000.0	20.03	.09508	32.00	19.96	16.16	14.87	13.53	.2000	34.
2207	140.0	2000.0	19.73	.09508	31.70	19.96	16.16	15.40	14.73	.2000	60.
2208	210.0	2000.0	20.83	.09508	31.50	19.96	16.16	15.70	15.11	.2000	88.
2209	280.0	2000.0	20.31	.09508	32.20	17.50	13.06	12.66	12.12	.2000	121.
2210	350.0	2000.0	20.71	.09508	32.20	17.50	13.06	12.63	12.37	.2000	168.
2211	70.0	3500.0	20.04	.09508	32.30	19.43	14.90	13.25	11.41	.2000	48.
2212	140.0	3500.0	19.94	.09508	31.60	19.43	14.90	13.82	12.87	.2000	95.
2213	210.0	3500.0	20.74	.09508	31.60	19.43	14.90	14.19	13.70	.2000	148.
2214	280.0	3500.0	20.03	.09800	32.30	17.97	14.32	13.74	13.22	.2000	192.
2215	350.0	3500.0	20.23	.09800	32.70	17.97	14.32	13.77	13.41	.2000	241.
2216	70.0	5000.0	20.62	.09508	29.40	18.15	13.17	12.25	9.14	.2000	60.
2217	140.0	5000.0	20.62	.09508	29.50	18.15	13.17	12.71	10.87	.2000	129.
2218	210.0	5000.0	20.62	.09508	29.00	18.15	13.17	13.39	12.74	.2000	196.
2219	280.0	5000.0	20.94	.09800	32.30	19.30	16.48	15.83	15.21	.2000	259.
2220	350.0	5000.0	20.14	.09800	32.30	19.30	16.48	15.91	15.46	.2000	328.
2221	280.0	570.0	20.31	.09508	31.00	17.01	12.20	11.75	11.30	.4385	51.
2222	140.0	3500.0	21.14	.09508	26.00	16.86	10.43	10.24	9.30	.2000	99.
2223	210.0	5000.0	21.14	.09508	26.50	16.86	10.43	9.71	9.06	.2000	200.
5201	70.0	570.0	14.22	.09710	21.06	19.34	12.85	12.35	11.53	.4385	16.
5202	350.0	2000.0	17.42	.09710	20.53	19.34	12.85	12.51	12.28	.2000	192.
5203	70.0	3500.0	19.92	.09710	22.33	19.34	12.85	12.00	11.10	.2000	57.
5204	70.0	570.0	20.0C	.09508	32.95	20.19	16.64	15.38	14.15	.4385	14.
5205	210.0	3500.0	19.34	.09640	27.66	14.50	8.29	7.71	7.12	.2000	165.
5206	70.0	5000.0	19.24	.09640	26.66	14.50	8.29	7.46	6.63	.2000	76.
5207	140.0	5000.0	19.04	.09640	27.33	14.50	8.29	7.61	6.90	.2000	146.
5208	70.0	3500.0	20.21	.09640	26.50	13.79	7.39	6.80	6.22	.2000	51.
5209	210.0	3500.0	20.10	.09640	26.17	13.79	7.39	6.93	6.45	.2000	165.

TABLE C.4

EXPERIMENTAL RESULTS   EMPTY TUBE

RUN NO.	TS DEG K	PTS KN/M2	VLO M/SEC	VGO M/SEC	PL KN/M3	EDPJ KN/M2/SEC	EDPB N/SEC	SURF M2/M3 1	2	3	FABS 2	3
2009	305.3	137.9	.1362	.6770	.222	.180	.00431	114.5	104.3	105.2	.404	.766
2010	305.3	137.9	.2724	.6159	.443	.394	.01724	224.9	0.0	0.0	.4771	.000
2012	305.3	137.8	.5448	.6554	1.020	1.224	.07931	90.2	105.2	100.1	.483	.905
2013	305.7	130.2	.6810	.6620	1.419	1.905	.13794	116.0	158.2	144.4	.296	.498
2014	305.9	131.7	.1362	3.0869	.399	1.286	.00776	224.4	223.0	220.3	.377	.509
2015	304.7	136.5	.2724	2.9366	.975	3.130	.03793	154.8	280.2	240.9	.351	.572
2016	304.8	135.0	.4086	2.9570	1.995	6.715	.11639	269.1	286.1	279.4	.317	.528
2017	304.1	136.4	.5448	2.9462	2.749	9.596	.21380	243.7	232.7	235.3	.283	.528
2018	305.6	137.7	.6810	2.9428	3.547	12.853	.34485	271.6	200.4	222.0	.186	.270
2019	304.4	137.9	.1362	5.3223	.665	3.630	.01293	268.6	357.2	327.5	.185	.313
2020	304.4	137.8	.2724	5.3005	1.552	8.648	.06035	409.8	340.1	359.5	.281	.411
2021	301.1	137.8	.4086	5.1378	2.572	14.263	.15001	332.8	435.2	401.8	.224	.345
2022	301.3	135.1	.5448	5.3129	4.079	23.894	.31726	336.3	443.5	405.3	.280	.404
2023	302.0	137.6	.6810	5.1628	5.587	32.646	.54313	326.1	443.5	385.7	.140	.197
2024	303.2	131.2	.1362	8.0599	1.153	9.448	.02242	302.3	426.8	385.7	.163	.238
2025	302.7	135.2	.2724	7.7522	2.306	18.501	.08966	378.0	456.0	458.0	.201	.265
2026	302.8	137.9	.4086	7.5528	3.857	30.710	.22501	304.6	529.4	458.0	.248	.362
2027	304.4	137.7	.5448	7.4921	4.966	39.909	.38623	445.1	575.7	532.5	.241	.419
2028	304.4	137.5	.6810	7.4577	7.271	59.179	.70694	693.4	602.9	628.9	.483	.672
2029	303.4	137.8	.5448	2.8115	2.705	9.077	.21036	249.3	472.1	401.3	.396	.679
2030	303.6	137.7	.6810	2.8394	3.547	12.487	.34485	387.7	410.7	401.5	.198	.292
5001	295.1	122.0	.1362	.8878	.222	.227	.00431	82.7	89.2	87.0	.265	.384
5002	294.8	108.2	.4086	.9612	.887	1.215	.05173	116.4	135.5	129.6	.084	.164
5004	296.1	126.5	.1362	3.2950	.443	1.521	.00862	233.9	122.2	155.7	.103	.156
5005	295.6	128.6	.1362	5.6547	.931	5.392	.01810	263.5	272.8	269.1	.284	.405
5008	297.1	130.8	.2724	.7933	.443	.472	.01724	105.4	132.2	123.8	.472	.750
5009	297.4	129.3	.5448	.6924	1.419	1.755	.11035	254.0	308.6	290.5	.499	.711
5010	297.6	133.5	.6810	.6741	1.818	2.463	.17673	179.1	283.6	250.9	.387	.567
5011	298.1	138.9	.6810	2.8026	3.990	13.901	.38795	479.0	691.1	622.7	.107	.159
5012	297.6	132.7	.4086	7.8811	4.168	34.549	.24312	348.2	367.7	361.2	.107	.159

EXPERIMENTAL DATA EMPTY TUBE

D CM	AL1 CM	AL2 CM	AL3 CM	BL CM	CL1 CM	CL2 CM	CL3 CM
1.348	110.6	256.0	366.5	300.7	233.7	123.2	132.8

RUN NO.	QL LIT/HR	QG LIT/HR	PT PSIA	X	T DEG C	BO ML	S1 ML	S2 ML	F CO2	DELP MM HG
1014	70.0	570.0	20.30	.02065	19.80	5.70	5.10	4.25	.4385	4.
1015	140.0	570.0	22.23	.02065	19.50	5.46	5.06	4.16	.4385	9.
1016	210.0	570.0	19.73	.02065	17.40	5.79	5.22	4.51	.4385	15.
1017	280.0	570.0	20.00	.02000	22.20	6.00	5.54	4.93	.4385	26.
1018	350.0	570.0	20.00	.02020	27.60	5.74	5.28	4.84	.4385	40.
1019	70.0	2000.0	20.00	.02130	20.00	5.72	5.25	4.57	.2000	10.
1020	140.0	2000.0	20.00	.02130	21.60	5.74	5.24	4.64	.2000	21.
1021	210.0	2000.0	20.00	.02130	20.40	5.80	5.30	4.67	.2000	37.
1022	280.0	2000.0	20.00	.02130	22.00	5.80	5.26	4.58	.2000	53.
1023	350.0	2000.0	20.10	.02000	23.80	5.44	5.01	4.36	.2000	71.
1024	70.0	3500.0	21.00	.02000	24.00	6.00	5.12	4.36	.2000	11.
1025	140.0	3500.0	20.30	.02000	24.20	5.93	5.13	4.33	.2000	32.
1026	210.0	3500.0	21.00	.02000	20.60	5.81	5.00	4.04	.2000	50.
1027	280.0	3500.0	20.00	.02000	21.80	5.98	5.18	4.31	.2000	90.
1028	350.0	3500.0	20.30	.02000	27.70	5.40	4.70	4.23	.2000	135.
1029	70.0	5000.0	20.00	.02000	21.20	5.67	4.26	3.41	.2000	25.
1030	140.	5000.	20.	.020	21.2	5.82	4.78	3.66	.20	46.
1031	210.	5000.	20.	.020	22.8	5.89	4.85	3.99	.20	73.
1032	280.	5000.	20.	.020	24.6	5.87	5.0	3.99	.20	104.
4001	350.0	570.0	20.56	.02030	27.60	6.27	5.92	5.47	.4385	31.
4002	350.0	2000.0	19.76	.02030	28.00	6.27	5.82	5.42	.2000	70.
4003	350.0	3500.0	19.96	.02010	32.00	6.06	5.67	4.98	.2000	100.
4004	280.0	3500.0	19.65	.02010	33.00	6.16	5.68	5.07	.2000	77.
4005	350.0	5000.0	20.25	.02010	33.00	6.16	5.39	4.44	.2000	131.
4006	280.0	5000.0	19.76	.02030	27.80	6.27	5.40	4.70	.2000	98.

EXPERIMENTAL DATA Tp-1 (H/D= 5.00)

D CM	AL1 CM	AL2 CM	AL3 CM	BL CM	CL1 CM	CL2 CM	CL3 CM	BR CM	WI CM
1.348	110.6	131.5	242.1	178.7	170.2	59.7	70.8	1.175	.075

RUN NO.	QL LIT/HR	QG LIT/HR	PT PSIA	X	T DEG C	BO ML	S1 ML	S2 ML	F CO2	DELP MM HG
1103	70.0	570.0	20.00	.02016	25.60	5.70	3.16	2.54	.4385	16.
1104	140.0	570.0	20.00	.02016	23.60	5.80	3.88	3.02	.4385	34.
1105	210.0	570.0	20.00	.02016	24.30	5.57	3.81	3.18	.4385	45.
1106	280.0	570.0	20.00	.02016	23.50	5.80	4.68	4.05	.4385	64.
1107	350.0	570.0	19.95	.02016	28.30	5.96	5.03	4.50	.4385	76.
1108	70.0	2000.0	19.95	.02016	24.20	5.69	3.93	3.52	.2000	41.
1109	140.0	2000.0	19.95	.02016	22.00	6.35	4.80	4.37	.2000	63.
1110	210.0	2000.0	20.00	.02016	21.80	6.61	5.41	4.89	.2000	91.
1111	280.0	2000.0	20.00	.02016	22.00	6.61	5.58	5.18	.2000	123.
1112	350.0	2000.0	19.95	.02016	27.80	5.99	5.03	4.69	.2000	153.
1113	70.0	3500.0	20.00	.02016	22.10	6.32	4.28	4.12	.2000	48.
1114	140.0	3500.0	20.00	.02016	21.60	6.00	4.03	3.74	.2000	95.
1115	210.0	3500.0	19.97	.02016	23.20	5.95	4.41	4.03	.2000	138.
1116	280.0	3500.0	19.95	.02016	27.10	6.08	4.76	4.46	.2000	174.
1117	350.0	3500.0	20.00	.02016	27.00	5.73	4.11	3.77	.2000	221.
1118	70.0	5000.0	19.96	.02016	24.40	6.20	4.01	3.90	.2000	65.
1119	140.0	5000.0	20.04	.02016	22.80	6.16	4.21	4.03	.2000	113.
1120	70.0	5000.0	20.00	.02016	23.30	5.88	4.79	4.77	.1000	64.
4101	70.0	570.0	20.09	.01928	27.25	5.23	3.23	2.31	.4385	18.
4102	140.0	570.0	20.09	.01928	27.50	5.23	3.84	3.04	.4385	33.
4103	210.0	570.0	19.90	.01928	28.50	6.44	5.37	4.45	.4385	56.
4104	70.0	2000.0	20.10	.01928	28.00	6.44	5.18	4.89	.2000	30.
4105	140.0	2000.0	20.42	.01928	28.50	6.57	5.52	5.06	.2000	60.
4106	210.0	2000.0	20.02	.01928	29.00	6.57	5.64	5.29	.2000	95.
4107	350.0	3500.0	19.68	.01928	28.50	6.51	5.77	5.11	.2000	219.
4108	350.0	5000.0	19.58	.01928	28.00	6.51	5.26	4.92	.2000	297.
4109	280.0	3500.0	19.95	.01928	28.00	6.54	5.21	4.95	.2000	178.
4110	280.0	5000.0	20.12	.01928	27.80	6.25	4.73	4.60	.2000	237.
4111	210.0	3500.0	20.12	.01928	28.00	6.25	4.86	4.66	.2000	137.
4112	140.0	3500.0	20.12	.01928	28.00	6.25	4.78	4.56	.2000	90.
4113	70.0	3500.0	19.32	.01928	28.40	6.25	4.63	4.46	.2000	49.

EXPERIMENTAL DATA Tp-2 (H/D= 9.32)

D CM	AL1 CM	AL2 CM	AL3 CM	BL CM	CL1 CM	CL2 CM	CL3 CM	BR CM	WI CM
1.348	110.6	131.5	242.1	178.7	170.2	59.7	70.8	1.242	.075

RUN NO.	QL LIT/HR	QG LIT/HR	PT PSIA	X	T DEG C	BO ML	S1 ML	S2 ML	F CO2	DELP MM HG
1201	70.0	570.0	20.00	.02020	29.50	6.24	4.64	3.72	.4385	12.
1202	140.0	570.0	20.00	.02020	28.00	5.78	4.77	3.73	.4385	23.
1203	210.0	570.0	20.01	.02020	28.60	6.18	5.36	4.66	.4385	33.
1204	280.0	570.0	20.01	.02020	29.10	6.18	5.50	5.19	.4385	49.
1205	350.0	570.0	20.00	.02020	29.50	6.24	5.60	5.10	.4385	64.
1206	70.0	2000.0	20.02	.02020	27.00	6.14	4.93	4.55	.2000	29.
1207	140.0	2000.0	20.02	.02020	26.90	6.14	5.19	4.78	.2000	55.
1208	210.0	2000.0	20.02	.02020	26.85	6.14	5.21	4.78	.2000	80.
1209	280.0	2000.0	20.00	.02020	28.40	6.30	5.59	5.15	.2000	104.
1210	350.0	2000.0	20.00	.02020	27.70	6.30	5.68	5.25	.2000	128.
1211	70.0	3500.0	20.00	.02020	28.70	5.91	4.46	4.13	.2000	40.
1212	140.0	3500.0	20.00	.02020	29.30	5.91	4.55	4.21	.2000	80.
1213	210.0	3500.0	20.00	.02020	26.60	5.99	4.69	4.36	.2000	121.
1214	280.0	3500.0	20.00	.02020	26.70	6.10	5.00	4.62	.2000	160.
1215	350.0	3500.0	20.00	.02020	27.10	6.10	5.12	4.73	.2000	195.
4201	280.0	570.0	20.38	.01928	30.60	6.24	5.26	4.63	.4385	45.
4202	280.0	3500.0	20.38	.01928	30.60	6.24	5.03	4.51	.2000	151.
4203	210.0	3500.0	20.04	.01928	31.40	7.32	6.05	5.67	.2000	112.
4204	140.0	3500.0	19.84	.01928	31.80	7.32	6.02	5.62	.2000	75.
4205	70.0	3500.0	19.64	.01928	32.20	7.32	5.88	5.61	.2000	46.
4206	350.0	5000.0	20.44	.01928	30.50	7.26	5.98	5.81	.2000	257.
4207	280.0	5000.0	20.01	.01928	32.00	7.30	5.88	5.70	.2000	205.
4208	210.0	5000.0	19.54	.01928	30.30	7.26	6.06	5.60	.2000	151.
4209	140.0	5000.0	20.61	.01928	32.20	7.30	5.85	5.20	.2000	100.
4210	70.0	5000.0	20.01	.01928	32.20	7.30	5.52	4.70	.2000	52.

EXPERIMENTAL RESULTS   EMPTY TUBE

RUN NO.	TS DEG K	PTS KN/M2	VLO M/SEC	VGO M/SEC	PL KN/M3	EDPJ KN/M2/SEC	KLOA/SEC			FABS	
							1	2	3	2	3
1014	293.0	140.0	.1362	.8486	.177	.175	.0174	.0131	.0144	.019	.047
1015	292.7	153.3	.2724	.7666	.399	.415	.0203	.0238	.0228	.026	.084
1016	290.6	136.0	.4086	.8442	.665	.833	.0472	.0315	.0363	.055	.124
1017	295.4	137.8	.5448	.8444	1.153	1.601	.0555	.0393	.0443	.058	.134
1018	300.8	137.8	.6810	.8554	1.773	2.725	.0828	.0429	.0553	.073	.143
1019	293.2	137.9	.1362	3.0588	.443	1.417	.0333	.0327	.0329	.010	.024
1020	294.8	137.9	.2724	3.0658	.931	3.108	.0755	.0638	.0675	.021	.046
1021	293.6	137.8	.4086	3.0432	1.640	5.663	.1081	.0989	.1021	.031	.071
1022	295.2	137.8	.5448	3.0467	2.350	8.440	.1666	.1805	.1775	.045	.102
1023	297.0	138.4	.6810	3.0505	3.148	11.747	.1551	.1799	.1733	.042	.106
1024	297.2	144.8	.1362	5.1704	.488	2.588	.0730	.0675	.0694	.010	.018
1025	297.4	139.9	.2724	5.3403	1.419	7.963	.1341	.1598	.1532	.018	.036
1026	293.8	144.7	.4086	5.0842	2.217	12.177	.1691	.2304	.2135	.027	.059
1027	295.0	137.7	.5448	5.3508	3.990	23.525	.2418	.3766	.3420	.036	.075
1028	300.9	139.7	.6810	5.3840	5.986	36.302	.3045	.1970	.2387	.039	.066
1029	294.4	137.8	.1362	7.6839	1.108	8.668	.1434	0.0000	0.0000	.011	.018
1030	294.4	137.8	.2724	7.6698	2.040	16.198	.1720	0.0000	0.0000	.016	.034
1031	296.0	137.7	.4086	7.7000	3.237	26.245	.2730	0.0000	0.0000	.024	.045
1032	297.8	137.7	.5448	7.7373	4.611	38.189	.2981	0.0000	0.0000	.027	.059
4001	300.8	141.7	.6810	.8382	1.374	2.088	.0605	.0406	.0467	.056	.127
4002	301.2	136.1	.6810	3.1529	3.104	11.899	.1960	.1243	.1478	.045	.085
4003	305.2	137.4	.6810	5.5634	4.434	27.686	.1796	.3113	.2729	.022	.061
4004	306.2	135.3	.5448	5.6747	3.414	21.233	.1967	.2600	.2434	.022	.049
4005	306.2	139.3	.6810	7.8510	5.808	49.555	.4303	0.0000	0.0000	.030	.068
4006	301.0	136.0	.5448	7.9216	4.345	36.787	.3556	0.0000	0.0000	.028	.050

RUN NO.	TS DEG K	PTS KN/M2	VLO M/SEC	VGO M/SEC	PL KN/M3	EDPJ KN/M2/SEC	KLOA /SEC 1	2	3	FABS 2	3
1103	298.8	137.8	.1452	.9128	1.194	1.263	.1452	.0882	.1155	.080	.100
1104	296.8	137.8	.2903	.8830	2.537	2.976	.1705	.1430	.1573	.121	.176
1105	297.5	137.7	.4355	.8653	3.357	4.367	.2373	.1466	.1911	.167	.227
1106	296.7	137.6	.5806	.8698	4.775	6.926	.1679	.1265	.1470	.142	.221
1107	301.5	137.2	.7258	.8833	5.670	9.124	.1984	.1512	.1749	.147	.231
1108	297.4	137.4	.1452	3.3040	3.059	10.550	.4429	0.0000	0.0000	.035	.043
1109	295.2	137.3	.2903	3.2612	4.700	16.693	.4149	0.0000	0.0000	.061	.078
1110	295.0	137.5	.4355	3.2425	6.789	24.971	.3598	.7540	.6002	.071	.102
1111	295.2	137.4	.5806	3.2408	9.177	35.068	.3742	.3377	.3701	.081	.113
1112	301.0	136.9	.7258	3.3061	11.415	46.023	.5427	.6516	.6470	.095	.128
1113	295.3	137.7	.1452	5.7451	3.581	21.094	0.0000	0.0000	0.0000	.044	.051
1114	294.8	137.5	.2903	5.7160	7.088	42.571	0.0000	0.0000	0.0000	.052	.065
1115	296.4	137.1	.4355	5.7506	10.296	63.690	.6055	0.0000	0.0000	.060	.073
1116	300.3	136.8	.5806	5.8293	12.982	83.210	.7172	0.0000	0.0000	.091	.111
1117	300.2	137.0	.7258	5.7800	16.488	107.269	1.8399	0.0000	0.0000	.017	.018
1118	297.6	137.3	.1452	8.3024	4.849	40.966	0.0000	0.0000	0.0000	.031	.034
1119	296.0	137.7	.2903	8.2126	8.431	71.685	0.0000	0.0000	0.0000	.017	.018
1120	296.5	137.6	.1452	8.2699	4.775	40.181	0.0000	0.0000	0.0000	.060	.088
4101	300.4	138.4	.1452	.9204	1.343	1.431	.0963	.0856	.0911	.084	.132
4102	300.7	138.4	.2903	.9074	2.462	2.949	.1185	.0994	.1088	.097	.181
4103	301.7	137.0	.4355	.9068	4.178	5.608	.1335	.1691	.1535	.024	.029
4104	301.2	138.5	.1452	3.3283	2.238	7.774	.1691	.1243	.1485	.040	.057
4105	301.7	140.5	.2903	3.2700	4.476	15.938	.2389	.3283	.2926	.053	.073
4106	302.2	137.6	.4355	3.3349	7.088	26.723	.3061	.2617	.2926	.040	.076
4107	301.7	134.8	.7258	5.9558	16.339	109.170	.3345	1.2363	.8392	.047	.060
4108	301.2	133.8	.7258	8.5656	22.158	205.880	.7020	0.0000	0.0000	.057	.069
4109	301.2	136.8	.5806	5.8514	13.280	85.417	.6948	0.0000	0.0000	.046	.050
4110	301.0	137.7	.5806	8.3227	17.682	157.428	.8630	0.0000	0.0000	.045	.052
4111	301.2	138.2	.4355	5.8119	10.221	63.855	.5805	0.0000	0.0000	.032	.036
4112	301.2	138.3	.2903	5.8203	6.715	41.031	.4628	0.0000	0.0000	.017	.019
4113	301.6	133.0	.1452	6.0815	3.656	22.763	.4971	0.0000	0.0000		

EXPERIMENTAL RESULTS   TP-2 (H/D= 9.32)

RUN NO.	TS DEG K	PTS KN/M2	VLO M/SEC	VGO M/SEC	PL KN/M3	EDPJ KN/M2/SEC	KLOA /SEC 1	2	3	FABS 2	3
1201	302.7	137.8	.1457	.9386	.895	.971	.0827	.0846	.0840	.051	.080
1202	301.2	137.8	.2914	.9209	1.716	2.080	.0868	.1272	.1088	.064	.130
1203	301.8	137.8	.4371	.9166	2.462	3.333	.1039	.1097	.1073	.078	.144
1204	302.3	137.8	.5828	.9208	3.656	5.497	.1131	.0562	.0829	.086	.125
1205	302.7	137.6	.7285	.9080	4.775	7.814	.1334	.1227	.1282	.101	.181
1206	300.2	137.9	.1457	3.3422	2.164	7.546	.1632	.2274	.2027	.024	.031
1207	300.1	137.8	.2914	3.3316	4.103	14.866	.2108	.2070	.2129	.038	.054
1208	300.0	137.7	.4371	3.3185	5.969	22.416	.3036	.3548	.3404	.055	.081
1209	301.6	137.5	.5828	3.3376	7.759	30.419	.2886	.3570	.3317	.056	.091
1210	300.9	137.4	.7285	3.3262	9.550	38.721	.2903	.3583	.3324	.061	.104
1211	301.9	137.7	.1457	5.9010	2.984	18.045	.2922	0.0000	0.0000	.016	.020
1212	302.5	137.6	.2914	5.9004	5.969	36.956	.4859	0.0000	0.0000	.031	.038
1213	299.8	137.4	.4371	5.8371	9.027	56.640	.5203	0.0000	0.0000	.044	.055
1214	299.9	137.2	.5828	5.8357	11.937	76.619	.4927	.7874	.7195	.050	.067
1215	300.3	137.1	.7285	5.8401	14.548	95.563	.5086	.6812	.6539	.055	.077
4201	303.8	140.3	.5828	.8872	3.357	4.935	.1707	.1458	.1582	.119	.195
4202	303.8	139.9	.5828	5.7933	11.266	71.831	.6517	0.0000	0.0000	.052	.075
4203	304.6	137.7	.4371	5.9200	8.356	53.120	.6102	0.0000	0.0000	.041	.053
4204	305.0	136.5	.2914	5.9990	5.596	35.198	.4684	0.0000	0.0000	.028	.037
4205	305.4	135.2	.1457	6.0816	3.432	21.372	.3950	0.0000	0.0000	.016	.018
4206	303.7	139.9	.7285	8.2949	19.174	173.015	.8186	0.0000	0.0000	.048	.055
4207	305.2	137.1	.5828	8.5132	15.294	139.119	1.0733	0.0000	0.0000	.043	.048
4208	303.5	134.1	.4371	8.6794	11.266	102.703	.4965	0.0000	0.0000	.027	.038
4209	305.4	141.7	.2914	8.2753	7.461	63.913	.5920	0.0000	0.0000	.022	.032
4210	305.4	137.7	.1457	8.5294	3.880	33.656	0.0000	0.0000	0.0000	.013	.020

APPENDIX C.

CHEMICAL ABSORPTION

EXPERIMENTAL DATA EMPTY TUBE

TABLE C.1

D CM	AL1 CM	AL2 CM	AL3 CM	BL CM	CL1 CM	CL2 CM	CL3 CM	BR CM	WI CM
1.348	110.5	256.0	366.5	300.7	233.7	123.2	132.8		

RUN NO.	QL LIT/HR	QG LIT/HR	PT PSIA	X	T DEG C	BO ML	B1 ML	S1 ML	S2 ML	F CO2	DELP MM HG
2009	70.0	570.0	20.00	.09620	32.10	21.20	20.39	19.19	17.85	.4385	5.
2010	140.0	570.0	20.00	.09620	32.10	21.20	20.39	19.36	18.57	.4385	10.
2012	280.0	570.0	20.00	.09620	32.10	21.80	21.05	20.79	20.39	.4385	23.
2013	350.0	570.0	18.90	.09620	32.50	21.80	21.05	20.80	20.45	.4385	32.
2014	70.0	2000.0	19.10	.09620	32.71	20.92	19.96	18.89	17.32	.2000	9.
2015	140.0	2000.0	19.80	.09625	31.50	20.31	18.20	17.85	16.85	.2000	22.
2016	210.0	2000.0	19.60	.09625	31.60	20.31	18.20	17.81	17.19	.2000	45.
2017	280.0	2000.0	19.80	.09620	30.90	20.73	18.94	18.66	18.24	.2000	62.
2018	350.0	2000.0	20.00	.09620	32.40	20.73	18.94	18.68	18.38	.2000	80.
2019	70.0	3500.0	20.00	.09625	31.20	16.81	11.62	10.85	9.12	.2000	15.
2020	140.0	3500.0	20.00	.09625	31.20	16.81	11.62	11.03	10.17	.2000	35.
2021	210.0	3500.0	20.00	.09625	27.90	19.10	15.78	15.38	14.51	.2000	58.
2022	280.0	3500.0	19.62	.09625	28.10	18.46	14.45	14.17	13.65	.2000	92.
2023	350.0	3500.0	20.00	.09625	28.80	18.46	14.45	14.22	13.70	.2000	126.
2024	70.0	5000.0	19.03	.09800	30.00	16.16	10.68	9.93	8.11	.2000	26.
2025	140.0	5000.0	19.63	.09800	29.50	16.16	10.68	10.19	9.13	.2000	52.
2026	210.0	5000.0	20.03	.09800	29.60	16.16	10.68	10.40	9.53	.2000	87.
2027	280.0	5000.0	20.00	.09625	31.20	17.61	13.09	12.71	11.89	.2000	112.
2028	350.0	5000.0	20.00	.09625	31.20	17.61	13.09	12.62	11.98	.2000	164.
2029	280.0	2000.0	20.00	.09625	30.20	19.40	16.55	16.30	15.66	.2000	61.
2030	350.0	2000.0	20.00	.09625	30.40	19.40	16.55	16.25	15.83	.2000	80.
5001	70.0	570.0	17.70	.09710	21.90	17.90	11.52	11.21	10.56	.4385	5.
5002	210.0	570.0	15.70	.09710	21.60	17.90	11.52	11.39	11.10	.4385	20.
5004	70.0	2000.0	18.35	.09710	22.93	16.73	10.45	10.03	9.59	.2000	10.
5005	70.0	3500.0	18.66	.09710	22.40	16.21	10.02	9.54	8.59	.2000	21.
5008	140.0	570.0	18.97	.09640	23.93	16.53	9.46	9.26	8.79	.4385	10.
5009	280.0	570.0	18.77	.09640	24.20	16.53	9.46	9.23	8.84	.4385	32.
5010	350.0	570.0	19.37	.09640	24.47	16.53	9.46	9.32	8.99	.4385	41.
5011	350.	2000.	20.17	.0964	24.93	16.12	9.40	9.21	8.80	.20	90.
5012	210.	5000.	19.27	.0964	24.47	16.12	9.40	9.17	8.70	.20	94.

TABLE C.2

EXPERIMENTAL DATA Tp-1 (H/D= 5.00)

D	AL1	AL2	AL3	BL	CL1	CL2	CL3		
CM	CM	CM	CM	CM	CM	CM	CM		
1.348	110.5	130.5	241.	178.7	170.2	59.7	70.8	1.175	.075

RUN NO.	QL LIT/HR	QG LIT/HR	PT PSIA	X	T DEG C	BO ML	B1 ML	S1 ML	S2 ML	F CO2	DELP MM HG.
2107	70.0	570.0	20.01	.09800	31.30	15.02	8.58	7.97	7.15	.4385	20.
2108	140.0	570.0	19.10	.09800	30.90	15.02	8.58	7.77	7.30	.4385	47.
2109	210.0	570.0	19.81	.09800	30.70	15.02	8.58	7.98	7.65	.4385	54.
2110	280.0	570.0	20.00	.09800	30.70	14.41	7.45	7.14	6.92	.4385	75.
2111	350.0	570.0	19.60	.09800	30.80	14.41	7.45	7.21	7.02	.4385	92.
2112	70.0	2000.0	20.00	.09800	31.40	13.38	6.70	5.57	4.49	.2000	44.
2113	140.0	2000.0	20.10	.09800	31.40	13.38	6.70	6.01	5.57	.2000	84.
2114	210.0	2000.0	20.30	.09800	31.50	13.38	6.70	6.14	5.81	.2000	119.
2115	280.0	2000.0	20.10	.09800	30.50	21.88	21.72	21.08	20.77	.2000	149.
2116	350.0	2000.0	20.10	.09800	30.50	21.88	21.72	21.16	20.93	.2000	182.
2117	70.0	3500.0	19.73	.09508	28.10	15.00	8.67	8.25	7.20	.2000	60.
2118	140.0	3500.0	20.43	.09508	28.30	15.00	8.67	8.42	7.72	.2000	118.
2119	210.0	3500.0	20.43	.09508	28.60	15.00	8.67	8.43	7.97	.2000	176.
2120	280.0	3500.0	19.83	.09800	30.40	21.30	20.62	20.00	19.40	.2000	225.
2121	350.0	3500.0	19.93	.09800	30.60	21.30	20.62	20.07	19.61	.2000	270.
2122	70.0	5000.0	19.65	.09508	27.10	14.19	7.75	7.42	4.83	.2000	80.
2123	140.0	5000.0	20.05	.09508	26.90	14.19	7.75	7.47	6.27	.2000	162.
2124	210.0	5000.0	20.15	.09503	27.10	14.19	7.75	7.51	6.83	.2000	236.
2125	280.0	5000.0	20.11	.09800	31.90	20.33	18.79	17.96	17.35	.2000	280.
2126	350.0	5000.0	20.01	.09800	31.90	20.33	18.79	18.12	17.56	.2000	366.
5101	70.0	2000.0	14.13	.09508	19.40	13.18	5.48	4.82	4.54	.2000	55.
5102	350.0	2000.0	17.13	.09508	20.40	13.18	5.48	4.89	4.75	.2000	235.
5103	350.0	3500.0	17.96	.09710	18.50	19.87	13.49	13.34	13.16	.2000	331.
5104	70.0	5000.0	16.23	.09508	21.33	21.09	15.17	13.86	12.93	.2000	91.
5105	140.0	5000.0	17.83	.09508	21.33	21.09	15.17	14.28	13.58	.2000	170.
5106	70.0	2000.0	19.24	.09640	25.90	15.74	9.35	8.77	8.24	.2000	51.
5107	350.0	2000.0	19.14	.09640	26.00	15.74	9.35	9.02	8.72	.2000	214.
5108	70.0	3500.0	19.98	.09640	25.60	15.55	8.96	8.26	7.56	.2000	64.
5109	140.0	3500.0	19.18	.09640	25.73	15.55	8.96	8.35	7.66	.2000	125.
5110	210.0	5000.0	19.68	.09640	26.13	15.55	8.96	8.34	7.78	.2000	248.
5111	280.0	2000.0	19.88	.09640	27.17	13.47	7.02	6.67	6.31	.2000	177.
5112	350.0	2000.0	18.88	.09640	27.67	13.47	7.02	6.79	6.58	.2000	211.

EXPERIMENTAL DATA Tp-2 (H/D= 9.32)

D CM	AL1 CM	AL2 CM	AL3 CM	BL CM	CL1 CM	CL2 CM	CL3 CM	BR CM	WI CM
1.348	110.5	130.5	241.	178.7	170.2	59.7	70.8	1.242	.075

RUN NO.	QL LIT/HR	QG LIT/HR	PT PSIA	X	T DEG C	BO ML	B1 ML	S1 ML	S2 ML	F CO2	DELP MM HG
2201	70.0	570.0	20.00	.09508	32.95	20.19	16.64	15.74	14.15	.4385	14.
2202	140.0	570.0	20.00	.09508	32.35	20.19	16.64	16.14	15.38	.4385	24.
2203	210.0	570.0	20.10	.09508	32.20	20.19	16.64	16.26	15.87	.4385	36.
2204	280.0	570.0	19.83	.09508	30.70	16.70	11.48	11.06	10.57	.4385	51.
2205	350.0	570.0	20.13	.09508	30.80	16.70	11.48	11.11	10.73	.4385	67.
2206	70.0	2000.0	20.03	.09508	32.00	19.96	16.16	14.87	13.53	.2000	34.
2207	140.0	2000.0	19.73	.09508	31.70	19.96	16.16	15.40	14.73	.2000	60.
2208	210.0	2000.0	20.83	.09508	31.50	19.96	16.16	15.70	15.11	.2000	88.
2209	280.0	2000.0	20.31	.09508	32.20	17.50	13.06	12.66	12.12	.2000	121.
2210	350.0	2000.0	20.71	.09508	32.20	17.50	13.06	12.63	12.37	.2000	168.
2211	70.0	3500.0	20.04	.09508	32.30	19.43	14.90	13.25	11.41	.2000	48.
2212	140.0	3500.0	19.94	.09508	31.60	19.43	14.90	13.82	12.87	.2000	95.
2213	210.0	3500.0	20.74	.09508	31.60	19.43	14.90	14.19	13.70	.2000	148.
2214	280.0	3500.0	20.03	.09800	32.30	17.97	14.32	13.74	13.22	.2000	192.
2215	350.0	3500.0	20.23	.09800	32.70	17.97	14.32	13.77	13.41	.2000	241.
2216	70.0	5000.0	20.62	.09508	29.40	18.15	13.17	12.25	9.14	.2000	60.
2217	140.0	5000.0	20.62	.09508	29.50	18.15	13.17	12.71	10.87	.2000	129.
2218	210.0	5000.0	20.62	.09508	29.00	18.15	13.17	13.39	12.74	.2000	196.
2219	280.0	5000.0	20.94	.09800	32.30	19.30	16.48	15.83	15.21	.2000	259.
2220	350.0	5000.0	20.14	.09800	32.30	19.30	16.48	15.91	15.46	.2000	328.
2221	280.0	570.0	20.31	.09508	31.00	17.01	12.20	11.75	11.30	.4385	51.
2222	140.0	3500.0	21.14	.09508	26.00	16.86	10.43	10.24	9.30	.2000	99.
2223	210.0	5000.0	21.14	.09508	26.50	16.86	10.43	9.71	9.06	.2000	200.
5201	70.0	570.0	14.22	.09710	21.06	19.34	12.85	12.35	11.53	.4385	16.
5202	350.0	2000.0	17.42	.09710	20.53	19.34	12.85	12.51	12.28	.2000	192.
5203	70.0	3500.0	19.92	.09710	22.33	19.34	12.85	12.00	11.10	.2000	57.
5204	70.0	570.0	20.0C	.09508	32.95	20.19	16.64	15.38	14.15	.4385	14.
5205	210.0	3500.0	19.34	.09640	27.66	14.50	8.29	7.71	7.12	.2000	165.
5206	70.0	5000.0	19.24	.09640	26.66	14.50	8.29	7.46	6.63	.2000	76.
5207	140.0	5000.0	19.04	.09640	27.33	14.50	8.29	7.61	6.90	.2000	146.
5208	70.0	3500.0	20.21	.09640	26.50	13.79	7.39	6.80	6.22	.2000	51.
5209	210.0	3500.0	20.10	.09640	26.17	13.79	7.39	6.93	6.45	.2000	165.

TABLE C.4

EXPERIMENTAL RESULTS   EMPTY TUBE

RUN NO.	TS DEG K	PTS KN/M2	VLO M/SEC	VGO M/SEC	PL KN/M3	EDPJ KN/M2/SEC	EDPB N/SEC	SURF M2/M3			FABS	
								1	2	3	2	3
2009	305.3	137.9	.1362	.6770	.222	.180	.00431	114.5	104.3	105.2	.404	.766
2010	305.3	137.9	.2724	.6159	.443	.394	.01724	224.9	0.0	0.0	.477	1.000
2012	305.3	137.8	.5448	.6554	1.020	1.224	.07931	90.2	105.2	100.1	.483	.797
2013	305.7	130.2	.6810	.6620	1.419	1.905	.13794	116.0	158.2	144.4	.296	.498
2014	305.9	131.7	.1362	3.0869	.399	1.286	.00776	224.4	223.0	220.3	.377	.509
2015	304.7	136.5	.2724	2.9366	.975	3.130	.03793	154.8	280.2	240.9	.351	.572
2016	304.8	135.0	.4086	2.9570	1.995	6.715	.11639	269.1	286.1	279.4	.317	.528
2017	304.1	136.4	.5448	2.9462	2.749	9.596	.21380	243.7	232.7	235.3	.283	.528
2018	305.6	137.7	.6810	2.9428	3.547	12.853	.34485	271.6	200.4	222.0	.186	.270
2019	304.4	137.9	.1362	5.3223	.665	3.630	.01293	268.6	357.2	327.5	.185	.313
2020	304.4	137.8	.2724	5.3005	1.552	8.648	.06035	409.8	340.1	359.5	.281	.411
2021	301.1	137.8	.4086	5.1378	2.572	14.263	.15001	332.8	435.2	401.8	.224	.345
2022	301.3	135.1	.5448	5.3129	4.079	23.894	.31726	336.3	356.5	349.3	.280	.404
2023	302.0	137.6	.6810	5.1628	5.587	32.646	.54313	326.1	443.5	405.3	.140	.197
2024	303.2	131.2	.1362	8.0599	1.153	9.448	.02242	302.3	426.8	385.7	.163	.238
2025	302.7	135.2	.2724	7.7522	2.306	18.501	.08966	378.0	456.0	458.0	.201	.265
2026	302.8	137.9	.4086	7.5528	3.857	30.710	.22501	304.6	529.4	458.0	.248	.362
2027	304.4	137.7	.5448	7.4921	4.966	39.909	.38623	445.1	575.7	532.5	.241	.419
2028	304.4	137.5	.6810	7.4577	7.271	59.179	.70694	693.4	602.9	628.9	.483	.672
2029	303.4	137.8	.5448	2.8115	2.705	9.077	.21036	249.3	472.1	401.3	.396	.679
2030	303.6	137.7	.6810	2.8394	3.547	12.487	.34485	387.7	410.7	401.5	.198	.292
5001	295.1	122.0	.1362	.8878	.222	.227	.00431	82.7	89.2	87.0	.265	.384
5002	294.8	108.2	.4086	.9612	.887	1.215	.05173	116.4	135.5	129.6	.084	.164
5004	296.1	126.5	.1362	3.2950	.443	1.521	.00862	233.9	122.2	155.7	.103	.156
5005	295.6	128.6	.1362	5.6547	.931	5.392	.01810	263.5	272.8	269.1	.284	.405
5008	297.1	130.8	.2724	.7933	.443	.472	.01724	105.4	132.2	123.8	.472	.750
5009	297.4	129.3	.5448	.6924	1.419	1.755	.11035	254.0	308.6	290.5	.499	.711
5010	297.6	133.5	.6810	.6741	1.818	2.463	.17673	179.1	283.6	250.9	.387	.567
5011	298.1	138.9	.6810	2.8026	3.990	13.901	.38795	479.0	691.1	622.7	.107	.159
5012	297.6	132.7	.4086	7.8811	4.168	34.549	.24312	348.2	367.7	361.2		

RUN NO.	TS DEG K	PTS KN/ M2	VLO M/ SEC	VGO M/ SEC	PL KN/ M3	EDPJ KN/M2/ SEC	EDPB N/ SEC	SURF M2/M3 1	2	3	FABS 2	3
2107	304.5	137.9	.1452	.8213	1.492	1.442	.02901	135.5	209.5	174.1	.252	.440
2108	304.1	131.5	.2903	.7747	3.507	3.734	.13636	435.9	424.5	423.1	.289	.787
2109	303.9	136.4	.4355	.7281	4.029	4.688	.23501	475.5	501.4	482.6	.304	.858
2110	303.9	137.6	.5806	.7725	5.596	7.572	.43521	318.8	299.3	307.2	.271	.652
2111	304.0	134.8	.7258	.7823	6.864	10.351	.66732	307.0	324.6	315.2	.292	.661
2112	304.6	137.7	.1452	3.1872	3.283	10.939	.06383	662.3	855.1	750.4	.207	.424
2113	304.6	138.2	.2903	3.1849	6.267	21.779	.24372	774.6	621.7	688.4	.169	.434
2114	304.7	139.5	.4355	3.1242	8.878	31.603	.51790	931.9	737.9	824.6	.190	.513
2115	303.7	138.0	.5806	3.0581	11.116	40.450	.86461	565.7	481.6	517.7	.238	.730
2116	303.7	137.8	.7258	3.0572	13.578	51.367	1.32013	626.3	484.3	549.3	.221	.759
2117	301.3	135.8	.1452	5.8127	4.476	26.670	.08704	195.8	518.7	366.3	.112	.157
2118	301.5	140.4	.2903	5.5785	8.804	51.667	.34236	214.7	646.1	439.6	.149	.202
2119	301.8	140.1	.4355	5.5825	13.131	79.021	.76596	299.6	633.4	470.7	.147	.224
2120	303.6	135.8	.5806	5.5374	16.787	102.701	1.30562	494.4	692.3	590.7	.263	.536
2121	303.8	136.3	.7258	5.5160	20.144	125.733	1.95843	536.3	670.2	599.8	.252	.554
2122	300.3	135.2	.1452	8.1935	5.969	49.770	.11606	162.3	1608.1	920.7	.193	.218
2123	300.1	137.6	.2903	8.0535	12.086	100.845	.47002	259.8	1303.9	796.4	.179	.221
2124	300.3	138.0	.4355	8.0714	17.607	149.782	1.02709	318.1	1042.4	683.1	.152	.206
2125	305.1	137.5	.5806	7.9955	20.890	179.154	1.62477	684.6	705.5	690.5	.187	.443
2126	305.1	136.4	.7258	8.0072	27.306	238.463	2.65476	657.7	816.4	730.7	.215	.473
5101	292.6	97.2	.1452	4.5253	4.103	19.165	.07979	813.9	366.1	575.2	.052	.175
5102	293.6	117.1	.7258	3.5429	17.533	74.841	1.70456	3335.9	1437.9	2368.3	.130	.680
5103	291.7	122.5	.7258	6.2341	24.695	171.873	2.40089	408.7	572.6	488.3	.098	.179
5104	294.5	111.5	.1452	9.9155	6.789	68.304	.13201	801.3	648.7	717.0	.069	.167
5105	294.5	122.2	.2903	8.9498	12.683	117.193	.49323	936.1	872.7	899.5	.104	.237
5106	299.1	132.4	.1452	3.3660	3.805	13.360	.07399	309.7	297.8	302.4	.100	.210
5107	299.2	131.1	.7258	3.2025	15.966	62.719	1.55224	869.2	1180.6	1022.1	.283	.595
5108	298.8	137.5	.1452	5.7172	4.775	27.992	.09284	372.5	392.9	381.9	.076	.151
5109	298.9	131.7	.2903	5.8462	9.326	57.228	.36267	659.6	870.8	765.7	.149	.281
5110	299.3	134.7	.4355	8.2105	18.503	159.972	1.07931	909.9	1012.9	957.5	.127	.268
5111	300.3	136.3	.5806	3.1148	13.205	48.800	1.02709	760.5	1085.8	922.5	.272	.537
5112	300.8	129.3	.7258	3.3594	15.742	64.309	1.53048	611.3	704.2	656.9	.198	.416

RUN NO.	TS DEG K	PTS KN/M2	VLO M/SEC	VGO M/SEC	PL KN/M3	EDPJ KN/M2/SEC	EDPB N/SEC	SURF M2/M3 1	2	3	FABS 2	3
2201	306.1	137.8	.1457	.7166	1.044	.901	.02031	116.9	317.0	220.9	.474	.743
2202	305.5	137.8	.2914	.7180	1.791	1.807	.06963	129.3	285.5	211.4	.453	.752
2203	305.4	138.4	.4371	.7499	2.686	3.188	.15667	147.6	202.0	175.9	.349	.689
2204	303.9	136.5	.5828	.6393	3.805	4.650	.29594	322.9	0.0	0.0	.585	1.000
2205	304.0	138.5	.7285	.6340	4.999	6.811	.48598	355.7	0.0	0.0	.567	1.000
2206	305.2	138.0	.1457	3.1629	2.537	8.393	.04932	401.5	566.3	482.2	.250	.490
2207	304.9	135.8	.2914	3.1956	4.476	15.609	.17408	470.9	551.9	509.6	.250	.533
2208	304.7	143.3	.4371	2.9829	6.565	22.454	.38298	388.3	686.8	542.4	.330	.587
2209	305.4	139.5	.5828	3.0065	9.027	32.403	.70213	508.5	1099.2	811.0	.403	.701
2210	305.4	142.1	.7285	3.0247	12.534	47.042	1.21858	696.2	645.6	666.5	.242	.643
2211	305.5	138.0	.1457	5.6431	3.581	20.731	.06963	553.6	823.6	684.8	.196	.372
2212	304.8	137.1	.2914	5.6262	7.088	41.942	.27563	713.2	817.0	759.9	.202	.432
2213	304.8	142.4	.4371	5.4717	11.042	65.244	.64411	641.2	542.6	587.2	.157	.383
2214	305.5	137.3	.5828	5.5841	14.325	88.338	1.11413	657.4	797.7	725.0	.228	.483
2215	305.9	138.5	.7285	5.5524	17.980	112.933	1.74808	762.6	697.4	726.1	.198	.499
2216	302.6	141.9	.1457	7.7920	4.476	35.532	.08704	315.7	1433.6	897.8	.232	.300
2217	302.7	141.6	.2914	7.7402	9.624	77.298	.37428	293.5	1489.2	912.0	.274	.343
2218	302.2	141.4	.4371	8.0526	14.623	124.144	.85301	-187.3	564.5	198.0	.145	.096
2219	305.5	143.3	.5828	7.7508	19.323	161.031	1.50291	590.5	739.2	662.0	.191	.390
2220	305.5	137.5	.7285	8.0916	24.471	215.838	2.37913	648.6	692.3	667.4	.173	.392
2221	304.2	139.8	.5828	.6348	3.805	4.633	.29594	322.3	0.0	0.0	.537	1.000
2222	299.2	145.3	.2914	5.3169	7.386	41.423	.28724	161.8	873.4	535.6	.200	.241
2223	299.7	144.9	.4371	7.6215	14.921	120.245	.87041	941.6	1042.3	987.8	.145	.306
5201	294.2	98.0	.1457	1.1327	1.194	1.526	.02321	184.5	333.7	263.6	.250	.402
5202	293.7	119.3	.7285	3.5117	14.325	60.739	1.39266	1122.6	1070.4	1092.2	.219	.542
5203	295.5	137.1	.1457	5.6561	4.253	24.673	.08269	468.4	538.4	503.2	.098	.190
5204	306.1	137.8	.1457	.7396	1.044	.925	.02031	175.1	268.8	220.9	.367	.743
5205	300.8	132.7	.4371	5.7784	12.310	76.513	.71809	866.9	1113.0	987.5	.191	.379
5206	299.8	132.3	.1457	8.5813	5.670	49.483	.11025	434.3	468.8	450.3	.063	.125
5207	300.5	130.7	.2914	8.5956	10.893	96.802	.42360	679.7	816.4	746.8	.107	.210
5208	299.7	139.1	.1457	5.7102	3.805	22.281	.07399	313.6	315.1	313.4	.063	.126
5209	299.3	137.9	.4371	5.5958	12.310	74.266	.71809	715.5	881.4	797.8	.155	.304

APPENDIX D.   PRESSURE DROP CORRELATIONS

CALCULATED VALUES OF RELS AND K FROM HUGHMARKS GRAPH   TABLE

RUN NO	TEMP DEG K	PT KN/M2	VLO M/SEC	VGO M/SEC	ROWL GM/ML	MUEL CENTI-POISE	DELPX KN/M3	RELS	AK
1014	293.0	140.0	.1362	.8486	1.000	1.0085	.177	13162.6	.595
1015	292.7	153.3	.2724	.7666	1.000	1.0160	.399	13785.6	.581
1016	290.6	136.0	.4086	.8442	1.000	1.0705	.665	15775.7	.550
1017	295.4	137.8	.5448	.8444	1.000	.9522	1.153	19667.4	.530
1018	300.8	137.8	.6810	.8554	1.000	.8423	1.773	24587.8	.495
4001	300.8	141.7	.6810	.8382	1.000	.8423	1.374	24312.6	.500
1019	293.2	137.9	.1362	3.0588	1.000	1.0036	.443	42912.2	.420
1020	294.8	137.9	.2724	3.0658	1.000	.9658	.931	46593.8	.412
1021	293.6	137.8	.4086	3.0432	1.000	.9940	1.640	46813.2	.410
1022	295.2	137.8	.5448	3.0467	1.000	.9567	2.350	50606.8	.385
1023	297.0	138.4	.6810	3.0505	1.000	.9173	3.148	54834.5	.390
4002	301.2	136.1	.6810	3.1529	1.000	.8350	3.104	61893.9	.375
1024	297.2	144.8	.1362	5.1704	1.000	.9131	.488	78340.3	.350
1025	297.4	139.9	.2724	5.3403	1.000	.9089	1.419	83240.2	.340
1026	293.8	144.7	.4086	5.0842	1.000	.9892	2.217	74853.9	.355
1027	295.0	137.7	.5448	5.3508	1.000	.9612	3.990	82680.9	.340
4004	306.2	135.3	.5448	5.6747	1.000	.7515	3.414	111562.5	.310
1028	300.9	139.7	.6810	5.3840	1.000	.8405	5.986	97274.0	.323
4003	305.2	137.4	.6810	5.5634	1.000	.7671	4.434	109732.3	.312
1029	294.4	137.8	.1362	7.6839	1.000	.9750	1.108	108115.5	.314
1030	294.4	137.8	.2724	7.6698	1.000	.9750	2.040	109803.6	.312
1031	296.0	137.7	.4086	7.7000	1.000	.9388	3.237	116423.7	.305
1032	297.8	137.7	.5448	7.7373	1.000	.9007	4.611	123956.9	.300
4006	301.0	136.0	.5448	7.9216	1.000	.8386	4.345	136085.8	.292
4005	306.2	139.3	.6810	7.8510	1.000	.7515	5.808	153043.1	.287
2009	305.3	137.9	.1362	.6770	1.100	1.0870	.222	11092.8	.617
5001	295.1	122.0	.1362	.8878	1.100	1.4767	.222	10282.0	.628
2010	305.3	137.9	.2724	.6159	1.100	1.0870	.443	12117.3	.604
5008	297.1	130.8	.2724	.7933	1.100	1.4552	.443	10859.3	.620
2011	305.3	137.9	.4086	.6714	1.100	1.0870	.709	14732.2	.576
5002	294.8	108.2	.4086	.9612	1.100	1.4873	.887	13656.7	.586
2012	305.3	137.8	.5448	.6554	1.100	1.1062	1.020	16088.6	.563
5003	296.6	116.8	.5448	.7234	1.100	1.4258	1.419	13189.2	.591
5009	297.4	129.3	.5448	.6924	1.100	1.4452	1.419	12694.0	.595
2013	305.7	130.2	.6810	.6620	1.000	1.0971	1.419	16501.6	.553
5010	297.6	133.5	.6810	.6741	1.100	1.4386	1.818	13967.4	.583
2014	305.9	131.7	.1362	3.0869	1.100	1.1024	.399	43351.9	.420
5004	296.1	126.5	.1362	3.2950	1.100	1.4425	.443	35271.8	.450
2015	304.7	136.5	.2724	2.9366	1.100	1.1301	.975	42106.3	.427

CONTINUED   TABLE D.1

RUN NO	TEMP DEG K	PT KN/ M2	VLO M/ SEC	VGO M/ SEC	ROWL GM/ ML	MUEL CENTI- POISE	DELPX KN/ M3	RELS	AK
2016	304.8	135.0	.4086	2.9570	1.100	1.1277	1.995	44253.0	.417
2017	304.1	136.4	.5448	2.9462	1.100	1.1482	2.749	45081.7	.416
2029	303.4	137.8	.5448	2.8115	1.100	1.1653	2.705	42708.2	.422
2018	305.6	137.7	.6810	2.9428	1.100	1.1130	3.547	48276.7	.403
2030	303.6	137.7	.6810	2.8394	1.100	1.1604	3.547	44986.0	.416
5011	298.1	138.9	.6810	2.8026	1.100	1.4017	3.990	36850.6	.443
2019	304.4	137.9	.1362	5.3223	1.100	1.1528	.665	70213.2	.362
5005	295.6	128.6	.1362	5.6547	1.100	1.4689	.931	58456.5	.383
2020	304.4	137.8	.2724	5.3005	1.100	1.1528	1.554	71684.8	.360
2021	301.1	137.8	.4086	5.1378	1.100	1.2226	2.572	67269.0	.364
2022	301.3	135.1	.5448	5.3129	1.100	1.2239	4.079	70965.8	.360
5006	295.3	133.2	.5448	5.2619	1.100	1.4889	4.966	57830.3	.385
2023	302.0	137.6	.6810	5.1628	1.100	1.2055	5.587	71877.7	.360
2024	303.2	131.2	.1362	8.0599	1.100	1.1630	1.153	104495.8	.313
2025	302.7	135.2	.2724	7.7522	1.100	1.1755	2.306	101227.0	.320
2026	302.8	137.9	.4086	7.5528	1.100	1.1730	3.857	100644.1	.322
5012	297.6	132.7	.4086	7.8811	1.100	1.4178	4.168	86698.4	.337
2027	304.4	137.7	.5448	7.4921	1.100	1.1457	4.966	104012.8	.313
5007	295.9	128.3	.5448	7.9880	1.100	1.4680	6.695	86186.6	.338
2028	304.4	137.5	.6810	7.4577	1.100	1.1457	7.271	105330.3	.312
1103	298.8	137.8	.1452	.9126	1.000	.8805	1.194	9773.3	.632
4101	300.4	138.4	.1452	.9204	1.000	.8497	1.343	10201.9	.630
1104	296.8	137.8	.2903	.8830	1.000	.9216	2.537	10357.6	.623
4102	300.7	138.2	.2903	.9074	1.000	.8442	2.462	11542.4	.615
1105	297.5	137.7	.4355	.8653	1.000	.9068	3.357	11669.4	.615
4103	301.7	137.0	.4355	.9068	1.000	.8260	4.178	13220.5	.592
1106	296.7	137.6	.5806	.8698	1.000	.9237	4.775	12774.2	.595
1107	301.5	137.2	.7258	.8833	1.000	.8296	5.670	15779.8	.568
1108	297.4	137.4	.1452	3.3040	1.000	.9089	3.059	30871.8	.465
4104	301.2	138.5	.1452	3.3283	1.000	.8350	2.238	33842.0	.455
1109	295.2	137.3	.2903	3.2612	1.000	.9567	4.700	30201.4	.472
4105	301.7	140.5	.2903	3.2700	1.000	.8260	4.476	35066.0	.450
1110	295.0	137.5	.4355	3.2425	1.000	.9612	6.789	31129.4	.465
4106	302.2	137.6	.4355	3.3349	1.000	.8171	7.088	37537.5	.441
1111	295.2	137.4	.5806	3.2403	1.000	.9567	9.177	32492.3	.460
1112	301.0	136.9	.7258	3.3061	1.000	.8386	11.415	39111.6	.435
1113	295.3	137.7	.1452	5.7451	1.000	.9544	3.581	50208.6	.400
4113	301.6	133.0	.1452	6.0815	1.000	.8278	3.656	61195.2	.380
1114	294.8	137.5	.2903	5.7160	1.000	.9658	7.088	50594.8	.400
4112	301.2	138.3	.2903	5.8203	1.000	.8350	6.715	59535.1	.378
1115	296.4	137.1	.4355	5.7506	1.000	.9301	10.296	54105.6	.392
4111	301.2	138.2	.4355	5.8119	1.000	.8350	10.221	60867.9	.380
1116	300.3	136.8	.5806	5.8293	1.000	.8516	12.982	61232.7	.380
4109	301.2	136.8	.5806	5.8514	1.000	.8350	13.280	62666.5	.375
1117	300.2	137.0	.7258	5.7800	1.000	.8535	16.488	62012.0	.375
4107	301.7	134.8	.7258	5.9558	1.000	.8260	16.339	65808.1	.370

CONTINUED

| RUN | TEMP | PT | VLO | VGO | ROWL | MUEL | DELPX | RELS | AK |
NO	DEG K	KN/ M2	M/ SEC	M/ SEC	GM/ ML	CENTI- POISE	KN/ M3		
1118	297.6	137.3	.1452	8.3024	1.000	.9048	4.849	75956.4	.353
1119	296.0	137.7	.2903	8.2126	1.000	.9388	8.431	73679.2	.355
1120	296.5	137.6	.1452	8.2699	1.000	.9280	4.775	73772.2	.355
4110	301.0	137.7	.5806	8.3227	1.000	.8386	17.680	86366.9	.340
4108	301.2	133.8	.7258	8.5656	1.000	.8350	22.158	90525.4	.333
2107	304.5	137.9	.1452	.8213	1.100	1.1387	1.492	7595.7	.672
2108	304.1	131.5	.2903	.7747	1.100	1.1482	3.507	8300.1	.658
2109	303.9	136.4	.4355	.7281	1.100	1.1531	4.029	9030.5	.646
2110	303.9	137.6	.5806	.7725	1.100	1.1649	5.596	10394.7	.622
2111	304.0	134.8	.7258	.7823	1.100	1.1624	6.864	11609.7	.615
2112	306.6	137.7	.1452	3.1872	1.100	1.0965	3.283	27196.9	.485
5106	299.1	132.4	.1452	3.3660	1.100	1.3889	3.805	22623.5	.514
2113	304.6	138.2	.2903	3.1849	1.100	1.1425	6.267	27219.5	.485
2114	304.7	139.5	.4355	3.1242	1.100	1.1401	8.878	27939.5	.480
2115	303.7	138.0	.5806	3.0581	1.075	1.1334	11.116	28076.7	.480
5111	303.3	136.3	.5806	3.1148	1.100	1.2540	13.205	26372.0	.490
2116	303.7	137.8	.7258	3.0572	1.075	1.1334	13.578	29190.1	.475
5102	293.6	117.1	.7258	3.5429	1.100	1.5774	17.533	24216.8	.502
5107	299.2	131.1	.7258	3.2025	1.100	1.3858	15.966	25367.6	.498
5112	300.8	129.3	.7258	3.3594	1.100	1.3233	15.742	27626.7	.480
2117	301.3	135.8	.1452	5.8127	1.075	1.3448	4.476	38746.4	.436
5101	292.6	97.2	.1452	4.5253	1.100	1.6163	4.103	25858.6	.491
5108	298.8	137.5	.1452	5.7172	1.100	1.4044	4.775	37354.9	.441
2118	301.5	140.4	.2903	5.5785	1.075	1.3389	8.804	38333.0	.437
5109	298.9	131.7	.2903	5.8462	1.100	1.4013	9.326	39189.3	.437
2119	301.8	140.1	.4355	5.5825	1.075	1.3303	13.131	39563.5	.432
2120	303.6	135.8	.5806	5.5373	1.075	1.1318	16.787	47272.2	.406
2121	303.8	136.3	.7258	5.5160	1.075	1.1271	20.144	48433.2	.404
5103	291.7	122.5	.7258	6.2341	1.100	1.6516	24.695	37710.5	.441
2122	300.3	135.2	.1452	8.1935	1.075	1.3941	5.969	52310.7	.395
5104	294.5	111.5	.1452	9.9155	1.100	1.5427	6.789	58359.7	.383
2123	300.1	137.6	.2903	8.0535	1.075	1.4002	12.086	52112.3	.395
5105	294.5	122.2	.2903	8.9498	1.100	1.5427	12.683	53599.6	.393
2124	300.3	138.0	.4355	8.0714	1.075	1.3941	17.607	53365.8	.393
5110	299.3	134.7	.4355	8.2105	1.100	1.3888	18.503	55712.2	.390
2125	305.1	137.5	.5806	7.9955	1.075	1.0977	20.890	68327.9	.363
2126	305.1	136.4	.7258	8.0072	1.075	1.0977	27.306	69578.0	.361
1201	302.7	137.8	.1457	.9386	1.000	.8084	.895	10653.6	.620
1202	301.2	137.8	.2914	.9209	1.000	.8350	1.716	11532.4	.616
1203	301.8	137.8	.4371	.9166	1.000	.8242	2.462	13046.1	.590
1204	302.3	137.8	.5828	.9208	1.000	.8154	3.656	14647.5	.578
4201	303.8	140.3	.5828	.8872	1.000	.7898	3.357	14783.8	.578
1205	302.7	137.6	.7285	.9080	1.000	.8084	4.775	16079.2	.562
1206	300.2	137.9	.1457	3.3422	1.000	.8535	2.164	32460.9	.460
1207	300.1	137.8	.2914	3.3316	1.000	.8554	4.103	33643.9	.456
1208	300.0	137.7	.4371	3.3185	1.000	.8573	5.969	34798.2	.450
1209	301.6	137.5	.5828	3.3376	1.000	.8278	7.759	37619.3	.442

CONTINUED

RUN NO	TEMP DEG K	PT KN/ M2	VLO M/ SEC	VGO M/ SEC	ROWL GM/ ML	MUEL CENTI- POISE	DELPX KN/ M3	RELS	AK
1210	300.9	137.4	.7285	3.3262	1.000	.8405	9.550	38320.2	.438
1211	301.9	137.7	.1457	5.9010	1.000	.8224	2.984	58400.1	.383
4205	305.4	135.2	.1457	6.0816	1.000	.7639	3.432	64750.0	.370
1212	302.5	137.6	.2914	5.9004	1.000	.8119	5.965	60577.2	.380
4204	305.0	136.5	.2914	5.9990	1.000	.7703	5.596	64867.7	.370
1213	299.8	137.4	.4371	5.8371	1.000	.8611	9.027	57877.9	.385
4203	304.6	137.7	.4371	5.9200	1.000	.7767	8.356	65013.1	.370
1214	299.9	137.2	.5828	5.8357	1.000	.8592	11.937	59340.4	.381
4202	303.8	139.9	.5828	5.7933	1.000	.7898	11.266	64124.6	.370
1215	300.3	137.1	.7285	5.8401	1.000	.8516	14.548	61266.9	.380
4210	305.4	137.7	.1457	8.5294	1.000	.7639	3.880	90201.7	.332
4209	305.4	141.7	.2914	8.2753	1.000	.7639	7.461	89074.5	.332
4208	303.5	134.1	.4371	8.6794	1.000	.7948	11.266	91106.9	.332
4207	305.2	137.1	.5828	8.5132	1.000	.7671	15.294	94188.5	.326
4206	303.7	139.9	.7285	8.2949	1.000	.7915	19.174	90557.7	.332
2201	306.1	137.8	.1457	.7166	1.075	1.1295	1.044	6518.6	.695
5201	294.2	98.0	.1457	1.1327	1.100	1.5538	1.194	7188.8	.683
5204	306.1	137.8	.1457	.7393	1.100	1.1988	1.044	6450.2	.696
2202	305.5	137.8	.2914	.7180	1.075	1.1435	1.791	7537.3	.672
2203	305.4	138.4	.4371	.7499	1.075	1.1459	2.686	8845.2	.646
2204	303.9	136.5	.5828	.6393	1.075	1.1696	3.805	8922.0	.646
2221	304.2	139.8	.5828	.6348	1.075	1.1498	3.805	9042.8	.646
2205	304.0	138.5	.7285	.6340	1.075	1.1672	4.999	9967.9	.628
2206	305.2	138.0	.1457	3.1629	1.075	1.1606	2.537	24342.3	.500
2207	304.9	135.8	.2914	3.1956	1.075	1.1678	4.476	25495.9	.495
2208	304.7	143.3	.4371	2.9829	1.075	1.1370	6.565	25683.2	.497
2209	305.4	139.5	.5828	3.0065	1.075	1.1207	9.027	27348.2	.486
2210	305.4	142.1	.7285	3.0247	1.075	1.1207	12.534	28597.0	.480
5202	293.7	119.3	.7285	3.5117	1.100	1.5726	14.325	23558.7	.508
2211	305.5	138.0	.1457	5.6431	1.075	1.1466	3.581	43110.6	.420
5203	295.5	137.1	.1457	5.6561	1.100	1.5066	4.253	33648.1	.458
5208	299.7	139.1	.1457	5.7102	1.100	1.3480	3.805	37957.4	.438
2212	304.8	137.1	.2914	5.6262	1.075	1.1633	7.088	43436.4	.417
2222	299.2	145.3	.2914	5.3169	1.075	1.3849	7.386	34579.3	.452
2213	304.8	142.4	.4371	5.4717	1.075	1.1633	11.042	43371.8	.417
5205	300.8	132.7	.4371	5.7784	1.100	1.3039	12.310	41650.2	.428
5209	299.3	137.9	.4371	5.5958	1.100	1.3600	12.310	38758.0	.440
2214	305.5	137.3	.5828	5.5841	1.075	1.1161	14.325	47181.2	.410
2215	305.9	138.5	.7285	5.5524	1.075	1.1070	17.980	48449.7	.404
2216	302.6	141.9	.1457	7.7920	1.075	1.3546	4.476	50036.6	.400
5206	299.8	132.3	.1457	8.5813	1.100	1.3329	5.670	57206.0	.385
2217	302.7	141.6	.2914	7.7402	1.075	1.3517	9.624	50736.7	.400
5207	300.5	130.7	.2914	8.5956	1.100	1.3125	10.893	59161.7	.382
2218	302.2	141.4	.4371	8.0526	1.075	1.3663	14.623	53059.6	.394
2223	299.7	144.9	.4371	7.6215	1.075	1.3359	14.921	51509.6	.398
2219	305.5	143.3	.5828	7.7508	1.075	1.1054	19.323	64373.6	.370
2220	305.5	137.5	.7285	8.0916	1.075	1.1054	24.471	68131.6	.360

PRESSURE DROP AND FRICTION FACTOR CALCULATION   TABLE D.2

PRESSURE DROP IN KN/M₃ , FRICTION FACTOR EXPERIMENTAL, MODIFIED AND S-L

RUN	DEPXN	DELPX	DELPC	UPRED	PDEV	FEXP	FMOD	FSL
1014	.218	.176	.133	24.76	-18.92	.01358	.01022	.00877
1015	.529	.398	.341	14.31	-24.58	.01030	.00882	.00788
1016	.949	.664	.632	4.83	-29.96	.00857	.00816	.00742
1017	1.310	1.152	.904	21.52	-12.03	.00950	.00746	.00693
1018	1.692	1.772	1.205	32.01	4.73	.01014	.00689	.00652
4001	1.672	1.373	1.190	13.37	-17.86	.00797	.00691	.00653
1019	.380	.442	.240	45.60	16.43	.01707	.00929	.00818
1020	1.033	.930	.701	24.63	-9.91	.01033	.00778	.00716
1021	1.810	1.639	1.268	22.66	-9.41	.00929	.00718	.00674
1022	2.712	2.349	1.957	16.72	-13.36	.00801	.00667	.00635
1023	3.493	3.147	2.571	18.31	-9.87	.00775	.00633	.00610
4002	3.521	3.103	2.622	15.52	-11.84	.00728	.00615	.00596
1024	.474	.487	.308	36.76	2.88	.01372	.00867	.00778
1025	1.373	1.418	.956	32.61	3.34	.01083	.00729	.00682
1026	2.380	2.216	1.696	23.45	-6.86	.00898	.00687	.00651
1027	3.674	3.989	2.698	32.37	8.57	.00943	.00637	.00613
4004	3.737	3.413	2.827	17.18	-8.64	.00713	.00591	.00577
1028	4.917	5.985	3.731	37.66	21.72	.00941	.00586	.00573
4003	4.969	4.433	3.812	14.01	-10.77	.00663	.00570	.00560
1029	.570	1.107	.372	66.39	94.26	.02560	.00860	.00772
1030	1.642	2.039	1.146	43.78	24.17	.01290	.00725	.00679
1031	2.999	3.236	2.182	32.58	7.91	.00968	.00653	.00625
1032	4.507	4.610	3.375	26.78	2.29	.00828	.00606	.00589
4006	4.546	4.344	3.435	20.93	-4.43	.00750	.00593	.00578
4005	6.013	5.807	4.674	19.50	-3.42	.00685	.00551	.00544
2009	.218	.221	.132	40.19	1.62	.01725	.01031	.00883
5001	.261	.221	.154	30.57	-15.00	.01601	.01112	.00932
2010	.520	.442	.334	24.38	-14.86	.01178	.00891	.00793
5008	.629	.442	.394	10.89	-29.59	.01068	.00951	.00832
2011	.906	.708	.604	14.69	-21.77	.00953	.00813	.00741
5002	1.164	.886	.758	14.46	-23.85	.01011	.00865	.00776
2012	1.297	1.019	.883	13.34	-21.40	.00891	.00772	.00712
5003	1.457	1.418	.968	31.73	-2.66	.01205	.00822	.00747
5009	1.437	1.418	.952	32.88	-1.26	.01233	.00828	.00751
2013	1.621	1.418	1.114	21.44	-12.50	.00960	.00754	.00699
5010	1.887	1.817	1.273	29.93	-3.70	.01129	.00791	.00725
2014	.418	.398	.265	33.49	-4.74	.01396	.00928	.00817
5004	.437	.442	.268	39.49	1.30	.01668	.01009	.00869
2015	1.114	.974	.750	23.06	-12.54	.01035	.00796	.00729

CONTINUED   TABLE D.2

RUN	DEPXN	DELPX	DELPC	UPRED	PDEV	FEXP	FMOD	FSL
2016	1.968	1.994	1.372	31.18	1.34	.01056	.00727	.00680
2017	2.873	2.748	2.046	25.55	-4.32	.00925	.00689	.00652
2029	2.808	2.704	1.994	26.27	-3.69	.00942	.00694	.00656
2018	3.831	3.546	2.787	21.40	-7.43	.00831	.00653	.00625
2030	3.752	3.546	2.712	23.52	-5.46	.00867	.00663	.00633
5011	3.833	3.989	2.711	32.03	4.08	.01031	.00701	.00661
2019	.531	.664	.339	48.89	25.17	.01772	.00905	.00803
5005	.551	.930	.342	63.23	68.91	.02656	.00976	.00848
2020	1.498	1.553	1.024	34.05	3.68	.01159	.00764	.00707
2021	2.674	2.571	1.881	26.83	-3.81	.00971	.00710	.00668
2022	4.037	4.078	2.913	28.58	1.01	.00934	.00667	.00635
5006	4.071	4.965	2.869	42.21	21.96	.01224	.00707	.00666
2023	5.333	5.586	3.924	29.76	4.64	.00906	.00636	.00612
2024	.651	1.152	.421	63.40	76.93	.02399	.00878	.00784
2025	1.820	2.305	1.256	45.49	26.68	.01368	.00745	.00693
2026	3.250	3.856	2.326	39.67	18.65	.01128	.00680	.00646
5012	3.349	4.167	2.346	43.69	24.42	.01276	.00718	.00674
2027	4.958	4.965	3.650	26.48	.14	.00862	.00633	.00610
5007	5.106	6.694	3.655	45.40	31.11	.01246	.00680	.00645
2028	6.724	7.270	5.039	30.68	8.13	.00873	.00605	.00588
1103	1.710	1.193	.580	51.38	-30.19	.05116	.02487	.02380
4101	1.665	1.342	.574	57.18	-19.37	.05724	.02450	.02348
1104	3.442	2.536	1.466	42.19	-26.29	.03520	.02035	.01983
4102	3.241	2.461	1.441	41.45	-24.05	.03348	.01960	.01916
1105	4.921	3.356	2.419	27.92	-31.79	.02489	.01794	.01765
4103	4.680	4.177	2.417	42.13	-10.73	.02968	.01717	.01696
1106	6.556	4.774	3.527	26.13	-27.16	.02242	.01656	.01640
1107	7.483	5.669	4.556	19.63	-24.23	.01848	.01485	.01481
1108	2.521	3.058	.966	68.40	21.33	.07068	.02233	.02158
4104	2.388	2.237	.956	57.26	-6.31	.05032	.02150	.02085
1109	5.398	4.699	2.639	43.83	-12.94	.03209	.01802	.01773
4105	4.942	4.475	2.603	41.83	-9.44	.02902	.01688	.01668
1110	8.211	6.788	4.653	31.44	-17.31	.02308	.01582	.01571
4106	7.480	7.087	4.602	35.06	-5.24	.02266	.01471	.01468
1111	10.864	9.176	6.821	25.66	-15.52	.01944	.01445	.01443
1112	12.483	11.414	9.014	21.03	-8.55	.01618	.01278	.01283
1113	3.065	3.580	1.218	65.96	16.82	.06354	.02163	.02096
4113	2.848	3.655	1.225	66.48	28.33	.06023	.02018	.01968
1114	6.588	7.087	3.438	51.48	7.57	.03507	.01701	.01681
4112	6.119	6.714	3.453	48.57	9.73	.03089	.01588	.01577
1115	9.942	10.295	6.172	40.05	3.56	.02435	.01460	.01457
4111	9.338	10.220	6.117	40.15	9.44	.02327	.01392	.01393
1116	12.717	12.981	9.145	29.55	2.07	.01820	.01282	.01288
4109	12.641	13.279	9.194	30.76	5.05	.01834	.01269	.01276
1117	15.983	16.487	12.406	24.75	3.15	.01593	.01199	.01207
4107	15.827	16.338	12.518	23.38	3.23	.01539	.01179	.01188

CONTINUED   TABLE D.2

RUN	DEPXN	DELPX	DELPC	UPRED	PDEV	FEXP	FMOD	FSL
1118	3.312	4.848	1.410	70.91	46.39	.07001	.02036	.01984
1119	7.333	8.430	4.059	51.84	14.96	.03355	.01615	.01602
1120	3.365	4.774	1.414	70.36	41.87	.06950	.02059	.02004
4110	14.544	17.679	11.065	37.41	21.55	.01950	.01220	.01228
4108	18.595	22.157	15.413	30.43	19.15	.01626	.01131	.01141
2107	2.049	1.491	.635	57.41	-27.19	.06326	.02694	.02557
2108	3.975	3.506	1.572	55.15	-11.79	.04846	.02173	.02105
2109	5.725	4.028	2.583	35.87	-29.62	.03017	.01934	.01893
2110	7.701	5.595	3.843	31.30	-27.33	.02576	.01770	.01744
2111	9.489	6.863	5.115	25.47	-27.66	.02219	.01654	.01637
2112	2.896	3.282	1.053	67.90	13.32	.07292	.02340	.02252
5106	3.404	3.804	1.100	71.07	11.77	.08976	.02596	.02473
2113	6.218	6.266	2.912	53.52	.77	.04029	.01872	.01837
2114	9.350	8.877	5.084	42.73	-5.05	.02866	.01641	.01626
2115	12.165	11.115	7.236	34.89	-8.62	.02329	.01516	.01509
5111	13.173	13.204	7.563	42.72	.23	.02731	.01564	.01554
2116	15.071	13.577	9.666	28.80	-9.90	.01992	.01418	.01418
5102	19.965	17.532	11.288	35.61	-12.18	.02463	.01585	.01574
5107	17.601	15.965	10.434	34.64	-9.29	.02327	.01521	.01514
5112	17.489	15.741	10.686	32.11	-9.99	.02181	.01480	.01476
2117	3.863	4.475	1.331	70.26	15.86	.08253	.02454	.02351
5101	4.078	4.102	1.258	69.32	.60	.08820	.02705	.02567
5108	3.982	4.774	1.354	71.62	19.90	.08747	.02482	.02375
2118	8.153	8.803	3.722	57.71	7.97	.04528	.01914	.01875
5109	8.543	9.325	3.870	58.50	9.16	.04646	.01928	.01887
2119	12.528	13.130	6.717	48.84	4.81	.03248	.01661	.01644
2120	15.329	16.786	9.901	41.01	9.50	.02390	.01410	.01409
2121	19.083	20.143	13.338	33.78	5.55	.01986	.01315	.01319
5103	25.321	24.694	15.077	38.94	-2.47	.02481	.01515	.01508
2122	4.376	5.968	1.538	74.23	36.39	.09360	.02411	.02314
5104	4.940	6.788	1.698	74.98	37.42	.09830	.02459	.02355
2123	9.454	12.085	4.410	63.50	27.82	.05149	.01879	.01842
5105	10.413	12.682	4.726	62.73	21.79	.05164	.01924	.01884
2124	14.649	17.606	8.033	54.37	20.18	.03570	.01629	.01614
5110	14.784	18.502	8.223	55.55	25.14	.03619	.01608	.01595
2125	17.297	20.889	11.902	43.02	20.76	.02340	.01333	.01337
2126	21.816	27.305	16.257	40.46	25.16	.02087	.01243	.01250
1201	1.179	.894	.437	51.07	-24.09	.03629	.01775	.01641
1202	2.544	1.715	1.120	34.71	-32.57	.02253	.01470	.01390
1203	3.896	2.461	1.908	22.49	-36.81	.01686	.01307	.01251
1204	5.228	3.655	2.754	24.66	-30.07	.01600	.01205	.01163
4201	5.058	3.356	2.683	20.06	-33.63	.01496	.01196	.01155
1205	6.547	4.774	3.645	23.65	-27.07	.01485	.01133	.01100
1206	1.828	2.163	.735	66.01	18.37	.04780	.01624	.01518
1207	4.203	4.102	2.058	49.82	-2.38	.02604	.01306	.01251
1208	6.713	5.968	3.660	38.67	-11.09	.01892	.01160	.01124
1209	9.088	7.758	5.390	30.52	-14.63	.01521	.01057	.01031

RUN	DEPXN	DELPX	DELPC	UPRED	PDEV	FEXP	FMOD	FSL
1210	11.658	9.549	7.257	24.00	-18.08	.01318	.01001	.00981
1211	2.190	2.983	.936	68.60	36.25	.04835	.01518	.01430
4205	2.154	3.431	.950	72.29	59.29	.05292	.01466	.01387
1212	5.134	5.964	2.698	54.75	16.17	.02671	.01208	.01166
4204	5.084	5.595	2.731	51.18	10.06	.02416	.01179	.01140
1213	8.519	9.026	4.892	45.80	5.96	.02021	.01095	.01066
4203	8.245	8.355	4.923	41.08	1.33	.01781	.01049	.01024
1214	11.916	11.936	7.382	38.15	.17	.01628	.01007	.00986
4202	11.519	11.265	7.351	34.74	-2.19	.01493	.00974	.00956
1215	15.213	14.547	9.982	31.38	-4.37	.01377	.00945	.00929
4210	2.436	3.879	1.107	71.46	59.25	.04975	.01419	.01347
4209	5.793	7.460	3.218	56.85	28.77	.02634	.01136	.01102
4208	9.796	11.265	6.015	46.60	14.99	.01904	.01017	.00995
4207	13.614	15.293	9.125	40.33	12.33	.01547	.00923	.00908
4206	17.570	19.173	12.274	35.98	9.12	.01377	.00881	.00870
2201	1.346	1.043	.445	57.28	-22.45	.04719	.02015	.01831
5201	1.860	1.193	.573	52.00	-35.82	.04552	.02184	.01962
5204	1.420	1.043	.465	55.38	-26.52	.04570	.02039	.01850
2202	2.891	1.790	1.148	35.89	-38.05	.02571	.01648	.01538
2203	4.521	2.685	1.996	25.66	-40.58	.01971	.01465	.01386
2204	5.873	3.804	2.733	28.17	-35.21	.01925	.01383	.01316
2221	5.795	3.804	2.709	28.78	-34.34	.01931	.01375	.01310
2205	7.436	4.998	3.660	26.76	-32.78	.01774	.01299	.01245
2206	2.146	2.536	.786	68.98	18.20	.05806	.01801	.01661
2207	4.957	4.475	2.217	50.45	-9.71	.02915	.01444	.01368
2208	7.572	6.564	3.789	42.27	-13.30	.02210	.01276	.01225
2209	10.408	9.026	5.641	37.49	-13.27	.01868	.01167	.01130
2210	13.281	12.533	7.608	39.29	-5.62	.01809	.01098	.01068
5202	16.916	14.324	8.820	38.42	-15.31	.01979	.01219	.01175
2211	2.580	3.580	.995	72.19	38.77	.06123	.01702	.01581
5203	2.910	4.252	1.017	76.08	46.14	.07939	.01898	.01739
5208	2.802	3.804	1.025	73.06	35.78	.06703	.01805	.01665
2212	6.140	7.087	2.895	59.15	15.42	.03337	.01363	.01299
2222	6.422	7.385	2.817	61.85	15.00	.03869	.01476	.01395
2213	9.873	11.041	5.197	52.92	11.83	.02562	.01206	.01164
5205	10.621	12.309	5.423	55.94	15.90	.02832	.01247	.01200
5209	10.635	12.309	5.327	56.72	15.74	.02945	.01274	.01223
2214	13.577	14.324	7.831	45.32	5.50	.01994	.01090	.01061
2215	17.455	17.979	10.688	40.55	3.00	.01716	.01020	.00998
2216	3.078	4.475	1.143	74.45	45.38	.06953	.01776	.01641
5206	3.190	5.669	1.211	78.63	77.68	.08109	.01732	.01606
2217	7.295	9.623	3.337	65.32	31.91	.04065	.01409	.01339
5207	7.580	10.892	3.567	67.25	43.69	.04171	.01366	.01302
2218	12.229	14.622	6.280	57.05	19.57	.02886	.01239	.01193
2223	11.854	14.920	6.107	59.06	25.86	.03018	.01235	.01189
2219	15.629	19.322	9.344	51.64	23.62	.02166	.01047	.01023
2220	20.806	24.470	13.252	45.84	17.61	.01803	.00976	.00958

TWO PHASE PRESSURE DROP   LOCKHART-MARTINELLI   TABLE D.3

RUN NO.	VGO M/ SEC	DELPX KN/ M3	P LM KN/ M3	RE L	RE G	PDEV	PHAIG	X
1014	.8510	.176	.214	1820.5	1379.5	-17.381	8.584	3.482
1015	.7689	.398	.454	3614.1	1367.2	-12.195	13.212	6.677
1016	.8474	.664	.769	5145.2	1353.9	-13.554	16.506	9.153
1017	.8432	1.152	1.075	7712.6	1330.7	7.241	19.541	11.541
1018	.8587	1.772	1.416	10898.6	1303.1	25.128	22.181	13.686
4001	.8384	1.373	1.409	10898.6	1313.0	-2.531	22.305	13.788
1019	3.0745	.442	.519	1829.3	4048.1	-14.804	4.674	1.213
1020	3.0693	.930	.986	3801.9	4017.2	-5.591	6.467	2.184
1021	3.0490	1.639	1.509	5541.1	4014.5	8.681	8.029	3.129
1022	3.0404	2.349	2.051	7676.2	3979.4	14.559	9.369	3.99
1023	3.0413	3.147	2.620	10007.5	3957.6	20.151	10.586	4.81
4002	3.1419	3.103	2.602	10993.8	3920.7	19.259	10.369	4.66
1024	5.1699	.487	.818	2010.7	7009.4	-40.349	3.691	.74
1025	5.3677	1.418	1.514	4039.9	6986.2	-6.289	4.922	1.33
1026	5.0995	2.216	2.196	5568.0	7034.0	.942	6.096	1.97
1027	5.3426	3.989	2.956	7640.3	6992.5	34.943	6.931	2.45
4004	5.6892	3.413	2.961	9772.3	6807.4	15.284	6.659	2.29
1028	5.3842	5.985	3.666	10921.9	6884.7	63.243	7.682	2.91
4003	5.5605	4.433	3.695	11966.9	6818.1	19.981	7.540	2.82
1029	7.6604	1.107	1.187	1883.0	10086.2	-6.681	3.205	.54
1030	7.6464	2.039	2.049	3766.1	10067.7	-.460	4.218	.98
1031	7.6853	3.236	2.929	5866.9	10000.6	10.515	5.033	1.39
1032	7.7280	4.610	3.832	8153.5	9938.4	20.323	5.742	1.77
4006	7.8977	4.344	3.807	8757.3	9855.3	14.114	5.669	1.73
4005	7.8552	5.807	4.723	12215.4	9696.6	22.948	6.290	2.08
2009	.6765	.221	.194	1857.9	1003.8	14.060	10.100	4.48
5001	.8881	.221	.236	1367.6	1241.0	-6.173	9.151	3.85
2010	.6155	.442	.341	3715.9	913.2	29.694	14.517	8.82
5008	.7939	.442	.499	2775.7	1174.0	-11.345	14.317	7.49
2011	.6709	.708	.601	5573.8	995.4	17.843	17.908	11.62
2012	.6580	1.019	.880	7302.7	971.0	15.844	22.076	15.25
5002	.9619	.886	.878	4073.6	1193.9	.981	17.152	9.65
5003	.7245	1.418	.943	5665.8	959.0	50.328	22.109	15.28
5009	.6913	1.418	1.121	5589.7	1011.0	26.583	24.182	15.34
2013	.6622	1.418	1.117	8367.4	924.4	26.985	25.160	18.07
5010	.6751	1.817	1.491	7019.2	1014.9	21.856	28.270	18.82
5004	3.2956	.442	.582	1400.0	3928.9	-23.901	4.811	1.28
2014	3.0962	.398	.533	1831.9	3611.0	-25.195	4.838	1.29
2015	2.9428	.974	1.021	3574.1	3586.0	-4.582	6.879	2.42
2016	2.9474	1.994	1.559	5372.6	3569.1	27.960	8.511	3.4
2017	2.9425	2.748	2.148	7035.6	3608.0	27.941	9.994	4.4
2029	2.7979	2.704	2.087	6932.3	3493.1	29.590	10.246	4.58
2018	2.9406	3.546	2.753	9072.6	3605.7	28.830	11.320	5.3

CONTINUED

RUN NO.	VGO M/ SEC	DELPX KN/ M3	P LM KN/ M3	RE L	RE G	PDEV	PHAIG	X
2030	2.8537	3.546	2.760	8702.0	3520.9	28.505	11.587	5.511
5011	2.8015	3.989	2.824	7204.0	3624.6	41.256	11.817	5.673
2019	5.3314	.664	.881	1751.8	6577.8	-24.530	3.806	.799
5005	5.6565	.930	.933	1374.8	6875.8	-.287	3.806	.799
2020	5.3058	1.553	1.598	3503.7	6546.1	2.783	5.151	1.456
2021	5.1236	2.571	2.313	4955.6	6472.6	11.172	6.378	2.133
2022	5.2848	4.078	3.162	6600.4	6554.1	28.976	7.297	2.677
5006	5.2923	4.965	3.272	5425.6	6639.3	51.735	7.455	2.773
2023	5.1740	5.586	3.974	8376.4	6459.4	40.579	8.304	3.303
2024	8.0408	1.152	1.268	1736.5	9545.8	-9.080	3.265	.568
2025	7.7439	2.305	2.164	3436.1	9489.8	6.557	4.358	1.056
2026	7.5492	3.856	3.068	5165.1	9424.7	25.702	5.275	1.521
5012	7.8799	4.167	3.276	4273.3	9767.5	27.195	5.271	1.519
2027	7.4941	4.965	4.041	7050.9	9246.0	22.880	6.079	1.962
5007	8.0085	6.694	4.343	5502.9	9672.3	54.139	6.066	1.955
2028	7.4489	7.270	5.025	8813.7	9190.2	44.669	6.820	2.391
1103	.9171	1.193	.812	1341.6	849.5	46.867	7.201	3.338
4101	.9198	1.342	.799	1390.2	852.0	67.911	7.131	3.290
4102	.9038	2.461	1.732	2797.5	837.2	42.136	10.639	5.803
1105	.8662	3.356	2.837	3907.0	811.5	18.305	14.084	8.473
4103	.9047	4.177	2.803	4289.2	824.2	49.051	13.543	8.042
1104	.8839	2.536	1.774	2562.6	832.4	42.972	10.940	6.029
1106	.8700	4.774	4.075	5113.5	819.3	17.162	16.783	10.679
1107	.8837	5.669	5.210	7117.4	805.0	8.828	18.835	12.418
1108	3.3210	3.058	2.579	1299.6	2561.9	18.581	4.718	1.231
4104	3.3138	2.237	2.506	1414.6	2541.8	-10.694	4.660	1.204
1109	3.2427	4.699	4.702	2468.5	2561.3	-.046	6.484	2.194
4105	3.2720	4.475	4.615	2859.1	2525.7	-3.022	6.354	2.119
1110	3.2328	6.788	6.959	3685.9	2553.5	-2.448	7.912	3.056
4106	3.3381	7.087	6.856	4335.9	2515.0	3.369	7.669	2.905
1111	3.2244	9.176	9.274	4937.1	2546.8	-1.055	9.158	3.855
1112	3.2976	11.414	11.486	7041.0	2498.7	-.620	10.048	4.448
1113	5.7591	3.580	4.065	1237.6	4522.6	-11.922	3.797	.795
4113	6.0922	3.655	4.111	1426.9	4449.2	-11.076	3.693	.749
1114	5.7062	7.087	7.060	2445.2	4507.1	.384	5.038	1.397
4112	5.8220	6.714	6.938	2828.3	4438.5	-3.224	4.928	1.340
1115	5.7350	10.295	10.050	3809.1	4476.7	2.446	5.999	1.91
4111	5.8094	10.220	9.898	4243.0	4428.9	3.257	5.899	1.86
1116	5.8350	12.981	13.044	5546.4	4421.3	-.477	6.763	2.35
4109	5.8252	13.279	12.903	5656.6	4413.9	2.921	6.737	2.34
1117	5.7976	16.487	16.208	6918.0	4393.0	1.723	7.569	2.84
4107	5.9679	16.338	16.283	7148.4	4413.6	.340	7.456	2.77
1118	8.3288	4.848	5.570	1305.5	6425.1	-12.946	3.306	.58
1119	8.1972	8.430	9.308	2515.6	6437.2	-9.429	4.317	1.03
1120	8.2726	4.774	5.569	1272.8	6457.5	-14.263	3.319	.59
4110	8.2991	17.679	16.510	5632.4	6327.0	7.082	5.715	1.75
4108	8.5501	22.157	20.511	7071.3	6319.6	8.026	6.279	2.07

CONTINUED

RUN NO.	VGO M/ SEC	DELPX KN/ M3	P LM KN/ M3	RE L	RE G	PDEV	PHAIG	X
2107	.8199	1.491	.850	1141.1	738.5	75.494	8.075	3.942
2108	.7725	3.506	1.839	2262.5	665.9	90.650	12.622	7.318
2109	.7295	4.028	2.970	3379.8	650.0	35.639	16.631	10.552
2110	.7724	5.595	4.340	4460.2	695.7	28.917	19.145	12.683
2111	.7826	6.863	5.744	5587.6	689.7	19.492	21.925	15.124
2112	3.1838	3.282	2.653	1185.0	2342.7	23.720	4.967	1.360
5106	3.3694	3.804	2.886	935.5	2489.0	31.799	4.998	1.376
2113	3.1935	6.266	5.022	2273.8	2377.8	24.789	6.817	2.389
2114	3.1217	8.877	7.370	3418.2	2353.0	20.448	8.381	3.352
2115	3.0597	11.115	9.721	4479.9	2292.2	14.341	9.796	4.278
5111	3.1061	13.204	10.058	4143.2	2311.5	31.284	9.894	4.344
2116	3.0732	13.577	12.378	5600.3	2288.2	9.693	11.039	5.127
5102	3.5439	17.532	14.251	4117.5	2396.9	23.029	11.014	5.110
5107	3.1925	15.965	13.223	4686.8	2343.4	20.738	11.198	5.238
5112	3.3537	15.741	13.371	4908.2	2400.9	17.723	10.884	5.020
5101	4.5168	4.102	3.415	803.9	2557.1	20.127	4.700	1.224
5108	5.7018	4.774	4.442	925.2	4398.5	7.483	4.004	.889
2118	5.5847	8.803	7.664	1896.1	4310.9	14.866	5.325	1.548
5109	5.8283	9.325	7.864	1853.8	4305.4	18.583	5.314	1.542
2119	5.6003	13.130	11.102	2862.9	4297.0	18.267	6.396	2.143
2120	5.5574	16.786	13.895	4486.2	4086.8	20.811	7.276	2.664
2121	5.5152	20.143	17.202	5631.6	4081.1	17.102	8.132	3.194
5103	6.2566	24.694	20.078	3932.5	4464.7	22.994	8.176	3.222
2122	8.2063	5.968	5.989	910.8	6141.8	-.336	3.494	.663
2117	5.8122	4.475	4.422	944.2	4350.0	1.198	3.959	.868
5104	9.9479	6.788	6.858	842.2	6351.8	-1.007	3.386	.618
2123	8.0689	12.085	10.159	1813.1	6151.5	18.968	4.585	1.167
5105	8.9764	12.682	10.997	1683.9	6283.4	15.328	4.527	1.138
2124	8.0513	17.606	14.347	2731.9	6175.5	22.717	5.445	1.612
5110	8.1958	18.502	14.496	2806.1	6169.2	27.633	5.443	1.611
2125	8.0022	20.889	17.518	4625.6	5921.4	19.242	6.079	1.962
2126	7.9995	27.305	21.489	5782.4	5882.6	27.067	6.756	2.353
1201	.9361	.894	.590	1431.6	832.6	51.628	7.072	3.250
1202	.9221	1.715	1.324	2772.0	824.6	29.556	10.706	5.853
1203	.9144	2.461	2.146	4212.5	817.7	14.715	13.719	8.182
1204	.9207	3.655	3.061	5677.3	818.9	19.434	16.346	10.313
1205	.9042	4.774	4.005	7158.1	804.3	19.202	18.972	12.53-
1206	3.3538	2.163	1.918	1355.9	2496.5	12.789	4.650	1.19-
1207	3.3426	4.102	3.562	2705.9	2488.2	15.159	6.358	2.12
1208	3.3292	5.968	5.289	4049.8	2478.2	12.851	7.778	2.97
1209	3.3505	7.758	7.117	5592.2	2464.8	9.010	8.969	3.73
1210	3.3318	9.548	8.993	6884.6	2465.0	6.189	10.138	4.50
1211	5.9218	2.983	3.056	1407.2	4356.3	-2.356	3.689	.74
4205	6.0875	3.431	3.064	1515.0	4316.3	11.975	3.638	.72

CONTINUED

RUN NO.	VGO M/ SEC	DELPX KN/ M3	P LM KN/ M3	RE L	RE G	PDEV	PHAIG	X
1212	5.8954	5.964	5.337	2850.8	4336.9	11.752	4.881	1.31
4204	6.0011	5.595	5.320	3004.8	4308.9	5.177	4.832	1.29
1213	5.8502	9.026	7.720	4031.9	4354.8	16.921	5.917	1.87
4203	5.9145	8.355	7.603	4470.1	4299.8	9.892	5.825	1.82
1214	5.8368	11.936	10.179	5387.8	4344.8	17.262	6.788	2.37
4202	5.8013	11.265	9.966	5861.3	4295.6	13.039	6.737	2.34
1215	5.8586	14.547	12.694	6794.9	4334.4	14.598	7.575	2.84
4210	8.5335	3.879	4.192	1515.0	6165.5	-7.453	3.207	.54
4209	8.2632	7.460	6.926	3030.0	6155.6	7.710	4.193	.97
4208	8.6666	11.265	10.041	4368.3	6179.9	12.197	4.934	1.34
4207	8.4903	15.293	12.849	6034.7	6134.3	19.026	5.624	1.70
4206	8.3114	19.173	15.785	7310.9	6154.2	21.468	6.312	2.09
2201	.7160	1.043	.580	1101.5	622.6	79.951	8.739	4.41
5201	1.1289	1.193	.745	819.3	753.7	60.057	7.570	3.59
5204	.7387	1.043	.603	1061.9	642.3	73.006	8.694	4.38
2202	.7200	1.790	1.336	2176.0	626.1	33.976	13.213	7.78
2203	.7516	2.685	2.254	3257.1	657.1	19.141	16.524	10.46
4201	.8859	3.356	2.999	5861.3	795.9	11.914	16.595	10.52
2204	.6374	3.804	3.037	4254.8	557.6	25.271	22.015	15.20
2221	.6334	3.804	3.023	4328.1	566.0	25.858	21.937	15.13
2205	.6342	4.998	4.050	5329.5	560.8	23.419	25.414	18.30
2206	3.1554	2.536	1.976	1071.9	2294.0	28.389	4.969	1.36
2207	3.2022	4.475	3.768	2130.7	2284.9	18.775	6.825	2.39
2208	2.9888	6.564	5.460	3282.6	2253.3	20.223	8.542	3.45
2209	2.9914	9.026	7.310	4440.4	2201.6	23.482	9.945	4.37
2210	3.0107	12.533	9.385	5550.6	2256.3	33.547	11.151	5.20
5202	3.5271	14.324	10.926	4047.5	2361.8	31.097	11.106	5.17
2211	5.6199	3.580	3.145	1085.0	4085.6	13.828	3.906	.84
5203	5.6721	4.252	3.386	844.9	4323.1	25.578	4.004	.88
5208	5.7276	3.804	3.352	944.3	4315.5	13.497	3.946	.86
2212	5.6246	7.087	5.616	2138.9	4063.8	26.194	5.231	1.49
2222	5.3005	7.385	5.661	1796.6	4210.2	30.468	5.394	1.58
2213	5.4774	11.041	8.120	3208.4	4104.9	35.977	6.342	2.11
5205	5.7705	12.309	8.506	2929.0	4138.3	44.712	6.354	2.11
5209	5.5798	12.309	8.457	2808.1	4202.8	45.551	6.432	2.16
2214	5.5673	14.324	10.619	4458.8	4022.4	34.893	7.244	2.64
2215	5.5675	17.979	13.396	5619.3	4024.8	34.209	8.111	3.18
2216	7.7851	4.475	4.365	918.4	5902.7	2.537	3.487	.66
5206	8.5960	5.66	4.700	955.0	6164.6	20.624	3.403	.62
2217	7.7585	9.623	7.526	1840.8	5847.5	27.874	4.591	1.17
5207	8.5786	10.892	7.970	1939.8	6074.2	36.659	4.453	1.10
2218	8.0365	14.622	11.031	2731.7	6093.3	32.559	5.389	1.58
2223	7.6412	14.920	10.710	2793.8	6000.1	39.312	5.484	1.63
2219	7.7291	19.322	13.361	4501.9	5827.1	44.613	6.123	1.98
2220	8.0790	24.470	16.886	5627.4	5837.1	44.911	6.727	2.33

CALCULATED RESULTS

AREA CREATION RATE KASTURI-STEPANEK

RUN	VLO	VGO	A	DELPX	EL	A/EL	ACRET
NO.	M/	M/	M2/	KN/		M2/	M2/
	SEC	SEC	M3	M3		M3	SEC

EMPTY TUBE

2009	.1362	.6770	104.30	.222	.4851	215.0	0.42E-02
5001	.1362	.8878	89.20	.222	.4674	190.8	0.37E-02
5008	.2724	.7933	132.20	.443	.5404	244.6	0.95E-02
5002	.4086	.9612	135.50	.887	.5575	243.0	0.14E-01
2012	.5448	.6554	105.20	1.020	.6506	161.7	0.13E-01
5009	.5448	.6924	308.60	1.419	.6491	475.4	0.37E-01
2013	.6810	.6620	158.20	1.419	.6825	231.8	0.23E-01
2014	.1362	3.0869	223.00	.399	.3255	685.1	0.13E-01
2015	.2724	2.9366	280.20	.975	.3587	781.2	0.30E-01
2016	.4086	2.9570	286.10	1.995	.3799	753.1	0.44E-01
2017	.5448	2.9462	232.70	2.749	.4039	576.1	0.45E-01
2018	.6810	2.9428	200.40	3.547	.4211	475.9	0.46E-01
5011	.6810	2.8026	691.10	3.990	.4424	1562.2	0.15
2019	.1362	5.3223	357.20	.665	.2841	1257.3	0.24E-01
5005	.1362	5.6547	272.80	.931	.2939	928.2	0.18E-01
2020	.2724	5.3005	340.10	1.552	.3006	1131.4	0.44E-01
2021	.4086	5.1378	435.20	2.572	.3208	1356.6	0.79E-01
2022	.5448	5.3129	356.50	4.079	.3330	1070.6	0.83E-01
2023	.6810	5.1628	443.50	5.587	.3503	1266.1	0.12
2024	.1362	8.0599	426.80	1.153	.2510	1700.4	0.33E-01
2025	.2724	7.7522	456.00	2.306	.2681	1700.9	0.66E-01
5012	.4086	7.8811	367.70	4.168	.2889	1272.8	0.74E-01
2027	.5448	7.4921	575.70	4.966	.2900	1985.2	0.15
2028	.6810	7.4577	602.90	7.271	.3015	1999.7	0.19
2030	.6810	2.8394	410.70	3.547	.4303	954.5	0.93E-01

TP-1 (H/D = 5.00)

2107	.1452	.8213	209.50	1.492	.4917	426.1	0.83E-02
2108	.2903	.7747	424.50	3.507	.5612	756.4	0.29E-01
2109	.4355	.7281	501.40	4.029	.6198	809.0	0.47E-01
2110	.5806	.7725	299.30	5.596	.6480	461.9	0.36E-01
2111	.7258	.7823	324.60	6.864	.6788	478.2	0.46E-01
2112	.1452	3.1872	855.10	3.283	.3559	2402.6	0.47E-01
5106	.1452	3.3660	297.80	3.805	.3668	811.9	0.16E-01

CONTINUED

RUN NO.	VLO M/ SEC	VGO M/ SEC	A M2/ M3	DELPX KN/ M3	EL	A/EL M2/ M3	ACRET M2/ SEC
2113	.2903	3.1849	621.70	6.267	.3828	1624.1	0.63E-01
2114	.4355	3.1242	737.90	8.878	.4069	1813.5	0.11
2115	.5806	3.0581	481.60	11.116	.4321	1114.6	0.87E-01
2116	.7258	3.0572	484.30	13.578	.4521	1071.2	0.10
5112	.7258	3.3594	704.20	15.742	.4443	1585.0	0.15
5108	.1452	5.7172	392.90	4.775	.3232	1215.7	0.24E-01
5109	.2903	5.8462	870.80	9.326	.3370	2584.0	0.10
2120	.5806	5.5374	692.30	16.787	.3562	1943.6	0.15
5103	.7058	6.2341	572.60	24.695	.3784	1513.2	0.15
2121	.7258	5.5160	670.20	20.144	.3705	1808.9	0.18
5104	.1452	9.9155	648.70	6.789	.2873	2257.9	0.44E-01
5105	.2903	8.9498	872.70	12.683	.3046	2865.1	0.11
5110	.4355	8.2105	1012.90	18.503	.3168	3197.3	0.19
2125	.5806	7.9955	705.50	20.890	.3159	2233.3	0.17
2126	.7258	8.0072	816.40	27.306	.3263	2502.0	0.24

TP-2   (H/D = 9.32)

RUN NO.	VLO M/ SEC	VGO M/ SEC	A M2/ M3	DELPX KN/ M3	EL	A/EL M2/ M3	ACRET M2/ SEC
5204	.1457	.7396	268.80	1.044	.5074	529.8	0.10E-01
2203	.4371	.7499	202.00	2.686	.6161	327.9	0.19E-01
2206	.1457	3.1629	566.30	2.537	.3626	1561.8	0.30E-01
2207	.2914	3.1956	551.90	4.476	.3870	1426.1	0.55E-01
2210	.7285	3.0242	645.60	12.534	.4554	1417.7	0.14
2211	.1457	5.6431	823.60	3.581	.3134	2628.0	0.51E-01
5203	.1457	5.6561	538.40	4.253	.3313	1625.1	0.32E-01
5208	.1457	5.7102	315.10	3.805	.3218	979.2	0.19E-01
2212	.2914	5.6262	817.00	7.088	.3290	2483.3	0.97E-01
2213	.4371	5.4717	542.60	11.042	.3464	1566.4	0.91E-01
5205	.4371	5.7784	1113.00	12.310	.3489	3190.0	0.19
5209	.4371	5.5958	881.40	12.310	.3558	2477.2	0.14
2214	.5828	5.5841	797.70	14.325	.3578	2229.5	0.17
2215	.7285	5.5524	697.40	17.980	.3703	1883.3	0.18
5207	.2914	8.5956	816.40	10.893	.3001	2720.4	0.11
5206	.1457	8.5813	468.80	5.670	.2900	1616.6	0.31E-01
2219	.5828	7.7508	739.20	19.323	.3211	2302.1	0.18
2220	.7285	8.0916	692.30	24.471	.3254	2127.5	0.21
2223	.4371	7.6215	1042.30	14.921	.3234	3222.9	0.19

LIQUID PHASE MASS TRANSFER COEFFICIENT (EMPTY TUBE)   TABLE E.2

RUN NO.	KLOX M/ SEC	KLOB M/ SEC	KLOKS M/ SEC	SHEXP	SHCAL	SC	PE	EU
1014	0.8654E-04	0.1173E-03	0.1791E-03	691.3	5724.2	597.7	0.1088E+07	.1286
1015	0.1144E-03	0.1431E-03	0.2003E-03	922.0	6455.4	607.2	0.2194E+07	.0725
1016	0.1272E-03	0.1577E-03	0.2103E-03	1089.8	7205.0	680.2	0.3500E+07	.0537
1017	0.1298E-03	0.1936E-03	0.3102E-03	971.4	9286.4	528.6	0.4077E+07	.0524
4001	0.1124E-03	0.2162E-03	0.3360E-03	736.8	8808.0	409.5	0.4463E+07	.0399
1019	0.1757E-03	0.1479E-03	0.4507E-03	1395.9	14321.4	591.4	0.1082E+07	.3219
1020	0.2320E-03	0.1821E-03	0.4935E-03	1763.9	15009.5	544.8	0.2071E+07	.1691
1021	0.2999E-03	0.2064E-03	0.5620E-03	2355.9	17660.3	579.3	0.3210E+07	.1324
1022	0.4604E-03	0.2307E-03	0.6291E-03	3464.3	18932.4	534.0	0.4099E+07	.1067
1023	0.4067E-03	0.2540E-03	0.7047E-03	2921.2	20243.6	488.7	0.4891E+07	.0915
1024	0.3125E-03	0.1598E-03	0.5488E-03	2233.2	15687.3	484.1	0.9733E+06	.3546
1025	0.5019E-03	0.2092E-03	0.8018E-03	3568.4	22802.9	479.4	0.1937E+07	.2578
1026	0.6309E-03	0.2231E-03	0.7637E-03	4929.2	23865.7	573.3	0.3192E+07	.1790
4004	0.4977E-03	0.2878E-03	0.1172E-02	2901.3	27314.4	325.0	0.3176E+07	.1551
1028	0.3704E-03	0.3126E-03	0.1467E-02	2421.8	38371.1	407.7	0.4453E+07	.1740
4003	0.5464E-03	0.3040E-03	0.1192E-02	3251.7	28382.3	338.6	0.4052E+07	.1289

LIQUID PHASE MASS TRANSFER COEFFICIENT (TP-1)   TABLE E.3

RUN NO.	KLOX M/ SEC	KLCB M/ SEC	KLOKS M/ SEC	SHEXP	SHCAL	SC	PE	EU
4101	0.1922E-03	0.1512E-03	0.9212E-03	767.2	14709.2	417.0	0.5796E+06	.5182
4102	0.1852E-03	0.1766E-03	0.8504E-03	734.1	13484.7	411.4	0.1151E+07	.2377
4103	0.2817E-03	0.2039E-03	0.9837E-03	1091.5	15245.9	393.4	0.1687E+07	.1792
1106	0.2044E-03	0.1985E-03	0.7511E-03	892.5	13121.3	495.9	0.2536E+07	.1152
1107	0.2224E-03	0.2195E-03	0.7975E-03	865.7	12415.9	396.9	0.2825E+07	.0876
4104	0.2503E-03	0.1734E-03	0.1563E-02	980.9	24500.4	402.2	0.5690E+06	.8635
4105	0.5389E-03	0.2074E-03	0.1581E-02	2088.1	24502.7	393.4	0.1125E+07	.4321
4106	0.3819E-03	0.2340E-03	0.1687E-02	1463.2	25859.0	384.9	0.1669E+07	.3040
1111	0.4852E-03	0.2292E-03	0.1391E-02	2203.1	25265.8	534.0	0.2636E+07	.2215
1112	0.8408E-03	0.2600E-03	0.1588E-02	3310.3	25002.6	405.9	0.2857E+07	.1763

LIQUID PHASE MASS TRANSFER COEFFICIENT (TP-2)

RUN NO.	KLOX M/ SEC	KLOB M/ SEC	KLOKS M/ SEC	SHEXP	SHCAL	SC	PE	EU
1201	0.1876E-03	0.1380E-03	0.6286E-03	694.0	9302.7	376.6	0.5391E+06	.3349
1202	0.2376E-03	0.1597E-03	0.5830E-03	909.0	8924.0	402.2	0.1115E+07	.1605
1203	0.1837E-03	0.1760E-03	0.5651E-03	693.3	8533.2	391.7	0.1650E+07	.1024
4201	0.2246E-03	0.1944E-03	0.6035E-03	811.4	8720.3	359.2	0.2105E+07	.0785
1205	0.1797E-03	0.2097E-03	0.6707E-03	664.9	9926.3	376.6	0.2695E+07	.0715
1206	0.4652E-03	0.1673E-03	0.1438E-02	1821.6	22520.9	420.8	0.5705E+06	.8097
1207	0.3464E-03	0.1961E-03	0.1360E-02	1359.8	21351.5	422.7	0.1144E+07	.3838
1208	0.5312E-03	0.2151E-03	0.1316E-02	2090.0	20709.3	424.6	0.1720E+07	.2482
1209	0.4891E-03	0.2339E-03	0.1330E-02	1854.5	20171.2	395.2	0.2210E+07	.1814
1210	0.4661E-03	0.2444E-03	0.1289E-02	1795.6	19869.1	407.7	0.2807E+07	.1429
1214	0.1030E-02	0.2555E-03	0.1969E-02	4060.1	31063.5	426.5	0.2298E+07	.2792
1215	0.8373E-03	0.2697E-03	0.1938E-02	3270.9	30278.5	418.9	0.2846E+07	.2177

MODULUS KLOA CALCULATED RESULTS

RUN NO.	VLO M/ SEC	VGO M/ SEC	VSUM M/ SEC	DELPX KN/ M3	EDPJ KN/M2/ SEC	KLOA / SEC	KLAMOD M3/KN/ SEC
EMPTY TUBE							
1014	.1362	.8486	.9848	.177	.175	.0131	.07401130
1015	.2724	.7666	1.0390	.399	.415	.0238	.05964912
1016	.4086	.8442	1.2528	.665	.833	.0315	.04736842
1017	.5448	.8444	1.3892	1.153	1.601	.0393	.03408500
1018	.6810	.8554	1.5364	1.773	2.725	.0429	.02419628
1019	.1362	3.0588	3.1950	.443	1.417	.0327	.07381490
1020	.2724	3.0658	3.3382	.931	3.108	.0638	.06852846
1021	.4086	3.0432	3.4518	1.640	5.663	.0989	.06030488
1022	.5448	3.0467	3.5915	2.350	8.440	.1805	.07680851
1023	.6810	3.0505	3.7315	3.148	11.747	.1799	.05714740
1024	.1362	5.1704	5.3066	.488	2.588	.0675	.13831967
1025	.2724	5.3403	5.6127	1.419	7.963	.1598	.11261451
1026	.4086	5.0842	5.4928	2.217	12.177	.2304	.10392422
1028	.6810	5.3840	6.0650	5.986	36.302	.1970	.03291012
4001	.6810	.8382	1.5192	1.374	2.088	.0406	.02954876
4003	.6810	5.5634	6.2444	4.434	27.686	.3113	.07020749
4004	.5448	5.6747	6.2195	3.414	21.233	.2600	.07615700
TP-1 (H/D =5.00)							
1106	.5806	.8698	1.4504	4.775	6.926	.1265	.02649215
1107	.7258	.8833	1.6091	5.670	9.124	.1512	.02666667
1111	.5806	3.2408	3.8214	9.177	35.068	.3377	.03679852
1112	.7258	3.3061	4.0319	11.415	46.023	.6516	.05708279
4101	.1452	.9204	1.0656	1.343	1.431	.0856	.06373790
4102	.2903	.9074	1.1977	2.462	2.949	.0994	.04037368
4103	.4355	.9068	1.3423	4.178	5.608	.1691	.04047391
4104	.1452	3.3283	3.4735	2.238	7.774	.1243	.05554066
4105	.2903	3.2700	3.5603	4.476	15.938	.3283	.07334674
4106	.4355	3.3349	3.7704	7.088	26.723	.2617	.03692156
TP-2 (H/D =9.32)							
1201	.1457	.9386	1.0843	.895	.971	.0846	.09452514
1202	.2914	.9209	1.2123	1.716	2.080	.1272	.07412587
1203	.4371	.9166	1.3537	2.462	3.333	.1097	.04455727
1205	.7285	.9080	1.6365	4.775	7.814	.1227	.02569634
1206	.1457	3.3422	3.4879	2.164	7.546	.2274	.10508317
1207	.2914	3.3316	3.6230	4.103	14.866	.2070	.05045089
1208	.4371	3.3185	3.7556	5.969	22.416	.3548	.05944044
1209	.5828	3.3376	3.9204	7.759	30.419	.3570	.04601108
1210	.7285	3.3262	4.0547	9.550	38.721	.3583	.03751832
1214	.5828	5.8357	6.4185	11.937	76.619	.7874	.06596297
1215	.7285	5.8401	6.5686	14.548	95.563	.6812	.04682431

MODULUS INTERFACIAL AREA RESULTS   TABLE E.6

RUN NO.	VLO M/ SEC	VGO M/ SEC	VSUM M/ SEC	DELPX KN/ M3	EDPJ KN/M2/ SEC	A M2/ M3	A/DELPX M2/ KN
EMPTY TUBE							
2009	.1362	.6770	.8132	.2220	.180	104.3	469.8
2012	.5448	.6554	1.2002	1.0200	1.224	105.2	103.1
2013	.6810	.6620	1.3430	1.4190	1.905	158.2	111.5
2014	.1362	3.0869	3.2231	.3990	1.286	223.0	558.9
2015	.2724	2.9366	3.2090	.9750	3.130	280.2	287.4
2016	.4086	2.9570	3.3656	1.9950	6.715	286.1	143.4
2017	.5448	2.9462	3.4910	2.7490	9.596	232.7	84.6
2018	.6810	2.9428	3.6238	3.5470	12.853	200.4	56.5
2019	.1362	5.3223	5.4585	.6650	3.630	357.2	537.1
2020	.2724	5.3005	5.5729	1.5520	8.648	340.1	219.1
2021	.4086	5.1378	5.5464	2.5720	14.263	435.2	169.2
2022	.5448	5.3129	5.8577	4.0790	23.894	356.5	87.4
2023	.6810	5.1628	5.8438	5.5870	32.646	443.5	79.4
2024	.1362	8.0599	8.1961	1.1530	9.448	426.8	370.2
2025	.2724	7.7522	8.0246	2.3060	18.501	456.0	197.7
2027	.5448	7.4921	8.0369	4.9660	39.909	575.7	115.9
2028	.6810	7.4577	8.1387	7.2710	59.179	602.9	82.9
2030	.6810	2.8394	3.5204	3.5470	12.487	410.7	115.8
5001	.1362	.8878	1.0240	.2220	.227	89.2	401.8
5002	.4086	.9612	1.3698	.8870	1.215	135.5	152.8
5005	.1362	5.6547	5.7909	.9310	5.392	272.8	293.0
5008	.2724	.7933	1.0657	.4430	.472	132.2	298.4
5009	.5448	.6924	1.2372	1.4190	1.755	308.6	217.5
5011	.6810	2.8026	3.4836	3.9900	13.901	691.1	173.2
5012	.4086	7.8811	8.2897	4.1680	34.549	367.7	88.2
TP-1 (H/D =5.00)							
2107	.1452	.8213	.9665	1.4920	1.442	209.5	140.4
2108	.2903	.7747	1.0650	3.5070	3.734	424.5	121.0
2109	.4355	.7281	1.1636	4.0290	4.688	501.4	124.4
2110	.5806	.7725	1.3531	5.5960	7.572	299.3	53.5
2111	.7258	.7823	1.5081	6.8640	10.351	324.6	47.3
2112	.1452	3.1872	3.3324	3.2830	10.939	855.1	260.5
2113	.2903	3.1849	3.4752	6.2670	21.779	621.7	99.2

CONTINUED   TABLE E.6

RUN NO.	VLO M/ SEC	VGO M/ SEC	VSUM M/ SEC	DELPX KN/ M3	EDPJ KN/M2/ SEC	A M2/ M3	A/DELPX M2/ KN
2114	.4355	3.1242	3.5597	8.8780	31.603	737.9	83.1
2115	.5806	3.0581	3.6387	11.1160	40.450	481.6	43.3
2116	.7258	3.0572	3.7830	13.5780	51.367	484.3	35.7
2120	.5806	5.5374	6.1180	16.7870	102.701	692.3	41.2
2121	.7258	5.5160	6.2418	20.1440	125.733	670.2	33.3
2125	.5806	7.9955	8.5761	20.8900	179.154	705.5	33.8
2126	.7258	8.0072	8.7330	27.3060	238.463	816.4	29.9
5103	.7258	6.2341	6.9599	24.6950	171.873	572.6	23.2
5104	.1452	9.9155	10.0607	6.7890	68.304	648.7	95.6
5105	.2903	8.9498	9.2401	12.6830	117.193	872.7	68.8
5106	.1452	3.3660	3.5112	3.8050	13.360	297.8	78.3
5108	.1452	5.7172	5.8624	4.7750	27.992	392.9	82.3
5109	.2903	5.8462	6.1365	9.3260	57.228	870.8	93.4
5110	.4355	8.2105	8.6460	18.5030	159.972	1012.9	54.7
5112	.7258	3.3594	4.0852	15.7420	64.309	704.2	44.7

TP-2   (H/D =9.32)

2203	.4371	.7499	1.1870	2.6860	3.188	202.0	75.2
2206	.1457	3.1629	3.3086	2.5370	8.393	566.3	223.2
2207	.2914	3.1956	3.4870	4.4760	15.609	551.9	123.3
2210	.7285	3.0247	3.7532	12.5340	47.042	645.6	51.5
2211	.1457	5.6431	5.7888	3.5810	20.731	823.6	230.0
2212	.2914	5.6262	5.9176	7.0880	41.942	817.0	115.3
2213	.4371	5.4717	5.9088	11.0420	65.244	542.6	49.1
2214	.5828	5.5841	6.1669	14.3250	88.338	797.7	55.7
2215	.7285	5.5524	6.2809	17.9800	112.933	697.4	38.8
2219	.5828	7.7508	8.3336	19.3230	161.031	739.2	38.3
2220	.7285	8.0916	8.8201	24.4710	215.838	692.3	28.3
2223	.4371	7.6215	8.0586	14.9210	120.245	1042.3	69.9
5203	.1457	5.6561	5.8018	4.2530	24.673	538.4	126.6
5204	.1457	.7396	.8853	1.0440	.925	268.8	257.5
5205	.4371	5.7784	6.2155	12.3100	76.513	1113.0	90.4
5206	.1457	8.5813	8.7270	5.6700	49.483	468.8	82.7
5207	.2914	8.5956	8.8870	10.8930	96.802	816.4	74.9
5208	.1457	5.7102	5.8559	3.8050	22.281	315.1	82.8
5209	.4371	5.5958	6.0329	12.3100	74.266	881.4	71.6

APPENDIX F.

PHYSICAL ABSORPTION   TP-1   (H/D= 5.00)

```
C  C  NP SHUKLA  PHYSICAL MASS TRANSFER COEFFICIENT  TP 1    25.8.1976
C     PRESSURE,TEMPERATURE,VOLUME AND VELOCITY CHANGES DUE TO THE
C     ABSORPTION HAVE BEEN DULY CORRCTED
C     D CM TEST SECTION INTERNAL DIAMETER
C     AL1, AL2, AL3, SAMPLING TAPS DISTANCES FROM THE INLET POINT
C     BL CM DISTANCE BETWEEN DELP PRESSURE DROP (MM OF MERCURY)
C     CL1, CL2, CL3, DISTANCE IN CM OF SAMPLING TAPS FROM
C     THE MID SECTION POINT WHERE TEST SECTION PRESS IS MEASURED
C     BR, WI CM BREADH AND THICKNESS OF THE TAPE
C     QL, QG LIT/HR OF LIQUID AND GAS FLOW RATES
C     PT, PSIA TEST SECTION PRESSURE
C     X, NORMALITY OF THE ACID USED FOR TITRATION
C     T DEGREES CENTIGRADE AVERAGE LIQUID TEMPERATURE
C     BO,S1,S2, BLANK, TAP 1 AND TAP 2 VOLUMES IN ML  OF ACID TO NEUTRALIZE
C     F, FRACTION OF CARBON DIOXIDE IN THE GAS PHASE
C     AKLOA 1,2, AND 3 ARE MASS TRANSFER COEFFICIENTS
C     FABS  FRACTION OF CARBON DIOXIDE ABSORBED
C     FUG VELOCITY CORRECTION DUE TO ABSORPTION
C     EDPJ  JEPSEN ENERGY DISSIPATION PARAMETER

      DIMENSION BD(5),FUG(5) ,FABS(5)
      DIMENSION V(5),C(5),AKLOA(20),P(5),CSTRK(5),CD(5),BSTRK(5)

      READ   300,D,AL1,AL2,AL3,BL,CL1,CL2,CL3,BR,WI
  300 FORMAT  (F5.3,2X,7(F5.1,2X),F5.3,2X,F5.3)
      DO 40 J=1,31
      READ 400,IRUN,QL,QG,PT,X,T,BO,S1,S2,F,DELP
  400 FORMAT   (I4,F6.1,F7.1,F7.2,F8.5,F7.2,3(F7.2),F6.4,F5.)
      PIB4=3.1428/4.
      WN=1.01325*10.**5.
      AR=PIB4*D*D-BR*WI
      TS=273.15+T

C     CALCULATION OF CO2 SOLUBILITY AND PRESSURES AT VARIOUS POINTS

   55 EX=1140./TS-5.3
      H=10.**EX
      PAT=PT/14.696
      YO=F/(1.-F)
      GM=QG*(1.-F)/22.4
      P(1)=PAT+(DELP*CL1)/(BL*760.0)
      P(2)=PAT+(DELP*CL2)/(BL*760.0)
      P(3)=PAT-(DELP*CL3)/(BL*760.0)
      PTS=((P(2)+P(3))/2.)*(WN/1000.)
```

CONTINUED

```
C       CONCENTRATIONS OF CO2 ABSORBED

        C(1)=0.0
        C(2)=X*(BO-S1)/4.0
        C(3)=X*(BO-S2)/4.0

C       TEST SECTION VOLUMES BETWEEN DIFFERENT SAMPLING POINTS

 1515   V(1)=(PIB4*D*D-0.0852)*AL1/1000.
        V(2)=(PIB4*D*D-0.0852)*AL2/1000.
        V(3)=(PIB4*D*D-0.0852)*AL3/1000.

C       VELOCITIES (M/SEC) AND PRESSURE DROP

        UG=QG*TS/(3.6*273.15*P(1)*AR)
        UL=QL/(3.6*AR)
        PL=DELP/BL
        UL=UL/100.
        UG=UG/100.

C       VOLUMETRIC MASS TRANSFER COEFFICIENTS KLOA
C       BETWEEN 0-1, 1-2 , AND 0-2 SAMPLING POINTS

        DO30 I=1,3
        FABS(I)=QL*C(I)/YO/GM
        FUG(I)=(1.+YO*(1.-FABS(I)))/(1.+YO)
        CSTRK(I)=((P(I)*(YO-QL*C(I)/GM))*H)/(1.0+YO-QL*C(I)/GM)
 2020   BSTRK(I)=(0.99)*CSTRK(I)
        CD(I)=CSTRK(I)-C(I)
        BD(I)=BSTRK(I)-C(I)
        AKLOA(I)=0.0
   30   CONTINUE
        UGAV=UG*0.5*(FUG(2)+FUG(3))*P(1)/(P(2)+P(3))*2.

C       PRESSURE DROP (KN/M3) AND EDPJ (KN/M2/SEC)

        PL=PL*WN/7.6 /1000.
        EDPJ=(UL+UGAV)*PL
        IF(BD(1))3,3,2
    2   IF(BD(2))3,3,1
    1   Z1=QL/(V(1)*3600.)
        AKLOA(1)=Z1 *      ((C(2)-C(1))/(CD(1)-CD(2)))*LOG(CD(1)/CD(2))
    3   IF(BD(2))6,6,5
    5   IF(BD(3))6,6,4
    4   Z2=QL/(V(2)*3600.)
        AKLOA(2)=Z2  *      ((C(3)-C(2))/(CD(2)-CD(3)))*LOG(CD(2)/CD(3))
    6   IF(BD(3))9,9,8
    8   IF (BD(1))9,9,7
    7   Z3=QL/(V(3)*3600.)
        AKLOA(3)=Z3  *      ((C(3)-C(1))/(CD(1)-CD(3)))*LOG(CD(1)/CD(3))
    9   PUNCH 100,IRUN,TS ,PTS,UL,UGAV,PL,EDPJ,
       1(AKLOA(I),I=1,3),(FABS(I),I=2,3)
  100   FORMAT (I4,2F6.1,2F8.4,2F8.3,3F7.4,2F5.3)
   40   CONTINUE
        STOP
        END
        PROGRAM ACCEPTEDZ     36930   45260     58939   59999
```

```
C  C  N P SHUKLA CHEMICAL MASS TRANSFER TP1          27.8.1976
C     PRESSURE,TEMPERATURE,VOLUME AND VELOCITY CHANGES DUE TO THE
C,    ABSORPTION HAVE BEEN DULY CORRECTED
C     UKR(I) IS REACTION RATE VELOCITY CONSTANT
C     UKLO(I) IS KL FOR CHEMICAL MASS TRANSFER RUNS
C     SURF(I) IS INTERFACIAL AREA SQUARE M/CUBIC M
C     EDPJ IS JEPSON ENERGY DISSIPATION PARAMETER  KN/M2/SEC
C     EDPB BANERGEE ENERGY DISSIPATION PARAMETER   N/SEC
      DIMENSION P(3),V(3),C(8),H(2),G(3),E(5),A(3),SUM(5),HS(5),B(3)
      DIMENSION FABS(5), FUG(5)
      DIMENSION UKLOA(5), DIFUS(5), UKR(5), UKLO(5), SURF(5), Z(5)

      READ   300,D,AL1,AL2,AL3,BL,CL1,CL2,CL3,BR,WI
  300 FORMAT   (F5.3,2X,7(F5.1,2X),F5.3,2X,F5.3)
      DO 40 J=1,40
      READ 400,IRUN,QL,QG,PT,X,T,BO,B1,S1,S2,F,DELP
  400 FORMAT   (I4,F6.1,F7.1,F7.2,F8.5,F7.2,4(F7.2),F6.4,F5.)
      PIB4=3.1428/4.
      WN=1.01325*10.**5.
      AR=PIB4*D*D-BR*WI
      T=T+273.15

C     CALCULATING PRESSURE TERMS AT VARIOUS POINTS

   55 PAT=PT/14.696
      FF=DELP/BL/760.
      P(1)=PAT+FF*(CL1-AL1/2.)
      P(2)=PAT+FF*(CL2-AL2/2.)
      P(3)=PAT+FF*(CL1-AL3/2.)
      PO=PAT+(DELP*CL1)/(BL*760.)
      PTS=PAT+DELP*(CL2-CL3)/(BL*2.*760.)

C     VOLUMES OF TEST SECTION BETWEEN VARIOUS SAMPLING TAPS

      V(1)=(PIB4*D*D-0.0864)*(AL1/1000.)
      V(2)=(PIB4*D*D-0.0864)*(AL2/1000.)
      V(3)=(PIB4*D*D-0.0864)*(AL3/1000.)
C     CALCULATING NORMALITIES OF NAOH AND NA2CO3
      C(1)=X*BO
      C(2)=X*B1
      C(3)=X*S1
 1515 C(4)=X*S2
      C(5)=C(1)-C(2)
      C(6)=C(1)-C(3)
      C(7)=C(1)-C(4)
      YO=F/(1.-F)
      GL=QL/2.
      GM=QG*(1.-F)/22.4
```

```
      FG=GM*YO-GL*C(2)
 2424 FR=GM/GL
      QG=QG*T/(PO*273.15)
      PL=DELP*WN/(7.6*BL*1000.)
      E(1)=(FG+GL*C(2))/(FG+GL*C(3))
      E(2)=(FG+GL*C(3))/(FG+GL*C(4))
      E(3)=(FG+GL*C(2))/(FG+GL*C(4))
      UG=QG/(3.6*AR)/100.
      UL=QL/(3.6*AR)/100.

C     CO2 SULUBILITY IN MIXED ELECTROLYTE SOLUTION

C     LOG10(HS/HW)=SUM(H*G)
 2020 EX=(1140./T-5.3)
      HW=10.**EX
      HG=(-1.3417+(8.44/1000.)*T-(1.3/100000.)*T*T)
      H(1)=0.157-HG
      H(2)=0.112-HG

C     CONCENTRATIONS OF NAOH AND NA2CO3

      G(1)=(C(2)+C(3))/2.
 2525 G(2)=(C(3)+C(4))/2.
      G(3)=(C(2)+C(4))/2.
      A(1)=(C(5)+C(6))/2.
      A(2)=(C(6)+C(7))/2.
      A(3)=(C(5)+C(7))/2.
 3030 B(1)=C(2)-C(3)
      B(2)=C(3)-C(4)
      B(3)=C(2)-C(4)

C     PHYSICO CHEMICAL DATA CALCULATION

      Z1=(4.736*T)/(10.**7.)
      Z2=(1.2189)/(10.**4.)
      DO 30 I=1,3
      FABS(I)=QL*B(I)/YO/GM/2.
      IF (FABS(I)-1.)12,12,13
   12 FUG(I)=(1.+YO*(1.-FABS(I)))/(1.+YO)
      GO TO 14
   13 FABS(I)=1.
      FUG(I)=(1.+YO*(1.-FABS(I)))/(1.+YO)
   14 Z(I)=(2.693*G(I))/(10.**6.)
      DIFUS(I)=Z1-Z2-Z(I)
      UKR(I)=EXP(2.303*(13.635-2895./T+0.132*G(I)))
```

```
      UKLO(I)= SQRTF(DIFUS(I)*UKR(I)*G(I))
      SUM(I)=H(1)*G(I) +H(2)*A(I)*6.
3535  HS(I)=(10.**SUM(I))/HW
      IF(E(I))2,2,3
   2  UKLOA(I)=0.
      GO TO 4040
   3  UKLOA(I)=GL*HS(I)*(B(I)+FR*LOGF(E(I)))/(V(I)*P(I))/3600.

C     CALCULATION OF INTERFACIAL AREAS
4040  SURF(I)= UKLOA(I)/UKLO(I)*100.
  30  CONTINUE
      UGAV=UG*(FUG(2)+FUG(3))*PO/PTS /2.
      PTS=PTS*WN/1000.
      EDPJ=(UL+UGAV)*PL
      EDPB=PL*QL/3600.
      PUNCH 100,IRUN,T,PTS,UL,UGAV,PL,EDPJ,EDPB,(SURF(I),I=1,3),
     1 (FABS(I),I=2,3)
 100  FORMAT (I4,2F6.1,F6.4,F7.4,F7.3,F8.3,F8.5,3F6.1,2F5.3)
  40  CONTINUE
      STOP
      END
      PROGRAM ACCEPTED    36930  48690    58539  59999
```

SLUG REYNOLDS NUMBER   RELS   **PROGRAM F.3**

```
C   C  N P SHUKLA  CALCULATION OF RELS , PRESSURE CORRELATION  4.9.1976

C      RELS CALCULATED USING VELOCITY= VSL+VSG  AND LIQUID PROPERTIES
C      TIMER - TIME RATIO FOR FLOW OF SAME VOLUME OF WATER AND SOLUTION
C      USED IN CALCULATION OF THE SOLUTION VISCOSITY

       READ 100, N
   100 FORMAT (2I5)
       PIB4=3.1428/4.
       DO 60 JSK=1,N
     1 READ 5, DPIPE,THICK,WIDTH,DBYH,CONTR
     5 FORMAT (5F10.4)
       READ 100,M
       DO 50 ISK=1,M
    15 READ 10,IRUN,VLO,VGO,T,DELPX,TIMER,ROWL ,PT
    10 FORMAT (I4,7F10.4)
       ROWL=ROWL*1.0E+06

C      CALCULATING VISCOSITIES OF WATER AND SOLUTION

       T=T-273.15
       TS1=T-8.435
       TS1SQ=TS1*TS1
       TSNU=SQRTF(8078.4+TS1SQ)
       FUNT=0.021482*(TS1+TSNU)-1.20
       VISW=1./FUNT
       VISSL=VISW*TIMER
       VIS=VISSL
       IF(CONTR-1.)20,20,30
    20 DH=DPIPE
       AREA=PIB4*(DPIPE**2)
       AREA=(0.0001)*AREA
       DH=DH*(0.01)
       GO TO 40

C      CALCULATING HYDRAULIC DIAMETER OF THE TEST SECTION

    30 AREA=PIB4*(DPIPE**2)-WIDTH*THICK
       DH=(4.0*AREA)/(3.1428*DPIPE+2.*WIDTH)
       AREA=(0.0001)*AREA
       DH=DH*(0.01)
    40 RELS=(DH*(VLO+VGO)*ROWL)/VIS
       T=T+273.15
       ROWL=ROWL/1.0E+06
       PUNCH 16,IRUN,T,PT,VLO,VGO,ROWL,VIS,DELPX,RELS
    16 FORMAT (I4,2F7.1,F6.4,F8.4,F7.3,F8.4,F8.3,F9.1)
    50 CONTINUE
    60 CONTINUE
       STOP
       END
```

FRICTION FACTOR AND PRESSURE DROP USINF RETP

PROGRAM F.4

```
**    N P SHUKLA FRICTION FACTOR CORRELATION ANALYSIS    10.9.1976
C     SMITHBERG LANDIS AND MODIFIED PRESUURE DROP FRICTION FACTORS
C     USING RETP FROM HUGHMARK,S  K FACTOR

      DIMENSION IRUN(70),VLO(70),VGO(70),PTS(70),RELS(70),AK(70)
      DIMENSION VL(70),RETP(70),F(70),DELPX(70),DELPC(70),PDEV(70)
      DIMENSION X(70),Y(70),DEPXN(70),ALPHAL(70),T(70),ROWL(70),VISL(70)
      DIMENSION UPRED(70),FEXP(70),FSL(70),ALFAL(70)
      READ5,M
    5 FORMAT (2I5)
      DO1400J=1,M
      READ 5,N
    1 READ 10,DPIPE,THICK,WIDTH,DBYH,CONTR,DH
   10 FORMAT (5F10.4,F10.6)
      PUNCH 5,N
      DO 500 I=1,N
      READ 20,IRUN(I),T(I),PTS(I),VLO(I),VGO(I),ROWL(I),VISL(I),
     1DELPX(I),RELS(I),AK(I)
   20 FORMAT (I4,2F7.1,F6.4,F8.4,F7.3,F8.4,F8.3,F9.1,F7.3)
      WM=1.01325*10.**2.
      PTS(I)=PTS(I)/WM
      DELPX(I)=DELPX(I)/WM
      ROWL(I)=(10.**6.)*ROWL(I)
      RG1=(1.+AK(I))*(VLO(I)+VGO(I))
      RG=VGO(I)/RG1
      ALFAL(I)=1.-RG
      VL(I)=VLO(I)/(1.-RG)
      RETP(I)=DH*VL(I)*ROWL(I)/VISL(I)
   15 IF(CONTR-1.)30,30,40
   40 AN=0.32*(1.+0.65*(DBYH**0.5))
      ODBYH=1./DBYH
      FP=2.51/((ODBYH-0.5)**1.07)
      FP1=(0.125+FP)/(RETP(I)**AN)
      F(I)=0.0014+FP1
      BN=0.2*(1.+1.7*(DBYH**0.5))
      FSL(I)=( 0.046+2.1/(ODBYH-0.5)**1.2) /RETP(I)**BN
      GOTO50
   30 F(I)=0.0014+0.125/RETP(I)**0.32
      FSL(I)=0.046/(RETP(I)**0.2)
   50 DELPC(I)=2.*F(I)*VL(I)*VL(I)*ROWL(I)/9.806/DH/1.033/10.**7.
      UPRED(I)=(1.0-DELPC(I)/DELPX(I))*100.0
      FEXP(I)=DELPX(I)*9.806*1.033E7*DH/2./VL(I)/VL(I)/ROWL(I)
  500 CONTINUE
      XT=0.0
      XZT=0.0
      YT=0.0
      XYT=0.0
```

```
      DO600 I=1,N
      X(I)=LOGF(F(I))
      Y(I)=LOGF(FEXP(I))
      XT=XT+X(I)
      YT=YT+Y(I)
      XZT=XZT+X(I)**2
      XYT=XYT+X(I)*Y(I)
600   CONTINUE
      PN=N
      XAVG=XT/PN
      YAVG=YT/PN
      BN=XYT-YAVG*XT
      BD=XZT-XAVG*XT
      B=BN/BD
      A=YAVG-XAVG*B
      A=EXPF(A)
      PUNCH 105, A,B
105   FORMAT (/5X,2HA=,E15.5,2X,2HB=,E15.5//)
      SUM=0.0
      DO 200 I=1,N
      DEPXN(I)=2.*A*F(I)**B*VL(I)**2.*ROWL(I)/9.806/DH/1.033E7
      PDEV(I)=((DELPX(I)-DEPXN(I))*100.)/DEPXN(I)
      SUM=SUM+DEPXN(I)
200   CONTINUE
      SUM=SUM/PN
      SUM1=0.0
      DO240I=1,N
240   SUM1=SUM1+(DEPXN(I)-SUM)**2
      STDEV=SQRTF(SUM1/PN)
      PUNCH 250,STDEV
250   FORMAT (2X,19HSTANDARD DEVIATION=,E15.5/)
      DO 300 I=1,N
      PTS(I)=WM*PTS(I)
      DELPX(I)=WM*DELPX(I)
      DELPC(I)=WM*DELPC(I)
      DEPXN(I)=WM*DEPXN(I)
      PUNCH 400,IRUN(I),VLO(I),VGO(I),VL(I),PTS(I),AK(I),RETP(I),
     1ALFAL(I)
      PUNCH 401,IRUN(I),DEPXN(I),DELPX(I),DELPC(I),UPRED(I),PDEV(I),
     1FEXP(I),F(I),FSL(I)
400   FORMAT (I4,3F8.4,F7.1,F6.3,F9.1,F7.4)
401   FORMAT (I4,3F8.3,2F8.2,3F8.5)
300   CONTINUE
1400  CONTINUE
      STOP
      END
```

CALCULATION OF PARAMETER X LOCKHART-MARTINELLI

```
C   C   N P SHUKLA CALCULATION OF X LOCKHART-MARTINELI 9.9.1976
        DIMENSION GMUE(10),WM(10),Y(10)
        READ 100, N
    100 FORMAT (2I5)
        PIB4=3.1428/4.
        DO 60 JSK=1,N
      1 READ 5, DPIPE,THICK,WIDTH,DBYH,CONTR
      5  FORMAT (5F10.4)
        READ 100,M
        DO 50 ISK=1,M
        READ   10,IRUN,T,PT,VLO,VGO,ROWL,VIS,DELPX,RELS
     10 FORMAT (I4,2F7.1,F6.4,F8.4,F7.3,F8.4,F8.3,F9.1)
        ROWL=ROWL*1.0E+06
        PTS=PT/(1.01325*10.**2.)
        IF(CONTR-1.)20,20,30
     20 DH=DPIPE
        AREA=PIB4*(DPIPE**2)
        AREA=(0.0001)*AREA
        DH=DH*(0.01)
        GO TO 40

C       CALCULATING HYDRAULIC DIAMETER OF THE TEST SECTION

     30 AREA=PIB4*(DPIPE**2)-WIDTH*THICK
        DH=(4.0*AREA)/(3.1428*DPIPE+2.*WIDTH)
        AREA=(0.0001)*AREA
        DH=DH*(0.01)

C       CALCULATING LIQUID REYNOLDS NUMBER

     40 TTS=T
        IF(DBYH-0.0)41,41,42
     41 FP=0.125
        GO TO 43
     42 FP=0.125+2.51/(1.0/DBYH-0.5)**1.07
     43 AN=0.32*(1.0+0.65*DBYH**0.5)
        REL=DH*VLO*ROWL/VIS
        FL=0.0014+FP/REL**AN
```

```
C      CALCULATING GAS VISCOSITY, DENSITY AND REYNOLDS NUMBER

       VISG=0.0
       GMUE(1)=0.0137*(TTS/273.15)**0.935
       GMUE(2)=0.01709*(TTS/273.15)**0.768
       Y(1)=0.4385
       Y(2)=0.5615
       WM(1)=44.0
       WM(2)=14.4
    45 DO 44 I=1,2
       J=3-I
       R1=GMUE(I)/GMUE(J)
       R2=WM(I)/WM(J)
       PHAI=1.0+R1**0.5/R2**0.25
       PHAI=PHAI**2/2.328/(1.0+R2)**0.5
       DENOM=1.0+Y(J)/Y(I)*PHAI
    44 VISG=VISG+GMUE(I)/DENOM
       ROWG=Y(1)*0.1235+Y(2)*0.0732
       ROWG=ROWG*PTS*273.15/TTS
       ROWG=ROWG*453.0/(0.3048)**3
    46 REG=DH*VGO*ROWG/VISG
       FG=0.0014+FP/REG**AN
       XX=FL/FG*ROWL/ROWG*(VLO/VGO)**2
       X=XX**0.5
       ROWL=ROWL/1.0E+06
       ROWG=ROWG/1.0E+06
       PUNCH 16,IRUN,ROWG,ROWL,VISG,VIS,FG,FL,REG,REL,X,DELPX
    16 FORMAT (I4,F7.5,F6.3,F6.4,F6.3,2F7.4,2F8.1,2F9.3)
    50 CONTINUE
       PUNCH 17,DH
    17 FORMAT (19HHYDRAULIC DIAMETER=,F10.6)
    60 CONTINUE
       STOP
       END
```

```
**    N P SHUKLA DELTp FROM LOCKHART-MARTINELLI      10.9.1976
      DIMENSION B(10),C(10)
   10 READ 20, (B(I),I=1,6), (C(I),I=1,6)
   20 FORMAT (6E12.5)
      DO 100 M=1,3
      READ 30, NRUN,DH
   30 FORMAT (I5,F10.6)
      DO 100 I=1,NRUN
   50 READ 40  ,IRUN,ROWG,ROWL,VISG,VIS,FG,FL,REG,REL,X,DELPX
   40 FORMAT (I4,F7.5,F6.3,F6.4,F6.3,2F7.4,2F8.1,2F9.3)
      WM=1.01325*10.**2.
      DELPX=DELPX/WM
      ROWL=(1.0E+06)*ROWL
      ROWG=(1.0E+06)*ROWG
      IF(REG-1000.)80,80,70
   70 PHAIG=B(1)
      DO 75 J=2,6
      N=J-1
   75 PHAIG=PHAIG+((LOGF(X))**N)*B(J)
      GO TO 90
   80 PHAIG=C(1)
      DO 85 J=2,6
      N=J-1
   85 PHAIG=PHAIG+((LOGF(X))**N)*C(J)
   90 VGO=REG*VISG/ROWG/DH
      PHAIG=EXPF(PHAIG)
      DELPG=FG*ROWG*VGO*VGO/DH/4.904/1.033E+07
      DELTP=(PHAIG**2)*DELPG
      PDEV=DELPX*100./DELTP-100.
      DELPX=WM*DELPX
      DELTP=WM*DELTP
  100 PUNCH 200,IRUN,VGO,DELPX,DELTP,REL,REG,PDEV,PHAIG ,X
  200 FORMAT (I4,F9.4,2F9.3,2F9.1,F8.3,2F9.3)
      STOP
      END

C     VALUES OF CONSTANTS B AND C FOR POLINOMIAL TO CALCULATE PHAI PARAMETE
14.45057E-0149.57215E-0257.61751E-03-1.16993E-03-4.28827E-0431.50219E-06
12.38666E-0153.13789E-0271.74654E-03-4.38638E-03-6.91229E-0411.99685E-06
```

```
C    C   N P SHUKLA CALCULATION OF KLO TP-1   28.9.1976

C        SCHIMDT, PECLET, EULER AND SHERWOOD DIMENSIONLESS GROUPS

     1 N=10
       DP=0.008135
       PI=3.1428
       ROW=10.**6.
       DO 90 I=1,N
       READ 200,RETP
   200 FORMAT (41X,F9.1)
       READ 100,IRUN,T,VLO,DELPX,AKLOA
   100 FORMAT (I4,F6.1,6X,F8.4,8X,F8.3,15X,F7.4)
       READ 400,QL
   400 FORMAT (4X,F6.1)
    10 DELPX=DELPX*10.**6.
C        EXPERIMENTAL KLO CALCULATION
       SURF=33.7*((RETP)**0.323)
       AKLO=AKLOA/SURF
C        DIFFUSIVITY AND VISCOSITY CALCULATION
       Z1=4.736*T/(10.**7.)
       Z2=1.2189/(10.**4.)
    15 DIFUS=Z1-Z2
       DIFUS=DIFUS/10.**4.
       TS=(T-273.15)-8.435
       TSSQ=TS*TS
       TSNU=SQRTF(8078.4+TSSQ)
    20 FUNT=0.021482*(TS+TSNU)-1.20
       VIS=1./FUNT
C        BANERJEE KLOB
       A=SQRTF(DIFUS)
       B=SQRTF(DELPX*DP/(4.*ROW))
       QL=QL/0.36/(10.**7.)
       C=(2.25*PI*DP*VLO)/(2.*QL)
    25 AKLOB=A*SQRTF(B*C)
C        KASTURI STEPANEK KLOK AND DIMENSIONLESS GROUPS
       SC=VIS/(ROW*DIFUS)
       PE=VLO*DP/DIFUS
       EU=DELPX*DP/(ROW*VLO*VLO)
       SH=0.25*PE*EU/SQRTF(SC)
    30 AKLOK=SH*DIFUS/DP
       SHEXP=AKLO*DP/DIFUS
       SHCAL=4.*SH
       PUNCH 300, IRUN,AKLO,AKLOB,AKLOK,SHEXP,SHCAL,SC,PE,EU
   300 FORMAT (I4,3E12.4,3F7.1,E11.4,F8.4)
    90 CONTINUE
       STOP
       END
       PROGRAM ACCEPTED   36930   39240      59129   59999
```

```
C       STRAIGHT LINE REGRESSION AND PERCENT DEVIATION
C       PREDICTED VALUE AND MAXIMUM, MINIMUM FOR 95 PERCENT VARIANCE
        DIMENSION X(200),Y(200),YPRED(200),AX(200),YY(200),IRUN(200)
        N=25
        XX=0.0
        YX=0.
        AVX=0.
        AVY=0.
        AN=N
        T=2.069
        YMEAN=0
   50   DO 90 I=1,N
        READ 130,IRUN(I),X(I)
  130   FORMAT (I4,37X,F9.1)
        READ 131,Y(I)
  131   FORMAT (58X,F6.1)
        AX(I)=X(I)
        YMEAN=YMEAN+Y(I)/AN
        YY(I)=Y(I)
        X(I)=LOGF(X(I))
        Y(I)=LOGF(Y(I))
        AVY=AVY+Y(I)/AN
        AVX=AVX+X(I)/AN
   90   CONTINUE
        DO 99 J=1,N
        X(J)=X(J)-AVX
        YX=YX+Y(J)*X(J)
   99   XX=XX+X(J)*X(J)
        B0=AVY
        B1=YX/XX
        B0=B0-B1*AVX
        B0=EXPF(B0)
        SUMSQ=0.0
        DO120I=1,N
        YPRED(I)=AVY+B1*X(I)
        DEV=Y(I)-YPRED(I)
  120   SUMSQ=SUMSQ+DEV**2
        VAR=SUMSQ/(AN-2.0)
        VAR=SQRTF(VAR)
  100   PUNCH 150,B0,B1,VAR
        STDER=0
        DO200I=1,N
        VARD=VAR*(1.0+1.0/AN+X(I)**2/XX)
        YMAX=YPRED(I)+VARD*T
        YMIN=YPRED(I)-VARD*T
        YP=EXPF(YPRED(I))
        YPMAX=EXPF(YMAX)
        YPMIN=EXPF(YMIN)
        ER=YY(I)-YP
        PDEV=ER/YP*100.
        STDER=STDER+PDEV**2/(AN-2.)
  200   PUNCH 140,IRUN(I),AX(I),YY(I),YP,PDEV,YPMAX,YPMIN
  140   FORMAT (I4,F9.1,5F6.1)
        STDER=SQRTF(STDER)
        PUNCH150,STDER
  150   FORMAT (5F25.20)
        STOP
        END
```

MODIFIED FRICTION FACTOR EQUATION   PROGRAM F.9

```
C   C   SOLUTION BY ITERATION AND FITTING OF STRAIGHT LINE   N P SHUKLA
        DIMENSION X(10),Y(10),RE(10)
        DIMENSION AX(10),AY(10),BX(10),BY(10)
        AVAX=0
        AVAY=0
        AVBX=0
        AVBY=0
        AXX=0
        BXX=0
        AYX=0
        BYX=0
        READ150,(RE(I),I=1,5)
10      DO100I=1,3
        READ150,DBYH
        XX=0
        YX=0
        AVX=0
        AVY=0
20      DO90J=1,5
40      F1=0.0014+0.125/RE(J)**.32
50      DO75K=1,20
        F2=0.464*SQRTF(F1)*DBYH**2
        F=LOGF(RE(J)*F1**0.5)
        F2=F2+0.0498/RE(J)*DBYH*(1125.0*F-3170.0)
        F2=F2+0.0014+0.125/RE(J)**0.32
        DIFF=ABSF(1.0-F1/F2)
60      IF(DIFF-0.002)80,80,70
70      F1=F2
75      CONTINUE
80      Y(J)=LOGF(F2-0.0014)
        X(J)=LOGF(RE(J))
        PUNCH200,DBYH,RE(J),F1,F2,K,Y(J),X(J)
        AVY=AVY+Y(J)/5.0
        AVX=AVX+X(J)/5.0
90      CONTINUE
        DO99J=1,5
        X(J)=X(J)-AVX
        YX=YX+Y(J)*X(J)
```

```
99      XX=XX+X(J)**2
        BO=AVY
        B1=YX/XX
        AN=-B1
        AI=EXPF(BO-B1*AVX)
        AAN=LOGF(AN/0.32-1.0)
        AHBYD=-LOGF(DBYH)
        BAI=LOGF(AI-0.125)
        BHBYD=LOGF(1.0/DBYH-0.5)
        BO=BO-B1*AVX
        AY(I)=AAN
        AX(I)=AHBYD
        AVAY=AVAY+AY(I)/3.0
        AVAX=AVAX+AX(I)/3.0
        BY(I)=BAI
        BX(I)=BHBYD
        AVBY=AVBY+BY(I)/3.0
        AVBX=AVBX+BX(I)/3.0
100     PUNCH300,BO,B1,AN,AI,AAN,AHBYD,BAI,BHBYD
101     DO102I=1,3
        AX(I)=AX(I)-AVAX
        BX(I)=BX(I)-AVBX
        AXX=AX(I)**2+AXX
        BXX=BX(I)**2+BXX
        AYX=AX(I)*AY(I)+AYX
102     BYX=BX(I)*BY(I)+BYX
        AB1=AYX/AXX
        BB1=BYX/BXX
        ABO=AVAY-AB1*AVAX
        BBO=AVBY-BB1*AVBX
103     PUNCH300,ABO,AB1,BBO,BB1
150     FORMAT(8F10.2)
200     FORMAT(2F10.1,2F10.5,I5,10X,2F12.5//)
300     FORMAT(//8F20.5//)
        STOP
        END
```

CALCULATION OF CARBONDIOXIDE CONCENTRATION IN THE LIQUID SAMPLE OBTAINED IN PHYSICAL ABSORPTION (126)

Since some sodium-carbonate may be present in the sample collector solution of sodium hydroxide, the reactions taking place are:

$$NaOH + HCl = NaCl + H_2O$$

$$Na_2CO_3 + HCl = NaHCO_3 + NaCl$$

Let V_S - volume of sodium hydroxide solution in the sample collector, ml

M_1 - concentration of sodium hydroxide in solution, mol/lit

M_2 - concentration of sodium carbonate in solution, mol/lit

V_C - volume of liquid sample drawn and added in the sample collector, ml

C - concentration of carbon dioxide in the sample, mol/lit

X - normality of hydrochloric acid used for titration

If Y ml of HCl solution is required for the first equivalence point of titration with, n, ml of NaOH blank, then

$$(M_1 + M_2) . n . 10^{-3} = X . Y . 10^{-3}$$
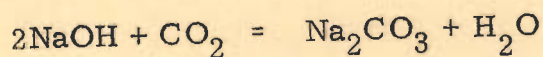
$$(M_1 + M_2) = \frac{X}{n} . Y \tag{G.1}$$

Moles of NaOH initially present in the sample collector,

$$= M_1 . V_S . 10^{-3}$$

Mole of Na_2CO_3 initially present in the sample collector,

$$= M_2 . V_S . 10^{-3}$$

CO_2 (in the liquid sample) reacts with NaOH as

$$2NaOH + CO_2 = Na_2CO_3 + H_2O$$

Total number of moles of Na_2CO_3 in the collector

$$= (M_2 V_S + C V_C). \, 10^{-3}$$

Moles of NaOH remaining in the collector

$$= (M_1 V_S - 2 C V_C). \, 10^{-3}$$

If q, ml HCl solution is required for the first equivalence point of the titration with m, ml alkali solution from the sample collector then

$$\frac{m}{V_S + V_C} \left[(M_2 V_S + C V_C) + (M_1 V_S - 2 C V_C) \right]. \, 10^{-3} = X. \, q. \, 10^{-3}$$

or $\frac{m}{V_S + V_C} \left[V_S (M_1 + M_2) - C V_C \right] = X . q$ \hfill (G.2)

From Equations G.1 and G.2

$$\frac{m}{V_S + V_C} \left[V_S \frac{X}{n} r - C V_C \right] = X \, q$$

$$V_S \frac{X}{n} Y - C V_C = X \left(\frac{V_S + V_C}{m} \right). \, q$$

$$C V_C = V_S \frac{X}{n} r - X (V_S + V_C). \frac{q}{m}$$

hence $C = \frac{X}{V_C} \left[\frac{V_S r}{n} - \left(\frac{V_S + V_C}{m} \right). \, q \right]$ \hfill (G.3)

In the case of present study

X   -   normality of HCl

V_C -   volume of sample drawn   =   4.0 ml

V_S -   NaOH solution in sample collector   =   4.0 ml

n   -   volume of NaOH blank   =   4.0 ml

m   -   total volume in the sample = 8.0 ml (since solutions are very dilute volume change on mixing can be neglected).

r   -   volume of HCl with 4.0 ml, NaOH blank, ml

q   -   volume of HCl with total sample (8.0 ml), ml

so Equation G.3 simplifies to

$$C = \frac{X}{4.0} \ (r - q) \hspace{3cm} (G.4)$$

Equation G.4 was used to calculate carbon-dioxide concentrations in different liquid samples obtained in physical absorption experiments.

REFERENCES

1. Scott D.S., in "Advances in Chemical Engineering" Vol. 4, Ed. Drew, T.B., Hoopes, J.W. and T. Vermeulen. Academic Press, New York p 200-273 (1963).

2. Alves G.E. "Concurrent Liquid-gas Flow in Pipeline Contactor" Chem. Engg. Progr. $\underline{50}$, 449 (1954).

3. Russel T.W. Hodgson and Govier G.W., Can. Jl Ch.E. $\underline{37}$, 9 (1959).

4. Govier G.W. and Aziz K. "The Flow of Complex Mixtures in Pipes" Van Nostrand Reinhold Co. New York (1972).

5. Baker O., Oil Gas Jl. $\underline{53}$, 185, (1954) cited in 1.

6. Hubbard M.G. Ph.D. Thesis, Univ. of Houston, (1965).

7. Reference 4, p.516.

8. Charles M.E., Govier, G.W. and Hodgson Can. Jl. of Chem. Engg. $\underline{39}$ 27 (1961).

9. Reference 3.

10. Govier G.W. and Omer M.M. "The Horizontal Pipeline Flow Air-Water Mixtures" The Can. Jl. Chem. Engg. $\underline{40}$ p. 93-104 (1962).

11. Bergelin O.P. and Gazeley C. "Cocurrent Gas-Liquid Flow-I. Flow in Horizontal Tubes" Heat Transfer and Fluid Mechanics Inst. Proc. p. 5 (May 1949).

12. Reference 2.

13. White P.D., Huntington R.L. "Horizontal Co-current Two-Phase Flow of Fluids in Pipe Lines" The Petroleum Engr. $\underline{27}$ (9) D 40 (Aug. 1955).

14. Baker O. "Simultaneous Flow of Oil and Gas" Oil Gas Jl. $\underline{53}$, 185 (July 1954).

15. Reference 1.

16. Hoogendoorn C.J. "Gas-Liquid Flow in Horizontal Pipes" Chem. Engg. Sci. $\underline{9}$, 205 (1959).

17. Hoogendoorn C.J. and Buitelaar A.A. i.b.i.d. 16 , 208 (1961).

18. Reference 4, p. 504-616.

19. Eaton B.A., Andrews D.E., Knowles C.R., Silberberg I.H. and Brown K.E., Petroleum Technol. 19 , 815 (1967).

20. Al-Shiekh J.N., Saunders D.E. and Brodkey R.S. "Prediction of Flow Patterns in Horizontal Two-Phase Pipe Flow" Can. Jl. Chem. Engg. 48 , 21 (1970).

21. Mandhane J.M., Gregory G.A. and Aziz K. "A Flow Pattern Map for Gas-Liquid Flow in Horizontal Pipes" Intern J. Multiphase Flow, 1 p. 537-553 (1974).

22. Taitel Y. and Duckler A.E. "A Model for Predicting Flow Regime Transition in Horizontal and Near Horizontal Gas-Liquid Flow" A.I.Ch.E. Jl. 22 (1) p. 47-55 (Jan. 1976).

23. Lockhart R.W. and Martinelli R.C. "Proposed Correlation of Data for Isothermal Two-Phase Two-Component Flow in Pipes" Chem. Engg. Progr. 45 (1) p. 39-48 (1949).

24. Hughmark G.A. Chem. Engg. Progr. 58 (4), 62 (1962).

25. Bankoff S.G. "A Variable-Density Single-Fluid Model for Two Phase Flow with Particular Reference to Steam-Water Flow" Jl. of Heat Transfer, Trans. A.S.M.E., C-82, 265 (1960).

26. Duckler A.E., Wicks M. and Clevel-and R.G. "Frictional Pressure Drop in Two-Phase Flow : B An Approach Through Similarity Analysis" A.I.Ch.E. Jl. 10 (1), 44, (Jan. 1964).

27. Hughmark G.A. "Holdup and Heat Transfer in Horizontal Slug Gas-Liquid Flow" Chem. Engg. Sci. 20 p. 1007-1010 (1965).

28. Oliver D.R. and Wright S.J., Brit. Chem. Engg. 9 , 590 (1964).

29. Chawla J.M. Chemic - Ing : Technik 41 , 328 (1969), Ref. 4.

30. Mamaev V. "Some Problems in the Hydrodynamics of Joint Transport of Gas and Liquid" Int. Chem. Engg. 5 (2), 318, (1965).

31. Guzhov A.L., Mamaev V.A. and Odishariya G.E. "A Study of Transportation in Gas-Liquid Systems" Tenth Int. Gas Conference, Hamburg (1967), cited in 4.

32. Greskovich E.J. Shrier A.L. and Bonnecaze R.H. Ind. & Engg. Chem. (Fundam) 8, 591, (1969).

33. Bertuzzi A.F., Tek M.R. and Poettmann F.H. "Simultaneous Flow of Liquid and Gas Through Horizontal Pipe" Jl. Pet. Tech., 207, 17 (Jan. 1956).

34. Gallyamov A.K. and Goldzberg V.L. Cite & Rd 4. p. 241.

35. Gregory G.A. and Scott D.S. "Physical and Chemical Mass Transfer in Horizontal Cocurrent Gas-Liquid Slug Flow" in Proc. Int. Symp. on Cocurrent Gas-Liquid Flow, Univ. of Water loo, Plenum Press, New York p. 633 (1969) and Chem. Engg. Jl. 2 (4) p. 287-296 (1971).

36. Bergles A.E. "Survey and Evaluation of techniques to Augment Convective Heat and Mass Transfer" in Progress in Heat and Mass Transfer Vol. I Ed. Grigull U. & Hahne E., Pergamon Press, New York p. 335 (1969).

37. i.b.i.d. p. 359.

38. See reference 36 p. 359.

39. Gambill W.R., Bundy R.D. and Wansbrough R.W. Heat Transfer, Burnout and Pressure Drop for Water in Swirl Flow through Tubes with Internal Twisted Tapes" Chem. Engg. Symp. Ser. 57 (32) p. 127-137 (1961).

40. Gambill W.R. and Bundy R.D. "An Evaluation of the Present Status of Swirl-Flow Heat Transfer" Paper No. 62-HT-42, Presented at A.S.M.E. - A.I.Ch.E. Heat-Transfer Conference and Exhibit., Houston, Texas, Aug. 5-8 (1962).

41. Reference 36 p. 360.

42. Colburn A.P. and King W.J. "Heat Transfer and Pressure Drop in Empty, Baffled and Packed Tubes" Ind. Engg. Chem. 23 (8), 919 (1931).

43. Evans S.I. and Sarjant R.J. "Heat Transfer in Gases Flowing Inside Tubes" Jl. of Institute of Fuel 24 p. 216 (1951).

44.   Kreith F. and Margolis D. "Heat Transfer and Friction in
      Turbulent Vortex Flow" Appl. Sci. Research, Section
      A 8 p. 457-473 (1959).

45.   Gambill W.R., Bundy R.D. and Wansbrough R.W. "Heat
      Transfer, Burnout and Pressure Drop for Water in
      Swirl Flow Through Tubes with Internal Twisted Tapes"
      ORNL - 2911 (1960), also Ref. 39.

46.   Smithberg E. and Landis F. "Friction and Forced
      Convection Heat Transfer Characteristics in Tubes
      with Twisted Tape Swirl Generators" Jl. Heat Transfer,
      ASME Series C-86 (1) p. 39-49 (1964).

47.   Gambill W.R. and Bundy R.D. "High-Flux Heat Transfer
      Characteristics of Pure Ethylene Glycol in Axial and
      Swirl Flow" A.I.Ch.E. Jl. 9 (1) p. 55-59 (1963).

48.   Seymour E.V. "A Note on the Improvement in Performance
      Obtainable from fitting Twisted-Tape Turbulence -
      Promoters to Tubular Heat Exchangers" Trans. Instn.
      of Chem. Engrs. 41 (4) p. 159-162 (1963).

49.   Lopina R.F. and Bergles A.E. "Heat Transfer and Pressure
      Drop in Tape Generated Swirl Flow" Technical Report
      No. 70281-47, Deptt. of Mech. Engg., M.I.T. (June 1967).

50.   Thorsen R. and Landis "Friction and Heat-Transfer
      Characteristics in Turbulent Swirl Flow Subjected to
      Large Transverse Temperature Gradients" Jl. Heat
      Transfer, Trans. ASME, Series C-90 (1) p. 87-97
      (1968).

51.   Kidd G.J. Jr. "Heat Transfer and Pressure Drop for Nitrogen
      Flowing in Tubes containing Twisted Tapes" A.I.Ch.E.
      Jl. 15 p. 581-586 (1969).

52.   Narasimhamurty G.S.R. and Vara Prasad S.S.R.K.
      "Effect of turbulence promoters in two-phase gas liquid
      flow in horizontal pipes" Chem. Engg. Sci. 24 (2)
      p. 331-341 (1969).

53.   Klepper O.H. "Heat Transfer Performance of Short Twisted
      Tapes" A.I.Ch.E. Symp. Ser. 69 (131) p. 87-93 (1973).

54.   Cumo M., Ferello G.E., Ferrari G. and Palazzi "The
      Influence of Twisted Tapes in Subcritical, Once-Through
      Vapor Generators in Counter Flow" Paper No. 74-HT-XX,
      Jl. of Heat Transfer, Trans. of ASME 96 C-3 p. 365 (1974).

55.   Bergles A.E., Lee R.A. and Mikie B.B. "Heat Transfer in Rough Tubes with Tape-Generated Swirl Flow" Jl. of Heat Transfer, ASME C-91 (3) p. 443-445 (1969).

56.   Seymour E.V. "Heat Transfer and Pressure Drop for Air in Forced Vortex Flow Through Tubes with Internal Twisted Tapes" Bechelor's Thesis, Univ. of Western Australia, Applecross, Australia (1962).

57.   Megerlin F.E., Murphy R.W. and Bergles A.E. "Augmentation of Heat Transfer in Tubes by use of Mesh and Brush Inserts" Jl. of Heat Transfer, Trans. of ASME 96 C-2 p. 145-151, (1974).

58.   Hicks R.E. and Mandersloot W.G.B. "The effect of viscous forces on heat and mass transfer in systems with turbulence promoters and in packed beds" Chem. Engg. Sci. 23 (10) p. 1201-1210, (1968),

59.   Collier J.G. and Wallis G.B. "Two Phase Flow and Heat Transfer" Vol. III. Notes for a summer course, July p. 10-22 (1966) Thayer School, Dartmouth College, Hanover, N.H,

60.   Sharma B.D. "Studies on the Momentum Transfer and Stability of Swirling Flow in Long Horizontal Tubes" Ph.D. Thesis, Univ. of Roorkee, Roorkee (1974).

61.   Date A.W. "Prediction of fully-developed flow in a tube containing a twisted-tape" Intn. Jl. Heat and Mass Transfer 17 p. 845-859 (1974).

62.   Sherwood T.K. and Pigford R.L. "Absorption and Extraction" McGraw Hill Co. Inc. New York (1952).

63.   Whitman W.G. Chem. & Met. Engg. 29 (4) (1923) cited in 62.

64.   Lewis W.K. and Whitman W.G., Ind. Engg. Chem. 16 1215 (1924) cited in 62.

65.   Astarita G. "Mass Transfer with Chemical Reaction" Elsevier Publishing Co. New York (1967).

66.   Higbie R. "The Rate of Absorption of a pure gas into a still liquid during short periods of exposure" Trans. A.I.Ch.E. 31 p. 365 (1935).

67. Danckwerts P.V. "Significance of Liquid Film Coefficients in Gas Absorption" Ind. Engg. Chem. $\underline{43}$, 1460 (1951); A.I.Ch.E. Jl. 1 456 (1955).

68. Treybal R.E. "Mass Transfer Operations" II Ed. McGraw Hill-Kogakusha Co. Ltd., Tokyo (1968).

69. Dobbins W.E. cited Reference 68 p. 53.

70. Joor H.L. and Marchello J.M., A.I.Ch.E. Jl. $\underline{4}$ 97 (1958).

71. Reynolds O. cited Reference 62, p. 59.

72. Von Karman T.H. Trans. ASME $\underline{61}$ 705 (1939).

73. Reference 62 p. 60.

74. Colburn A.P. Ind. Engg. Chem. $\underline{22}$ 967 (1930).

75. Chilton T.H. and Colburn A.P. Ind. Engg. Chem. $\underline{26}$, 1183 (1934).

76. Sherwood T.K. and Gilliland E.R. Ind. Engg. Chem. $\underline{26}$, 516 (1934).

77. Linton W.H. and Sherwood T.K. : Chem. Engg. Progr. $\underline{46}$, 258 (1950).

78. Varlamove etal cited Reference 1 p. 266-267.

79. Baird M.H.I. and Davidson J.F. "Gas absorption by large rising bubbles" Chem. Engg. Sci. $\underline{17}$ pp. 87-93 (1962).

80. Beek W.J. and Van Heuven J.W. "Gas absorption in narrow gas lifts" Chem. Engg. Sci. $\underline{18}$ p. 377-390 (1963).

81. Heuss J.M., King C.J. and Wilke C.R. "Gas Liquid Mass Transfer in Cocurrent Froth Flow" A.I.Ch.E. Jl. $\underline{11}$ (5) p. 866-873 (1965).

82. Collins D.E. Ph.D. Thesis, Purdue University (1958).

83. Jepsen J.C. "Mass Transfer in Two-Phase Flow in Horizontal Pipelines" A.I.Ch.E. Jl. $\underline{16}$ p. 705-711 (1970).

84.   Banerjee S., Scott D.S. and Rhodes E. "Studies on
           Cocurrent Gas-Liquid Flow in Helically Coiled Tubes
           II Theory and Experiments on Turbulent Mass Transfer
           without and with Chemical Reaction" Can. Jl. Chem.
           Engg. p.542-551 (1970) also S. Banerjee, Ph.D.
           Thesis, Univ. of Waterloo, Canada (1968).

85.   Kulic E., M.A.Sc   Thesis, Univ. Waterloo (1970).

86.   Danckwerts P.V. "Gas Absorption Accompanied by Chemical
           Reaction" A.I.Ch.E. Jl. 1 (1955).

87.   Jagota A.K., Rhodes E. and Scott D.S. "Mass Transfer in
           Upwards Cocurrent Gas-Liquid Annular Flow" The
           Chem. Engg. Jl. 5 p.23-31 (1973).

88.   Golding J.A. and Mah C.C. "Gas Absorption in Vertical
           Slug Flow" Can. Jl. Chem. Engg. 53 (4) p.414 (1975).

89.   Wicks M. and Duckler A.E. "Entrainment and Pressure
           Drop in Cocurrent Gas-Liquid Flow : Air-Water in
           Horizontal Flow" A.I.Ch.E. Jl. 6 (3) p.463-468 (1960).

90.   Anderson J.D., Bollinger R.E. and Lamb D.E. "Gas Phase
           Controlled Mass Transfer in Two-Phase Annular
           Horizontal Flow" A.I.Ch.E. Jl. 10 (5) p.640-645 (1964).

91.   Ciborowski J.W. and Rychlicki R.M. Int. Jl. Heat Mass
           Transfer 14, 1261 (1971).

92.   Kropholler H.W. and Carr A.D. i.b.i.d. 5, 1191 (1962).

93.   Scott D.S. and Hayduk W. "Gas Absorption in Horizontal
           Cocurrent Bubble Flow" Can. Jl. Chem. Engg. 44
           p.130-136 (1966).

94.   Levenspiel O., Weinstein N.J. and Li J.C.R. Ind. Engg.
           Chem. 48, 324 (1956).

95.   Wales C.E. "Physical and Chemical Absorption in Two-
           Phase Annular and Dispersed Horizontal Flow"
           A.I.Ch.E. Jl. 12 p.1166-1171, (1966).

96.   Cichy P.T., Ulman J.S. and Russel T.W.F. "Two-Phase
           Reactor Design - Tubular Reactors" Ind. Engg. Chem.
           61 (8) p.6-15 (1969).

97.   Lamont J.C. and Scott D.S. "Mass Transfer from Bubbles
          in Cocurrent Flow" Can. Jl. Chem. Engg. <u>44</u>
          p.201-208 (1966).

98.   Lamont J.C. "Gas Absorption in Cocurrent Turbulent
          Bubble Flow" Ph.D. Thesis, Univ. of Britsh
          Columbia, Canada (1966).

99.   Reference 35.

100. Hughmark G.A. "Mass Transfer in Horizontal Annular
          Gas-Liquid Flow" Ind. Engg. Chem. (Fandam)
          <u>4</u> p.361-363 (1965).

101. Davison R.L. and Kessler D.P. "Mass Transfer in
          Horizontal Cocurrent Annular Flow" A.I.Ch.E.
          66th Natnl. Meeting, Portland, Aug. 24-27 (1969).

102. Kasturi G. and Stepanek J.B. "Two-Phase Flow-III, Inter-
          facial Area in Cocurrent Gas Liquid Flow" Chem. Engg.
          Sci. <u>29</u> p.713-719 (1974).

103. Kasturi G. and Stepanek J.B. "Two-Phase Flow-IV, Gas
          and Liquid Side Mass Transfer Coefficients" Chem.
          Engg. Sci. <u>29</u> p.1849-1856 (1974).

104. Horvath C., Solomon B.A. and Engasser "Measurement of
          Radial Transport in Slug Flow using Enzyme Tubes"
          Ind. Engg. Chem. (Fandam) <u>12</u> (4), 431, (1973).

105. Shah A.K. and Sharma M.M. "Mass Transfer in Gas-
          Liquid Horizontal Pipelines" Can. Jl. Chem. Eng.
          <u>53</u> (5), 572 (1975).

106. Thomas D.G. "Effect of Wires Located Near the Edge of
          Laminar Boundary Layer on the Rate of Forced.
          Convention From a Flat Plate" A.I.Ch.E. Jl. <u>11</u>
          p.848 (1965).

107. Zarnett G.D. "A Study of Horizontal Two-Phase Flow
          with Chemical Reaction in Rifled Tubes" Ph.D. Thesis,
          Univ. of Toronto, Canada, (1972).

108. Morris W.D. and Misson P. "An Experimental Investi-
          gation of Mass Transfer and Flow Resistance in the
          Kenics Static Mixtures" Ind. Engg. Chem.;
          Proc. Des. & Devlp. <u>13</u> (3) p.270-275 (1974).

109. Duckler A. E. and Hubbard M. G. "A Model for Gas-Liquid Slug Flow in Horizontal and Near Horizontal Tubes" Ind. Engg. Chem. (Jandam) $\underline{14}$ (4) p. 337-347 (1975) and Hubbard M.G., Ph.D. Thesis, Univ. of Houston (1965).

110. Vogel A. I. "A Text Book of Quantitative Inorgan Analysis including Elementary Instrumental Analysis" III Ed. p. 249, Orient Longmans Pvt. Ltd. Calcutta (1961).

111. Hewitt G.F., King R.D. and Lovegrove P.C. "Techniques for Liquid Film and Pressure Drop Studies in Annular Two Phase Flow" AERE - R 3921, UKAEA, Harwell, England, (1962).

112. Perry J.H. Ed. "Chemical Engineers Handbook" IIIrd Ed. McGraw Hill Book Co., New York (1950).

113. Reference 62. p. 127.

114. Himmelblau "Process Analysis by Statistical Methods" John Wiley & Sons Inc. New York (1970).

115. Reference 86. p. 19.

116. Danckwerts P.V. Trans. Fara. Soc. $\underline{46}$, 300 (1950).

117. i. b. i. d. $\underline{46}$ p. 701 (1950).

118. Perry R.H. and Pigford R. L. Ind. Engg. Chem. $\underline{45}$ 1247 (1953).

119. Van Krevelen D.W. and Hoftizer P.J. Rec. Trans. Chim. $\underline{67}$, 563, (1948).

120. Brian P.L.T., Hurley J.F. and Hasseltine E.E.H. "Penetration Theory for Gas Absorption Accompanied by a Second Order Chemical Reaction" A.I.Ch.E. Jl. $\underline{7}$, 226 (1961).

121. Porter K.E. "The effect of contact time distribution on gas absorption with chemical reaction" Instn. Chem. Engrs. $\underline{44}$ T. 25 (1966).

122. Reference 86. p. 115-118.

123. Danckwerts P.V. and Sharma M.M. "The Absorption of Carbondioxide with solutions of Alkali and Amines" The Chem. Engr. 44 CE 244 (1966).

124. Pinsent B.R.W., Pearson L. and Roughton F.J.W. "The Kinetics of Combination of CO_2 with (OH) ions" Trans. Far. Soc. 52 1512 (1956).

125. Porter K.E., King M.B. and Varshney K.C. "Interfacial Areas and Liquid Film Mass Transfer Coefficients for a Bubbe Plate Derived from absorption rates of CO_2 into water and NaOH solutions" Trans. Instn. Chem. Engg. 44 T 274 (1966).

126. Jagcta A.K. "Hydrodynamics and Mass Transfer in Upwards Cocurrent Gas-Liquid Annular Flow in Vertical Tubes" Ph.D. Thesis, Univ. of Waterloo, p.321 (1970).

127. Duckler A.K., Wicks M., and Cleveland R.G. "Frictional Pressure Drop in Two Phase Flow : A Comparison of Existing Correlations for Pressure Drop and Holdups" A.I.Ch.E. Jl. 10 (1) p.38-43 (1964).